

Copyright is owned by the Author of the thesis. Permission is given for a copy to be downloaded by an individual for the purpose of research and private study only. The thesis may not be reproduced elsewhere without the permission of the Author.

Ovine Paratuberculosis

Transmission Dynamics and Cost- Effectiveness of Interventions

A thesis presented in partial fulfilment of the requirements for the degree of Doctor of
Philosophy at Massey University

Nelly Marquetoux

2017

Institute of Veterinary, Animal and Biomedical Sciences

Massey University

Palmerston North, New Zealand

Abstract

This thesis aimed at enhancing the knowledge about the epidemiology and control of paratuberculosis caused by infection with *Mycobacterium avium* subsp. *paratuberculosis* (MAP) in the New Zealand farming system, with a primary focus on sheep.

The potential for pathogen transmission between farms was explored in two studies. Four years of livestock movement records to and from 112 corporately owned farms in New Zealand, involving 1.15 million sheep, cattle and deer were analysed using social network analysis. In the first study, topologic features favouring pathogen spread in this network of farms were established. Hub-farms were identified as targets for risk-based movement control strategies to effectively decrease the potential for large epidemics. Inferences about movement control were not specific to MAP, so could apply to any pathogen transmission. In a second study, the potential for MAP transmission between farms was evaluated. In 2010, cross-sectional MAP screening using faecal culture and genotyping of cultures was performed on a subset of 102 farms in this network at the herd/flock level. These data were merged with the data about livestock movements. Multiple regression methods adapted to network data showed associations between past livestock movements and current strain type distribution in this population of farms. Farms in the same livestock movement network community were found to be twice as likely to share the same strains of MAP compared to farms in different communities ($p=0.033$). These studies showed that livestock movements between farms favour pathogen transmission and likely contribute to the high level of MAP infected farms in New Zealand. Results suggest that MAP can establish in a flock following the introduction of infected animals, and that biosecurity applied to trade may reduce the spread of MAP.

In a second part, a compartmental infection model was developed to simulate paratuberculosis on a typical self-replacing Romney sheep farm in New Zealand. This was preceded by a review of the literature on the physio-pathology of MAP infection in sheep, clinical outcomes and pathways following MAP infection to inform the model structure. A review of MAP enumeration methods *in vitro* identified comparative biases in estimating MAP doses in experimental studies. Subsequently, a systematic review and meta-analysis of experimental infection of sheep with MAP quantitatively estimated parameters for the simulation model, and identified relevant challenge-dose effects. The meta-analysis also enabled to integrate the effect of age at exposure, strain of MAP and type of inoculum on the

outcomes of experimental infection with MAP. It determined that MAP is highly infectious, with only 76 live ingested organisms required to cause histological lesions in the small intestine in 50% of inoculated sheep. However, 8.9×10^6 MAP organisms were necessary to cause progression to clinical disease in 50% of sheep infected as lambs or hoggets, and 7.7×10^9 in sheep infected as adults.

Simulations using the model were carried out for a range of clinical incidence scenarios, to study the impact of ovine Johne's disease (OJD) on a New Zealand pastoral sheep farm and the cost-effectiveness of interventions, *e.g.* vaccination. The impact of OJD is low on the majority of NZ pastoral sheep farms. These would not economically benefit from vaccination. However, vaccination with Gudair™ drastically reduced OJD mortality in flocks with high (1%) to very high (2%) annual clinical incidence of OJD in ewes, and was cost-effective. At a level of 1% OJD cases/annum in the ewe flock, the time to positive return on investment was 23 years, dropping to five years for 2% OJD cases/annum. After 30 years, farms with 2% OJD could expect NZD 2.4 return (net present value) for each dollar invested, with a total net profit of NZD 2,435 per 100 ewes in the flock. Meat price fluctuations had a strong impact on the economic evaluation.

Besides, annually replacing 1% of the flock with infected ewes tended to negate the beneficial impact of vaccination on reducing clinical disease incidence, through maintaining high levels of pasture contamination. The movements of MAP-infected animals can thus jeopardize the success of vaccination strategies. In the current context of high endemic prevalence of MAP infection in New Zealand farms, and given evidence about transmission between farms, it seems unrealistic to prevent MAP re-/introductions on farms in the absence of a certification program.

The network analysis undertaken in this thesis enhanced the understanding of the role of livestock movement in transmission of MAP. Combined with the simulation model, this work provides options to support farmers' decision-making and veterinary advice for managing sheep flocks with high OJD mortality.

Acknowledgments

All my gratitude goes to my four supervisors Cord Heuer, Peter Wilson, Anne Ridler and Mark Stevenson for their support, encouragements and all the knowledge they shared with me. Thanks Cord for taking me on-board, sharing your experience so generously and for your great optimism. It was so pleasant to be invariably granted a big welcoming smile upon knocking at your door. I loved how you always pulled out the ‘big picture’ about my work or my technical questions, and you were always keen to teach me. I also thoroughly enjoyed hearing the fantastic “tales” of all your personal and professional adventures! Your rich life and your enthusiasm durably populated my imagination. You are more than a supervisor to me and my best achievements were the times when you were happy with me, or proud of me. I will never forget how Hilli and you welcomed me in New Zealand like family. I feel so lucky to know you guys, and your family. Peter, you know how much I appreciated your contribution to this work. Your high standards in science, in ethics and in your approach of life are real models for me both academically and personally. If I improved even slightly my writing skills in all those years, I owe it to you. Anne your input in this thesis was simply essential; you made this computer-based PhD relevant to actual sheep farming in New Zealand. Thank you so much for your great diligence, your guidance and support and for always picking essential bits that nobody else picked in the manuscripts! Mark, it was such a pleasure to have you next door for a couple of years, during which I learned a lot from you. I truly appreciate how generous you were in sharing all your fantastic epi resources and the very amiable way in which you did it. The EpiCentre is a great place to learn and my research (and me as a scientist) greatly benefited from the many precious inputs. I would also like to thank my examiners David Hayman, Navneet Dhand and Pauline Ezanno, for their excellent examination and insightful contribution to this thesis.

Special thanks to Masako, Matthieu and Simon for the great help in the last week or two in wrapping up this thesis. The beers helped but without you guys it would have been simply impossible. It was super nice to see how much I could count on you when I needed you! A special thanks to Sabrina for nicely proof-reading one manuscript for me.

I am also grateful to all the people who helped me in my work throughout the years: Rebecca Mitchell for a very insightful collaboration and for welcoming me in your house (with Ymir); it was so stimulating to work with you and I learned a lot. Carolyn Gates, it is so nice that you came along; our quick (but efficient!) collaboration made me only regret that we did not have

time to do more. I greatly admire the extent of your knowledge and how smart you are. Matthieu, working with you was a highlight in this PhD. Your input in trying to link the meta-analysis and the model was essential in giving me confidence in my home-brewed methods. It took a great deal of figuring out and patience on your end. Thank you for your scientific contribution, your dedication, your time and a very much-appreciated help in proof-reading this thesis. I am extremely grateful to Geoff Jones and Chris Jewell for always giving me spot on statistical advice. It was great to have your robust input when I was very lost from time to time and it makes me trust myself a little more. I would like to sincerely thank Karren Plain and Richard Whittington for welcoming me in their lab in Camden. I really appreciated the world of new knowledge about PCR I learned there, with your generous contribution and the help of Anna Waldron. It was wonderful how well it worked to set up the PCR here and it will greatly benefit future research at Massey. Thanks to Doug Begg for sharing his expertise about ovine paratuberculosis. My thoughts also go to Gordon Williams (Landcorp), for his great help in building a meaningful livestock movement database and understanding the raw data, thanks for a very diligent contribution. A special dedication to Neville for sharing my Hopkirk adventure (although to no avail), being by my side in the difficulties and for showing me the way around the lab. Also, a big hug to Helen and Phil who welcomed me so generously in their house in Tauranga, giving me the means of a very fruitful writing retreat when I needed focusing on this work.

I very gratefully acknowledge the Graduate Research School (Massey University), in particular Fiona McNish, for excellent support for being very understanding and flexible. This was much appreciated. I sincerely thank Massey University and Education New Zealand for their very generous and essential support through my doctoral scholarship. The New Zealand Johne's Disease Research Consortium partially funded this research, for which they are gratefully acknowledged. I also thank Chris Cunningham and Wendy Maharey for their administrative support.

Life at the EpiCentre would not be nearly as nice without all the great friends I came across. Masako, I am so glad that you are the one who ended up sharing 'our' office, and became my alter-ego! What a great time we had! There could not have been a better friend AND a better office mate for me. You and Ilyas really gave me a family here. Thanks for always sitting next to me with a beer and we watch the world (in awe) alongside each other. Thanks for sharing your perspective with me and showing me a different life philosophy, which helped me to embrace life differently. Thanks for all your encouragement in particular in the last few weeks, and your wise advice. And thanks for giving to the world such a great person as Ilyas, whom I love!

Simon, you are the most helpful person in the EpiCentre, always fixing stuff for everybody and popping in the next 2 minutes whenever we need you. Thank you for the innumerable morning coffees (“or tea, if you prefer”...). Thank you for introducing us to Ultimate Frisbee and being so encouraging with me (despite my total lack of natural ability). Juan and Dani, you made our life in New Zealand so much more fun, so much more homely, too! Juan it was great to always hang together in the office. The shorts&flip-flop gang. I loved your relax yet super knowledgeable approach to epi. Dani, your visits were the highlight of the day, your super friendly smile, a balm. You are such an unspeakably nice person! More importantly, all the BBQ, all the jokes, the smiles, the laughter, the beers, the pisco, the camping trips, (...the fish?), the parties, the talking til 4 am and much more. You guys, with Magda and Isabel, represent the epitome of friendship and happiness for me.

Thanks to Emilie for being a dear friend and for sharing a ‘kind of French spirit’ with me. You will know what I mean... was nice to have you to talk to. Another great highlight in my time here was to travel and do field work with you, a unique opportunity to discover the “real NZ”.

A special word to my dear friend Kruno to say how much I value our friendship, we shall keep this alive.

A special thanks to Sebou: we came here together all those years ago, it was a pretty big leap and I don’t know if I would have committed that far on my own... And we loved it so much that we both lingered, although not together! I could not have stayed all these years without you by my side though; your company and your support meant that I was never alone. We roamed this country together (at least in the first few years), and all the little paths smelt of hazelnut for us! And it was so much fun. I am glad to be your friend and wish you all the best for your future life mate!

I now remember fondly all the “old” EpiCentre folks: Anou, Melvin, Lesley, Alberto, Marta, Kandarp, Ben, Eutteum, Long, Ray & Belinda, Sarah, it was great to befriend with you.

Thanks to all the “current” EpiCentre folks for making our life better: Alicia for all your support and your delightful craziness (stay just the way you are!), Arata thanks for all the years of friendship and all of your great inputs, Jun, Katja, Sabrina, Yuni and Chris. Thanks also to Naomi and Tim for their friendly support along the years.

Cristobal, I inherited from your paraTB PhD and in some aspects you are like a big brother to me. I greatly appreciate your friendship and the life tricks you shared with me, for this PhD and

otherwise ;). Milan, you are the next generation and I am so glad to pass my stuff on to you, of anybody. It is great to work with you and to be your friend.

Matthieu, I am so grateful for the time we spent together so far, and how you showed me another (wonderful) way. Did I tell you how much I love your van? Thank you for the time and efforts you invested on me, I hope you will be rewarded, maybe beyond expectations ;)

This work would not have been possible without the great support, at a distance, from my beloved family. I missed you all a great deal in all those years; this is the only (and huge) negative point of being here. Big thanks to my Mum and Dad for the love and encouragements, which paved my way in this life. Your upbringing gave me the confidence I could achieve what I want in life, with the help of all the comforting and cherished (and super fun!) childhood memories I carry with me. Mamy, a big hug to you and thanks for all the fun and the love we share. To my sister Chloé, the moments we shared when you visited here were the best! Thanks for always having good advice for me, too! And thanks to my dear Léo: I love you to bits; you are a lovely little boy and I miss you a lot. Finally, thanks to Martine for giving us the amazing opportunity of becoming sisters again, and a big kiss to each of the last two little additions to the family: Alex and Jonah! You guys are adorable. A special thought to my godson baby Jonah, the “real” Kiwi bloke!

List of Abbreviations

AIC	Akaike Information Criterion
AGID	Agar Gel Immunodiffusion
CI	Confidence Interval
CFU	Colony Forming Unit
Ct	Cycle threshold
DNA	Deoxyribonucleic Acid
FMD	Foot-and-Mouth Disease
GAMM	Generalised Additive Mixed Models
GLM	Generalised Linear Models
GOF	Goodness-of-fit
GSCC	Giant Strongly Connected Component
GWCC	Giant Weakly Connected Component
IFN _γ	Interferon Gamma
IL	Interleukin
JD	Johne's disease
LC	Landcorp
MAP	<i>Mycobacterium avium</i> subsp. <i>Paratuberculosis</i>
<i>M. bovis</i>	<i>Mycobacterium bovis</i>
MC	Monte Carlo
MPN	Most probable Number
<i>M. tb</i>	<i>Mycobacterium tuberculosis</i>
NAIT	National Animal Identification and Tracing Scheme

NZ	New Zealand
NZD	New Zealand Dollar
OD	Optical Density
ODE	Ordinary Differential Equation
OJD	Ovine Johne's Disease
OR	Odds Ratio
PCR	Polymerase Chain Reaction
PTB	Paratuberculosis
qPCR	quantitative Polymerase Chain Reaction
RFLP	Restricted Fragment Length Polymorphism
SNA	Social Network Analysis
SSR	Short-Sequence-Repeat
TB	Tuberculosis
Th1	T helper 1
Th2	T helper 2
VNTR	Variable-Number Tandem-Repeat
WGS	Whole Genome Sequencing

List of Journal Publications

Marquetoux, N., M. Stevenson, P. Wilson, A. Ridler and C. Heuer (2016) 'Using social network analysis to inform disease control interventions', *Preventive Veterinary Medicine* 126: 94-104.

Marquetoux, N., C. Heuer, P. Wilson, A. Ridler and M. Stevenson (2016) 'Merging DNA typing and network analysis to assess the transmission of paratuberculosis between farms', *Preventive Veterinary Medicine* 134: 113-121.

List of Conference Presentations

Oral presentations

Marquetoux, N., C. Heuer, P. Wilson., A. Ridler and M. Stevenson (2016) 'The role of livestock movements between farms in the spread of paratuberculosis', *GeoVet Conference*, Valdivia, Chile - senior oral presentation.

Marquetoux N., R. Mitchell, P. Wilson, M. Stevenson, A. Ridler and C. Heuer (2016) 'Modelling paratuberculosis in a typical sheep flock in New Zealand', *International Colloquium on Paratuberculosis*, Nantes, France.

Marquetoux N., R. Mitchell, P. Wilson, M. Stevenson, A. Ridler and C. Heuer (2015) 'Meta-analysis of the transmission of *Mycobacterium avium* subsp. *paratuberculosis* in experimentally infected sheep to inform mathematical modelling', *International Symposia on Veterinary Epidemiology and Economics*, Merida, Mexico.

Marquetoux N., M. Stevenson, P. Wilson, A. Ridler, and C. Heuer (2014) 'Molecular epidemiology of paratuberculosis: using strain typing data to inform the transmission between farms via livestock movements', *International Colloquium on Paratuberculosis*, Parma, Italy.

Marquetoux, N., C. Heuer, P. Wilson and M. Stevenson (2013) 'Can we assess the transmission of paratuberculosis between farms? Description of a network analysis of livestock movements', *New Zealand Veterinary Association Epi branch Conference*, Palmerston North, New Zealand.

Marquetoux, N., R. Mitchell, P. Wilson, A. Ridler, M. Stevenson, C. Verdugo and C. Heuer (2013) 'Comparative Cost-Benefits Of Johne's Disease Control In Sheep Flocks Using Simulation', *International Sheep Veterinary Congress*, Rotorua, New Zealand.

Marquetoux, N., P. Wilson and C. Heuer (2011) 'Test-and-cull and evaluation of its cost-effectiveness for JD control in deer', *Deer Branch of the New Zealand Veterinary Association Conference*, Queenstown, New Zealand.

Poster presentation

Marquetoux N., C. Heuer, P. Wilson and A. Ridler (2015) 'Using pathogen strain-typing to inform transmission dynamics in social networks of livestock movements', *International Symposia on Veterinary Epidemiology and Economics*, Merida, Mexico.

Marquetoux N., R. Mitchell, P. Wilson., M. Stevenson, A. Ridler, and C. Heuer (2014) 'Meta-analysis of paratuberculosis progression in experimental sheep studies informing mathematical modelling', *International Colloquium on Paratuberculosis*, Parma, Italy.

Marquetoux N., A. Ridler, P. Wilson and C. Heuer (2014) 'Economics of ovine paratuberculosis: estimation of economic losses due to paratuberculosis in the meat sheep industry in New Zealand', *International Colloquium on Paratuberculosis*, Parma, Italy.

Marquetoux, N., R. Mitchell, P. Wilson, A. Ridler, M. Stevenson, C. Verdugo and C. Heuer (2012) 'A within-herd state transmission model for MAP infection in farms co-grazing deer and sheep in New Zealand', International Symposia on Veterinary Epidemiology and Economics proceedings, *International Symposia on Veterinary Epidemiology and Economics*, Maastricht, the Netherlands.

Marquetoux, N., C Heuer, P. Wilson, and M. Stevenson, (2012), 'Between-farm movements of livestock: epidemiological implications for the transmission and control of paratuberculosis in New Zealand', *International Colloquium on Paratuberculosis*, Sydney, Australia.

Table of Contents

Abstract.....	iii
Acknowledgments.....	v
List of Abbreviations	ix
List of Journal Publications	xi
List of Conference Presentations	xiii
Table of Contents.....	xv
List of Figures	xxii
List of Tables	xxix
Chapter 1. General Introduction.....	1
1.1 Definitions.....	1
1.2 Aetiology of paratuberculosis	2
1.3 Prevalence of MAP infection and incidence of clinical paratuberculosis	3
1.4 Production effects of paratuberculosis in sheep in New Zealand	4
1.4.1 Production effects associated with clinical paratuberculosis.....	4
1.4.2 Production effects associated with subclinical paratuberculosis	5
1.4.3 Production effects and economic losses at the industry level	6
1.5 Justification for this thesis	6
1.6 Thesis aim and objectives	7
1.7 Thesis outline	7
1.8 Declaration.....	9
Chapter 2. Using social network analysis to inform disease control interventions	11
2.1 Abstract.....	11
2.2 Introduction	12
2.3 Material and methods	13
2.3.1 Movement data	15
2.3.2 Data analysis	15

2.4	Results	20
2.4.1	Consistency of the contact pattern over time.....	21
2.4.2	Description of the degree distribution	23
2.4.3	Small-world properties of the network and overall connectivity	24
2.4.4	Effect of network properties on the basic reproduction number (R_0)	25
2.4.5	Efficacy of targeted control strategies to disrupt the transmission via livestock movements	27
2.5	Discussion	30
2.5.1	Consistency of the contact pattern over time.....	31
2.5.2	Description of the degree distribution	32
2.5.3	Small-world properties and connectivity	33
2.5.4	Effect of network properties on the basic reproduction number (R_0)	34
2.5.5	Efficacy of targeted control strategies to disrupt the transmission via livestock movements	35
2.6	Conclusions.....	37
2.7	Acknowledgements	38
Chapter 3. Merging DNA typing and network analysis to assess the transmission of paratuberculosis between farms.....		39
3.1	Abstract	39
3.2	Introduction.....	39
3.3	Material and methods	41
3.3.1	Animal movement data	41
3.3.2	Paratuberculosis culture.....	41
3.3.3	Data analysis.....	42
3.4	Results	48
3.4.1	Descriptive results	48
3.4.2	Association between MAP strain type pattern and movement pattern between farms	49
3.5	Discussion	52

3.5.1	Measure of livestock movements	53
3.5.2	Species	54
3.5.3	Euclidian distance	55
3.5.4	Island	56
3.5.5	Genetic resolution	57
3.5.6	Statistical Methods	59
3.6	Conclusion	59
3.7	Acknowledgements	60
Chapter 4. A synthesis of the patho-physiology of <i>Mycobacterium avium</i> subspecies <i>paratuberculosis</i> infection in sheep to inform mathematical modelling of ovine paratuberculosis		
		61
4.1	Abstract	61
4.2	Introduction	62
4.3	Assumptions for a candidate model structure	63
4.3.1	Pathological outcomes following artificial inoculation with MAP	64
4.3.2	Progression pathways	69
4.3.3	Conclusions and assumptions for a candidate model	75
4.4	Modelling the force of MAP infection after natural exposure in a pastoral environment	76
4.4.1	Probability of infection in lambs prior to weaning	76
4.4.2	Probability of infection after weaning	77
4.4.3	Conclusions: modelling the force of infection	78
4.5	Effect of covariates	78
4.5.1	Effect of age at exposure on infection	79
4.5.2	Effect of age at exposure on progression	79
4.5.3	Effect of MAP dose on progression	80
4.5.4	Effect of MAP strain on progression	82
4.5.5	Effect of inoculum type on progression	82

4.5.6	Conclusions: effect of covariates.....	84
4.6	Field data for model validation	84
4.6.1	Prevalence of histological lesions in sheep naturally infected with MAP	87
4.6.2	Incidence of clinical cases in sheep naturally infected with MAP	89
4.6.3	Conclusion: Field data for model validation.....	90
4.7	Conclusion	92
Chapter 5. Enumeration methods of <i>Mycobacterium avium</i> subsp. <i>paratuberculosis</i> <i>in vitro</i> from animal samples		
		93
5.1	Abstract	93
5.2	Introduction.....	93
5.3	Different methods of MAP enumeration	94
5.3.1	Culture based methods	94
5.3.2	Pelleted weight.....	100
5.3.3	Direct microscopic counts of MAP cells	101
5.3.4	Direct PCR.....	103
5.3.5	Other methods	105
5.4	Equivalence between estimates from the different methods:	105
5.4.1	Viable MAP versus microscopic direct count	105
5.4.2	Plate count versus end point titration.....	107
5.4.3	Weight of pelleted bacteria versus “theoretical” total number or other methods 107	
5.4.4	McFarland units versus qPCR or direct microscopic count	108
5.4.5	McFarland units versus plate counts.....	109
5.4.6	qPCR versus plate counts	109
5.5	Summary.....	110
5.6	Conclusion: application for interpreting inoculum doses of experimental challenge models.....	111
Chapter 6. Meta-analysis of experimental infection of sheep with <i>Mycobacterium avium</i> subsp. <i>paratuberculosis</i> to inform mathematical modelling of ovine paratuberculosis		
		113

6.1	Abstract.....	113
6.2	Introduction	114
6.3	Materials and methods	115
6.3.1	Literature search	115
6.3.2	Data extraction and standardisation	117
6.3.3	Data analysis and parameter estimation	121
6.4	Results.....	129
6.5	Discussion.....	147
6.5.1	Probability of active infection	148
6.5.2	Probability of progression (χ).....	150
6.5.3	Rate of progression from early to severe disease in the progressor track (δ) .	152
6.5.4	Rate of recovery from shedding in the non-progressor track (γ)	153
6.5.5	Effects of covariates.....	155
6.5.6	Methods.....	158
6.6	Conclusion.....	160
6.7	Acknowledgments.....	160
Chapter 7.	Modelling paratuberculosis in a typical sheep flock in New Zealand	163
7.1	Abstract.....	163
7.2	Introduction	164
7.3	Materials and methods	166
7.3.1	Model description	166
7.3.2	Farm gate profit of sheep farming	173
7.3.3	Simulation scenarios	175
7.3.4	Sensitivity analysis	178
7.4	Results.....	179
7.4.1	Infection dynamics.....	179
7.4.2	Cost of OJD.....	180
7.4.3	Vaccine effect.....	181

7.4.4	Cost-effectiveness of vaccination	183
7.4.5	Effect of purchasing infected stock	185
7.4.6	Effect of changing the replacement rate and pasture spelling	186
7.4.7	Sensitivity analysis	187
7.4.8	Model validation	188
7.5	Discussion	190
7.5.1	Dynamics of infection	190
7.5.2	Flock demographics	193
7.5.3	Model validation	194
7.5.4	Interventions to control OJD	196
7.6	Conclusion	202
7.7	Acknowledgements	202
Chapter 8.	General discussion	203
8.1	Overview of results	203
8.2	Farm-to-farm transmission of paratuberculosis (Chapters 2 and 3)	205
8.2.1	Assessing the impact of livestock movements on MAP spread	205
8.2.2	Spatial spread and comparison with TB	206
8.2.3	Genetic resolution and influence of species	207
8.2.4	Methods	208
8.3	Within-flock transmission (Chapters 4, 5, 6)	209
8.3.1	From physiopathology of ovine paratuberculosis to within-flock dynamics	209
8.3.2	Evaluating the effect of MAP dose	210
8.3.3	Methods to estimate model parameters	210
8.3.4	From experimental infection to natural challenge	212
8.3.5	Modelling within-flock dynamics	214
8.4	Control of ovine PTB	214
8.4.1	Vaccination	214
8.4.2	Biosecurity on Farms	216

8.4.3	What is the real incentive for control?	216
8.5	Future work.....	218
8.6	Concluding comments	220
Chapter 9.	References	223
Chapter 10.	Appendices.....	239
10.1	Appendix A (Chapter 3).....	239
10.1.1	A.1. Inter-dependencies and hypothesis testing in social network analysis	239
10.1.2	A.2. Results of univariate analysis.....	240
10.1.3	A.3. Supplementary Figures	241
10.2	Appendix B (Chapter 6).....	243
10.2.1	B.1. Method 1: overall fit	243
10.2.2	B.2. Method 2: fitting using the median time.....	244
10.2.3	B.3. Results.....	245
10.3	Appendix C (Chapter 7).....	247
10.3.1	C.1. Model Ordinary Differential Equations.....	247
10.3.2	C.2. Euler method: first order approximation of ODE solutions.....	249
10.3.3	C.3. Model algorithm	250
10.3.4	C.4. Updating the value of the underlying initial population at risk of infection (exposed to MAP) $E_{age,0}$ after demographic events	254
10.3.5	C.5. Calculation of death rate due to paratuberculosis parameters (μ_c) and shedding parameters (σ_{low} and σ_{high}).....	257

List of Figures

- Figure 2-1 : Frequency of pairs of farms being connected in only one year or repeatedly in multiple years (2006 – 2010). 22
- Figure 2-2 : un-weighted degree distribution for the 107 LC farms involved in the network in 2009-2010. 24
- Figure 2-3 : correlations observed in the LC network in 2009-10 between the number of contacts in and out per farm (un-weighted degree, a) or the number of animals in and out per farm (weighted degree, b), respectively for transfers (green), agistments (red) and the total of both movements (black). R_{in-out} corresponds to the Pearson correlation coefficient between the total in- and out-degree. 27
- Figure 2-4: representation of the network of LC farms in 2009-2010, showing the importance of high-degree farms (in red) and high-betweenness farms (big size) in the contact structure. Each farm is represented as a node, the links between nodes are livestock movements. (a) projection according to the contact pattern only, not the geographical space, although the two main clusters correspond to farms of the North Island versus farms of the South Island, (b) contact pattern projected on a map of New Zealand according to the spatial coordinates of farms. 28
- Figure 2-5: Line plots showing the effect of targeted (in red and blue) or random (in black with 95% credible limits) removal of farms on two measures of potential spread: (a) showing the size of the largest strongly connected component as a function of the number of farms removed, (b): showing the value of $R_0(\text{reduced network}) / R_0(\text{full network})$ as a function of the number of farms removed. 29
- Figure 3-1: The principle of matrix correlation analysis applied to a theoretical network of six farms infected by MAP (i, j, k, l, m, n) connected by livestock movements (black lines). Colours represent particular MAP strains. Proximity of farms in the network is expressed by the shortest path length between farms or the network community to which farms belong (represented by the shape of the farms: square=community #1, circle=community #2) based on the livestock movement pattern. 44
- Figure 3-2: Distribution of 11 VNTR/SSR strain types of MAP, categorised A – K, from 54 isolates typed from 47 pools of 33 Landcorp Ltd. properties of sheep, deer, beef and dairy cattle. The number of isolates of each type is indicated above each bar. 49

Figure 3-3: : Spatial locations of all 112 Landcorp Ltd. farms of which 2010 movement data were available coloured by their network community (a); spatial locations of the 33 farms of which MAP isolates were genotyped, coloured by MAP VNTR/SSR type (b); Fruchterman-Reingold layout of farms (circles) and the network of livestock movements (lines), coloured by VNTR/SSR type (c), as in (b), and including farms without isolates or not sampled (white circles). Only the 33 MAP-positive farms and the farms that were along the shortest path between them were included. For illustration, red lines display all shortest paths linking farms of a single strain (green).51

Figure 4-1: structure for a candidate state-transition mathematical model of ovine paratuberculosis, based on evidence gathered in Part 1 of this review91

Figure 6-1: hypothesised model structure for transmission dynamics of ovine paratuberculosis. F is the rate of entry into active infection following exposure through contaminated environment. χ is the proportion of infected animals entering the progressor track, δ the rate of progression from mild to severe disease, γ the rate of exit from early, transient shedding into a recovered state, μ_c the rate of mortality due to clinical paratuberculosis, sigma the rate of shedding into the environment (high or low shedding)..... 115

Figure 6-2: Steps of parameter estimation for the distribution of time from ingestion of MAP to onset of active infection from observed histological data of the meta-analysis for dose 10^4 MAP..... 124

Figure 6-3: Method to estimate the value of χ from the predicted probabilities of *model 1* (in blue) and *model 2* (in red), for a specific set of covariates. 126

Figure 6-4: Distributions of the age at inoculation (a.) the time from inoculation to *post-mortem* (b.), and inoculum dose (c.) for individual sheep (across all experiments)...132

Figure 6-5: Raw daily frequency histogram of sheep with histological lesions of known type over time (left) and sheep detected with severe lesions or clinical signs over time (right), all datasets combined..... 134

Figure 6-6: Monthly proportion of shedders (n=161, repeated measurements) and histological lesions of PTB at *post-mortem* (n=627)..... 135

Figure 6-7: Predicted probability of active infection, i.e. presence of histological lesions in the guts versus time from *model 1* (blue curve) and 95% confidence interval (grey area) (covariate levels: MAP dose = 105, tissue homogenate inoculum, ovine strain). Points

represent the raw data from individual experiments. Each point corresponds to the observed proportion of sheep histology positive in 3-monthly time slots, grouped by dose (red: observations with inoculum dose above the median dose; green: observations with inoculum dose below the median dose) and inoculum type (square: pure culture; triangle: tissue homogenate). 137

Figure 6-8: Predicted probabilities of active infection over time from *model 1* and successive transformations for the purpose of fitting a Weibull distribution (a = predicted probabilities; b= predicted probabilities scaled to one for each stratum, c = transformation to a linear form), stratified by increasing MAP challenge dose 10 to 10¹² MAP (ovine MAP strain, tissue homogenate inoculum). 138

Figure 6-9: Relationships between the dose-dependent Weibull parameters α_{dose} and k_{dose} and the dose-dependent plateau $\max(P T < t)_{dose}$ and the inoculum dose to model the probability of active infection as a function of time from inoculation to *post-mortem*. 138

Figure 6-10: Predicted probability of active infection (blue) and progression (red) over time from inoculation to *post-mortem*, for combinations of age and inoculum dose, with confidence intervals (blue and red shading). All predicted probabilities were based on the ovine MAP strain (*model 1*) and tissue homogenate inoculum. 141

Figure 6-11: Estimated probability of progression upon infection (χ) as a function of inoculum dose for sheep less than one year old (left) and older sheep (right) showing data-driven predictions (obtained from *model 1* and *model 2*, in blue) and simulated (red) data. 142

Figure 6-12: Illustration of the effect of smoothing on the curves and the appearance and position of the “main peak” 145

Figure 6-13: Parametric survival results (exponential distribution) for exit of transient shedding in sheep inoculated with MAP for various covariate patterns 146

Figure 7-1: Modelled age compartment sizes of management groups (/100 lambing ewes), transitions between production groups, reproductive periods and timing of management events in a typical North Island hill country sheep flock. 168

Figure 7-2 : Transitions between mutually exclusive disease states for ovine paratuberculosis (transmission from the environment Env, *i.e.* the pasture). E represents Exposed sheep. P (progressor track) and N (non-progressor track) represent sub-clinical infection associated with early/mild disease, low shedding and no visible production

effects. A represents the (sub-clinically then clinically) Affected stage, experiencing production effects and high shedding. R represents a stage of Recovery from disease/shedding. Flock demographic parameters are not shown. Details of parameters and equations for transition between stages are given in Appendix C....172

Figure 7-3 Evaluation of the cost of OJD and of the cost effectiveness of vaccination over time, showing the evolution of annual farm gate profit after seeding MAP infection and after the onset of vaccination. This figure is for explanatory purposes only and benefits/costs are not discounted.177

Figure 7-4: Loss in revenue due to paratuberculosis in the flock, in NZD/year/100 ewes, for different levels of clinical incidence and different reference years for farm-gate prices.181

Figure 7-5: Simulation of Gudair™ trial conditions (Reddacliff et al., 2006) showing the effect of vaccine on the total number of OJD deaths in the flock (for 100 lambing ewes in the flock). Two possible vaccine effects were simulated (separately): a preventive vaccine effect (in blue) or a therapeutic effect (orange); the red dashed line represents onset of vaccination (whole flock).182

Figure 7-6: Cost-effectiveness of vaccination with varying levels of pre-vaccination OJD clinical incidence in the flock using present value (discounting rate 6%): a. cumulative benefit and cost of vaccination at equilibrium (30 years after vaccination start, for 100 ewes in the flock, with average meat prices), b. benefit-cost ratio of vaccination at equilibrium, c. time to return on investment (RoI) after onset of vaccination, d. time to break-even (B-E) after onset of vaccination.184

Figure 7-7: Effect of vaccination and purchase of ewes in a flock with high clinical incidence of OJD (1% in ewes pre-vaccination), in two different scenarios, describing (a.) MAP infection, (b.) OJD incidence level and (c.) cost-effectiveness of vaccination (using average market prices). The baseline scenario (in blue) was to purchase one uninfected ewe/100 ewes/year. The alternative scenario (in orange) was to purchase one infected ewe/100 ewes/year (in the P compartment) after the red dashed line.185

Figure 7-8: Effect of changing the replacement rate (RR) from 25 to 20% (in orange) or to 30% (in green) and vaccination (in blue) and in a flock with high clinical incidence of OJD (1% in ewes pre-intervention), describing (a.) MAP infection, (b.) OJD mortality and (c.) cumulative net profit of alternative strategy compared to the baseline (using average market prices). Crosses in plot c. represent combination of RR changes and

vaccination. These are not shown in plot a. and b. as they are blended with the blue curve. 186

Figure 7-9: Effect of pasture spelling (in green) and vaccination (in blue) or both (in orange) in a flock with high clinical incidence of OJD (1% in ewes pre-intervention), describing (a.) MAP infection and (b.) OJD mortality. 187

Figure 7-10: effect of contact rate C (proportion of MAP in pasture that is ingested by sheep through grazing) on the disease dynamics. 188

List of Tables

Table 1-1: Herd/flock true prevalence of MAP infection, based on faecal culture or ELISA positivity at the herd/flock level, proportion of positive herds/flocks with clinical paratuberculosis, and reported annual incidence, from (Verdugo et al., 2014a) and Verdugo (2013)	3
Table 2-1: Definitions of social network terms used in this study.....	14
Table 2-2: Total number of livestock movements between farms and number of animals of each species moved (in parentheses) in four years.....	21
Table 2-3 : Similarity between years 1 to 4 for the top 10% ranked LC farms according to one measure of the degree.....	23
Table 2-4 : Impact of the correlation between in- and out-degree in the LC farm network on R_0 , the estimated potential initial spread of epidemics in year 2009-2010.....	26
Table 2-5 : Size of the giant strong component (GSC) and giant weak component (GWC) in the network, during the fourth year of the study period	26
Table 3-1: Odds ratio (OR) and p-value obtained using MR-QAP for the association between MAP molecular similarity on farm (farms harbouring common VNTR/SSR strains) and the directed (dSPL) or undirected (uSPL) shortest path length between farms, or belonging to the same network community.	50
Table 4-1: Summary of field PTB outcomes from natural challenge experiments and heavily infected commercial flocks	85
Table 6-1: reference list for the 38 experiments included in the meta-analysis (n=767 sheep) with details of the experimental protocol	130
Table 6-2: frequency of different pathological outcomes for 767 sheep experimentally infected with MAP (all datasets combined).....	133
Table 6-3: correspondence between different pathological outcomes measured at the time of <i>post-mortem</i> , for the subset of sheep for which it was possible to establish the individual correspondence between different outcomes from the data.	133
Table 6-4: results of the parametric part of <i>model 1</i> (presence/absence of histological lesions at <i>post-mortem</i>).....	136

Table 6-5: results of the parametric part of <i>model 2</i> (presence/absence of markers of progression at <i>post-mortem</i>)	140
Table 6-6: results of the parametric part of the <i>model 3</i> for the presence of mild-moderate lesions at <i>post-mortem</i> (reference=no early lesions, ie. no specific lesions or severe lesions).....	143
Table 6-7: Results of the parametric part of <i>model 4</i> for the presence of severe lesions at <i>post-mortem</i> (reference=no severe lesions, i.e. no specific lesions or mild-moderate lesions)	144
Table 6-8: Results of <i>model 5</i> (parametric survival using the exponential distribution) for factors associated with the duration of transient shedding in sheep classified as non-progressors (Figure 6-1).	146
Table 7-1: Summary of experiments of survival of MAP organisms on pasture	170
Table 7-2: Parameters to evaluate the annual economic benefit of sheep farming (Romney type production, North Island farming system).	174
Table 7-3: Annual range of daily exposure to MAP from grazing for each age group, and the corresponding values taken by the plateau of infection, for an annual clinical incidence of OJD of 0.2% (NZ national average).....	180
Table 7-4: Total annual farm-gate profit (in NZD/100 ewes) for a self-replacing North Island Hill country Romney flock at baseline (no paratuberculosis).....	180
Table 7-5: Cumulative net profit, Benefit cost ratio, time to return on investment (RoI) and time to break-even (B-E) for different scenario of levels of clinical incidence and meat price scenario	185
Table 7-6: lamb crop, comparison between industry figures and outcomes from the model (in an OJD-free flock)	189
Table 7-7: Infection dynamics observed in the simulations (for various annual OJD levels and two age groups) compared to that of observational studies	189

Chapter 1. General Introduction

This thesis is a comprehensive study of the transmission dynamics and economic impact of *Mycobacterium avium* subsp. *paratuberculosis* infection, particularly in sheep, and presents a model that can be applied to the control of ovine paratuberculosis on New Zealand sheep farms. This model could be adapted to other pastoral sheep-farming systems.

1.1 Definitions

In the literature, paratuberculosis (PTB) is classically defined as a chronic granulomatous enteritis caused by infection of the intestinal tract with *Mycobacterium avium* subsp. *paratuberculosis* (MAP). In this thesis, more specific terminology is used to disambiguate the different terms related to the epidemiology and infection with MAP, as follows:

- **Paratuberculosis** is a generic term describing all aspects of epidemiology and infection with MAP. It encompasses asymptomatic (latent) infection, pathology and clinical disease caused by MAP.
- **Latent infection** with MAP refers to the presence of the organism in the host tissues, not associated with pathology or disease. It can be assessed by tissue culture or PCR of ileal tissue and mesenteric lymph nodes.
- **Active infection** caused by MAP refers to the presence of granulomatous inflammation in the small intestine, *i.e.* pathology, caused by the host immune response to MAP, whether subclinical or resulting in clinical disease.
- **Affected** by MAP refers to sheep presenting severe histological changes in the small intestine, altering the intestinal function and causing production effects. Effects due to MAP can range from subclinical to clinical.
- **Clinical disease** caused by MAP is a fatal wasting condition occurring in a minority of infected animals. Clinical paratuberculosis is also called Johne's disease (JD), the terms 'clinical PTB' and 'JD' being used interchangeably in this thesis.

Where the reference pertains specifically to sheep, we use the terms ovine paratuberculosis, and for clinical disease the term ovine Johne's disease (OJD).

1.2 Aetiology of paratuberculosis

The causative agent of paratuberculosis is *Mycobacterium avium* subsp. *paratuberculosis* (MAP) (Chiodini et al., 1984; Harris and Barletta, 2001). This is a gram-positive, acid-fast micro-organism that grows slowly *in vitro* and requires mycobactin in the culture media (Cocito et al., 1994). It can be differentiated from other micro-organisms of the *Mycobacterium avium* complex by molecular genetics, with the presence of 14 to 18 copies of the insertion sequence IS900 in its genome (Motiwala et al., 2006). The genetic variation within MAP subspecies can be assessed by various techniques, the classical one being restriction fragment length polymorphism (RFLP) using the IS900 sequence as a probe (Collins et al., 1990). Using this technique in the late 1980's, genetic diversity of isolates from New Zealand allowed differentiation of 29 strains, which mostly fell into 2 distinct groups. These were called cattle strains (C strain) and sheep strains (S strain) as they appeared to be host species-specific (Collins et al., 1990). At the time this observed segregation of strains from sheep and strains from cattle suggested a strain-host preference (Motiwala et al., 2006).

The relative difficulty to culture organisms from the S strain could favour the under-reporting of bovine infection with the S strain, although S strain isolates were identified from cattle in Australia and Iceland (Whittington et al., 2001). Apparent strain specificity could also partially be due to a lack of mixing opportunities between cattle and sheep strains (Motiwala et al., 2006). Further molecular work (Stevenson et al., 2002) identified genetic differences between pigmented isolates (corresponding to the "ovine" strain) and non-pigmented isolates (corresponding to the "cattle" strain). This latter paper introduced a new nomenclature to classify MAP strains based on phenotypic and genotypic characteristics. Strain type I corresponds to a group of organisms difficult to grow in culture and showing a strong host preference for sheep; strain type II corresponds to organisms easy to grow in culture, commonly isolated from cattle but also from a broad range of species including deer and sheep (Stevenson et al., 2002).

Recent molecular epidemiology studies in New Zealand demonstrated the absence of strain-species-specificity, with 86% of infected sheep flocks, 80% of infected beef herds and 10% of infected dairy herds infected with strains of type I (Verdugo et al., 2014b). The authors concluded that transmission of MAP between livestock species is frequent in the pastoral context of New Zealand where co-grazing is common.

1.3 Prevalence of MAP infection and incidence of clinical paratuberculosis

Johne's disease was first reported in New Zealand in 1912, in an imported Jersey cow in the North Island (de Lisle, 2002). It became well established in dairy herds in the Taranaki region over the next decade. Ovine JD was first reported in sheep in 1952 on a farm of the South Canterbury region and within a few years in 15 more properties in the same region (Gumbrell, 1986). The first reported case of ovine JD in the North Island was in Hawkes Bay in 1972, probably following introduction of sheep from the South Island. In deer, the first isolation of MAP was identified in 1985. The number of laboratory confirmed infections steadily increased subsequently, with 619 farmed deer culture positive in 299 herds (representing 6% of the national deer farm population) between 1986 and 2000 (de Lisle et al., 2003). Most of these were identified during routine abattoir surveillance for *M. bovis*. Hence, since the early 1900's, MAP infection in New Zealand spread throughout all livestock industries and all regions.

The first comprehensive nation-wide farm-level prevalence study in New Zealand was conducted in 2009 in deer, beef and sheep farms, showing that paratuberculosis was endemic in all livestock species (Verdugo et al., 2014a). However, clinical manifestations of paratuberculosis were rare, except in dairy. Laboratory or veterinary confirmed clinical cases of OJD were reported from 5.4% of randomly selected surveyed flocks (Verdugo, 2013) although farmer diagnosis indicated that 55% of flocks that tested positive had cases of clinical paratuberculosis. Based on farmer diagnosis, the mean annual clinical incidence was estimated at 0.16% among test positive flocks. A summary of farm-level paratuberculosis in New Zealand is given in Table 1-1.

Table 1-1: Herd/flock true prevalence of MAP infection, based on faecal culture or ELISA positivity at the herd/flock level, proportion of positive herds/flocks with clinical paratuberculosis, and reported annual incidence, from (Verdugo et al., 2014a) and Verdugo (2013)

	True prevalence of infection at herd/flock level [95% probability interval]	% of positive herd/flocks reporting clinical cases	Reported annual clinical incidence in positive herds/flocks [95% confidence interval]
sheep	76% [70-81%]	54%	0.16% [0.09-0.24%]
beef	42% [35-50%]	24%	0.04% [0.01-0.08%]
deer	46% [38-55%]	55%	0.32% [0.05-0.6%]

1.4 Production effects of paratuberculosis in sheep in New Zealand

The economic burden of paratuberculosis on farm can be due to both clinical disease and subclinical losses of production (Gonda et al., 2007). Losses due to clinical JD are more obvious and readily identifiable as illness and mortality. Sub-clinical losses are difficult to estimate, primarily because sub-clinically affected animals are a challenge to detect.

A review of economic losses due to paratuberculosis in dairy cattle identified direct versus indirect losses (Hasonova and Pavlik, 2006). Direct losses can be due to JD mortality, reduced milk yield or growth rates, impaired reproduction, decrease in productive life-time and increased susceptibility to other diseases. Indirect losses can be due to loss in genetic value of culled animals, loss of breeding animals prematurely culled, increased cost of replacement, cost of diagnostic tests and other veterinary costs related to JD, and eventually costs of control programs or trade restrictions (Hasonova and Pavlik, 2006). However, while these are plausible causes of loss, there is limited evidence quantifying most of these losses in most species.

1.4.1 Production effects associated with clinical paratuberculosis

To assess the production effect of clinical paratuberculosis in New Zealand sheep breeds, a longitudinal study was performed over 8 birth cohorts between 1971 and 1978 on one sheep station heavily impacted with paratuberculosis (Morris et al., 2006). The incidence of clinical paratuberculosis was closely monitored in naturally infected adult ewes in pure Merino, Merino crosses and Romney breeds. The diagnosis of paratuberculosis was confirmed in clinically affected ewes by histopathology and tissues from all clinically “normal” culled ewes also underwent histopathology. The overall annual clinical incidence in mated ewes was 1%, being 0.9% in Romney and 1.2% in Merino/Merino-crosses (significantly different between Romney and Merino). The analysis showed a significantly lower pre-mating live weight, between 0.8 to 9.5 kg/ewe depending on the age of the ewe (on average 3.46), for clinical cases in their final year of production compared with clinically normal ewes in the flock. Individual reproductive performance was also significantly lower in clinically affected ewes compared with clinically normal ewes in the same flock, with 13% fewer lambs born and the total weight of weaned lambs 46% lower over the lifetime of a ewe. These production losses were for clinically affected animals in one heavily infected flock. Therefore it is hard to

generalize to all flocks in New Zealand, given the diversity of management systems, infection pressure, environment and sheep genetics. Nevertheless, it demonstrates potentially significant production effects associated with clinical paratuberculosis. Despite the lack of external validity, it provides plausible estimates for the possible extent of these production effects in a flock with 1% clinical incidence of OJD.

In sheep, a breed effect was also reported, whereupon Merino appear more likely to express clinical disease than Romney or other British breeds, both at the flock (Lugton, 2004) and at the individual levels (Morris et al., 2006).

1.4.2 Production effects associated with subclinical paratuberculosis

Production effects associated with subclinical disease, which are more difficult to establish, were partially addressed in a vaccine trial by Thompson et al. (2002). Two commercial farms with confirmed OJD, on which it was “considered to be a problem”, were recruited: one crossbred and one pure Merino. On each farm one cohort of replacement ewe lambs was randomly allocated to vaccinated (either Gudair™ or Neoparasec™ vaccine) and control groups. The aim was to evaluate potential subclinical effects due to paratuberculosis by comparing vaccinated and control over time, assuming vaccination was effective in “suppressing or minimizing” those effects. After 3.5 years, “no consistent differences” in productivity between control and vaccinated could be detected (body weight, fleece weight, reproductive performances). The only statistically significant effects of vaccination with Gudair™ were reported as “slightly” lower body weight at the final weighing and “slightly” lower fleece weights at the first shearing in vaccinated animals on one of the two properties. Given that 1657 animals were enrolled, the power of the analysis was probably enough to detect a biologically significant production difference should such a difference exist. However, that vaccinated and control sheep were run together might have biased the estimated effect towards the null, or alternatively the results could be attributed to lack of efficiency of the vaccine to protect against subclinical disease. A randomized clinical trial with replication, involving a representative sample of flocks, would allow a more robust evaluation of subclinical as well as clinical effects of ovine PTB.

To measure the impact of paratuberculosis in the national population of farms rather than at the individual level, a national cross-sectional study was conducted in 2009 (Verdugo, 2013). One hundred-and-sixty-two sheep flocks were included and data about productivity were

collected by mail survey. The study design and number of flocks allowed robust estimates of average national production effects, unlikely to be biased by farm-level confounding factors, although recall biases might be present. The number of tailed lambs in flocks with history of OJD was significantly lower by 20%, compared to uninfected flocks. Additionally, culling rate in MAP test positive flocks with no history of OJD was substantially lower than that of uninfected flocks (11.5% versus 15.5%). The latter effect was non-plausible and likely spurious, hence non-causal.

1.4.3 Production effects and economic losses at the industry level

In the 1980's, OJD was the main laboratory-diagnosed cause of ill-thrift or diarrhoea in adult sheep in New Zealand, with 23% of cases of ill-thrift or diarrhoea confirmed as OJD (Gumbrell, 1986). However, the effects of clinical disease on farm production were believed to be limited (Gumbrell, 1986).

In a report about the economics of control strategies for paratuberculosis in all livestock industries in New Zealand (Brett, 1998), the cost of clinical disease was estimated across all industries as NZD 30 million (most likely) or NZD 57 million (worst-case scenario). The economic burden attributed to paratuberculosis was thus considered small "relative to the value of the industries". These estimates are now nearly two decades old. They were based on scarce evidence, biased by the poor performance of diagnostic tests to detect infection, and under-reporting of the disease. Subclinical production effects were overlooked.

1.5 Justification for this thesis

MAP infection is endemic in all livestock species in New Zealand, and an estimated 76% of sheep flocks are infected (Verdugo et al., 2014a). Infection with -and mixing of- MAP strains occurs between species within farms, associated with co-grazing (Verdugo et al., 2014a). However, the dynamics of MAP transmission from farm-to-farm has not been studied so far.

The economic impact of PTB in New Zealand remains poorly understood, but has been associated with production limiting effects in all affected livestock species (Morris et al., 2006; Hunnam et al., 2009; Lombard, 2011). The industry-wide average clinical incidence in sheep is estimated to be below 0.2%, with a maximum reported within-flock annual OJD mortality of around 3% (Verdugo, 2013). For the higher incidence farms, tailored control of paratuberculosis would be desirable. There is little data to inform which control strategies

might be most biologically effective in specific circumstances, or the incidence level at which control strategies may be economic.

However, given that the overall impact upon the sheep industry is limited, it is difficult to justify expensive field epidemiological or controlled studies evaluating methods of control. Alternative methods may be more appropriate. In this context, simulation modelling is an appropriate means of assessing biologically effective and economically viable control measures. There is a plethora of simulation models for bovine paratuberculosis, but there is a scarcity of models for ovine paratuberculosis in a pastoral environment. A modelling approach would enable bringing together within-flock dynamics of paratuberculosis and the impact of multiple re-introductions of MAP via sheep movements between farms. It would inform on-farm control strategies for OJD and contribute to better characterize the population of farms in New Zealand that would benefit from vaccination against OJD.

1.6 Thesis aim and objectives

This thesis was aimed at enhancing knowledge about the epidemiology and control of paratuberculosis in the New Zealand context, with a primary focus on sheep.

The objectives were:

- To use network analysis to evaluate the effect of livestock movements between farms as a risk factor for infection with MAP using data on infection *per se*, and strain type.
- To review literature on patho-physiology of MAP infection in sheep and MAP quantification methods used in experimental studies, with the purpose of informing the development of a simulation model for ovine PTB.
- To perform a meta-analysis of the pathobiology of MAP infection in sheep with the dual purpose of (1) testing assumptions generated in the literature review, (2) estimating parameters for the ovine PTB model.
- To develop a simulation model with the purpose of evaluating the biological and economic effectiveness of vaccination for ovine PTB on New Zealand pastoral farms

1.7 Thesis outline

Chapter 2 describes and analyses, using social network analysis, the pattern of livestock movement in a nation-wide commercial livestock enterprise of 112 farms in New Zealand. The objective was to identify specific features that might favour the spread of infectious diseases.

Risk-based strategies of movement controls were tested to inform targeted control measures to mitigate this risk.

While Chapter 2 addressed pathogen spread in the network in general, Chapter 3 applied the network analysis approach to assess the specific risk of MAP transmission via livestock movements, in the New Zealand context. The same movement data as in Chapter 2 were used. They were combined with two layers of farm-level MAP data: MAP infection status *per se*, complemented by strain typing of MAP isolated from those farms. Novel methodology of multivariate matrices correlations was used to investigate associations between cross-sectional strain type distribution on farm and past livestock movements. Associations between strain type sharing and species on farm, and Euclidian distance between farms and island, were also evaluated.

Chapter 4 reviewed the current understanding of patho-physiology of ovine PTB. The review was used to synthesise information and generate assumptions about within-host MAP infection dynamics, thus informing the development of a mathematical model. Consequently, Chapter 5 reviewed methods of enumeration of MAP *in vitro* to assess possible biases in the estimation of inoculum dose and dose effects in experimental challenge models of ovine PTB.

The review process aforementioned highlighted methodological difficulties for robust parameters estimation and the need to carry a systematic review and meta-analysis of experimental infection with MAP, presented in Chapter 6. The meta-analysis was used to quantitatively estimate important parameters for the model of ovine paratuberculosis presented in Chapter 7. A secondary objective was to test hypotheses generated in Chapter 4 and 5, in particular the effect of age at exposure, dose ingested, strain type, sheep breed and inoculum type on the outcome of experimental infection with MAP.

Chapter 7 then incorporated the findings of previous chapters in a simulation model of ovine paratuberculosis in a pastoral sheep farm typical of New Zealand. Conclusions were drawn about infection dynamics of MAP in a hypothetical New Zealand Romney sheep flock, the cost of ovine paratuberculosis associated with different levels of clinical incidence, effectiveness and cost-effectiveness of vaccination and the impact of trade.

The thesis concludes with a General Discussion that brings together findings about paratuberculosis transmission unravelled in this thesis. It also provides an opportunity to critique the methods used and outcomes, and to highlight the contribution of this thesis to a

wider perspective of disease control in animal populations. It concludes with a series of suggestions for future research.

1.8 Declaration

Each research chapter was written as a manuscript intended for publication in a refereed journal, hence some repetitions of background information occur throughout the thesis. Chapter 2 and Chapter 3 have been published in Preventive Veterinary Medicine. Chapter 4, 5 and 6 are intended for submission in Veterinary Research and Chapter 7 and 8 in Preventive Veterinary Medicine or PLoS ONE.

Chapter 2. Using social network analysis to inform disease control interventions

Nelly Marquetoux^a, Mark Stevenson^b, Peter Wilson^c, Anne Ridler^c, Cord Heuer^a

^a *EpiCentre, Institute of Veterinary, Animal and Biomedical Sciences, Massey University, New Zealand*

^b *Faculty of Veterinary and Agricultural Sciences, The University of Melbourne, Werribee, Victoria, Australia*

^c *Institute of Veterinary, Animal and Biomedical Sciences, Massey University, New Zealand*

2.1 Abstract

Contact patterns between individuals are an important determinant for the spread of infectious diseases in populations. Social network analysis (SNA) describes contact patterns and thus indicates how infectious pathogens may be transmitted. Here we explore network characteristics that may inform the development of disease control programmes.

This study applies SNA methods to describe a livestock movement network of 180 farms in New Zealand from 2006 to 2010. We found that the number of contacts was overall consistent from year to year, while the choice of trading partners tended to vary. This livestock movement network illustrated that a small number of farms central to the network played a potentially dominant role for the spread of infection in this population. However, fragmentation of the network could easily be achieved by “removing” a small proportion of farms serving as bridges between otherwise isolated clusters, thus decreasing the probability of large epidemics.

This is the first example of a comprehensive analysis of pastoral livestock movements in New Zealand. We conclude that, for our system, recording and exploiting livestock movements can contribute towards risk-based control strategies to prevent and monitor the introduction and the spread of infectious diseases in animal populations.

Key words: network analysis; livestock movements; epidemiology; infectious diseases dynamics; basic reproduction ratio; control strategies

2.2 Introduction

Movement of livestock between farms or markets is a strong determinant of spread of transmissible pathogens in animal populations (Keeling and Eames, 2005; House and Keeling, 2011). Detailed knowledge about movement of livestock can be a useful tool to inform strategies to control the spread of contagious pathogens. A classic example is provided by the foot-and-mouth disease (FMD) epidemics of 2001 in the UK. A few long-range movements, mostly via markets and dealers, spread the infection widely at an early stage (Kao, 2002; Shirley and Rushton, 2005; Kao et al., 2006). Consequently, more stringent and accurate livestock tracing systems, in addition to mandatory movement restrictions, were implemented in the UK (Vernon, 2011). Analysis of animal movement can also provide a useful framework to study the spread of endemic diseases and has been extensively used for tuberculosis, both in cattle populations (Gilbert et al., 2005; Woolhouse et al., 2005) and wildlife (Corner et al., 2003; Porphyre et al., 2008; Drewe et al., 2011).

Landcorp Farming Limited (LC) is a state-owned enterprise, comprised of 122 farms¹ located throughout New Zealand, representing the regional variety of farm types of the country's pastoral livestock industry. New Zealand farming is characterised by all-year pastoral farming in which pasture availability drives the annual production cycle and different livestock species are often co-grazed on the same pasture. LC farms are typical of this farming system and most LC farms host multiple livestock species (cattle, sheep and/or deer – mostly red deer). LC keeps detailed records of the shipments of livestock off and onto their farms. Most movements occur between LC farms with a small proportion of movements to non-LC farming enterprises. The movement records of LC were unique in New Zealand, in that they provided a complete set of movement events over several years within a corporate group of farms representing a relatively closed population. We propose that this information could be used to provide some insight into factors that are potentially influential in disease spread. A better understanding of these factors is a necessary first step in development of rational interventions to limit disease spread.

In this study we analysed the contact pattern arising from movements of sheep, cattle and deer to and from LC farms from 2006 to 2010. Our aim was to use social network analysis (SNA) to describe the trading pattern of LC farms and to understand how contact through

¹ 122 farms as per 2012, this number is subject to annual changes and increased to 137 in 2014. The number of different LC properties involved in the network analysis is 112.

trading might influence the spread of infectious diseases. A preliminary step was to assess the consistency of network characteristics over time, and a sequel was to discuss the effect of targeted control measures with respect to various aspects of disease spread in this particular network. This analysis will help to prioritise the allocation of resources to enhance biosecurity in this network of farms.

2.3 Material and methods

Definitions of the technical terms related to SNA used in this paper are provided in Table 2-1.

Table 2-1: Definitions of social network terms used in this study.

Parameter	Definition
General terms:	
Directed path	The pathway between nodes (farms) accounting for the direction of the contacts (<i>i.e.</i> livestock movements). A movement from nodes A to B or a movement from nodes B to A thus defines two different pathways.
Undirected path	The pathway between nodes (farms) ignoring the direction of the contacts. A movement from nodes A to B or a movement from nodes B to A thus defines the same pathway.
Neighbour	The k -nearest neighbours of a node i are all nodes that are within k steps of node i . The set of adjacent nodes defines the neighbourhood of node i . In graph theory, adjacency is defined according to the edges of the network, not according to spatial distance.
Measures of centrality:	
In-, out-degree	The number of contacts to or from a node (farm), respectively, during a defined period. In-degree is potentially positively correlated with the probability of introduction of infectious agents. Out-degree is potentially positively correlated with the probability of spreading infection.
Weighted in-, out-degree	The weighted in- and out-degree were defined as the total number of animals (as opposed to the total number of contacts) received or sent by a farm, respectively, during a defined period.
Measures of cohesion:	
Clustering coefficient	Clustering coefficient (CC) can be either a local or a global network attribute. In this study CC is expressed as a global measure, corresponding to the probability that any two nodes j and k are connected to a node i and nodes j and k are in turn connected to each other (Kiss et al., 2006). As a global measure CC quantifies 'cliquishness' within the network (Watts and Strogatz, 1998).
Strongly connected component	The section of a network where any node could be reached from any other node by following the direction of existing paths (Christley et al., 2005).
Weakly connected component	The section of a network where all nodes are linked to each other irrespective of the direction of the path (Christley et al., 2005).

2.3.1 Movement data

The data available for analysis included all livestock movement records to and from the properties of LC for the period 1 July 2006 to 30 June 2010 (inclusive). LC farms primarily exchange livestock within the company, but some movements also involved properties outside LC. Livestock classes involved in the movements were dairy cattle, beef cattle, sheep and deer. Two types of movements were recorded. A transfer was defined as the *permanent movement* of livestock from one property to another (equivalent to a sale). The format for a transfer was an annual summary record: for every pair of farms between which livestock transfers occurred in a given year, there was one summary record for each species moved corresponding to the sum of all the annual transfers for this species. Agistments were defined as *temporary movements* of livestock (equivalent to a lease). These occurred when animals were sent from one LC property to another -or to a property outside LC- for a limited period for grazing management, followed by another agistment movement record back to the property of origin. Detailed data for agistments were available, thus each agistment corresponded to an actual shipment of animals including the date on which the movement event occurred.

The LC movement database contained: the source and destination property; the type of movement (transfer or agistment); the date (year for transfers, calendar date for agistments); the species involved: sheep, beef, dairy or deer; and the total number of animals of each species moved in one year for transfers, or the actual batch size for agistment events.

Using these data, we constructed yearly networks consisting of all recorded livestock movements within the LC enterprise from the 01st July to the 30th of June and we described the contact pattern in terms of consistency over time, size, centrality measures and cohesion (see Table 2-1). We finally analyzed the characteristics of this contact pattern that were believed to be a key for disease transmission.

2.3.2 Data analysis

The consistency of farm movement events was evaluated across successive years. All subsequent analyses were carried out using data for the year 2009-2010 only, as movement records were most complete for this year. The recorded data represented a census of the movements to/from the LC farms. However, some non-LC farms traded with LC farms, thus acting as satellites of this network. For these commercial farms, only the movements to/from LC farms were known while movements to/from other commercial farms were not included in the data. To avoid biases, all the movements were used to calculate farm-level network

properties (such as degree or betweenness) but only measures for the LC farms were reported. Similarly, network-level statistics (degree distribution, standard deviation and average degree, degree correlations and effect of targeted control) were calculated using only the LC farms. Since the non-LC farms contributed to the overall connectivity, they were kept to calculate measures of network cohesion. The analyses were performed using the software package Pajek for SNA (Batagelj and Mrvar), and the *igraph* package (Csárdi, 2006) within R (R Development Core Team, 2014). Networks were plotted using Gephi (Bastian et al., 2009).

2.3.2.1 Consistency of the contact pattern over time

Networks are dynamic structures, therefore evaluating the consistency (or the lack of it) of global and individual network properties can reveal important evolutions in the network topology (Kossinets and Watts, 2006; Robinson et al., 2007). Year to year consistency was first assessed in terms of the number of contacts of each type (transfers and agistments). In addition, we analysed the consistency of the pair-wise relationships between farms. To do this, we identified each unique pair of farms (two farms with at least one movement occurring between them) and how many years this link existed between 2006 and 2010.

To assess the consistency over the years of the identity of the more central farms in the network, according to different centrality measures, farms were ranked by their in- or out-degree (weighted or not) and their betweenness for each of the four years. The top 10% farms (or ‘hubs’) according to each centrality measure were then identified for each year (*i.e.* the 12 top farms in each year). We then calculated the proportion of farms among those 48 top farms that were present at least three years out of four. This proportion was called a similarity index and was used to compare how similar across years the hub farms were, according to different centrality measures. In addition, we computed the probability of the estimated similarity index if the rank of the farms followed a random order using a Fisher test (corresponding to a p-value).

2.3.2.2 Description of the degree distribution

A common feature of many real-world networks is the heterogeneity in patterns of contact (Barabási and Albert, 1999; Albert and Barabasi, 2002), whereupon small numbers of nodes are highly connected whereas most other nodes in the network have relatively few connections. Heterogeneity in the number of contacts can have a strong influence on the spread and persistence of an infectious disease (Hethcote, 1978) and infection can spread more readily via hub nodes. It is therefore important to examine the distribution of the number of contacts per node to determine where the heterogeneity lies, between the

assumption of homogenous mixing and that of pure scale-free connectivity, when the degree distribution follows a power law (Bansal et al., 2007).

We used standard statistical methods combining maximum-likelihood (ML) and goodness-of-fit (GOF) tests to fit a parametric probability distribution to the degree distribution data (number of contacts per farm) for the 107 LC farms involved in the network in 2009-10.

We assessed the observed data for consistency with the power law distribution. The guidelines described by Clauset et al. (2009) provided the framework, while the implementation was carried using the functions `plfit` and `plpva`². The `plfit` function computes a ML estimate for the power-law exponent and determines the best cut-off value for a power-law tail in the observed distribution with a Kolmogorov-Smirnov GOF test. The `plpva` function then computes a p-value to test the plausibility of a power-law fit for the observed data, by comparing the observed GOF test to that obtained with n random samples from a true power-law distribution. Hence a high p-value indicates that a large proportion of the power-law samples fluctuates “further away” from the model than the observed data, which is unlikely to occur by chance and indicates that the power-law model fit is a plausible for this data (Clauset et al., 2009). The `plpva` function allowed adjustment for finite-size bias (small sample size) and the p-value for the power law tail was computed over 1000 non-parametric repetitions of the fitting procedure.

When attempting to fit a power-law to a distribution, it is good practice to check if the data could also be fitted with other skewed distributions (Clauset et al., 2009). The package *fitdistrplus* implemented within R (Delignette-Muller and Dutang, 2015) was used to assess the best fit from the following empirical distributions: gamma, Weibull, exponential and lognormal.

2.3.2.3 Small-world properties of the network and overall connectivity

Many networks found in nature, unlike random networks, are highly structured and display strong clustering (or clique behaviour), meaning that two connected nodes are likely to share social ties with a common third node, forming a triangle of inter-connected nodes. This property is referred to as ‘small-world’ (Watts and Strogatz, 1998). The tendency to form social (or regional) groups with more contacts within than between tends to enhance transmission within clusters, making it more difficult for pathogens to overcome local structures and spread

²available on the webpage <http://tuvalu.santafe.edu/~aaronc/powerlaws/>

globally. This can result in smaller effective reproduction rates and smaller final epidemic (Keeling, 1999; Cross et al., 2005). However, the presence of a few long-range connections via hub-nodes, acting like short-cuts between communities, can result in a fast dissemination of pathogens through all parts of the network and increase the likelihood of rapid disease spread (Keeling and Eames, 2005).

We assessed the small-world properties of the network of LC farms in 2009-2010 by calculating the average path length between connected LC farms and the clustering coefficient and by comparing these values with those obtained from 10000 simulated random Erdos-Renyi network of the same size (Watts and Strogatz, 1998). We assessed the overall connectivity of the network by determining the size of the largest or 'giant' weakly connected component (GWCC) and of the largest, giant strongly connected component (GSCC).

2.3.2.4 Effect of network properties on the basic reproduction number (R_0)

At the farm level, the basic reproduction rate (R_0) is the expected number of farms infected by a first infected farm during its infectious period in a fully susceptible, homogenous population at equilibrium (Anderson and May, 1979; Diekmann et al., 1990). In homogenous mixing populations, $R_0 > 1$ classically represents the threshold for pathogen invasion (Diekmann et al., 1990; Anderson and May, 1991). Heterogeneity in the contact pattern may enhance the transmission of infection throughout a network (Pastor-Satorras and Vespignani, 2001); however, this partly depends on the correlation between in- and out-degree (Woolhouse et al., 2005; Kiss et al., 2006). In the absence of correlations between the in-degree and the out-degree in a directed network, the heterogeneous structure of the contact pattern (that is, the presence of hubs) is unlikely to have an effect on the value of R_0 (Woolhouse et al., 2005). A positive correlation between in-degree and out-degree increases the value of R_0 at a given infectious rate of a pathogen whereas a negative correlation decreases it (Woolhouse et al., 2005; Bansal et al., 2007). These network properties should be accounted-for in calculations of R_0 .

We used the method of Volkova et al. (2010) to estimate the basic reproduction number for the network, taking into account the variance and covariance in contact rates, as follows:

$$R_{0(network)} = \rho_0 \times \sqrt{(m_{in} \times m_{out}) + (SD_{in} \times SD_{out} \times r_{in-out})} \quad \text{Equation 1}$$

In Equation 1 ρ_0 is an unknown constant depending on pathogen specific virulence characteristics, such as the probability of infection given contact or the duration of the infectious period; m_{in} (m_{out}) is the average in-degree (resp. out-degree), SD_{in} (SD_{out}) is the standard deviation of the in-degree (resp. out-degree) distribution and r_{in-out} is the Pearson correlation coefficient between the in- and the out-degree. The in- and out-degree were calculated using all the movements since they represented a census of LC movements; however, the mean, standard deviation and correlations were calculated after removing the non-LC farms for which degree calculations were biased (but keeping the edges between those and the LC farms). By using the Pearson correlation coefficient in this equation, the assumption was that only the linear part of the correlations had an impact on disease spread. In a homogenous-mixing population of farms, there would be no variability in the contact rate between farms; hence the standard deviations would be zero. In this case, according to Equation 1, the expression for R_0 reduces to:

$$R_0 (homogenous) = \rho_0 \times \sqrt{(m_{in} \times m_{out})} \quad \text{Equation 2}$$

It is noteworthy that by aggregating farm contacts in a static yearly network, our approach would more adequately address chronic diseases, while overestimating the transmission of infections such as FMD. Nonetheless the principle of this analysis was not specific to any given pathogen, hence we were not interested in the absolute value of R_0 *per se*, rather in the relative increase that could be attributed to the presence of highly connected farms. Thus, we assumed that ρ_0 was constant and calculated a relative value defined as $R_{0(network)}/R_{0(homogenous)}$, to evaluate the multiplicative impact of heterogeneity and correlations in the contact pattern in 2009-2010 on the value of R_0 (Volkova et al., 2010).

2.3.2.5 Efficacy of targeted control strategies to disrupt the transmission via livestock movements

The farms potentially playing a key role in the transmission of infectious agents via livestock movements could be of two kinds:

- Farms with high degree: high degree farms are more likely to exchange livestock with a number of different trading partners. They therefore could be more at risk of becoming infected and/or to pass the infection on;
- Farms with high betweenness; high betweenness farms act as links between inter-connected cliques, acting as short-cuts and resulting in a ‘small-world’, highly navigable

network. This can favour epidemics of large size involving most nodes in the network, due to percolation behaviour in connectivity.

We first wanted to explore whether a highly connected farm was also more likely to control the flow between clusters of inter-connected farms. We therefore examined the correlation between total degree and betweenness for the LC farms.

Next, we simulated a targeted ban of movements to/from the farms within the LC network. The list of all the 107 LC farm identifiers involved in the network in 2009-10 was sorted in descending order of total degree. One-hundred-and-six simulations ($n-1$) were then carried out wherein for each simulation the LC farm with the highest total degree was removed from the network, simulating a movement ban to/from this farm. The effect of farm removal was then quantified in terms of: (1) the size of the remaining largest GSCC (which provided an estimate of the lower bound of potential final epidemic size); and (2) $R_{0(\text{reduced network})}/R_{0(\text{full network})}$, where the reduced network was the result of a targeted farm removal. Farm removal was cumulative: once removed a farm was not eligible anymore and the next highest-degree farm was determined in the next step. The value of R_0 at each step, called $R_{0(\text{reduced network})}$, was calculated using Equation 1 (with average in- and out-degree being calculated after excluding the non-LC farms for which the complete set of movements was unknown, to avoid bias). $R_{0(\text{reduced network})}/R_{0(\text{full network})}$ represented the proportion of the contribution of the movement pattern to R_0 after the movement ban for a given number of target farms. A second set of simulations were then carried out where farm removal was on the basis of betweenness (instead of total degree).

To evaluate the specific effect of a targeted control of movements towards key-farms, we compared these results with those obtained with a simulated ban of movements to/from randomly chosen farms. To do this we simulated the removal of farms in 100 randomly generated orders and computed the size of the largest GSCC and $R_{0(\text{reduced network})}/R_{0(\text{full network})}$ on each occasion. The mean and 95% quantiles for both quantities were then calculated, representing the effect of a random ban of movements on the potential of disease spread throughout the network.

2.4 Results

During the four-year study period there were 3,531 movement events, involving a total of 180 farms (112 LC farms and 68 non-LC farms in total). Most movements occurred between LC farms; 312 (9%) occurred between a LC farm and a farm outside LC.

2.4.1 Consistency of the contact pattern over time

The frequency of movements of each type (transfers and agistments) or each species was consistent over the first 3 years of the study period. In year 4 (2009-2010) the total number of movements increased by a factor of 1.8 from the value recorded for 2008-2009 (see Table 2-2). The change was due to an increase in the number of recorded agistments (temporary movements), particularly for dairy cows for which it was common practice to graze and mate heifers outside the property of origin before the first calving. This apparent increase in the frequency of agistments in the final year was due to a change in LC's recording policy: unlike transfers, most agistments were not accurately recorded before 2009. The pattern of transfers was consistent throughout the observation period. The data for 2009-2010 were therefore considered to be the most complete and robust of the LC network dataset. During 2009-2010, the average distance travelled by livestock in this network was 150 kilometres (median: 71 kilometres, range: 0.8 to 1091 kilometres).

Table 2-2: Total number of livestock movements between farms and number of animals of each species moved (in parentheses) in four years.

	Agistments	Transfers	Total contacts	Sheep	Beef	Deer	Dairy
2006/7	62	708	770	266 (214,295)	258 (23,414)	49 (15,076)	197 (17,147)
2007/8	45	719	764	282 (232,422)	232 (24,052)	52 (17,767)	198 (19,860)
2008/9	30	682	712	234 (201,555)	216 (24,125)	55 (13,724)	207 (24,159)
2009/10	586	699	1285	310 (216,689)	261 (25,544)	62 (15,457)	652 (63,660)
Total years	723	2808	3531	1092 (864,961)	967 (97,135)	218 (62,024)	1254 (124,826)

pairs only connected between 2006 and 2009
 pairs also connected in 2009–10

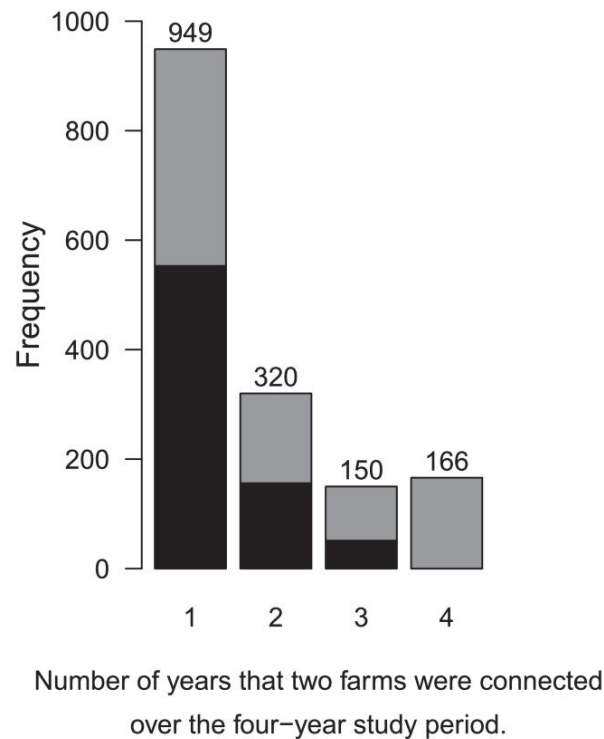


Figure 2-1 : Frequency of pairs of farms being connected in only one year or repeatedly in multiple years (2006 – 2010).

The frequency with which a pair of farms was found to be connected throughout the study period (from one year only, to all four years) is shown in Figure 2-1. Only 20% of the directed movements connecting two farms were repeated in at least three years out of four between 2006 and 2010, while 60% of the pairs occurred only once. This low frequency of pairs consistently trading with each other over the years was not due to the lack of reporting of some movements before 2009, as indicated by the stratification by 2006-2009 and 2009-2010 (Figure 2-1). This shows that trading partners tended to vary from one year to the next in the network of LC farms, based on the 4 years of data available for analysis.

Farms with the highest centrality scores in a given year tended to have similar scores in subsequent years (Table 2-3), with 48 to 71% of farms being among the top 10% highest degree farms in at least three years during the study period. For betweenness centrality however, only 40% of the farms were consistent hubs.

Table 2-3 : Similarity between years 1 to 4 for the top 10% ranked LC farms according to one measure of the degree

Outcome	Similarity % ^a	<i>p</i> -value
In-degree	48% (23/48)	<i>p</i> < 0.0001
Out-degree	65% (31/48)	<i>p</i> < 0.0001
In-degree (weighted)	71% (34/48)	<i>p</i> < 0.0001
Out-degree (weighted)	63% (30/48)	<i>p</i> < 0.0001
Betweenness	40% (19/48)	<i>p</i> < 0.01

^a Percentage of LC farms that are present at least 3 years out of the four-year study period among the 10% highest ranked, according to different centrality measures

2.4.2 Description of the degree distribution

The methodology proposed by Clauset et al. (2009) was used to assess the presence of a power law tail for the degree distribution. For the total degree distribution the best cut-off for a power law tail in the empirical distribution was more than 19 contacts per farm, and the exponent of the power law was $\gamma=3.09$. The GOF test for the tail of the distribution (>19 contacts per farm) indicated that the power law was a plausible fit for these data (*p*-value=0.854). With only 50 observations above 19 contacts/farm, the power to reject the assumption of a power-law fit was limited; nevertheless, the high *p*-value indicated that there was no evidence for lack of fit. Similarly, a power law fit could not be ruled out for the tail of the distribution of in-degree ($x_{min}=8$, $\gamma=2.62$, $n=47$ observations, *p*-value=0.22) or for out-degree ($x_{min}=11$, $\gamma=2.87$, $n=39$ observations, *p*-value=0.4).

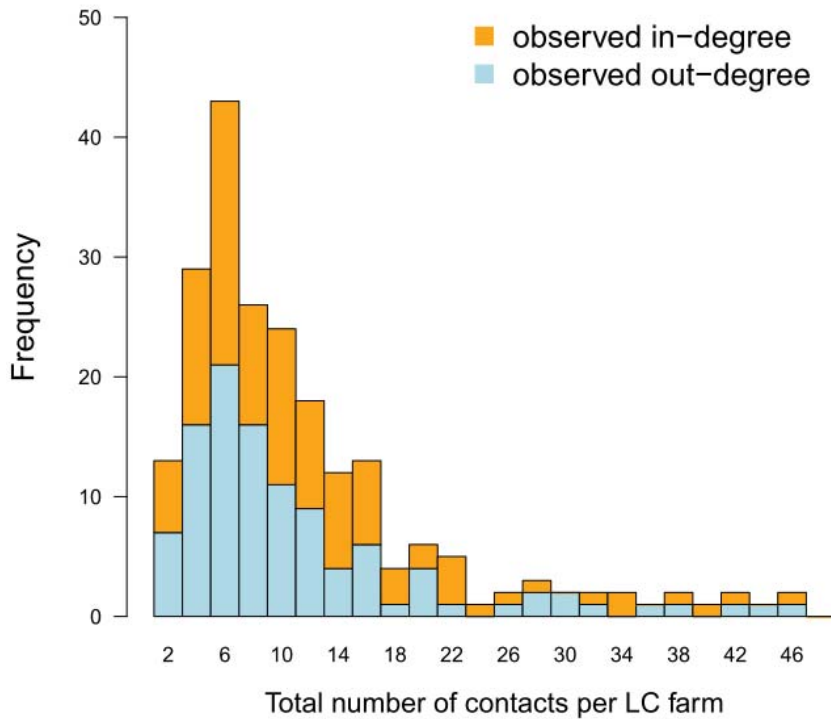


Figure 2-2 : un-weighted degree distribution for the 107 LC farms involved in the network in 2009-2010.

Considering other skewed distributions, the lognormal distribution provided the best fit for in-degree, and total degree and the Weibull distribution for the out-degree distribution, based on the lowest Akaike Information Criterion (among lognormal, gamma, Weibull, or exponential distributions). This did not indicate that these distributions appropriately fitted the observed distribution, but only that the other distributions provided a worse fit. Different GOF statistics were performed to test the plausibility of the fit. The less sensitive of the four tests (Kolmogorov Smirnov test) could not rule out the null hypothesis for the following distributions: lognormal fit for the total degree and in-degree, Weibull fit for the out-degree. However, the authors of the package indicated that that “this approximate test may be too conservative” (Delignette-Muller and Dutang, 2015).

2.4.3 Small-world properties of the network and overall connectivity

The network of LC farms during the commercial year 2009-2010 had a diameter of nine. This means that there existed a directed pathway between any two pairs of farms of the network,

with no more than nine steps to reach one farm from another. The average path length between any two pairs of farms was of 3.9 steps and the clustering coefficient was 0.34. By way of comparison, the 95% quantiles of the distribution of clustering coefficients obtained with 10 000 simulated Erdos-Renyi random networks comprising 164 nodes and 1285 ties were between 0.088 and 0.1. Hence, the observed clustering in the LC network was about 4-fold stronger than that of a random network. The short path length between farms observed in the network of LC farms, associated with high clustering, is characteristic of a small-world network. Graphical representation of the network (Figure 2-4) clearly shows the clustering of farms into two groups corresponding to North Island and South Island farms. Livestock movements occurred preferentially within the same island (97% of movements), but the North and South Island farms were interconnected by small numbers of trans-island movement events (3%) that acted as short-cuts between the two main clusters. Thus, despite high clustering and even topographic separation into two islands, the network of LC farms showed a high level of overall cohesiveness, as assessed by the size of the interconnected components of the network (Table 2-5). In 2009-2010, 100% of the total number of farms was weakly interconnected, meaning that an (undirected) pathway existed between all pairs of farms, while 79% of farms were strongly connected (Table 2-5).

2.4.4 Effect of network properties on the basic reproduction number (R_0)

Estimates of the increase in the magnitude of R_0 that could be attributed to the heterogeneity of the contact network are shown in Table 2-4.

Pearson's correlation coefficient for the un-weighted in- and out-degree was strongly positive (Table 2-4), indicating a linear correlation between the numbers of contacts in and out of farms in 2009-2010. As can be seen in Figure 2-3, this correlation was mostly due to the agistments. This type of movement corresponded to a temporary lease of unproductive livestock (typically dairy heifers or replacement lamb ewes) to a farm in a different region than the farm of origin, according to seasonal and regional variations of pasture availability, followed by a return to the farm of origin. Given this correlation between the in- and the out-degree and the variance in the degree distribution of the observed contact pattern, the initial spread was estimated to be 118% of the spread that would occur in a homogenous mixing population with similar average degree (Table 2-4). Our inference is that the presence of highly connected hubs is likely to enhance the potential for pathogen spread by farms that both send

and receive large number of contacts, phenomenon amplified by the inherent features of agistments that increased correlations. For the animal-weighted degree the Pearson coefficient of 0.01 was not significant, hence there was no overall linear association between the number of animals received or sent per farm, despite an apparent high correlation when considering agistments only (Figure 2-3). Therefore, the high variance observed in the contact pattern (see standard deviation in Table 2-4) did not significantly contribute to increase the value of when movements were expressed in number of individual animals moved, according to Equation 1 (Table 2-4).

Table 2-4 : Impact of the correlation between in- and out-degree in the LC farm network on R_0 , the estimated potential initial spread of epidemics in year 2009-2010

	Un-weighted degree (number of contacts)	Weighted degree (number of animals moved)
m_{in}	10.8	2642.3
m_{out}	11.3	2903.2
SD_{in}	9.4	5062.8
SD_{out}	9.2	3585.5
r_{in-out} [95% CI]	0.56 [0.42–0.68]	0.01 [-0.18–0.20]
$R_{0(network)}/R_{0(homogenous)}$ [95% CI]	1.18 [1.14–1.22]	1.02 [0.76–1.22]

Table 2-5 : Size of the giant strong component (GSC) and giant weak component (GWC) in the network, during the fourth year of the study period

	2009–10
Total number of farms	164
Size of GSC	129
% Network	79%
Size of GWC	164
% Network	100%

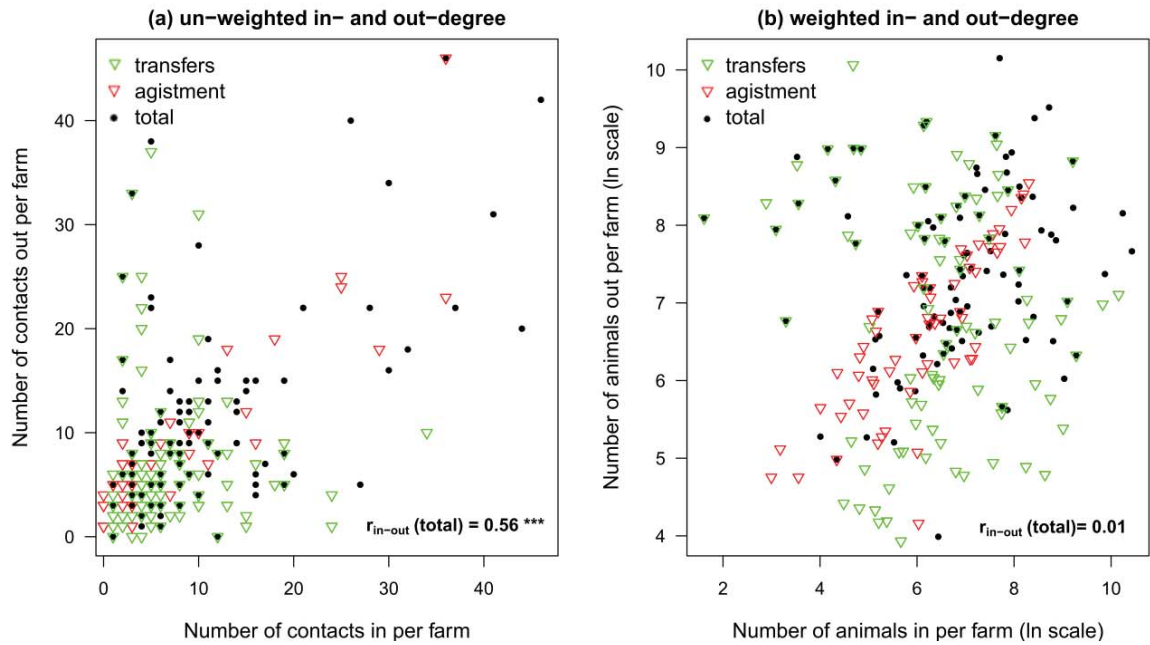


Figure 2-3 : correlations observed in the LC network in 2009-10 between the number of contacts in and out per farm (un-weighted degree, a) or the number of animals in and out per farm (weighted degree, b), respectively for transfers (green), agistments (red) and the total of both movements (black). R_{in-out} corresponds to the Pearson correlation coefficient between the total in- and out-degree.

2.4.5 Efficacy of targeted control strategies to disrupt the transmission via livestock movements

The total degree and the betweenness of LC farms were highly positively correlated (Spearman's rank correlation coefficient 0.7, $p < 0.0001$). Thus, farms with a number of contacts well above the average also tended to control the flow by being on the path in between many pairs of farms (see Figure 2-4). These central farms tended to link different communities of farms (results not shown), thus forming one giant interconnected component as can be seen in Figure 2-4. In particular, high degree/betweenness farms often received/sent livestock across islands, thus linking together the cluster of the North Island farms and the cluster of the South Island farms.

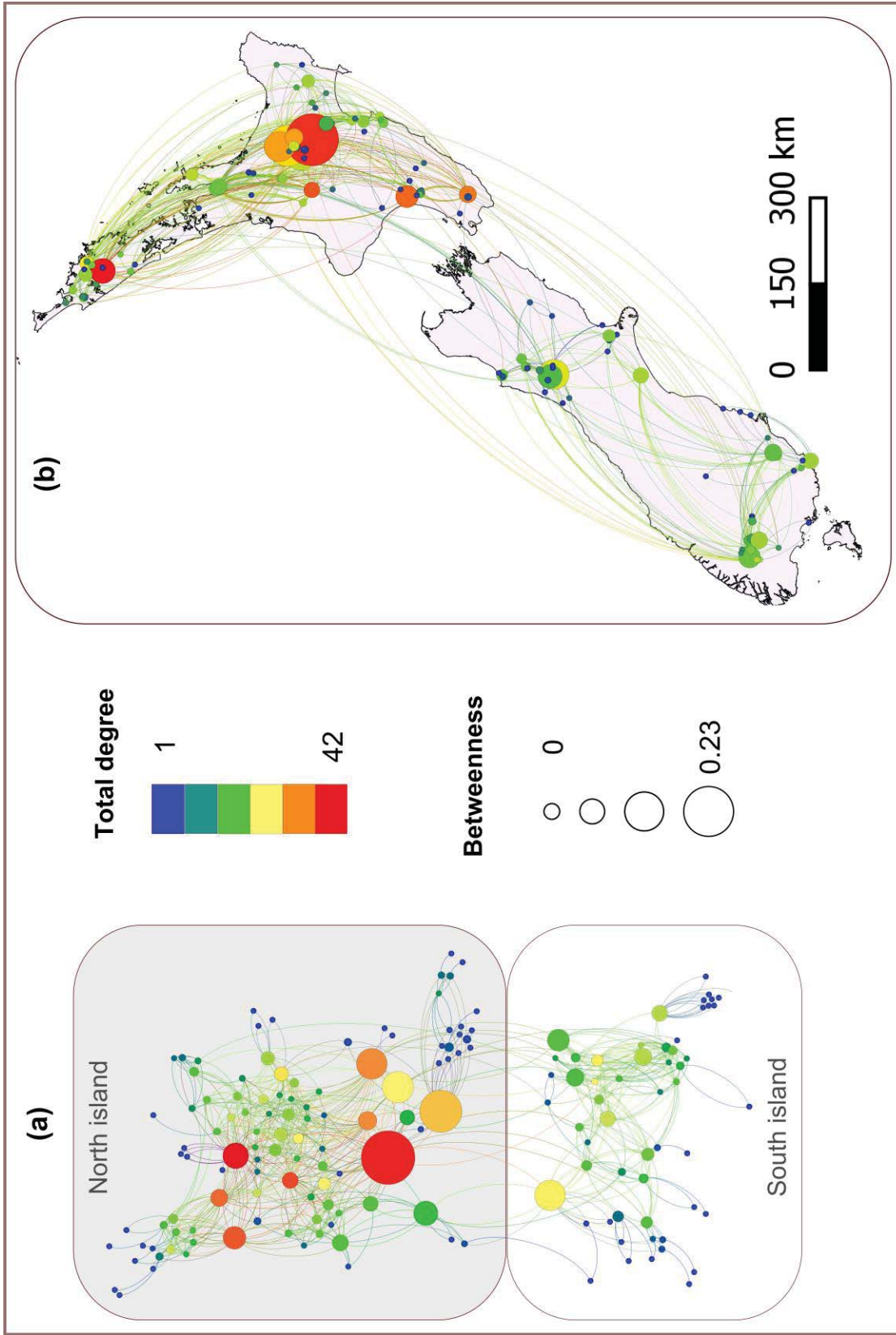


Figure 2-4: representation of the network of LC farms in 2009-2010, showing the importance of high-degree farms (in red) and high-betweenness farms (big size) in the contact structure. Each farm is represented as a node, the links between nodes are livestock movements. (a) projection according to the contact pattern only, not the geographical space, although the two main clusters correspond to farms of the North Island versus farms of the South Island, (b) contact pattern projected on a map of New Zealand according to the spatial coordinates of farms.

As expected from the high correlation between degree and betweenness, a ban on the movements to and from both high-degree or high-betweenness farms would be an effective measure for decreasing the potential of disease spread throughout the network (Figure 2-5).

More specifically, the removal of farms with the highest betweenness scores would be the most efficient way to decrease the size of the largest GSCC of the network. After the removal of just 10% of farms with the highest betweenness scores (16 of 164 farms in 2009-2010), the size of the largest GSCC was decreased from 129 farms to just 17 farms whereas the number of different strong components in the network increased from 27 to 71. Thus, the targeted removal of bridge-farms efficiently disrupted network connectivity by isolating clusters of farms. On the other hand, the proportion of the contribution of the movement pattern to the initial spread of infection ($R_{0(\text{reduced network})}/R_{0(\text{full network})}$) was most efficiently reduced by targeting the farms with the highest total degree. Removal of 10% of the highest-degree-farms resulted in a drop to 40% of the full network spreading potential.

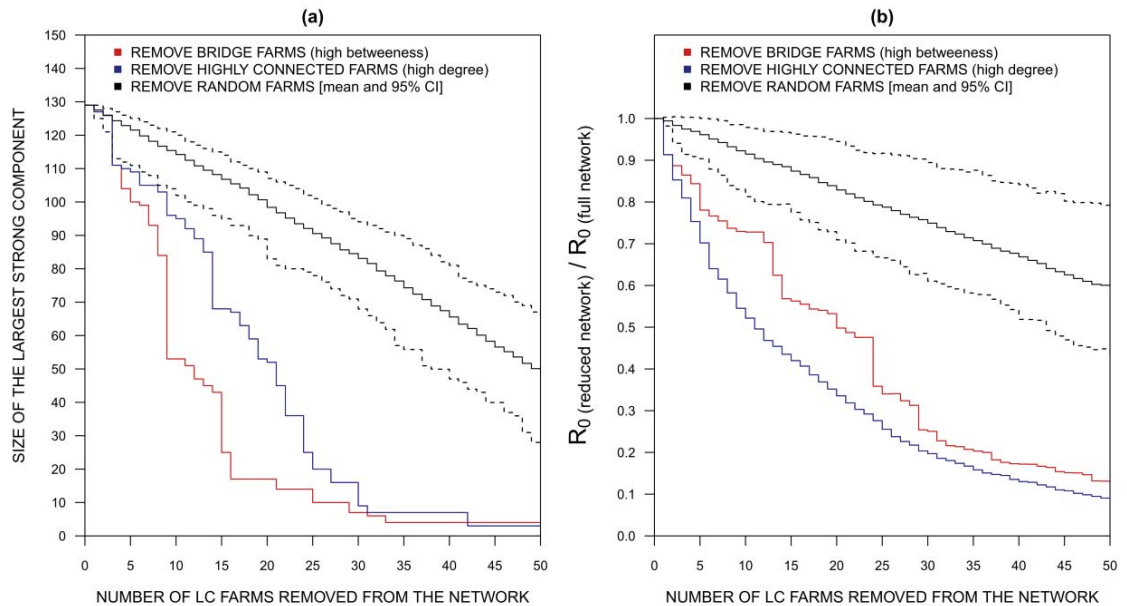


Figure 2-5: Line plots showing the effect of targeted (in red and blue) or random (in black with 95% credible limits) removal of farms on two measures of potential spread: (a) showing the size of the largest strongly connected component as a function of the number of farms removed, (b): showing the value of $R_0(\text{reduced network}) / R_0(\text{full network})$ as a function of the number of farms removed.

These results show how by removing high betweenness farms the network is transformed into a set of unconnected, smaller components (that is, a highly fragmented network). Similar effects were obtained by targeting high degree farms (Figure 2-5), which could be expected considering those farms with high degree were also those with high betweenness. In contrast,

random removal of farms provides a relatively inefficient means for reducing reduce the network connectivity and the spreading potential of infectious agents.

2.5 Discussion

In New Zealand, the National Animal Identification and Tracing Scheme (NAIT) was launched in July 2012. Until then, little data were available to conduct detailed studies of farm-to-farm movement of livestock in New Zealand. Prior to NAIT studies of farm-to-farm movement of livestock, individuals and animal product were based on cross sectional questionnaires (Lockhart et al., 2010). Sanson (2005) conducted a prospective study of movement of livestock off farms in the North Island of New Zealand to establish realistic parameters to inform a simulation model of FMD. That study addressed all types of off-farm movements occurring during three-week time slots, including people, material and manure; less than 4% of the total number of reported movements were actually livestock.

In the absence of a national livestock tracing scheme, the study of Sanson (2005) represented the only realistic way of quantifying farm movement patterns in New Zealand, but with key drawbacks. Firstly, it provided little insight into contact patterns for all livestock premises throughout the country. Secondly, it was a one-off cross-sectional study from which the consistency of the documented contact patterns over time could not be evaluated. Accurate recording of livestock movement data could only arise, in the absence of a mandatory system, from recording the source and destination of all animal shipments moved onto and off a given farm enterprise, the number of animals moved and movement date, similar to the system implemented in this study by LC. The recorded data represented a census of the movements to/from the LC farms. However, LC farms also traded with commercial farms outside LC that were not central but rather behaved like satellites of this network. The presence of movements to farms outside LC meant that this network would be embedded into a larger network of NZ farms rather than isolated. The focus of the study was limited to the LC farms but the effect of links to commercial farms outside LC notably on the spread of infectious diseases should not be ignored from a biosecurity perspective. An overall livestock network was considered in this study, encompassing movement of cattle, sheep and deer. This approach is suitable for infections shared by all Ruminant species. It is particularly relevant in the New Zealand context where different species are often co-grazed on the same pastures, enhancing the possibility of inter-species pathogen transmission.

The contact pattern presented in this study is unlikely to be representative of all livestock enterprises in New Zealand. However, these analyses provide an indication of how a large corporate farming enterprise can derive value from routinely recorded movement data to identify individual farms at risk for contagion.

2.5.1 Consistency of the contact pattern over time

We analysed the consistency of the pairs of farms exchanging livestock together in successive years. Most pairs of farms (60%) had been exchanging livestock for only one of the four years of the study period. This effect was not affected by the sub-optimal reporting of agistments observed before 2009 since the same pattern was observed when only data for the first three years of the study were analysed (Figure 2-1). We conclude that a characteristic feature of this network was that farms tended to interact with different partners (other farms) in subsequent years. It is possible that over a longer period of time (more than four years) consistency of farm-to-farm trading relationships would, if they were present, become more apparent.

While overall network properties in the LC network (such as scale-free, small-world properties) remained similar from one year to the next (results not shown), the properties of individual nodes (farms) could still vary from year to year (Kossinets and Watts, 2006). When evaluating the consistency of the hub's identity year after year, we found that 40 to 71% of the top 10% farms with the highest centrality measure were similar every year. Considering this level of similarity between years, it can be assumed that decisions about targeted control strategies based upon the contact pattern observed in previous years would still be effective in future years, although sub-optimal. Based on a one-year time frame to measure contacts, Volkova et al. (2010) analysed movements of sheep in Scotland and showed that the top 20% farms contributing most to the spread of infectious disease varied from year to year, similar to the LC network. Hence the effect of targeting the 'hubs' for control strategies based on the previous year contact network instead of real-time data consistently showed a reduced efficacy. Regular up-dates of farm-to-farm contact patterns are recommended to inform biosecurity measures, since we observed in the LC network significant variations in the efficacy of control strategies for small changes in the identity of the targeted farms (results not shown). When working at the national level the high volumes of data and the computational power can be a limitation in this respect (Martínez-López et al., 2009).

Our analyses were on a one-year basis rather than aggregated for the whole study period. This represented a compromise in terms of time-scale aggregation, since livestock movements

occur daily, but not all movement dates were available for analysis. As commercial ties between farms were not constant over the entire study period, aggregation of network data could result in an artificial co-existence of links that did not actually co-exist temporally. For this reason it was postulated that static networks appear to be constantly inaccurate for making predictions through epidemic simulations, as they fail to capture the intermittence of the connections between farms, thus artificially increasing the density and clustering of contacts (Vernon and Keeling, 2009). In a study of cattle movement patterns in the UK (Vernon and Keeling, 2009), a fully dynamic network was the only type to render appropriate temporal correlations in cattle movement patterns. The inaccuracy of predictions about final epidemic size arising from the representation of evolving networks as static would however, be minimal for diseases with low transmission probability and long infectious periods (Cross et al., 2005; Vernon and Keeling, 2009), such as mycobacterial infections.

2.5.2 Description of the degree distribution

In veterinary epidemiology, most social network studies claim ‘scale-free properties’ based on the fact that degree distributions are skewed (Kiss et al., 2006; Porphyre et al., 2008; Lockhart et al., 2010; Aznar et al., 2011). A visual method to ‘test’ this hypothesis consists in plotting the cumulative distribution of the number of contacts per node at the log-log scale. A tail falling on a straight line is a necessary condition for a degree distribution following a power law and is therefore commonly used as a criterion to assess the scale-free nature of a network (Kiss et al., 2006; Porphyre et al., 2008; Aznar et al., 2011). However, such conclusions can be ‘substantially incorrect’ since a variety of skewed distributions other than power law could also be fitted by a linear regression at a double-logarithmic scale (Clauset et al. 2009), and the assumptions underlying ordinary least square regression are violated (Jones and Handcock, 2003). This visual evaluation of contact heterogeneity in networks is nevertheless sufficient for highlighting the preponderant role of ‘hubs’ in the network and for assessing the effect of risk-based movement control strategies as is often of interest in veterinary science (Woolhouse et al., 1997; Woolhouse et al., 2005).

However, it can also be useful to unravel the mathematical properties of the observed contact pattern when attempting to model the spread of infectious disease. The theoretical law that best fits the empirical set of contacts can be incorporated as an approximation of the underlying heterogeneity of contacts in epidemic models (Keeling and Eames, 2005; Bansal et al., 2007). Robust mathematical methods to assess the scale-free nature of networks are often lacking in the graph literature, casting doubts as to whether scale-free properties indeed

always arise from real-world networks (Li et al., 2005; Snijders et al., 2006; Clauset et al., 2009; Worby et al., 2014). Statistical methods to evaluate a power-law fit, combining maximum-likelihood fit and goodness-of-fit tests (Clauset et al., 2009), were presented here as an example; these methods should be preferred to specifically assess the fit with a power law. There is at least one previous example in the field of veterinary epidemiology where the above framework was implemented (Dorjee et al., 2013). When applied to the LC network data, this approach indicated that a power law tail was highly plausible for the degree distribution for the period 2009-2010. However, even robust methods such as this present an inherent lack of power for small datasets, the LC network.

2.5.3 Small-world properties and connectivity

In most real-world networks, scale-free properties are associated with social clustering that also impacts pathogen spread. Similarly, the network of LC farms exhibited small-world properties, with a clustering coefficient approximately 4 times greater than expected in a random network of same size. We observed a specific and strong geographical clustering of contacts within islands (either North or South Island of New Zealand), with few trans-island contacts (less than 3% of total volume of movements). In such structured networks, the navigability for pathogens can be limited to localised neighbourhoods (Eguíluz and Klemm, 2002). Clustering or even fragmentation of the network can therefore prevent the occurrence of large epidemics despite values of R_0 greater than one (Cross et al., 2005), whereupon a group-level R^* describing pathogen invasion through structured groups could be a much better predictor for pandemics. In the network of livestock movements in Great Britain in 2003-2004, Kao et al. (2006) assessed the risk of spread of an incursion of FMD; they showed that clustering of contact protected against epidemic spread, with a large epidemic of FMD only possible when R_0 was greater than 4. Hence $R_0 > 1$ is a necessary, albeit not sufficient, condition for infection spread in a structured network such as the network of LC farms.

Complementary to knowledge about R_0 , the size of the largest GSCC in the network represents an estimate of the total number of farms that a pathogen could reach if introduced into the network (Christley et al., 2005; Kao et al., 2006; Kiss et al., 2006; Robinson et al., 2007). Along these lines, we looked at the size of the largest GSCC or GWCC to assess the overall connectivity. Depending on the year, the largest GSCC in the LC network comprised 79% to 95% of the total number of farms in the network. This number represented the lower bound for the potential final epidemic size. Additionally, infection could spread to all the sink nodes receiving animals from (but not sending animals to) farms in the GSCC, thus reaching virtually

all the farms in the LC network. Hence, despite the presence of community structures, the density of contacts as well as the presence of bridge-farms linking communities allowed for a very high overall connectivity in this network. Previous research additionally shows that large epidemics are more likely to occur in such a structured meta-population for chronic diseases than acute infections (Cross et al., 2005).

2.5.4 Effect of network properties on the basic reproduction number (R_0)

In homogenous-mixing populations, the value of R_0 depends primarily on the average number of contacts per node, so called *first order moment* of the network (May and Lloyd, 2001). In skewed networks the heterogeneity in the number of contacts induces a second order relationship between nodes (May and Lloyd, 2001; Volkova et al., 2010). This corresponds to a non-null variance and covariance in contact rates and modifies the threshold value of infectious rates above which pathogens are propagated (Bansal et al., 2007; Volkova et al., 2010). In a network in which farms with a high in-degree tend to have few off-farm movements (for example finishing farms), those farms -once infected- would be unlikely to spread infection to other farms. By contrast, we observed a strong correlation between in-degree and out-degree (un-weighted) for the LC network in 2009-2010. In that year, 46% of movement were 'agistments' which correspond to temporary exchanges of young stock, particularly dairy cattle, leased to graze in areas of the country with better pasture availability and later returned to their farm of origin. This practice, well exemplified by the LC corporation movement pattern, is typical of the pastoral system in New Zealand. It contributes greatly to the circulation of livestock in all parts of the country; moreover, the inherent back-and forth nature of this type of movements increases the correlation between in and out degree, as observed for the LC network in our study. This in turn could favour the transmission of infectious diseases.

Methods to assess the epidemic invasion in a network include a range of simulation modelling procedures. Other, more tractable methods have also been described to estimate values of R_0 that take into account the variance and covariance in contact rates, so that a negative correlation in the degree would lead to a decrease in the value of R_0 (May and Lloyd, 2001; Volkova et al., 2010). We used the approach of Volkova et al. (2010) to evaluate the impact of the second order moment on the basic reproductive number (R_0), compared to what it would be in a network of same size with homogenous mixing (that is, a network in which the variance

of the degree distribution was 0). In the paper by Volkova et al. (2010) in- and out- degree correlations were examined for Scottish sheep farms during the period 2003-2007. The correlation between the number of contacts in and out was close to zero, whereas it appeared much stronger when taking into account the numbers of animals per batch (still weak on an absolute scale), ranging from 0.18 to 0.36. For the LC network this relationship was reversed. The number of contacts in and out (in-degree and out-degree) were strongly positively correlated (Pearson's $\rho=0.56$ [0.42 - 0.68]), whereas correlations between the number of animals imported and exported per farm (weighted in-degree and out-degree) were not correlated. According to Volkova et al. (2010), different scales used to define contacts could apply to different diseases, with unweighted contact more appropriate to study the spread of highly contagious diseases (such as FMD) and weighted contact for diseases with low intra-herd prevalence (such as mycobacterial infections). For the LC network, the presence of few highly connected farms could contribute enhancing the initial spread of a pathogen by 20% (un-weighted model), which could be a cause of concern in the case of an incursion, such as a FMD epidemic. Our analyses confirm that the way the contacts were weighted had a strong influence on the inferences.

We calculated relative values of R_0 . Absolute values for R_0 could not be computed and would be meaningless, since they depend upon pathogen properties, such as the duration of the infectious period and the probability of infection given contact.

Finally, it should be noted that even higher order relationships ignored in this study, such as assortative or dis-assortative mixing also have an impact on disease spread in networks (Kiss et al., 2006).

2.5.5 Efficacy of targeted control strategies to disrupt the transmission via livestock movements

While scale-free properties are not easily defined, the vulnerability to targeted removal of hub-nodes represents the most prominent feature of scale-free networks (Li et al., 2005). This phenomenon is known in statistics as the Pareto principle. Applied to infectious diseases it means that "20% of the host population contributes to at least 80% of the net transmission potential, as measured by the basic reproduction number R_0 " (Woolhouse et al., 1997).

We explored the impact of removing farms from the LC network that ranked highly for either their total degree (total number of contacts per farm) or their betweenness centrality. Farms

with high betweenness had a strong tendency to also display a high total degree, thus the removal of farms according to their betweenness or to their degree both had a strong effect on the potential spread of infection. By contrast, the removal of randomly chosen farms was always significantly less effective (Figure 2-5). Removing high degree farms was the most efficient way to reduce R_0 (Figure 2-5 b), while targeting high-betweenness farms was most effective to fragment the network into smaller, unconnected components (Figure 2-5 a). We observed percolation-type transitions (Kiss et al., 2006): as important bridge-farms acting as short-cuts between socially or geographically remote clusters were removed, the size of the largest GSCC suddenly dropped, thus the network connectivity fell apart. Commonly, livestock markets act as easily identifiable 'bridges' in a network of livestock farms and are often primary targets for livestock movement control. However, some farms (trader holdings) can also play a role as a bridge between cliques (Lockhart et al., 2010) or links between markets (Kao et al., 2006). Although these farms tend to be less readily identifiable than livestock markets (Ortiz-Pelaez et al., 2006), they might represent a very high risk to spread infectious agents (Dubé et al., 2010). Betweenness centrality is a measure of how each node lies 'in between' pairs of other nodes, therefore providing an indication of farms that control connectivity in the network (Ortiz-Pelaez et al., 2006). In the case of the LC network, the livestock operations displaying high betweenness were farms that sent/received livestock trans-island.

This feature could be exploited to decrease the risk of large epidemics, if the most influential farms for the overall connectivity are identified and targeted for control measures, such as movement bans, quarantines or other biosecurity measures. An obvious example in the case of the LC network is related to the topography of the country: if only trans-island movements were banned, the network would be disconnected into two independent clusters of farms; a pathogen introduced in one island could not spread to LC farms of the other island, no matter how contagious. This principle of isolation between the two main islands is already exploited by the Ministry of Primary Industries to implement legal biosecurity measures for pest control in New Zealand. In particular, the South Island is declared at the time of writing "controlled area" regarding the unwanted didymo algae to prevent the spread to waterways of the North Island³; similarly, a movement control of bee colonies and other risk goods from the North to

³ <http://www.biosecurity.govt.nz/didymo>

the South Island was enforced until *Varroa destructor* finally became established in the South Island⁴.

Our results, similar to previous work (Dubé et al., 2009), suggest that risk-based control strategies for biosecurity regulations could be efficient to reduce farm-to-farm spread of infection after an incursion. Risk-based surveillance targeting farms importing livestock from a large number of trading partners could also be implemented routinely for incursion detection. In an attempt to assess the possibility of spread throughout a contact network, considerations both on the magnitude of R_0 and on the presence of a GSCC in the network should be made as they inform two different aspects of the dynamics of an epidemic.

2.6 Conclusions

This study represents the first example of an analysis of a comprehensive contact network of livestock farms in New Zealand.

As one of the largest corporations of farms in the country, LC is well suited for implementing routine records of livestock movements. Although the results presented here are unlikely to be representative of all livestock enterprises in New Zealand, they show the value of such data for epidemiological studies. Our findings illustrate the contribution of a very common practice in the New Zealand pastoral farming industry, which consists of dispatching young stock to lease farms in different areas depending on pasture availability and scarcity for a temporary period. This contributes to increase correlations in the contact pattern which could favour the transmission of pathogens. Similar insights would likely be obtained if the methodologies applied in this study were applied to movement data collected from a wider, more representative cross-section of the population of livestock farms in New Zealand. Notably, the network of LC farms presents very similar structural properties as most other published animal movements, despite that farming systems are different between countries and production types.

Our findings emphasise the value of control measures targeted on smaller numbers of ‘at risk’ farms to control contagious disease spread, as opposed to blanket policies applied to the general population of farms. Selective interventions do not only include movement bans; the key-player farms identified in this study could also be subject to enhanced biosecurity measures and could be prioritised for active surveillance of infectious diseases since they

⁴ <http://www.biosecurity.govt.nz/pests/varroa>

would be at higher risk of becoming infected and transmitting infection. We thus propose that there is a value in documenting and analysing movement events, either at the national or, as demonstrated here, at corporate farming level. In the future, more comprehensive and detailed network analysis, encompassing all livestock movements in New Zealand, should become possible as the National Animal Identification and Tracing system comes into full operation.

2.7 Acknowledgements

This study was partially funded by the New Zealand Johne's Disease Research Consortium and stipends were granted by Massey University and New Zealand International Doctoral Research Scholarship. The main author is particularly grateful to Landcorp farming limited for providing us the data for this analysis and Gordon Williams for invaluable help in managing these data and understanding the movement pattern in relation with Landcorp policies and production needs. We are also especially grateful to Carolyn Gates for her insightful comments concerning the analysis and the manuscript.

Chapter 3. Merging DNA typing and network analysis to assess the transmission of paratuberculosis between farms

Nelly Marquetoux^a, Cord Heuer^a, Peter Wilson^b, Anne Ridler^b, Mark Stevenson^c

^a EpiCentre, Institute of Veterinary, Animal and Biomedical Sciences, Massey University, New Zealand

^b Institute of Veterinary, Animal and Biomedical Sciences, Massey University, New Zealand

^c Faculty of Veterinary and Agricultural Sciences, The University of Melbourne, Werribee, Victoria, Australia

3.1 Abstract

Paratuberculosis, a chronic enteric infection caused by *Mycobacterium avium* subsp. *paratuberculosis* (MAP), is endemic in all farmed ruminant species in New Zealand. The use of genotyping in combination with network analysis of livestock movement events from one farm location to another has the potential to contribute to our understanding of between-farm transmission events. We studied a population of 122 farms from a corporate commercial livestock enterprise in New Zealand, trading with each other in near isolation from other commercial farms. The data consisted of longitudinal movements to and from these farms between 2006 and 2010, as well as the results of cross-sectional MAP screening and genotyping performed in 2010. We explored associations between past livestock movements and current strain type distribution in this population of farms using quadratic assignment procedure. Our results show that measures of farm clustering within the movement network were significantly associated with sharing of MAP strains. For example, farms closely related by trade were twice as likely to share the same strains of MAP ($p=0.033$). Other covariates were also associated with the probability of sharing the same strains of MAP, such as being located on the same island (OR=5.8 to 8.7, $p<0.01$), farming the same livestock species and Euclidian distance between farms. The novel approach we used supports the hypothesis that livestock movement is indeed a significant contributor to farm-to-farm transmission of MAP.

3.2 Introduction

Paratuberculosis (PTB) is a chronic infection of ruminants caused by *Mycobacterium avium* subsp. *paratuberculosis* (MAP). While most infections are asymptomatic, some result in

chronic wasting, leading to production loss and pre-mature culling or death of affected animals (Chiodini et al., 1984; Garcia and Shalloo, 2015). Paratuberculosis has a worldwide distribution among farmed ruminants and its control remains a challenge. In New Zealand, a nation-wide prevalence study showed that PTB was present at endemic levels in beef (42%), deer (46%) and sheep (76%) in the general population of pastoral farms (Verdugo et al., 2014a). The economic impact of PTB in New Zealand remains poorly understood but has been associated with production effects in all affected livestock species (Lombard et al., 2005; Morris et al., 2006; Hunnam et al., 2009). Because paratuberculous livestock are not treated and since MAP is resilient in the farm environment, infection with MAP is virtually impossible to eradicate from farms or regions (Whittington and Sergeant, 2001). Possible control strategies therefore aim at reducing the presence of MAP in the farm environment and preventing the introduction of MAP in naïve farms. Hence, a full understanding of the transmission between farms is desirable. The purchase of infected stock has been hypothesised to be an important route for introducing MAP onto disease free farms (Sweeney, 1996; Whittington and Sergeant, 2001). To the best of our knowledge few studies have addressed the issue of quantifying the probability of farm-to-farm transmission of MAP arising from the transfer of animals from one geographic location to another. Filling this knowledge gap would improve our understanding of the extent to which livestock movements contribute to high prevalence levels in New Zealand. This, in turn, would inform policies for the control of paratuberculosis.

Molecular epidemiology has become a powerful approach to assess transmission pathways of infectious diseases (Kao et al., 2014). High genetic resolution is desirable for the study of pathogen transmission dynamics both within and between farms (Amonsin et al., 2004; Motiwala et al., 2005; Thibault et al., 2008; Oakey et al., 2014). In the past decade, MAP genotyping combining multilocus Short-Sequence-Repeat (SSR) and mycobacterial interspersed repetitive unit Variable-Number Tandem-Repeat (VNTR) were found to achieve a high level of discrimination between strains using a limited number of loci of the MAP genome (Thibault et al., 2008). This approach identified important epidemiological features, such as strain specific susceptibility to MAP in red deer (O'Brien et al., 2006) and inter-species transmission of MAP by co-grazing multiple species in a pastoral environment (Verdugo et al., 2014b).

Data combining molecular evidence of MAP and livestock movement in a closed population should provide evidence for farm-to-farm transmission of MAP via livestock movements. The objective of this study was to combine MAP strain typing information with social network

analysis (SNA) to provide evidence to support the hypothesis that MAP is transferred from one farm location to another via livestock movements.

3.3 Material and methods

3.3.1 Animal movement data

The animal movement data for this study were provided by Landcorp Farming Limited (LC), a corporate commercial livestock enterprise comprised of 122 farms located in both the North and South Islands of New Zealand (as per 2012, the number of farms is subject to annual changes and increased to 137 in 2014). Pastoral dairy, beef, deer and sheep LC farms are managed under conditions that are typical of livestock farming in New Zealand, with nearly half of the farms hosting at least two different livestock species.

Landcorp Farming Ltd. kept records of all livestock movements on and off their farms before it became mandatory to declare farm-to-farm movements of livestock with the launch of the National Animal Identification and Tracing scheme in July 2012. Details of the movements between 01 July 2006 and 30 June 2010 were retrieved for analysis, involving a total of 112 different LC farms over the four years. An additional 68 commercial farms outside the LC Corporation sent or received livestock to/from LC farms. These commercial farms were only satellites in this network. However, they contributed, though minimally, to its connectivity and hence were included to calculate shortest path lengths and for community detection (see below).

Data included permanent *transfers* of animals between farms (equivalent to a sale) and temporary transfers (*agistments*) for the purpose of grazing (Marquetoux et al., 2016b). The movement database contained the following details for each movement event: the source and destination property, type of movement (transfer or agistment), date (year for transfers, calendar date for agistments), species moved (sheep, beef, dairy or deer) and the total number of animals of each species moved in one year for transfers, or the actual batch size for agistment events.

3.3.2 Paratuberculosis culture

Between May and September 2010, 102 of the 112 LC farms involved in the movement network analysis were tested for PTB infection, including 162 breeding herds/flocks of sheep, deer, dairy or beef cattle. The remaining 10 LC farms had either been sold in the meantime or

did not have breeding stock (were finishing or growing farms) so were excluded from PTB testing. The 68 other commercial farms that were involved in livestock exchanges with LC were also not tested.

For each species within a farm a random sample of 20 healthy individuals was selected for individual faecal sampling per rectum. Mixed age breeding ewes/cows (above two years old) and 1-2-year-old deer of either sex were selected. Additional samples were collected from up to five Johne's disease clinical suspects (wasting or diarrhoea) present at the time of sampling. Faecal samples were pooled (1 × 20/pool for sheep and 2 × 10/pool for cattle and deer, and clinical suspect animals' faeces pooled separately within farm and species) and tested for the presence of MAP by liquid culture using the medium BACTEC 12B. Details of the sampling scheme and culture method are described in (Verdugo et al., 2014a).

Additionally, culture positive faecal pools were typed using 6 loci identified by VNTR, and 1 locus identified by SSR sequencing analysis, 'SSR8' (Collins et al., 2002; Amonsin et al., 2004; Thibault et al., 2007). The combination of the specific number of repeat sequences detected for each locus allowed the classification of each isolate into one particular VNTR/SSR strain type.

3.3.3 Data analysis

In the context of this study a trade relationship between two farms was said to exist if animals were moved from one farm location to the other. The unit of observation was a *dyad*, consisting of a pair of farms and the different kinds of relationships existing between them (example: trade or MAP strain type sharing). The set of all dyads thus formed a network. Dyadic observations are typically represented by $n \times n$ sociomatrices, with n being the number of nodes (farms) in the network and each cell $A_{i,j}$ a sociomatrix A characterising a particular relationship for the pair of nodes (i,j) . Two sociomatrices formed the basis of the data for this study, one with ties informing on the relationship between the farms in the livestock movement network, the other with ties representing whether pairs of farms had strains of MAP in common.

The objective of our analysis was to estimate the presence and extent of associations between farms that shared the same MAP strains and the contact structure between farms, adjusting for the presence of other determinants for strain type sharing. This corresponds to testing for statistical associations between matrices as represented in Figure 3-1.

3.3.3.1 Outcome: strain type sharing

For every pair of farms for which MAP organisms were isolated and typed from both farms, the outcome of interest was whether or not the farms harboured a common strain type of MAP (coded as 1) or not (coded as 0), see Figure 3-1. If farms were infected with more than one ST, strain sharing referred to at least one common strain type being isolated in the two farms (*i.e.* farm A being infected with strains 1 and 2 and farm B with strains 1 and 3, the pair AB was considered to share a common strain of MAP, strain 1 in this example).

Pairs with farms either not tested or negative were not used for the correlation analysis, since the outcome (strain type sharing) was not available for such pairs.

3.3.3.2 Exposure of interest

For each pair of farms, we used three measures of connectedness in the network of livestock movement as three distinct exposure variables: undirected and directed shortest path length and community belonging.

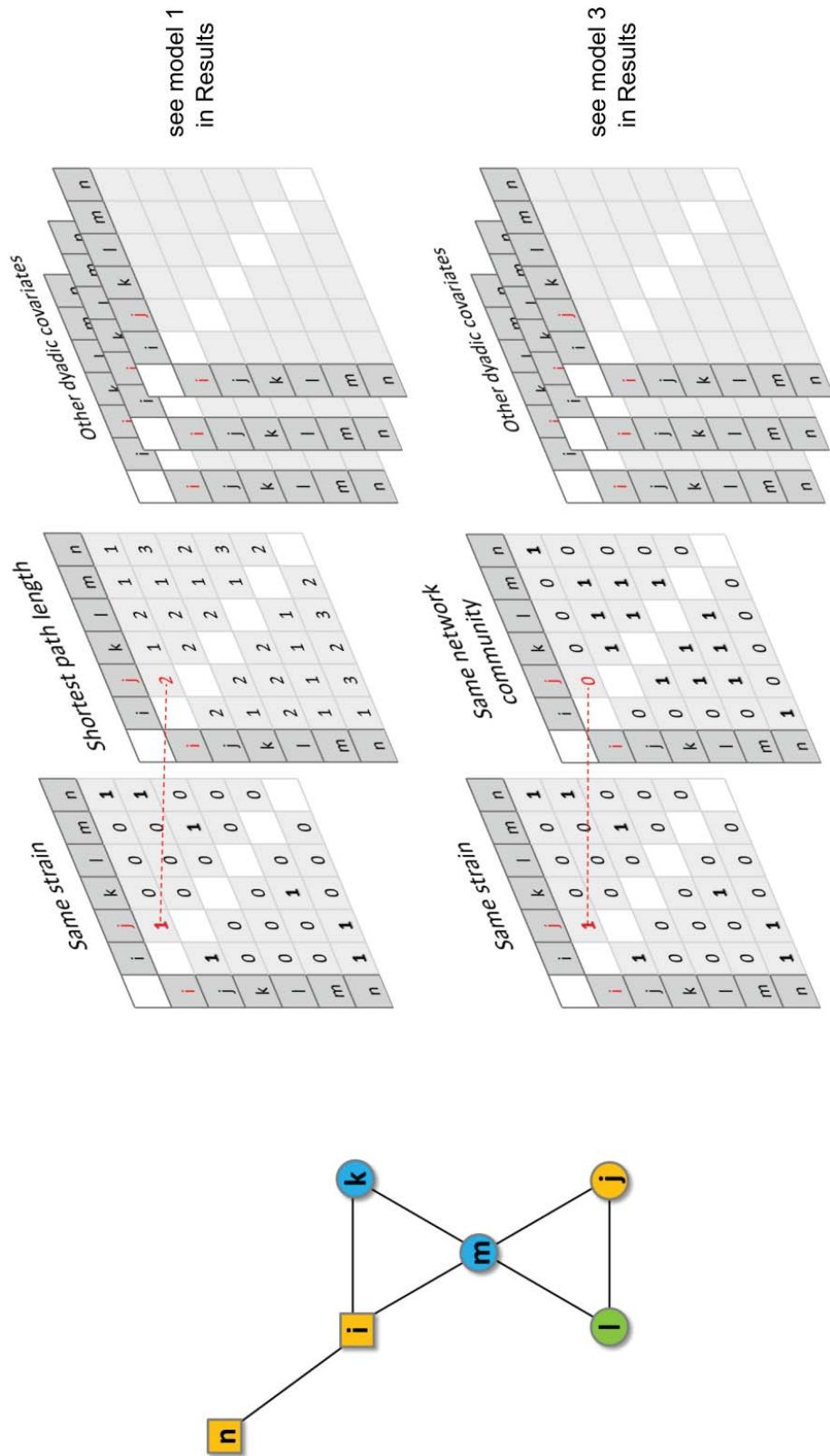


Figure 3-1: The principle of matrix correlation analysis applied to a theoretical network of six farms infected by MAP (i, j, k, l, m, n) connected by livestock movements (black lines). Colours represent particular MAP strains. Proximity of farms in the network is expressed by the shortest path length between farms or the network community to which farms belong (represented by the shape of the farms: square=community #1, circle=community #2) based on the livestock movement pattern.

3.3.3.2.1 Shortest path length

The movement data were used to build a directed network $G(n,m)$ with n farms and m edges representing the movement of livestock between farms. We used un-weighted network edges such that for a pair of farms (i,j) , the edge X_{ij} represents the presence/absence of movements from i to j over the four year study period irrespective of the number of animals moved. Hence $X_{ij} = 0$ if there were no movements between i and j , and $X_{ij} = 1$ if there was at least one movement from farm i to farm j in any of the four years.

We computed the shortest path length (SPL) between pairs of farms in the network using the *igraph* package (Csárdi, 2006) implemented in R (R Development Core Team, 2014). The SPL represents the number of steps between two LC farms following livestock movements, indicating how closely related or far apart are any two farms in the network. We computed both directed and un-directed SPL by taking into account or ignoring the direction of edges. This is shown in the Figure A1 of Appendix A.

3.3.3.2.2 Community detection

The network of LC farms presented small-world properties with high clustering of contact (Marquetoux et al., 2016b). We used this property to identify communities of farms, defined as groups of nodes with dense connections within the group but sparsely connected with other nodes (Girvan and Newman, 2002). This is therefore another way to identify clusters of farms closely related by livestock movements. We used the Louvain method for community detection (Blondel et al., 2008), more precisely a generalisation of this method developed by Mucha et al. (2010) making use of the four successive years of movement data as multiple layers. We implemented this method in MATLAB (Inderjit et al. 2014, MATLAB code available on the webpage <http://netwiki.amath.unc.edu/GenLouvain/GenLouvain>).

We defined yearly sub-networks $G(k)$ with $k \in \{1,2,3,4\}$ corresponding to the four years of the study period. For each year, we took into account the number of animals moved along the edges, with $A_{ij}(k)$ = total number of animals sent from i to j in year k . The GenLouvain algorithm (Mucha et al., 2010) was used on the four resulting matrices to identify the community structure that maximized the modularity (a numeric value providing a measure of the quality of the partition of farms in communities). Additionally, because the analytical model to which these results will be fed required a unique community structure for the study period, the next step was to allocate each farm to a single community across the four years. This was achieved by increasing the value of the “interlayer coupling parameter” used in the

implementation of the GenLouvain algorithm to the smallest value that produced the desired feature.

Based on the results of this community detection procedure, the “community belonging” variable informed whether a pair of farms belonged to the same community based on the livestock movement network (same community = 0 or 1).

3.3.3.3 Other covariates

To adjust for possible confounding effects and explore the effect of other potentially epidemiologically relevant factors on the probability that two farms harboured the same strain type, we considered other covariates at the pair level. Thus, “same species” was a sociomatrix informing whether the pair of farms hosted the same livestock species. Farms with the same livestock species may be more likely to exchange animals and MAP subtypes may be host species specific, hence species could be a confounder. In the coding of this variable, beef and dairy were considered two distinct species since they represent distinct production systems. In reality, beef and dairy farms are unlikely to be particularly connected via livestock movement. In addition, they tend to harbour distinct strain types in the New Zealand context (Verdugo et al., 2014b). Similarly, “same island” was a sociomatrix informing whether both farms of a pair were situated on the same island of New Zealand (coded 0 or 1). Livestock movements are strongly clustered within each of the two main islands of New Zealand (North Island versus South Island). Moreover, strains of MAP strongly segregate within each island of New Zealand (Verdugo et al., 2014b), for evolutionary and ecological reasons that might not be only due to the clustering of movements within islands. Finally, “spatial distance” corresponded to the geographical distance between two farms, measured by the Euclidian distance (per 100 km). This variable allowed us to quantify the effect of geographical distance between farms on the probability of sharing the same strain type, over and above the effect of livestock movements and island.

3.3.3.4 Model building

Associations were assessed using three different models for the three measures of the exposure of interest: undirected SPL (uSPL), directed SPL (dSPL) and whether the pair of farms belonged to the same community (same community = 0 or 1).

All variables of the model were at the level of the pair of farms (dyad). Standard tests of statistical significance rely on the assumption that observations are independent while dyadic observations used in SNA are inherently dependant (Dekker et al., 2007; Borgatti et al., 2013;

Scott, 2013). For robust statistical inference, we therefore used the Multiple Regression Quadratic Assignment Procedure (MR-QAP) (Krackhardt, 1988). More information can be found in Appendix A.

We implemented the MR-QAP using the *netlogit* function from the R package “sna” (Butts, 2008) performing logistic regression for binary outcomes, adapted to relational data. The estimation of regression coefficients was achieved by standard GLM routines on the vectorised sociomatrices (Butts, 2008). Robust standard errors for the coefficients cannot be obtained by this method due to the lack of independence inherent to dyadic observations. Instead, p-values for the significance of the regression coefficients were estimated by a method of permutation of the model’s residuals using double-semi-partialling (Dekker et al., 2007). We used 10,000 permutations to ensure a stable p-value estimate for the final multivariable models and 1000 permutations for bivariate analysis and model building.

A univariate analysis was performed first to explore if the presence of the same strain type in two farms versus a different strain type could be explained by contact network measures between the farms, whether the two farms were located on the same island and whether they hosted the same livestock species and the Euclidian distance between them.

Multivariable logistic regression provided an estimate of the association between the network measures (linear effect of directed SPL or undirected SPL or the fact of belonging to the same network community) and sharing the same subtype, adjusting for the effect of the other covariates, according to the hypothesised pathway shown in the Figure A2 in Appendix A. The different network exposure variables carried a high level of collinearity and their effect was assessed independently in the three models, as described above.

The effect of possible relevant interactions was assessed, between the network measures (SPL or community belonging) and same species, the network measures (SPL or community belonging) and same island and between same island and Euclidian distance.

Model building was based on hypothesis generated using causal diagrams (see Figure A2 in Appendix A) and biological relevance while model selection was based upon the Wald test and minimizing the Akaike Information Criterion (model parsimony).

3.4 Results

3.4.1 Descriptive results

There were a total of 3,532 movement events involving 1,148,946 animals and 112 LC farms between 2006 and 2010. Of the 102 farms tested for PTB in 2010 there were three beef-only, two deer-only, 12 sheep-only, 37 dairy-only, 33 sheep/beef, one deer/sheep, 12 beef/sheep/deer and two dairy/sheep farms.

3.4.1.1 *MAP molecular data*

Of the 162 herds/flocks tested for MAP, 38 were culture positive from 36 farms and isolates from 47 faecal pools from 33 farms were typed. The seven VNTR/SSR loci used for strain typing defined 11 distinct strain types in this population of isolates, nominally named A-K (Figure 3-2). This resulted in the identification of 54 isolates of distinct strain types, with some pools of faeces containing isolates of two different strains.

Of the 33 farms where strains of MAP were typed, four harboured two strains and two harboured three. On all farms, multiple strains were from a single livestock species rather than different strains segregating in different species on the same property. The number of strains present on a property (1,2,or 3) in 2010 was not associated with the number of incoming movements, the number of outgoing movements or the number of animals imported or exported in 2009-2010. Further analyses were therefore not confounded by number of strains per property.

3.4.1.2 *Livestock movement pattern*

The network was characterised by a relatively short average path length between any two farms (3.9) indicating high connectivity and the presence of few highly connected “hub” farms with high in- and out-degree (Marquetoux et al., 2016b). The movements of livestock were clustered within island: 3% of movements were between the two islands. This network feature was confirmed in our community detection analyses. Detected communities of farms were always located on the same island, even though the community detection algorithm was based on livestock movement records and not on spatial proximity (Figure 3-3).

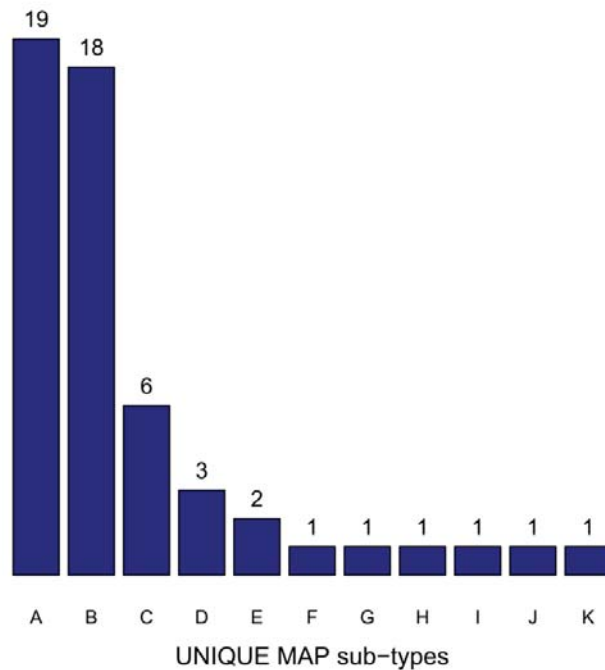


Figure 3-2: Distribution of 11 VNTR/SSR strain types of MAP, categorised A – K, from 54 isolates typed from 47 pools of 33 Landcorp Ltd. properties of sheep, deer, beef and dairy cattle. The number of isolates of each type is indicated above each bar.

3.4.2 Association between MAP strain type pattern and movement pattern between farms

Results of the univariate analysis can be seen in Table A1 in Appendix A.

Multivariable analysis indicated that over and above the effect of clustering of the MAP strains within species and within island, and in addition to a spatial distance effect, livestock movement pattern had a significant impact on whether two farms harboured a common MAP strain type (Table 3-1; $p < 0.05$).

An interaction existed between SPL and species (models 1 and 2), such that the effect of SPL was stronger when two farms hosted different species. This was probably because species accounted for some of the SPL effect in the ‘same species’ stratum. We assumed a continuous linear effect of SPL on the outcome; hence the OR suggested that each step further along the network path decreased the odds of sharing the same strain of MAP by 62% (uSPL) to 53% (dSPL), for pairs of farms not hosting the same species. The effect of species alone was not significant in both models with SPL (p-values of 0.4 or 0.8 respectively for model 1 and 2).

Species was therefore removed as a main effect in these models although the significant interaction between SPL and species was kept (corresponding to the models with the lowest AIC). The OR in Table 3-1 were estimated by adding the SPL effect and the interaction with species.

Table 3-1: Odds ratio (OR) and p-value obtained using MR-QAP for the association between MAP molecular similarity on farm (farms harbouring common VNTR/SSR strains) and the directed (dSPL) or undirected (uSPL) shortest path length between farms, or belonging to the same network community.

	OR	QAP p-value*
Model 1: un-directed shortest path length (uSPL):		
uSPL in same species	0.76	0.1611
uSPL in different species	0.38	0.0001
same island	5.77	0.0008
spatial distance (on a 100 km scale)	1.16 ^a	0.0121
Model 2: directed shortest path length (dSPL):		
dSPL in same species	0.87	0.2251
dSPL in different species	0.47	<0.00001
same island	5.82	0.0011
Spatial distance (on a 100 km scale)	1.15	0.0159
Model 3: same community:		
same community	2.08 ^b	0.033
same species	4.51	0.0001
same island	8.69	0.0001
spatial distance (on a 100 km scale)	1.24	0.0022

* MC p-values, note that it is not possible to obtain directly standard error estimates with this method.

^a For a 100-km increase in the distance between two farms the odds of sharing the same strain increased by a factor of 1.16.

^b If two farms belonged to the same network community the odds of sharing the same strains of MAP were 2.08 times that of farms belonging to different network communities.

Belonging to the same network community was a strong risk factor for harbouring a common MAP strain type on farm (OR = 2.08, model 3). Over and above this network effect, hosting the same species on farm increased the odds of harbouring the same strains of MAP 4.51 times, illustrating again the host-specificity effect of MAP strains.

Being located in the same island was also a strong risk factor for sharing the same MAP strain type on farm (OR between 5.77 or 8.69 depending on the model, Table 1). In the case of Euclidian distance between farms, after accounting for the effect of island and network proximity, increasing distance between farms increased the odds of sharing the same strain.

Goodness-of-fit tests performed on all three models supported an adequate fit of the data.

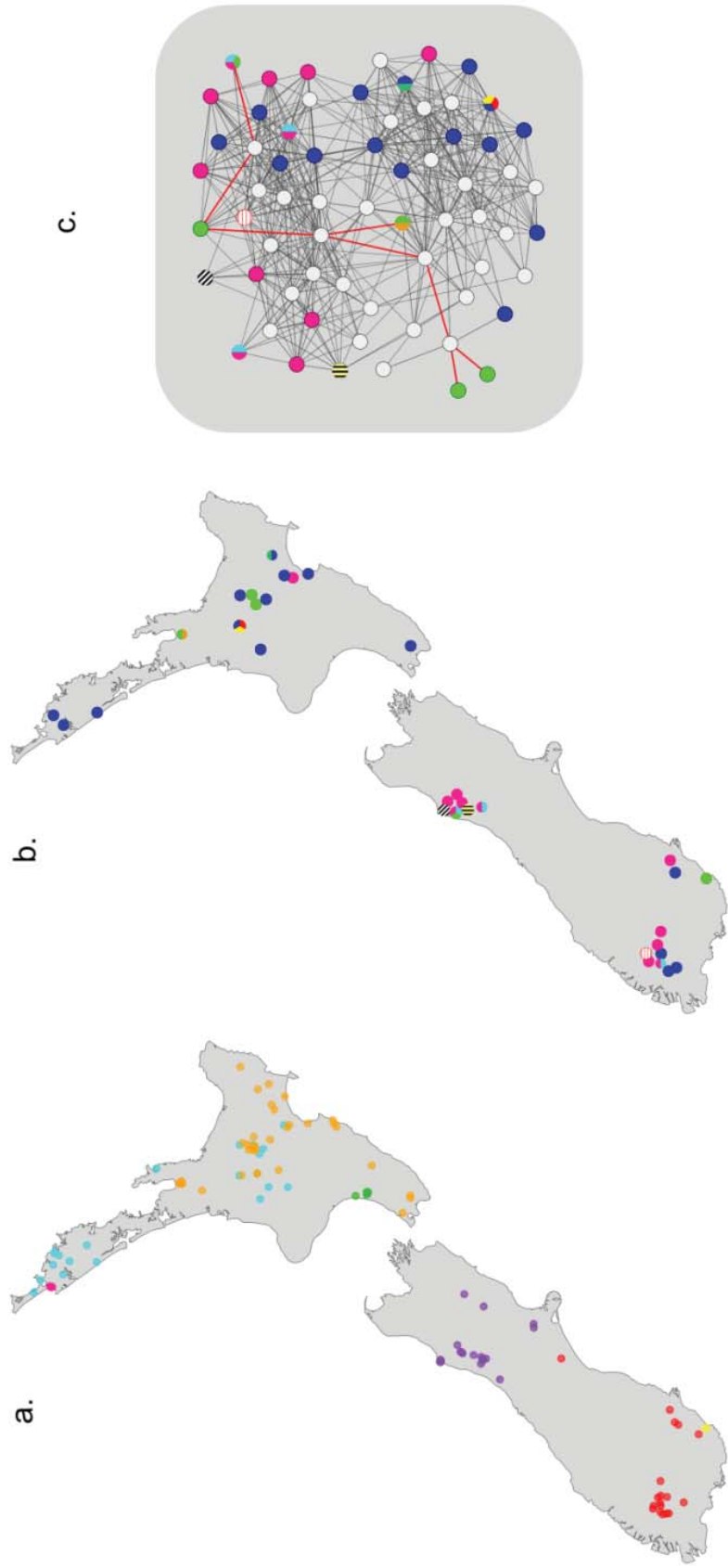


Figure 3-3: : Spatial locations of all 112 Landcorp Ltd. farms of which 2010 movement data were available (a); spatial locations of the 33 farms of which MAP isolates were genotyped, coloured by MAP VNTR/SSR type (b); Fruchterman-Reingold layout of farms (circles) and the network of livestock movements (lines), coloured by VNTR/SSR type (c), as in (b), and including farms without isolates or not sampled (white circles). Only the 33 MAP-positive farms and the farms that were along the shortest path between them were included. For illustration, red lines display all shortest paths linking farms of a single strain (green).

3.5 Discussion

This paper reports on one of few opportunities to analyse potential transmission pathways to support the hypothesis for transmission of MAP between farms. The results presented are consistent with biologically and epidemiologically plausible assumptions on this topic. This observational cross-sectional study of MAP presence on farms showed a significant association between the livestock movement pattern in previous years and the distribution of MAP strains. The specificity of these data is that all observations and corresponding analysis were at the pair level (dyad), hence the results have a dyadic interpretation. Farms that were directly connected via livestock movements were more likely to have strains of MAP in common than farms that were only indirectly connected. Every step further apart along the movement network made it less likely for farms to share a MAP strain. Similarly, farms belonging to the same network community of livestock trade were twice as likely to have common strains of MAP. Hence the clustering of livestock movement and the clustering of strain types were strongly associated, suggesting that livestock movements contributed to the spread of MAP infection from farm to farm.

To the best of our knowledge, there is no similar example in the literature where a longitudinal set of contact data and a cross-section of molecular MAP data were available for the same set of farms. Landcorp Ltd. (LC) is one of the largest farming companies in New Zealand and they represent a relatively closed network of farms with limited contact to farms outside LC (Marquetoux et al., 2016b). This constitutes a very favourable setup to study pathogen transmission.

The consistency of the observed associations across models using various measures of clustering of the livestock movements suggests that our findings are robust. It is noteworthy that the data came from the LC farming population, which is endemically infected with MAP (although to a slightly lesser extent) as is the general farm population in New Zealand (Verdugo et al., 2014a). Hence the LC farms are representative of the wider farm population in NZ. Although one could expect farm to farm spread of paratuberculosis to be more difficult to demonstrate in such endemic areas, our results indicate that it does occur. The national farm-level true prevalence in New Zealand in 2010 was 69% of farms with at least one species on-farm infected with MAP (Verdugo et al., 2014a); livestock movements is likely to be the main driver for maintenance of such a high prevalence level. Comparable outcomes have already been reported for bovine tuberculosis (TB), if not for paratuberculosis. Nationwide cattle movements reportedly had a major impact at spreading bovine TB in the UK, “consistently

outperform environmental, topographic and other anthropogenic variables as the main predictor of disease occurrence” (Gilbert et al., 2005).

In order to draw causal inferences, a longitudinal approach with follow-up of the farms and multiple testing would, however, be preferable for evaluating the temporal change in distribution of MAP strain types on farm over time and relative to trading patterns. We did not have longitudinal strain typing data in each of the years for which movement data were available; hence it was impossible to infer which farm infected which farm. In this respect, it is interesting to note that the undirected SPL was a better predictor for a pair of farms harbouring the same strain type than directed short path length, indicating that trying to infer a direction for transmission of MAP via movements was less efficient than not to. The focus of the analysis was to account for a number of possible confounders by performing multivariable network regression. Consequently, our analysis delivered adjusted measures of association that supported a causal link between livestock movement and MAP transmission. However, the present data cannot be used to infer which MAP strain could become dominant in the case of multiple or sequential introductions from various sources or between an endemic strain and a recently introduced strain. This also depends upon within-herd infection dynamics and the relative virulence of MAP strains, so that such inferences are beyond the scope of this study. Further evidence and more specific study design would therefore be required if more compelling evidence was needed.

3.5.1 Measure of livestock movements

In the present study, a livestock movement event included any of four species (sheep, deer, dairy or beef cattle). We analysed the entire movement network of all species because individual species-specific networks were highly fragmented, rendering them of little use for analysis. In addition, half of the LC farms were mixed-species farms, which meant they could import/export different species with subsequent spread to other species hosted on the recipient farm. The underlying assumption was that given a farm was infected with MAP, the transmission to another farm could occur irrespective of which species was moved, and that different species on the same farm were likely to exchange MAP types. This was a reasonable and plausible assumption for pastoral farms where MAP infection is primarily driven by indirect contact via contaminated pasture and different species are often co-grazed on the same pasture, either concurrently or sequentially. Strong evidence indeed exists from previous research in New Zealand that different livestock species co-grazing in the same pasture were

likely to transmit MAP between each other (Verdugo et al., 2008) and to harbour common MAP strains (Verdugo et al., 2014b).

Both network measures used in the analysis (SPL and community) were a proxy for how closely related via livestock trade the farms were. As such, they were more informative than simply the number of animals moved between farms, as indicated in our analyses (results not shown). The shortest path length represented a measure of distance (as the number of steps) between farms via livestock trade. This LC network was typically “small-world” (Marquetoux et al., 2016b), so that local heterogeneity in the distribution of contacts induced a community structure with denser connections within than average. Hence farms in the same community are more likely to trade with each other compared with farms selected at random. More importantly, they are also likely to share common covariate features (such as farm type or species farmed) and thus play a similar role in the network (Fortunato, 2007). The detection of such communities is therefore highly relevant for epidemiological studies. The LC network consisted of four yearly contact patterns (four layers) evolving over time from 2006/7 to 2009/10 and this longitudinal structure contains information that would be lost if the data are aggregated. Null models underlying the original Louvain method, similar to other network algorithms, cannot handle “multilayer” data (Mucha et al., 2010). Therefore, a generalization of the Louvain method was developed by Mucha et al. (2010) to address the specificity of time-evolving networks that can be represented as a succession of static networks over time. This generalized Louvain method was therefore ideally suited to detect communities in the LC network, while keeping the multilayer format arising from the four year’s data.

3.5.2 Species

It is now well understood that there is no strict specificity between host and MAP type. Ample evidence shows that the main types (type I and II) of MAP organisms, formerly known as respectively sheep and cattle types, can both be isolated from a wide range of hosts (Stevenson et al., 2002). However, a relative specificity of MAP VNTR/SSR sub-types cannot be excluded. A host preference was observed in epidemiological studies (Whittington and Sergeant, 2001). Moreover, it is plausible that farms with the same livestock species cluster within the movement network. Hence the species hosted on a farm may represent a factor confounding the crude effect of movements on MAP strain sharing. We therefore adjusted for this possible confounding effect of species in our multivariable models. In that, we categorized beef and dairy cattle as two distinct species since molecular epidemiology studies in New Zealand show that they tend to harbour different strains (Verdugo et al., 2014b). There was a

significant interaction between SPL and species, the effect of SPL being weaker and not significant when farms hosted the same livestock species. This may be interpreted as a positive host-specificity effect of MAP strains that interfered with the negative effect of increasing network distance (SPL), in other words species accounted for some of the SPL effect in the 'same species' stratum. This observation also indirectly supports the hypothesis that transmission of MAP occurs between species on the same farm (Verdugo et al., 2008; Verdugo et al., 2014b).

3.5.3 Euclidian distance

Local spread occurs over a limited distance and is supposedly not due to direct movements of animals between farms but to more diffuse phenomena, such as run-off waters, fence-to-fence livestock contact with neighbouring pastures or the impact of wildlife reservoirs. The possibility of local spread was evaluated in our study in several ways but was not supported by our data. First, we tested the effect of different buffer distances (farms being at 30, 50 or 100 kilometres from each other) on the probability of sharing the same strain types and there was no significant association (results not shown). Further, we used the Euclidian distance in our models to account for any local spread effect (as would be suggested by a negative association between distance and sub-type sharing). Our results not only did not support a local transmission effect, but increasing distance had an unexpected positive effect on two farms sharing the same MAP strain. This was independent of, or in addition to, the network contact pattern (SPL or network community) and the island effect.

The Euclidian distance between farms, for a fixed SPL, may represent a proxy for movement length; hence the observed positive association could be related to the duration of transport being a stress factor for increased excretion of MAP. Moreover the increase in odds of sharing common strains of MAP when distance increased was two to three times more important for pairs of farms situated across islands than for farms on the same island (results not shown) although the interaction between Euclidian distance and same island was not significant. This suggests that crossing the Cook Strait by ferry, causing animals to be on trucks for extended periods of time, may increase the excretion of MAP as a consequence of transport stress. This could facilitate the transmission of infection to the destination farm. Another plausible explanation may be that older animals (breeding stock) could be more likely to be transported long distances whereas young stock would travel shorter distances for agistment purposes. Although young animals can shed MAP in their faeces, the probability and the amount of

shedding tends to increase with age (Antognoli et al., 2007) which could contribute to the observed association with distance.

Previous work about the spread of bovine tuberculosis in brushtail possum populations in New Zealand found little evidence of local spread (Porphyre et al., 2008). This observation is consistent with our findings for paratuberculosis, although the epidemiology of paratuberculosis and tuberculosis are distinctly different. However, our study was not ideally suited to observe the local transmission of MAP from spatial neighbourhood. LC farms were mostly located too far apart for any physical spatial contact through wildlife, run-offs, water ways, or effluents, hence likely exceeding the range at which local transmission can occur.

3.5.4 Island

Our data show that a pair of farms on the same island was more likely to share the same MAP strain than a pair of farms on different islands. This strong effect of strain clustering within islands was consistent with a previous study (Verdugo et al., 2014b). The observed island effect may be attributable to island ecology and evolution. The vast majority (97%) of movements between LC farms occurred within either the North or South Island. It is hypothesised that the observed island segregation of MAP strains was either caused by independent initial pathogen introductions to each of the two islands and/or further strain evolution with mixing primarily within island due to the topographic constraints limiting trans-island movements across the Cook Strait. Even though this observed island effect was likely due to clustering of livestock movements within island, it remained highly significant after adjusting for the effect of livestock movements. This may indicate that four years of movement data only were insufficient to show long-term effects on strain distribution. The island effect may thus be a proxy for past movements, capturing decades of evolution driven by livestock movements clustering within island which was not represented in our movement data. This was a very strong factor for strain sharing (ORs for island in the two models were 5.8 and 8.7, respectively).

Since movements were highly clustered within island, there was a high collinearity between the measures of SPL or community and island. As an example, two farms that were not on the same island never belonged to the same network community (see Figure 3-3). This collinearity caused a large standard error for the estimated coefficients (that translated in our results by larger p-values). However, since island had a strong effect on the MAP strain distribution irrespective of the movement pattern, we preferred to adjust for this “island effect”, even though the strong collinearity would have justified removing island as a covariate, especially

for the model with community as exposure of interest. Nevertheless, a model without island and distance (the effect of distance without adjusting for island would be meaningless in our study) resulted in similar coefficients for both community (0.83 instead of 0.73) and species (1.45 instead of 1.51), but with much smaller p-values for community exposure ($p=0.007$ instead of $p=0.033$).

3.5.5 Genetic resolution

The degree of genetic resolution to identify MAP strains was important for evaluating farm-to-farm transmission. VNTR genotyping is a PCR-based subtyping method with good discriminatory power (Thibault et al., 2007), offering an effective alternative to the technically demanding yet poorly discriminating restriction fragment length polymorphism (RFLP) or the more costly whole genome sequencing (WGS). Further use of SSR sequencing adds to the resolution of VNTR, since SSR analysis was demonstrated to be highly discriminatory for characterising different strains as well as for identifying epidemiologically and genetically related strains of MAP (Amonsin et al., 2004). These features are required for suitable molecular epidemiologic studies. The combination of VNTR and SSR typing was therefore deemed appropriate as a marker for epidemiological tracking of longitudinal transmission of MAP (Thibault et al., 2008).

Tandem VNTR and SSR genotyping was also used in Australia in 2014 to explore the incursion of MAP in low-prevalence areas of the country (Oakey et al., 2014). By combining these genotyping methods with trace-forward cattle movement history, the analysis allowed clarification of how two cases of infected farms in Queensland were likely to have resulted from two independent incursions rather than an existing epidemiological link via cattle movements between the farms.

However, recent work comparing whole genome sequencing versus VNTR typing shows some limitations of the latter (Ahlstrom et al., 2015). First, VNTR typing may not capture the same amount of genetic variation as WGS, due to lack of discriminatory power and a frequently observed phenomenon of convergent evolution. As a result, VNTR may fail to uncover the true genetic diversity based on the number of SNP differences. In our study, the two most frequent strain types were detected in a total of nearly 70% of isolates (Figure 3-2). It is possible that a more discriminant genotyping method may have detected more distinct genetic lineages among these groups. In our analysis, additional information provided by SSR8 addressed this problem only partially by breaking the third most frequent strain type into three further groups, but leaving the dominant strain type the same. Increased discriminatory power to

detect the relationship between isolates may help in clarifying the transmission patterns between farms. On the other hand, if the genetic diversity had resulted in many more than the 11 distinct strains as in our analysis, it could have become more difficult to see an association between communities of strains and communities of movements. The extreme would be to find different strains on each farm, which would result in a strain-type -sharing network completely disconnected. This problem was noted by VanderWaal et al. (2014). Secondly, the opposite phenomenon was also observed in about 10% of Canadian MAP isolates, for which less than ten SNP differences existed (hence were virtually from the same lineage) although they belonged to different VNTR types (Ahlstrom et al., 2015). Incorrectly classifying strains as different when they were the same would equally impair inferences about transmission and represents another possible limitation of VNTR/SSR genotyping.

The increased resolution of WGS compared with the MAP lineage, could prove more useful than VNTR genotyping for inferences about MAP transmission. A study following an outbreak investigation of *M. tuberculosis* in British Columbia showed how the additional resolution of WGS over VNTR genotyping helped to clarify the role of social interactions between individuals (as per contact tracing surveys) by detecting relevant epidemiological linkages (Gardy et al., 2011). It would be desirable to gain more insights into the genetic diversity and relatedness of MAP organisms in New Zealand through WGS in comparison to the current genotyping system.

In the present study the genetic criterion for inferring a transmission was that two farms shared the same strain, rather than phylogenetic trees and genetic distances based on minimum spanning trees as is often done with VNTR-SSR typing (Thibault et al., 2008; Pradhan et al., 2011; Oakey et al., 2014). Sharing the same strain seems a more robust epidemiologic criterion than genetic distance (VanderWaal et al., 2014; Ahlstrom et al., 2015). Moreover, even where WGS data are available, previous research shows that inferring transmission networks from genetic distance based on phylogenetic trees can be misleading, sometimes no better than random source attribution in building infection trees (Worby et al., 2014). Similarly, a high level of uncertainty was obtained in developing a transmission network from WGS data for a real-world TB outbreak investigation (Didelot et al., 2014). For bovine TB transmission between cattle herds or between badgers and cattle using WGS, “despite unprecedented resolution” the direction of transmission was impossible to infer (Biek et al., 2012).

3.5.6 Statistical Methods

For analysing dyadic data, the dependency structure inherent to social relationships should be considered (Borgatti et al., 2013; Scott, 2013). Two main families of methods can be identified in the literature to address inference making in social networks: permutation methods and Exponential Random Graph Models (Snijders, 2011).

We used a permutation-based method of QAP as a straightforward tool for evaluating an association between the distribution of MAP strains in the farm population and the movement pattern between farms, while adjusting for important possible confounders (Pinter-Wollman et al., 2013). Appropriate QAP methods thus allow epidemiological inferences to be made for relational data with robust inference. A simple derivation of the Mantel test is not necessarily appropriate when analysing social network data where multi-collinearity, correlations and right-skewness are prominent features (Anderson and Legendre, 1999). Double semi-partialling QAP is a permutation method based on Monte Carlo simulation that was developed to handle multiple regression of multi-collinear data with auto-correlation typical of that observed in network adjacency matrices (Dekker et al., 2007). This method was well suited for our data, especially since we wanted to account for possible confounding effects.

Due to multiple correlations between covariates (for example between community belonging and being on the same island), the fully adjusted models potentially overestimated the standard errors for network exposure variables leading to overly conservative inferences. However, the multivariable approach to network regression allowed us to estimate adjusted, high resolution network effects, which is particularly suited for epidemiological inferences.

MR-QAP was similarly implemented by VanderWaal et al. (2014) who addressed a similar problem: assessing inter-species transmission of pathogens among ungulates in Kenya. The results of the VanderWaal et al. (2014) study showed that sharing similar strains of *E. coli* was positively associated with: (a) ungulates of the same species, (b) samples being collected on the same side of a river and (c) individuals of different species that were more frequently associated with each other. The authors thus inferred transmission dynamics and pathways for this pathogen.

3.6 Conclusion

This study combines social network analysis and molecular evidence from pathogen strain typing to assess the potential of farm to farm spread of MAP, the causative agent of paratuberculosis. We report a strong association between longitudinal movement data of four

livestock species between farms across four years and the cross-sectional distribution of MAP strains in the same population of farms. This association remained significant after adjusting for confounders, such as geographic location (North Island versus South Island) and species on-farm, both known to be determinants of the MAP strains found on farm. Our results support the hypothesis that livestock movements contribute to the spread of paratuberculosis in a population where a large proportion of farms were already infected. This highlights the relevance of risk-based trade as implemented in Australia or the Netherlands or movement restriction as in Denmark (Geraghty et al., 2014) for the control of paratuberculosis.

3.7 Acknowledgements

This study was partially funded by the New Zealand Johne's Disease Research Consortium and Landcorp Farming Ltd. and stipends were granted by Massey University and New Zealand International Doctoral Research Scholarship. We thank Gordon Williams from LC for access to the movement data, G. DeLisle and D. Collins (AgResearch NZ) for culture and strain typing, Marian Price-Carter (AgResearch NZ) for her expert advice and help in interpreting the strain typing data. Gratefully acknowledged are Geoff Jones (Massey University's Mathematics and Statistics Group), Ian Dohoo (Atlantic Veterinary College, Prince Edward Island, Canada) and Christopher Jewell (Lancaster University) for invaluable comments about statistical data analysis, Carter Butts (University of California, Irvine) for elaborate explanations about permutation methods for network models and ERGM specification, Peter Mucha (University of North Carolina) for helping to implement the generalized Louvain method, and Matthieu Vignes (IFS, Massey University) for his help with the Matlab code.

Chapter 4. A synthesis of the patho-physiology of *Mycobacterium avium* subspecies *paratuberculosis* infection in sheep to inform mathematical modelling of ovine paratuberculosis

Nelly Marquetoux^a, Rebecca Mitchell^b, Peter Wilson^c, Anne Ridler^c, Cord Heuer^a

^a *EpiCentre, Institute of Veterinary, Animal and Biomedical Sciences, Massey University, New Zealand*

^b *Department of Population Medicine and Diagnostic Sciences, Cornell University, Ithaca, NY, USA*

^c *Institute of Veterinary, Animal and Biomedical Sciences, Massey University, New Zealand*

4.1 Abstract

To inform a mathematical disease simulation model, we reviewed and synthesized evidence about the pathogenesis of ovine paratuberculosis (PTB). The main outcome was the model structure, shown in Figure 1 at the end of this chapter, which served as a basis to develop a compartmental PTB model. Several possible outcomes following exposure to MAP were identified: (1) mere colonization of the small intestine (latent infection), (2) active infection with the presence of inflammatory histopathology in the intestinal tissues (mild disease), associated with low faecal shedding, (3) affection by MAP causing severe intestinal pathology, reduced production, onset of clinical signs and high faecal shedding. Latent infection was an uninformative outcome for modelling ovine paratuberculosis. Conversely, the presence of histological lesions and their grade appeared as a good marker of active infection and progression through different disease stages. It is possible to recover from mere infection and from early disease. We therefore identified two possible pathways following infection with MAP: (1) non-progression leading to recovery and (2) progression to clinical disease and death. Findings from studies using experimental and natural exposure to MAP were generally comparable. This review suggested that host-level characteristics (age at exposure and breed) as well as pathogen-level covariates (MAP dose, strain and inoculum type for experimental infection) had a strong influence on the outcome of exposure to MAP. However, the review

was an aggregation of disparate studies with low numbers of sheep and the presence of study level confounders, hindering comparisons between and across studies. Hence, it was very difficult to formally validate the stated assumptions and to quantitatively estimate model parameters using this review process. For example, from individual studies it was not possible to calculate a consistent value for the proportion of sheep exposed to MAP entering the pathway to clinical disease versus the recovery pathway. We conclude that a meta-analysis should be conducted to complement this work. This would enable; (1) a systematic approach, (2) pooling of the data across studies to increase power for testing stated assumptions generated in this review and, derive meaningful model parameters and (3) bias to be quantified and adjusted for.

4.2 Introduction

Ovine paratuberculosis (PTB) is a chronic enteritis that can result in a fatal wasting condition, caused by infection of the intestinal tract with *Mycobacterium avium* subsp. *paratuberculosis* (MAP). A proportion of sheep infected with MAP experience subclinical- and clinical-production effects and mortality detrimental to animal wellbeing and farm economics. For the purpose of this review, the term PTB refers to clinical and subclinical manifestation of MAP infection, *i.e.*, the presence of pathology due to MAP, as distinct from MAP latent infection *per se*. The terms ‘clinical PTB’ and ‘ovine Johne’s disease’ (OJD) are used interchangeably. With reference to MAP ‘strain type’, we only consider the main types, so-called ‘cattle strain’ for MAP type II and ‘sheep strain’ for MAP type I/III. However, throughout this document ‘ovine PTB’ refers to sheep presenting paratuberculosis pathology, irrespective of the strain type.

Historically, sheep were commonly used as a convenient ruminant subject for experimental infection with MAP, either as a model for bovine paratuberculosis (Brotherston et al., 1961a), or to better understand ovine PTB in countries where OJD was perceived as a problem (Begg and Whittington, 2008). Hence, published data of experimental or natural infection of sheep with MAP are abundant.

We aimed to develop a compartmental mathematical model to simulate MAP infection in a sheep flock as well as the subsequent pathology and associated production effects at the flock level. This modelling approach enables the study of the infection dynamics, epidemiology, economics, and possible control strategies of paratuberculosis within a flock. Developing a compartmental model for ovine PTB requires synthesizing important phases of the pathogenesis of ovine PTB. The model ideally captures mechanisms of infection and

transmission including shedding stages, shedding levels and force of infection. It should also identify disease stages in which animals are affected by MAP and potential production effects.

The purpose of the present review was to synthesize information to inform an evidence-based, state-transition model of MAP infection and ovine PTB. The initial intentions were to inform the design of the model structure (qualitative synthesis of the pathogenesis), and to parameterize the model (quantitative synthesis of the pathogenesis). However, it proved difficult to draw robust quantitative estimates to parameterize the model because evidence gathered in this review was too disparate. This necessitated narrowing the scope of this work to a qualitative study of pathogenesis of ovine PTB. This work was then complemented with a systematic review and meta-analysis (Chapter 6) that enabled robust quantitative parameter estimation.

This paper synthesizes knowledge from natural and experimental infection of sheep with MAP. The objectives were to:

- Review current knowledge to synthesize an updated understanding of the patho-physiology of PTB to inform a mathematical model of MAP.
- Identify knowledge gaps and generate biologically plausible assumptions that can thus be further explored using a meta-analysis framework.

A model structure was developed based on the results of the first part of this review, presented in Figure 4-1.

4.3 Assumptions for a candidate model structure

The first objective was to establish the patho-physiological pathway following infection with MAP, and identify relevant infection stages. These could then be used to build the simplest possible model that adequately captures the dynamics of infection with respect to transmission and production effects. For that purpose, we have mostly used published evidence of experimental challenge studies with MAP, as well as limited input from observational studies about the pathogenesis of paratuberculosis. These observational studies all presented evidence of natural challenge with MAP under commercial farming conditions. The aim was to model natural paratuberculosis in a sheep flock. Findings from experimental challenge therefore needed to be extrapolated to naturally occurring paratuberculosis. It will be indicated whenever evidence reviewed pertains to natural challenge rather than experimental infection.

4.3.1 Pathological outcomes following artificial inoculation with MAP

Understanding the pathological outcomes of infection with MAP allows the definition of relevant stages in disease progression, as the compartments of a state-transition model.

4.3.1.1 Infection with MAP

A sheep becomes infected with MAP following ingestion of a dose high enough to cause uptake of the bacterium in the intestinal wall. This is followed by replication and at least short-term persistence (as opposed to passive passage in which ingested organisms pass through the intestinal tract without invasion of intestinal wall *per se*). This obligatory colonization of tissues with MAP corresponds to 'mere' tissue infection. An *in vivo* study of lamb intestinal loops shows that this uptake occurs within hours of MAP being in contact with the intestinal wall (Ponnusamy et al., 2013). Another study on ovine macrophage cultures (Abendaño et al., 2014) showed that uptake of 52 to 86% of MAP inoculum occurred within two hours, for various strains of MAP (both C and S type).

This early infection stage is ordinarily referred to as latent infection. It is not necessarily associated with, nor predictive of pathological outcomes such as faecal shedding, intestinal histopathology or gross lesions, and clinical signs. Hence, in the absence of such markers of disease, mere colonization of the intestinal tract by MAP can be difficult to recognise. Identification, based on diagnostic tests such as tissue culture, also have poor sensitivity at this stage of infection. Tissue PCR is at this stage the most sensitive technique (Delgado et al., 2012; Preziuso et al., 2012). More information about the relative sensitivity of different diagnostic tests can be found in Chapter 5. Although tissue PCR is not commonly used to detect MAP infection, few studies using this technique found that nearly all experimentally inoculated sheep had PCR-positive tissue (Fernandez et al., 2014; Fernandez et al., 2015). This indicates the presence of MAP DNA within the intestinal wall. One study demonstrated, by using tissue PCR, that even low inoculum doses of MAP (approximately 10^3 CFU repeated four times) were sufficient to establish intestinal infection in most artificially challenged sheep despite the absence of detectable tissue lesions and while faecal culture was always negative (Delgado et al., 2012). Similarly, infection was undetectable by tissue and faecal culture after 14 weeks, in sheep inoculated with doses below 10^4 MAP (Reddacliff and Whittington, 2003). These sheep had been successfully exposed to MAP, as a fraction of them developed a positive

IFN γ response. Mere colonization can be only transitory in some animals because complete clearance of infection has been observed (Gilmour et al., 1977).

Latent infection does not contribute to infection dynamics in the absence of faecal shedding, and is not associated with any detectable production loss. Moreover, for animals that go on to develop specific histological lesions, the latent stage can be relatively short with intestinal lesions appearing as early as a few weeks post exposure to MAP (Begara-McGorum et al., 1998). Hence, it is irrelevant to model the latent stage. It is more appropriate to model the rates at which susceptible sheep enter into an “active” infection stage, associated with some detectable modification of the histological structure of the intestine and faecal shedding following ingestion of MAP.

4.3.1.2 Pathology caused by MAP

Active infection, as opposed to mere colonization (here onwards referred to as latent infection), can be defined as a stage during which MAP can be detected in tissues, combined with at least some detectable inflammatory host immune response to MAP.

Onset of active infection and progression through disease stages can thus be assessed by monitoring intestinal histological lesions typical of PTB (Clarke and Little, 1996). Intestinal lesions of naturally infected sheep can be located in the jejunum, ileum and ileal lymph nodes. The small intestine, in particular the ileal wall, is more severely affected than the afferent lymph nodes (Kluge et al., 1968; Dennis et al., 2010; Preziuso et al., 2012). Hence, while latent infection is often assessed by culture or PCR of intestinal and afferent mesenteric lymph node tissues (Brotherston et al., 1961a; Brotherston et al., 1961b), active infection may be better ascertained by histopathology of intestinal tissue (ileum and jejunum) rather than mesenteric lymph nodes (Nisbet et al., 1962; Begg et al., 2010). Mycobacterial presence is more abundant in intestinal mucosa than in the draining mesenteric lymph nodes (Clarke and Little, 1996; Dennis et al., 2010), thus making the assessment of pathology more accurate in the former.

The severity of lesions determines whether the ileal wall ultrastructure, and therefore its function, is affected or not. A histological scoring system, grading lesion severity as type 1, 2, 3a, 3b and 3c, was developed by Pérez et al. (1996) to score ileal wall lesions. Type 1 and 2 are defined as mild lesions consisting of small focal granulomata of epithelioid cells limited to the Peyer patches (type 1), or extending to the mucosa adjacent to Peyer patches (type 2). Acid Fast Bodies (AFB) are absent or very scant (Pérez et al., 1996). Severe lesions (type 3) present a multifocal to diffuse cellular infiltration, which extends to areas of the mucosa not associated

with lymphoid tissues (Pérez et al., 1996). They extend beyond the lamina propria into the submucosa (Clarke and Little, 1996), resulting in a thickening of the intestinal mucosa and atrophy of villi. This alters the capacity of absorption of the small intestine, which is likely to cause clinical PTB. Type 3b and 3c lesions, involving diffuse granulomatous enteritis, are considered the more advanced type (Pérez et al., 1996; Clarke, 1997). They are associated with typical macroscopic lesions at *post-mortem*. The multifocal nature of type 3a lesions is evocative of early development of type 3b lesions (Pérez et al., 1996). Although not as severe as diffuse lesions, and not usually described in clinical cases of PTB, they cause an alteration of the ultrastructure of the ileal wall with the enlargement of involved villi (Pérez et al., 1996). These lesions have been shown to be likely predictive of the development of clinical PTB (D. Begg, Personal Communication, February 2012).

The degree of MAP tissue colonization also allows for the differentiation between paucibacillary lesions presenting no or few AFB and multibacillary lesions presenting abundant AFB (Clarke and Little, 1996; Kurade et al., 2004). For diffusely infiltrated lesions, the paucibacillary type (3c) and the multibacillary type (3b) differ, beyond the relative paucity/abundance of AFB, by the nature of the cellular infiltrate. Multibacillary lesions are characterized by a diffuse granulomatous enteritis with massive infiltration of mostly macrophages and epithelioid cells (Pérez et al., 1996; Smeed et al., 2007; Smeed et al., 2010; Preziuso et al., 2012), while lymphocytic and neutrophilic infiltration is usually mild (Clarke and Little, 1996). These lesions were described historically as lepromatous-type lesions (Clarke and Little, 1996). On the other hand, the dominant cell type in paucibacillary lesions in sheep is lymphocytic (Pérez et al., 1996; Preziuso et al., 2012), with T cells and eosinophils (Smeed et al., 2007) located mainly within the lamina propria (Kluge et al., 1968; Preziuso et al., 2012). Paucibacillary lesions were also referred to as tuberculoid-type lesions (Clarke and Little, 1996). In one study of natural infection, where serial biopsies of the same set of animals were performed over time, one animal (out of 77 followed up) interestingly evolved from 3c paucibacillary lesions to 3b multibacillary. In lesions of type 3a, two distinct patterns of infiltration (tuberculoid and lepromatous) are present (Kurade et al., 2004). This suggests these lesions might represent a “crucial transition stage” between the two pathogenesis types. Type 3a lesions are thus sometimes also called “borderline lepromatous” (Pérez et al., 1996). In pathogenesis studies of clinical PTB, paucibacillary lesions usually refer to the most severe 3c lesions rather than mild type 1 and 2 lesions, which are less commonly observed in advanced cases (Clarke and Little, 1996; Preziuso et al., 2012).

While the onset of histological lesions represents entering an active infection stage, the evolution to type 3 lesions represents an adequate marker of progression towards clinical disease. However, a number of studies dichotomize the lesion type between pauci- versus multibacillary rather than severe versus mild. As such, the progression to multibacillary lesions in terminal ileum appears as an end-stage, irreversible condition (Dennis et al., 2010). This is associated with permanent faecal shedding of high concentrations of MAP (Whittington et al., 2000; Kurade et al., 2004; Reddacliff et al., 2006; Kawaji et al., 2011). Moreover, diffuse intestinal lesions (3b, 3c) are nearly always associated with the expression of clinical disease, both in naturally and artificially infected sheep (Clarke and Little, 1996; Whittington et al., 2000; Kurade et al., 2004; Reddacliff et al., 2006; Dennis et al., 2010; Preziuso et al., 2012). The multibacillary stage of the disease would also be a phase where infection is more likely to disseminate to extra-intestinal tissues (Clarke and Little, 1996; Smeed et al., 2007).

In a pathological study of naturally infected sheep, between three and five years old, presenting with advanced PTB (ELISA positive animals presenting histological lesions), MAP was detected by tissue PCR in the udder. In this study, all 10 sheep showing type 3b lesions were positive to MAP in the udder, as well as six out of nine sheep presenting type 3c lesions (Preziuso et al., 2012). All sheep with 3b lesions were clinically affected, along with some sheep with 3c lesions. From studies where the Perez score was used, it appears that the type of paucibacillary lesions associated with clinical disease is the diffuse type 3c (Clarke, 1997; Preziuso et al., 2012). Multifocal 3a lesions were not reported in clinical cases, hence representing the early development of the pathognomonic pathological presentation of the disease in sheep (Clarke, 1997).

Thus, it is important to emphasise that, in sheep at least, both pauci- and multibacillary types can be pathogenic and it is not clear whether they “represent sequential or divergent stages of PTB” (Clarke, 1997). As a result, the fate of sheep presenting severe lesions appears similar irrespective of MAP abundance in the tissues: to progress to clinical disease. However, the shedding level between pauci- and multibacillary animals may differ by several orders of magnitude (see 4.3.1.3), and hence their relative contribution to the infection dynamics in the flock is different. It is therefore relevant to estimate their relative proportion among the subset of clinically affected animals. In a study where 77 naturally challenged sheep were followed over three years (Dennis et al., 2010), 12 sheep developed clinical PTB, among which 10 had multibacillary and two had paucibacillary gut lesions at the time of death. Similarly, in a random sample of clinical cases of PTB from heavily infected flocks (n=45 sheep) (Clarke and Little, 1996), all animals harboured severe lesions and 14 were classified as paucibacillary with

lesions corresponding to type 3c. In a vaccine trial (Reddacliff et al., 2006) in which sheep were followed for 3.5 to 4.5 years and mortalities closely recorded, the cumulative number of clinical cases over the study period among the controls was 80, among which 88% were multibacillary. Lastly, in a longitudinal experiment mimicking natural infection of PTB, 22 sheep died following the onset of typical clinical signs of PTB, among which 15 animals underwent histopathology and all of them presented with multibacillary lesions in their guts (Abbott et al., 2004). If we pool these results, we obtain a proportion of $(14+2+10+0) / (45+12+80+15) = 17\%$ clinically affected sheep presenting paucibacillary lesions and the rest with multibacillary lesions. Relative shedding levels for these categories have yet to be investigated.

4.3.1.3 Shedding level of infectious sheep

Semi-quantitative shedding data can be obtained using quantitative PCR. Kawaji et al. (2011) experimentally inoculated 38 sheep with MAP. They compared shedding rates according to the histological status. This showed that sheep harbouring multibacillary lesions (n=10) shed about 10^4 times more (in femtograms of DNA) than the sheep with paucibacillary lesions (n=18). In this experiment, the average shedding level of inoculated sheep which were histology negative at necropsy (n=10) was not significantly different to that of the sheep with paucibacillary lesions.

There is not only a scale difference in the amount shed between low and high shedders, but among the low shedders, shedding is often only intermittently detected (Stewart et al., 2004; Begg et al., 2010). On the other hand, continuous shedding is associated with multibacillary cases (Whittington et al., 2000). Quantitative faecal excretion of MAP was studied in an experiment involving seven naturally infected sheep selected based on AFB present in their feces, from a flock with clinical PTB (Whittington et al., 2000). Daily excretion was monitored by culture for 11 days and two groups were identified: four sheep retrospectively classified as multibacillary were shedding every day. While three sheep, with no other detected evidence of infection, were shedding intermittently on days 1/11, 3/11 and 4/11. This represents a shedding occurrence on average 24% of the time (on a daily basis) for intermittent shedders. Faeces from five of these sheep, including four multibacillary persistent shedders and one intermittent shedder, were pooled and prepared to estimate the total amount of MAP excreted over 15 days by end-point titration. The total faecal output was estimated to contain 6.27×10^{12} MAP. Considering the contribution of the intermittent shedder as negligible compared with the amount shed by the multibacillary cases, we calculated a daily excretion of MAP for multibacillary animals as approximately 1×10^{11} MAP per day. Given that paucibacillary

cases shed 10^4 times less and on average only 24% of the time, the average excretion rate for paucibacillary animals could be estimated at 2.4×10^6 CFU/day. The design of this experiment was robust and measured our outcome of interest (shedding quantities and frequencies in sheep with natural PTB), with little possible bias despite, being based on a small number of animals over a limited period.

These figures thus inform mathematical models about the rate of environmental contamination of MAP for compartments of paucibacillary and multibacillary shedding sheep.

4.3.1.4 Conclusion: pathological outcomes

- Latent MAP infection does not contribute to the transmission of infection or to sub-/clinical production effects of ovine PTB. Hence, there is little justification for inclusion of a latent infection status in a mathematical model of infection dynamics and economic effects.
- Animals presenting severe lesions, usually referred to as sub-clinically and clinically affected sheep, are a subset of actively infected sheep suffering production losses due to PTB.
- Paucibacillary lesions (type 1, 2, 3a, 3c) are associated with low and possibly intermittent shedding. Multibacillary lesions are associated with high and persistent shedding. It is biologically plausible that the presence of few or numerous AFB in lesions in the small intestine should correlate well with low or high shedding of MAP in faeces, respectively. This must be reflected in the shedding rates of the various active infection compartments.

4.3.2 Progression pathways

A number of studies support the existence of two possible pathological pathways following infection with MAP: one leading to recovery and the other to progressive disease. These distinct pathways can be evaluated by multiple testing strategies identifying infection load within host tissues, damage to the host and shedding into the environment. Recovery can be illustrated by a variety of outcomes, *e.g.*, a lack of progression to clinical disease, a regression of specific lesions (recovery from disease) and the potential clearing of MAP infection from the tissues (recovery from infection).

4.3.2.1 Immunological response

The feature of immuno-pathology of PTB is a polarization of the immune response for a given animal at a given point in time. The host immune response is either predominantly cell mediated (Th1 oriented) in paucibacillary animals, or predominantly humoral (Th2 oriented) in multibacillary animals (Chiodini et al., 1984; Pérez et al., 1996). This polarisation of immunity is controlled by the activation of distinct cellular receptors and cytokines (Abendaño et al., 2014). This determines two differing patterns of T cell activation in the two pathological types (Smeed et al., 2007; Smeed et al., 2010). Cytokines such as IFN γ and interleukin-10 (IL-10) are thought to be pivotal in the establishment or the failure, respectively, of a Th1 mediated protective immune response.

Pro-inflammatory IFN γ mediates the adaptive immune response against intra-cellular pathogens (Koets and Gröhn, 2015). High levels of IFN γ are observed in early stages of infection, whereas a decline of IFN γ is predictive of progression to severe pathology and disease (de Silva et al., 2013). Genetic expression of IFN γ is up-regulated in intestinal tissues of sheep presenting paucibacillary disease compared to multibacillary (Smeed et al., 2007).

On the other hand, IL-10 is an immuno-suppressive cytokine induced by MAP to evade the cell-mediated adaptive immune system, thus allowing the persistence of MAP in the macrophages (de Silva et al., 2013; Koets and Gröhn, 2015). In the early days of infection, a correlation was noted between an increased anti-apoptotic, anti-destructive response by macrophages infected in vitro, and the survival of MAP in these macrophages (Abendaño et al., 2014). This was mediated by differential cytokine regulation, in particular upregulation of anti-inflammatory IL-10 and down-regulation of pro-inflammatory IL-2. The level of IL-10 increases progressively in infected animals as the disease progresses (de Silva et al., 2011; de Silva et al., 2013). However, the precise role of IL-10 is not yet fully elucidated. The cytokine is thought to be associated with the failure of Th1 mediated adaptive immune response and hence is used as a marker of disease progression. However, an elevation of IL-10 levels in peripheral blood can be observed as early as four months post-inoculation in experimentally infected sheep (de Silva et al., 2011) and, is associated with resistance to disease later in the course of progression (de Silva et al., 2013). This suggests that the immunosuppressive effect of IL-10 might have a protective effect at the animal level by limiting the damage of the intestinal tissues (de Silva et al., 2013; Koets and Gröhn, 2015), at least in animals that control the infection. It is not clear however, whether measures of the adaptive immune response adequately reflect the local intestinal immunity (Koets and Gröhn, 2015). High peripheral blood levels of IL-10 could also

result from a failure act locally. A variation of the adaptive immune response and particularly the expression of IL-10 can be observed at various sites (blood versus mesenteric lymph nodes versus ileal tissue). The existence of distinctly different immune pathways can also be illustrated by the clear differences in the IL-10 response pattern between paucibacillary and multibacillary sheep. IL-10 is upregulated in the ileal wall of sheep with multibacillary disease presenting a Th2 dominant response (Smeed et al., 2007). On the other hand, de Silva et al. (2011) observed that the secretion of IL-10 in the mesenteric lymph nodes was lower in multibacillary sheep compared to paucibacillary.

This immune polarization was thought to be relatively antagonistic (Clarke, 1997). Thereupon the cell-mediated immune response would correspond to a “controlled” infection observed in early stages and paucibacillary disease. A later switch to a non-protective humoral response would then be associated with multibacillary disease, determining the onset of clinical disease. An excessive cell-mediated immune response reportedly led to advanced inflammation of the intestine walls in severe paucibacillary cases referred to in 4.3.1.2. (Chiodini et al., 1984; Clarke, 1997). Thus, paucibacillary infection can also be at the end stage of PTB in sheep unlike cattle (Smeed et al., 2007). A switch between Th1 and Th2 responses could be triggered by various factors: T cell exhaustion, MAP exposure dose, macrophage bursting size and other host-level metabolic triggers (Koets and Gröhn, 2015).

However, recent research suggests a more complex immunologic response to MAP infection than the classical switch hypothesis (early predominance of Th1, then Th2 response). This was based on the observation that half the sheep experimentally infected with MAP actually presented a combined antibody and $INF\gamma$ response at an early stage of infection (Begg et al., 2011). Simultaneous cellular and humoral responses were also observed (Fernandez et al., 2015), as well as a lack of early interferon gamma production in sheep with only focal intestinal lesions. A transient early elevation of IL-10, as well as B cells, was noted in cattle (Koets and Gröhn, 2015). Moreover, recent research on bovine tuberculosis suggests that $INF\gamma$ may be more correlated with bacterial load and lesion severity, which can fluctuate over time within an individual, rather than a marker of protection (Koets and Gröhn, 2015). These recent breakthroughs in immuno-pathology of mycobacterial infection conclude that progression to disease could result from a generalised failure of the immune system where the Th1 response fails first, rather than switches.

4.3.2.2 Presence of MAP in intestinal tissues

The presence of MAP organisms in intestinal tissues of infected sheep can be demonstrated directly by culture, or indirectly by the presence of microscopic lesions characteristic of PTB. These methods, based on serial biopsies or sequential necropsies, can show the onset of infection or pathology. This is followed by two possible pathways, a progressive infection towards disease in some sheep or, a recovery (resolution of lesions and/or clearing of infection) in others.

According to the experiment of Begara-McGorum et al. (1998), neonatal lambs can become histologically positive in their Peyer's patches as early as 18 days after inoculation, although such early lesions may not harbour visible MAP. Those authors proposed early MAP distribution as an indication of initial local propagation within intestinal tissue followed by a dissemination phase.

Similarly, one month after the end of a 10-week challenge period in which 1.8×10^8 total CFU was administered, MAP could be detected by culture in the intestinal mucosa of 13/14 sheep slaughtered early in the study. MAP was detected in quantities estimated between 1.6×10^4 to 10^6 viable MAP/g of mucosa, thus indicating an intestinal location of MAP with likely active division of the organism (Gilmour et al., 1965b). In a second group slaughtered nine months post challenge, 9/14 were intestinal culture positive, suggesting a decrease⁵ of infection load in the guts over time for some of the sheep. A second experiment in the same paper, using the same inoculum dose, suggested a possible recovery from pathology. While 8/10 sheep culled at any point in the first year after inoculation harboured MAP specific intestinal lesions, only 3/8 sheep culled 18 months after inoculation did⁵.

A 1968 study involved three-week-old lambs (n=18) given a single oral challenge of 10^{10} to 10^{11} MAP (cattle strain) from a tissue homogenate. The aim was to describe the chronology of infection and pathological processes using sequential necropsy of animals at one, four, eight, 16 days and one, two, four, eight, and 16 months post inoculation (Kluge et al., 1968). The first AFB were identified within macrophages in lymph follicles of the intestinal wall at 1-month post challenge, along with the first intestinal lesions. The peak of lesions in the intestine corresponded with a sudden peak in the number of AFB detected in tissues, between four and eight months after inoculation. This period corresponded with the onset of clinical signs at five and six months post-inoculation. After 16 months, the authors noted that surviving lambs were

⁵ The results are marginally significant as per Fisher exact test, suggesting a decreasing trend.

recovering from disease, with histological recovery of tissue lesions in which very few AFB could be detected and few viable MAP could be grown. The fast onset of extensive multibacillary lesions and clinical signs could be related to the high inoculum dose of likely potent (not laboratory attenuated) MAP from a tissue homogenate. It is also noticeable that despite onset of relatively severe pathology in the first year, the sheep that were not culled during this time appeared to be recovering from disease around 16 months post-inoculation. This propensity to recover from extensive lesions was noted elsewhere as a characteristic of PTB in sheep infected with the cattle strain of MAP (see 4.5.4) although at the time of the study, technologies to allow such distinction were not available.

Gilmour et al. (1977) inoculated 30 sheep with an oral challenge with a total dose estimated at 10^9 MAP over 10 weeks. *Post-mortem* examinations were performed with histology and tissue culture on a proportion of animals at regular intervals over 27 months. Necropsies performed in the first year after inoculation demonstrated more frequent and higher concentrations of bacteria and more histologic damage than those performed throughout the second year. Of those sacrificed between 22 and 27 months post inoculation (n=11), six had no lesions and five harboured mild lesions suggestive of healing of previously active lesions. Five of the sheep underwent serial biopsies, allowing a follow up of the evolution of infection status. At five and 11 months post challenge, all five were infected according to either histology or culture of intestinal wall. Between 17 and 27 months, two sheep became consistently negative to both tissue culture and histological lesions up until necropsy. One sheep apparently cleared infection from its tissues although microscopic lesions were seen at *post-mortem* after 27 months and two sheep developed more severe pathology. The authors conclude that sheep infected orally become colonised initially. Some then totally recover from infection while others become permanent carriers (with lesions), among which a further proportion become clinical while the rest recover from sub-clinical infection.

In a more recent experiment, 30 weaned Merino sheep were inoculated with a moderate to high dose (5×10^8 viable MAP) of an ovine strain obtained directly from a tissue homogenate (Begg et al., 2005). Sequential culling was performed at different times. All of a random subset of six animals were tissue culture positive 13 months after inoculation and five presented histological lesions. In the following year, 10 of the sheep became clinically affected, six with severe histological lesions, though only three were tissue culture positive. At the end of the trial (22 months post inoculation), the six animals that had survived were all tissue culture negative, and only half presented minor lesions. Since the infection rate one year post-challenge was nearly 100%, it is likely that this level of experimental challenge achieved active

infection of all the sheep. These results suggest that infected sheep could experience a primary phase of active infection where MAP invades the tissues, causing lesions in most animals. Some sheep harbouring severe lesions expressed the disease clinically. All the clinically affected animals in this experiment were identified based on weight loss between 11 to 21 months post challenge, with a median time of 15 months (Begg et al., 2005). The six sheep without clinical signs after 22 months recovered and even cleared (or controlled) the infection below detection limits.

An observational study of natural infection with MAP (Dennis et al., 2010), followed 77 sheep from a flock with clinical PTB from 10 to 36 months of age. Serial biopsies of intestinal tissues and mesenteric lymph nodes were performed by laparotomy. Among the 46 (60%) infected sheep detected by tissue culture, six cleared MAP from their tissues by the end of the trial and 12 died of clinical disease. Thus, the proportion which recovered from infection was at least 13%. As sheep were naturally infected rather than experimentally challenged, we do not know when infection took place. If infection took place early in life, there is no way to tell how many of the 31 sheep had already been infected but recovered before the study began. All 12 sheep dying of clinical PTB had progressed in less than two years from having no intestinal lesions to more advanced intestinal pathology, with 11/12 severe multibacillary lesions at the time of death. Serial biopsies are very rare in the literature of ovine PTB. By allowing disease progression within an animal to be monitored, this technique is well suited to establish a progression pattern although the stress of anaesthesia/surgery might alter the natural course of the disease.

4.3.2.3 MAP in faeces

Faecal shedding is more difficult to detect than histo-pathology due to the sub-optimum sensitivity of faecal culture and the intermittence of shedding (possibly confounded by shedding levels below the limit of detection). However, shedding can be monitored by repeatedly collecting samples over time.

Stewart et al. (2004) inoculated either at six months of age with a cattle-type (10 sheep) or at 10 months of age with an ovine-type of MAP (10 sheep), and monitored them for 54 and 35 months, respectively, equivalent to a typical productive life of sheep. Faecal culture revealed that shedding started as early as two months post inoculation in nearly all of the 12 shedders. Thereafter, two patterns were apparent: ten sheep shed intermittently and transiently at some point between two and 16 months after challenge and thereafter stopped shedding permanently. The other two sheep were persistent shedders and were the only animals that

developed clinical disease, occurring at 20 and 32 months after challenge (Stewart et al., 2004). Although the evidence is tenuous, this study is the only one to follow the sheep long enough to suggest a long-term pattern. Findings suggested that only a proportion of infected sheep progressed towards disease, while all those that did not progress shed only transiently before stopping shedding for an extended period compatible with the rest of their productive life. These animals might either eliminate MAP infection or control it below the level of detection by faecal culture.

In another trial (Kawaji et al., 2011), 38 four-month-old sheep were inoculated and followed up to 13 months after challenge. Faecal shedding was detected via direct quantitative PCR. At eight months post-challenge, all 38 animals shed detectable MAP. At thirteen months, qPCR failed to detect MAP in faecal samples from five sheep. This suggests that these were transient shedders, although intermittent shedding could not be ruled out. At the first sampling at four months, all shedders excreted low levels of MAP DNA, while subsequent samplings allowed the distinction of low and high shedders. At the last sampling 13 months after challenge, there was a clear difference between low and high shedders that were several orders of magnitude apart in MAP DNA quantities, plus a proportion that stopped shedding as described by Stewart et al. (2004). Sheep shedding high loads of MAP at 13 months post-challenge had concomitant signs of disease progression, *i.e.* advanced pathology at *post-mortem*.

4.3.2.4 Conclusions: progression pathways

- All measurable outcomes of PTB infection (histology, tissue infection and faecal shedding) display a similar pattern of an early transient active infection stage followed by either control/remission or irreversible progression to severe disease/high shedding.
- This dichotomy in the disease is mediated by a polarization of the underlying immune response.
- This can be modelled by two possible pathways following infection with MAP: a non-progressor pathway leading to recovery and a progressor pathway leading to disease.

4.3.3 Conclusions and assumptions for a candidate model

- The relevant disease stages and pathways identified above were synthesised into a model structure for PTB in sheep as can be seen in Figure 4-1.
- Quantitative parameters for this model could, however, not be estimated from this review. Low sample size prevented parameter estimation from individual studies.

Heterogeneity in the study design prevented the direct comparison of infection outcomes between studies. Combining findings across studies to obtain consistent parameter estimates was hindered by study level confounding factors. A meta-analysis therefore appeared necessary for robust quantitative parameter estimation.

- Important assumptions and considerations for conducting this meta-analysis are as follows:
 - (1) Active infection can be measured by histo-pathological changes in the small intestine as a proxy for shedding.
 - (2) Results of histo-pathological examinations of sheep exposed to MAP are abundant in the literature as most studies of ovine PTB examine histo-pathology in the experimental animals. On the other hand, faecal shedding data are less reliable due to the intermittence of early faecal shedding and the lack of sensitivity of culture-based methods compared with histology.
 - (3) We therefore selected observation of lesions in the small intestine as the outcome to measure the rate of onset of active infection in the meta-analysis.
 - (4) The presence of severe lesions or clinical signs in sheep can be used to evaluate the proportion of infected animals entering the progressor pathway towards disease (versus the non-progressor pathway towards recovery).

4.4 Modelling the force of MAP infection after natural exposure in a pastoral environment

This section reviews modes of transmission of MAP under natural exposure to derive a mathematical expression for the force of infection.

4.4.1 Probability of infection in lambs prior to weaning

Infection with MAP is faecal-oral and thought to occur very early in life by exposure to MAP from an infectious dam via suckling, as well as from a contaminated farm environment (Chiodini et al., 1984; Whittington and Sergeant, 2001).

Some data suggests that direct transmission from the dam might play a dominant role in lambs before weaning from infectious dams (Reddacliff et al., 2004). This direct transmission in neonatal lambs would include both vertical and pseudo-vertical infection.

Previous work indicates that true vertical transmission of MAP occurred in 1/54 (1.9%) sub-clinically infected ewes and 5/5 (100%) clinically affected ewes (Lambeth et al., 2004).

In a field experiment, “tracer” ewes from a farm free of MAP were set to co-graze a pasture with home-bred ewes on a known MAP-positive farm just before the lambing season (Reddacliff et al., 2004). Lambs born from home-bred ewes and those born from the tracer ewes were raised from birth in the same contaminated paddock. The prevalence of Agar gel immunodiffusion (AGID) test positive animals in the homebred ewe flock was around 15% in clinically normal animals, confirming the heavily infected status of the homebred flock, while the tracer ewes were from a flock negative to all tests.

Infection was followed in both groups of lambs by serial culling and tissue culture. Positive tissue culture appeared earlier in the home-bred lambs compared to the tracer lambs born from uninfected ewes. The cumulative proportion of lambs that were culture positive up to eight months of age was also significantly higher in the home-bred group. This suggests that the home-bred lambs were exposed earlier and/or more heavily than the tracer lambs. One can assume that vertical transmission was negligible in these clinically normal animals (Lambeth et al., 2004). Hence the extra-challenge in neonates from infected dams compared to neonates from PTB-free dams, born and raised on the same contaminated pasture, could be due to pseudo-vertical transmission in lambs from infected ewes. By that we mean a close contact with infected and potentially shedding dams, most likely through suckling contaminated teats, on top of the baseline pasture-based exposure. These anecdotal observations confirm earlier observations about infection in neonates (Chiodini et al., 1986; Whittington and Sergeant, 2001). Nevertheless, this experiment also suggests that tracer lambs can acquire infection from contact with a contaminated pasture, prior to weaning (Reddacliff et al., 2004). This is consistent with the observation that lambs in a pastoral environment can eat substantial amounts of grass from a very early age.

4.4.2 Probability of infection after weaning

In a pastoral environment, in addition to direct dam-to-lamb transmission, MAP infection occurs indirectly via grazing contaminated pasture. The quantity of MAP present on pasture is the product of faecal shedding by infectious sheep and survival of MAP in the environment. The quantity of MAP accumulated on pasture thus represents the infectious compartment of the model, effectively a “dose” of MAP inoculum. The probability of infection can therefore be

modelled via an indirect force of infection driven by the dose of MAP to which susceptible animals are orally exposed by grazing (Heuer et al., 2012).

The contact between susceptible sheep and the infectious compartment (contaminated pasture) may depend on the density of sheep grazing the pasture. Assuming that MAP shed on pasture disperses evenly over the grazing surface and the dry matter intake/sheep/day is constant, then the grazing density (sheep/ha) does not influence the intake of MAP from pasture. This is a valid assumption as long as pasture management is adequate and overstocking does not occur. The dose of MAP ingested per sheep can thus be defined as a proportion of the total dose available in the environment divided by the total number of sheep. This is in contrast to an earlier model of ovine PTB by Sergeant (2002), in which increased grass density decreased the probability of infection by MAP from the pasture.

4.4.3 Conclusions: modelling the force of infection

- In a pastoral environment, acquisition of MAP infection mostly occurs via exposure to the contaminated environment (indirect transmission). This can be modelled with an indirect force of infection, function of the estimated dose of MAP ingested through grazing. Constants in the formula of the force of infection can be estimated from a meta-analysis of experimental data.
- Indirect transmission via pasture occurs in neonates as in other age groups, hence needs to be modelled with an indirect force of infection for sheep prior weaning.
- Direct, dam-to-lamb transmission occurring in neonates potentially encompasses both vertical (in utero) and pseudo-vertical (close contact/suckling after birth) transmission.
- The frequency of vertical transmission was estimated at 100% in clinically affected ewes and 1/54 in sub-clinically infected ewes.
- Anecdotal evidence suggests a possible extra challenge in neonates due to pseudo-vertical transmission. Although biologically plausible, these results come from low numbers of sheep from an experiment that was not replicated (Reddacliff et al., 2004), hence this effect is impossible to measure robustly. This mode of transmission was thus not incorporated in the model, which only accounted for vertical transmission and indirect transmission.

4.5 Effect of covariates

The outcome of challenge with MAP may further depend upon a number of biological covariates such as: the challenge dose of MAP, strain of MAP, age of sheep at inoculation,

breed, number of inoculum doses used, whether MAP organisms were obtained from subculture or directly from tissue homogenates (Hines et al., 2007; Begg and Whittington, 2008), and individual host susceptibility. These variations make it difficult to compare the outcomes of different studies. There is therefore a need to establish which of these covariates should be considered and what their effect is.

4.5.1 Effect of age at exposure on infection

Historically, it was accepted that susceptibility to infection was reported to decrease with age based on evidence from cattle (Whittington and Sergeant, 2001; Windsor and Whittington, 2010). Adult animals were thus often considered resistant to infection. However, more recent data about ovine PTB does not support the assumption of an age-based resistance to infection *per se*. Recent works suggest that older animals can be infected when subjected to high doses and continued exposure, in both sheep and cattle (Fecteau et al., 2010; McGregor et al., 2012). Experimental data where sheep were challenged with MAP and followed to monitor their infection status allow estimation of the incidence rate of infection. A number of experiments failed to demonstrate a difference in infection rates between animals infected as young or as adults (Reddacliff et al., 2004; McGregor, 2009; Dennis et al., 2010; Fecteau et al., 2010; Delgado et al., 2012; McGregor et al., 2012). Adult sheep from seven to 10 years old were successfully infected by MAP as assessed by tissue PCR, even with low doses around 10^3 CFU. A proportion of sheep in the high dose group developed histo-pathological lesions (Delgado et al., 2012; Delgado et al., 2013).

4.5.2 Effect of age at exposure on progression

Lambs and adult sheep may be equally susceptible to infection, but the proportion developing signs of disease (as in severe lesions, modelled as *progression*) may depend on age.

This assumption can be evaluated by exposing sheep of different ages experimentally to MAP. In an experimental study, different age groups were inoculated with various doses of MAP (Delgado et al., 2012). Lambs were challenged at one month of age, while the age of ewes challenged ranged from two to ten years. All animals but one ewe in the high dose group presented histopathological lesions in the intestines compatible with PTB, thus were classified as infected. Half of the eight infected lambs presented severe, multifocal lesions (type 3a) with few to moderate numbers of AFB at 220 days. The 12 infected ewes presented only mild focal lesions with no AFB visualised (type 1 or 2 lesions). The more severe lesions in half of the lambs in this study were considered a satisfactory proxy for progression to clinical disease,

even though lesions of histological grade 3a were not strictly multibacillary (Clarke and Little, 1996).

In another experiment, uninfected sheep of different age groups were grazed on pastures contaminated with MAP and followed for 2.5 years (McGregor et al., 2012). The lamb group was 8 to 12 weeks of age at the beginning, “hoggets” were 2-year-olds and adults were more than three years old when first exposed. There was a significant association between age and the outcome of infection: the lower the age at exposure, the greater the number of lesions in the intestine, the greater the severity of lesions and the greater the likelihood and the earlier the occurrence of faecal shedding. There was no significant difference in lesion frequency between lambs and hoggets, approximately half of them presented severe lesions (type 3a or 3b). However, there was a significant difference between young animals (lambs and hoggets) and adults, with around 5% of adults harbouring severe histological lesions (McGregor et al., 2012). This study indicated that sheep up to two years of age seem more prone to progress to disease when infected with MAP, compared to adults.

4.5.3 Effect of MAP dose on progression

Dose at exposure can influence the outcome of experimental challenge studies and, is also reflected in the outcome of natural exposure through contaminated pastures with different levels of contamination.

In an experimental infection model using weaner Merino sheep, (Reddacliff and Whittington, 2003), a challenge dose of 10^3 to 10^8 MAP resulted in negative tissue cultures after 7 or 14 weeks. On the other hand, challenge with 10^8 MAP resulted in positive tissue culture in all sheep. This could indicate that colonization of the intestine was unlikely to occur at a low inoculum dose. This is in contrast with other results showing that inoculum doses around 10^3 were infectious (Brotherston et al., 1961a; Delgado et al., 2012). Alternatively, inoculation with such low doses may result in subsequent clearing of infection within the first few months, unlike infection with higher doses.

(Brotherston et al., 1961a) inoculated sheep with a total dose of 10^3 (low), 10^6 (medium) and 10^9 (high) MAP CFU and compared the outcome by tissue culture of subgroups of sheep slaughtered at regular intervals. One month after challenge, all of 12 necropsied animals (four per group) were tissue culture positive in the small intestine, irrespective of the dose. After nine months however, only 5/12 sheep were still intestinal culture-positive, which could indicate that as many as 7/12 sheep might have recovered from infection. However, the

proportion of potentially recovered sheep depended on the dose, with 3/4 negative at nine months in the low and the medium dose group but only 1/4 negative in the high dose group. Another paper (Nisbet et al., 1962) described the pathology occurring in this experiment. The low and medium dose groups presented a very similar pattern of exclusively focal lesions with a “peak” occurring at five months (6/8 animals necropsied at that time were histology positive). The pattern was, however, different in the high dose group. With the exception of one animal culled at nine months, all other sheep necropsied at one, five or nine months were histology positive. They presented extensive epithelioid cell infiltration involving the submucosa and mucosa (severe lesions), with few to many AFB, in most animals. Moreover, progression to clinical disease was only observed in 2/11 of the sheep in the high dose group, as early as three months after the first dose was administered. These results, despite a limited sample size, demonstrate that following the onset of initial infection, some animals can clear or control the infection. It also suggests that the outcome of MAP infection may differ depending on the dose, with low/medium doses resulting in a high proportion of sheep recovering from infection/disease while, high doses trigger the progression towards severe pathology and clinical disease. It is also relevant to note the differences in the temporal pattern of intestinal infection (as per tissue culture) versus histo-pathology, with a peak of intestinal infection occurring one-month post challenge, while the peak of histo-pathology seemed delayed around five to nine months. Moreover it was possible, in the later course of the disease, to observe mild lesions in tissue culture negative animals (Nisbet et al., 1962). These may represent healing lesions.

In a study assessing natural infection in sheep described by McGregor et al. (2012) sheep of different age groups were grazed on low, medium and highly contaminated pastures. There was a significant effect of exposure to highly contaminated pasture versus low contamination. The odds ratio of shedding MAP in faeces in high versus low dose paddocks was 3.5, and the odds of dying of clinical PTB between those doses was 18.2. The animals experiencing a higher environmental exposure shed 3.4 times earlier and succumbed to clinical PTB 18.6 times earlier than the sheep in low exposure paddocks. The highest mortality rate occurred in the high exposure group showing a higher proportion of sheep progressed to disease irrespective of the age. Hence, the pattern of the dose related onset of disease observed in experimental and natural challenge studies are similar.

4.5.4 Effect of MAP strain on progression

Stewart et al. (2004) inoculated 10 sheep with a cattle (C) MAP strain at six months of age and another 10 sheep with an ovine (S) strain at 10 months of age. Histopathology was not performed, thus making interpretation of disease progression difficult. However, both groups had the same incidence of clinical disease (1/10 sheep) and similar shedding patterns, with seven in the cattle strain group and five in the ovine strain group. No formal conclusion could be derived from this study due to small sample size.

In another experiment (Verna et al., 2007), 19 lambs were inoculated with C strains of various origins and sub-types and 5 lambs with a gut homogenate containing an S strain. Histopathological examination was performed at 150 days post-infection. It revealed that only sheep inoculated with the S strain had extensive lesions, with abundant AFB presence in the intestines, suggesting that the S strain induces more severe lesions in sheep than the C strain. These observations only pertain to the early stages of infection, until 150 days post-inoculation. In a similar experimental challenge study (Fernandez et al., 2014), sheep infected with a C strain (n=12) initially showed more severe and diffuse disease in the small intestine. These lesions tended to regress over time, unlike lesions induced by the S strain in the other group (n=12). This pattern was consistent with a significantly higher IFN γ response in sheep infected with the C strain versus the S strain, suggesting that the former triggers a stronger cellular immune response. The authors thus suggest a tendency towards resolution of disease after strong initial tissue lesions in lambs infected with the C strain compared with the S strain.

4.5.5 Effect of inoculum type on progression

Another factor influencing infection outcomes is the type of inoculum. A low passage pure culture of MAP and MAP organisms directly harvested from infectious tissues without *in vitro* passage (tissue homogenate inoculum) are not equivalent.

An experimental infection model of ovine paratuberculosis (Begg et al., 2005) showed that challenge with tissue homogenate (ground-up small intestine from a clinical case) caused “higher levels of infection and disease” than challenge with a pure MAP culture obtained from a low-passage-number (3 passages) culture medium, despite a 20 times higher dose of MAP in the pure culture (10^9 MAP). Moreover, in a distinct experiment the same authors report that sheep inoculated with 10^9 MAP of the same isolate in pure culture, but continuously-passaged (> 10 passages) did not result in any infection or gut histopathology in the inoculated sheep.

The organisms in pure culture versus tissue homogenate were collected from different animals but were both of the S strain of MAP.

A similar outcome was obtained in the experiment of Verna et al. (2007), where one-month-old lambs were inoculated with either a bovine strain cultured *in vitro* (n=5) or the same bovine strain directly purified from tissue homogenate (n=5) at a similar dose. The *in vitro* cultured strain induced milder forms of disease with mainly focal lesions located in the lymph nodes, while the purified gut homogenate inoculum induced more lesions, and more diffuse and multifocal lesions.

In another experiment (Stewart et al., 2004), 10 sheep were inoculated with gut homogenate and 10 with a pure culture of MAP with the same strains across groups (5 sheep with a C strain and 5 with a S strain, in each group). Shedding was followed for 34 months (S strain) or 56 months (C strain). In the pure culture group, shedding occurred only transiently at two months post-inoculation in two sheep inoculated with the cattle strain and no further shedding could be identified. No signs of clinical disease were present in this group. In the gut homogenate group, all 10 sheep shed MAP either transiently for several months or continuously until the end of the experiment, and two animals developed clinical disease (one for each strain type). No differences in the shedding pattern or the occurrence of clinical disease could be attributed to the strain type. However, the MAP dose (organisms/g) was not determined for the tissue homogenate; hence dose is a possible confounder for these findings.

In a similar comparative study where several experiments were reported (Begg et al., 2010), one experiment described MAP inoculation of 4-month-old lambs with a dose approximating 3×10^8 MAP (Kawaji et al., 2011), either with gut homogenate from infectious sheep or with a pure culture of MAP. In this experiment, there was no significant difference between the two groups in terms of the proportion of sheep progressing to disease after 13 months of follow-up. However, the sheep inoculated with gut homogenate started shedding and had clinical signs earlier than pure culture inoculated sheep (Begg et al., 2010).

Another experiment, involving 14 sheep, was specifically designed to assess possible virulence attenuation due to *in vitro* passage (Fernandez et al., 2015). The results show significantly higher IFN γ response in the group dosed with tissue homogenate, while the IFN γ peripheral response of the culture group was no different to that of the controls. The homogenate inoculum was also more pathogenic, inducing more severe and more extended lesions compared to the pure culture group, for a comparable dose of MAP. The authors concluded

that even low passage of MAP *in vitro* induces an attenuation of virulence compared with direct tissue homogenate.

4.5.6 Conclusions: effect of covariates

- Age at exposure and dose, strain and inoculum type of MAP all interact with the onset and severity of tissue lesions in sheep, thus confounding each other.
- The effect of these covariates should be evaluated in a meta-analysis to quantify these effects across all studies and tease them apart when estimating parameters for a mathematical model of PTB.

4.6 Field data for model validation

In this section, we review evidence about natural PTB from field-based studies. Cross-sectional data of gut histopathology in the flock resulted in estimates for the proportion of sheep in the flock in various disease stages. Longitudinal data of OJD mortality resulted in estimates of annual incidence rate of OJD. These represent plausible field outcomes against which simulated outcomes of a mathematical model of OJD in a sheep flock could be retrospectively validated.

Six longitudinal studies involving 14 flocks are summarised in Table 4-1.

Table 4-1: Summary of field PTB outcomes from natural challenge experiments and heavily infected commercial flocks

Study	(1)	(2)				(3)							
Flock ID	1	1	2	3	T	1H	2H	3H	1E	2E	3E	T	
Cross-sectional sampling:													
age at sampling (yrs)	2	3	5	7.5	MA	2	2	2	4.5	4	3.5	MA	
# tested for histopathology	73	254	270	258	782	10	15	18	44	60	40	187	
# histology +ve	15	21	15	7	43	2	13	5	9	16	16	61	
% histology +ve	15/73 = 21%	8%	6%	3%	6%	20%	87%	28%	20%	27%	40%	33%	
# sheep with diffuse histological lesions ^d	7	17	11	2	30	2	7	3	3	5	4	24	
% sheep with diffuse histological lesions	7/73 = 10%	7%	4%	1%	4%	20%	54%	17%	7%	8%	10%	13%	
% sheep with diffuse lesions among histology +ve	7/15 = 47%	81%	73%	14%	67%	100%	47%	60%	33%	31%	25%	39%	
Longitudinal follow-up:													
Total follow-up period (yrs)	2	2.5	2.5	2.5	2.5	NA	NA	NA	NA	NA	NA	4 ^b	
cumulative # clinical cases	12	5	2	0	7	NA	NA	NA	NA	NA	NA	80	
population at risk	75 ^a	263 ^e	275 ^e	268 ^e	806 ^e	NA	NA	NA	NA	NA	NA	525 ^c	
annual incidence of clinical disease (%)	12/(2*75) = 8%	0.8%	0.3%	0%	0.35%	NA	NA	NA	NA	NA	NA	3.8%	

Legend:

T: total

MA: mixed age adult animals

NA: not available

H: Hogget cull at 2 years of age

A: Adult, culling at the end of the experiment

^a 77 sheep in total minus two sheep that died for reasons unrelated to PTB

^b on average on the three properties

^c approximate estimates based on information provided by the authors that 200 control sheep/farm were included at the beginning of the study, normal culling management occurred thereafter so that roughly 150 control sheep/farm would remain at the end of the study period, hence the population at risk over the three farms was ((200+150)/2)*3=525.

Table 4-1(continued):

Study	(4)	(5)							Grand Total
flock ID	1	1	2	3	4	5	6	T	
Cross-sectional sampling:									
age at sampling (yrs)	3	5	MA	MA	5	3	4	MA	MA
# tested for histopathology	452	272	73	93	308	441	192	1379	2873
# histology +ve	54	30	17	8	38	87	44	224	397
% histology +ve	54/452=12%	11%	23%	9%	12%	20%	22%	16%	14%
# sheep with diffuse histo lesions ^d	14	21	9	5	16	33	26	110	185
% sheep with diffuse lesions in the flock	14/452=3%	8%	12%	5%	5%	7%	14%	8%	6%
% sheep with diffuse lesions among histo +ve	14/54=26%	70%	53%	63%	42%	38%	59%	49%	47%
Longitudinal follow-up:									
Total follow-up period (yrs)	2.5	NA	NA						
cumulative # clinical cases	22	NA	NA						
population at risk	485	NA	NA						
annual incidence of clinical disease (%)	22/(485*2.5)=1.8%	NA	2.2%						

^d only diffuse intestinal lesions 3b and 3c (Perez score), except for (McGregor et al., 2012) where lesions 3a (severe multifocal) are included as well.

^e calculated as the average between the number of sheep included at the beginning and the number of sheep remaining at the end of the experiment in each group, according to figures in (McGregor, 2009).

(1) Dennis et al. (2010)

(2) (McGregor et al., 2012)

(3) Reddacliff et al. (2006)

(4) Abbott et al. (2004)

(5) Sergeant et al. (2003)

4.6.1 Prevalence of histological lesions in sheep naturally infected with MAP

In two field-studies, a three-year longitudinal follow-up was carried out to study natural exposure to MAP via contaminated pasture (Abbott et al., 2004; McGregor et al., 2012). The trial sheep originated from PTB-free flocks (McGregor et al., 2012) or a mixture of infected and PTB-free flocks (Abbott et al., 2004). Sheep were kept in paddocks with various initial MAP contamination levels, mimicking natural exposure to MAP. Co-grazing clinical case shedding with the trial flocks ensured high pasture contamination for periods of time. Sheep were enrolled at weaning and monitored for 2.5 years (McGregor et al., 2012) or from birth up to three years old (Abbott et al., 2004). Hence, the latter trial was about natural exposure to MAP via contaminated pasture as well as maternal exposure. At the end of the study, all surviving sheep underwent necropsy with tissue culture and histology. The proportion of histology positive sheep at three years old was 8% (McGregor et al., 2012) and 12% (Abbott et al., 2004), towards the low end of the spectrum. These observations were representative of low clinical incidence flocks (Table 4-1).

A vaccine efficacy field trial was conducted in New South Wales (Australia) in three heavily infected Merino farms with annual OJD mortality between 5 and 15%. Lambs were recruited, managed under usual farming practices and followed between 3.5 and 4.5 years depending on the farm (Reddacliff et al., 2006). Clinically normal hoggets were culled at two years of age. Histopathology was performed on a random sample of 43 unvaccinated hoggets in total, 12 of which presented severe lesions (proportion = 28%, Table 4-1). At the end of the trial a random sample of 144 clinically normal ewes (on average four years old) was necropsied for histological examination. The proportion of sheep with severe lesions at this second sampling was 12/144 (8.3), more than three times lower than it was among two-years-old sheep. This pattern of progression to severe disease in young adults in the face of high natural challenge suggests that sheep surviving up to four years old are likely to harbour milder lesions and thus represent animals in the pathway to recovery.

In Dennis et al. (2010) a cohort of naturally challenged sheep (n=77) from a 'heavily MAP infected' flock were followed from 10 months old onwards. Sheep underwent intestinal biopsy for histopathological examination at two years of age, representing a cross section of disease status. Fifteen sheep out of 73 presented histological gut lesions (21%) among which 7/73

presented severe lesions (10%). This naturally infected flock was the most impacted by OJD mortality (Table 4-1).

A cross-sectional study included six known infected flocks in New South Wales, Australia, to estimate the sensitivity of ELISA and AGID tests. All animals (n=1379) underwent necropsy with histology (Sergeant et al., 2003). Sheep at necropsy were adult mixed-age ewes over three years old. The overall prevalence of all histology lesions was 16%, versus 8% for severe lesions (Table 1), hence 50% of sheep presenting histological lesions were actually harboring 'severe' lesions, similar to observations in Dennis et al. (2010).

The overall proportion of severe lesions among sheep detected with histological lesions was notably high at 47%. Studies in commercial flocks usually recruited flocks experiencing high mortalities. This could have contributed to a skewed representation of disease severity (towards more severe lesions), compared to random MAP infected flocks, which would mostly experience low PTB mortality. The sensitivity of histopathology may also be lower for mild lesions, *i.e.* small focal granulomas. These can easily be missed, especially when many of the examined animals harbour extensive severe lesions. For field studies unlike experimental challenge, low-grade lesions (type 1) could possibly be considered unspecific and overlooked. This would explain the low proportion of such mild lesions in the results presented here. In contrast, the histology study of Pérez et al. (1996) included sheep from four infected flocks with low prevalence in Spain. All the sheep culled for any reason during 18 months underwent histopathological examination. Of the 166 sheep in the study, about 50% presented with lesions in their small intestine and of those 40/82 (49%) presented type 1 lesions, which were rare in contrast to the observational field studies. As a result, the proportion of severe lesions among histology positive sheep was lower than in the observational studies in Table 4-1(33%). A better sensitivity towards low grade lesions in the histology study of Pérez et al. (1996) might explain these differences. Alternatively, the Pérez et al. (1996) study and studies presented in Table 4-1 represent two distinct populations of flocks, respectively low and high incidence of OJD.

In a study of diagnostic test accuracy for OJD, Dhand et al. (2010) estimated a multi- to paucibacillary ratio of 20:80 in a "typical" (median prevalence) flock. Moreover, the same authors estimated a plausible multi- to paucibacillary ratio of 10:90 in a low prevalence flock (N. Dhand, personal communication, March 3, 2013). The multibacillary stage can be a proxy for disease progression. This illustrates that the overall proportion of 47% of severe lesions among sheep detected histology positive on farm (Table 4-1) may not be representative of all

flocks with PTB. Nevertheless, these field observations provide a plausible range for prevalence of various disease stages in natural PTB for model validation.

4.6.2 Incidence of clinical cases in sheep naturally infected with MAP

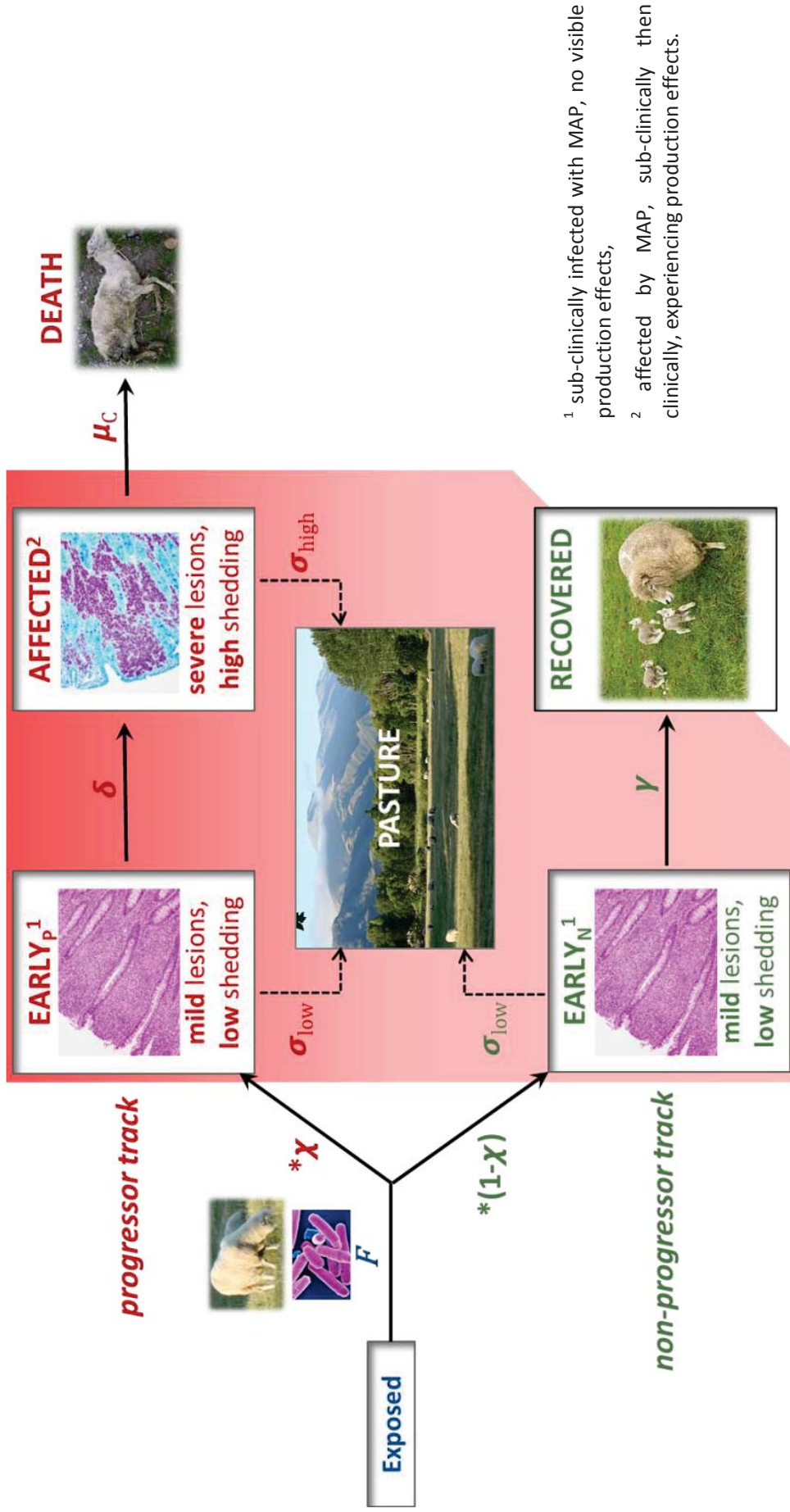
The lowest clinical incidences were obtained in the grazing trials where OJD-free ewes were co-grazed with clinical cases to mimic natural exposure to MAP. An overall annual clinical incidence of respectively 0.35% (McGregor et al., 2012) and 1.8% (Abbott et al., 2004) was presented, thus representing low clinical incidence flocks (Table 4-1).

Prior to the start of the vaccine efficacy trial of Reddacliff et al. (2006), annual mortality rates of mixed-age ewes in 3 flocks were reported between 5% and 15%. Clinical cases were primarily 2-, 3-, and 4-year-old sheep. During the trial, the sheep were closely monitored throughout the four-year study period (average duration over the three properties). OJD mortality in the control group provided insights into the natural distribution of clinical disease in these New South Wales flocks. However, the clinical incidence among controls was likely reduced by the presence of vaccinated counterparts in the same pasture. Assuming OJD deaths were evenly spread over the study period, the average annual clinical incidence rate was 3.8% per year (Table 4-1). The paper describes the age distribution of clinical cases, showing a peak of mortality in young adults between 1.5 and three years old, with only 20% of deaths occurring earlier or later. These observations are corroborated by the high annual mortality rate of 8% observed in Dennis et al. (2010), where sheep from a heavily infected flock were only monitored up to three years of age. Similarly, in a pasture-based experimental study mimicking natural PTB (Abbott et al., 2004), 4.4% of the total number of enrolled weaners died of clinical PTB between weaning and 3 years of age. The earliest clinical case died at 1.5 years old.

The occurrence of clinical cases in young sheep with naturally occurring PTB highlights that ovine PTB can progress rapidly to clinical disease in natural PTB as well as experimental challenge studies. It is possible that in a heavily contaminated environment, the infection cycle is enhanced and a permanent high dose challenge from a young age causes more sheep to enter the progressor track, whereupon they progress relatively quickly to disease. Clinical cases in older sheep may be caused by a late recrudescence from a stage of disease recovery or simply new infections occurring later in life, since age-based resistance to infection does not seem to occur in sheep (see 4.5.1).

4.6.3 Conclusion: Field data for model validation

- Experimental challenge studies enable a better understanding of the pathogenesis of ovine PTB, contributing to the development and parametrisation of an ovine PTB model. However, it is important to review evidence from field-based studies against which the simulated outcomes of the model could be retrospectively validated.
- We found five studies pertaining to 14 heavily infected commercial sheep flocks, from which natural PTB outcomes could contribute to retrospective model validation.
- The overall trend was that 14% of sheep across these infected flocks presented histological lesions of PTB and 6% presented severe lesions indicative of progression to clinical disease. The overall annual clinical incidence of OJD was 2.2%.
- Importantly, natural PTB exhibited a great variation between flocks. The prevalence of histological lesions in individual flocks ranged from three to 87% and the proportion of animals with severe lesions ranged from 1% to 54%.
- This range of plausible values for prevalence of different disease stages and annual clinical incidence can be retrospectively compared to simulated proportions of sheep in different model compartments, for model validation purpose.
- Overall, the results were comparable with those of experimental challenge studies presented in previous sections. In particular, the mean proportion of sheep histology positive with severe lesions was 47%, an unexpectedly high proportion for natural PTB. Other evidence suggests that such high proportions are not representative of all flocks and may be inaccurate for low prevalence flocks.
- In these field studies, death due to OJD appeared to occur in young sheep around two years of age, mostly before three years old. This is similar to experimental challenge studies, where fast progression to disease is observed.



¹ sub-clinically infected with MAP, no visible production effects,
² affected by MAP, sub-clinically then clinically, experiencing production effects.

Figure 4-1: structure for a candidate state-transition mathematical model of ovine paratuberculosis, based on evidence gathered in Part 1 of this review ⁶

⁶ References for the pictures: MAP bacterium from Oregon State University website (<http://smallfarms.oregonstate.edu/sfn/f11Johndisease>); histological lesions in the small intestine: (Smeed et al., 2007). Figures 2 and 3; Ewe and triplet lambs: https://en.wikipedia.org/wiki/Sheep_farming_in_New_Zealand; dead ewe: picture credit Stefan Smith; NZ sheep pasture: picture credit primary author.

4.7 Conclusion

The aim of this synthesis was primarily to inform mathematical modelling. It identified potential pathways for the pathogenesis of ovine PTB and specified the main stages of this progressive disease, leading to developing a model structure for ovine PTB.

The outcomes of individual experimental challenge models appeared confounded by experimental conditions, *e.g.* age, dose and strain type. Therefore, a secondary aim was to generate important assumptions to conduct a systematic review and meta-analysis of ovine PTB pathogenesis. In this respect, this review specified appropriate clinical outcomes to use as markers for the occurrence of different disease stages. It also identified important covariates to consider in the meta-analysis to (1) measure their effect on paratuberculosis pathophysiology and (2) adjust for their confounding effect on the outcomes. Main biological factors potentially influencing the course of infection/disease were age at inoculation, inoculum dose, strain type of MAP, and the exposure dose to MAP.

Chapter 5. Enumeration methods of *Mycobacterium avium* subsp. *paratuberculosis* *in vitro* from animal samples

Nelly Marquetoux^a, Peter Wilson^b, Anne Ridler^b, Cord Heuer^a

^a EpiCentre, Institute of Veterinary, Animal and Biomedical Sciences, Massey University, New Zealand

^b Institute of Veterinary, Animal and Biomedical Sciences, Massey University, New Zealand

5.1 Abstract

Enumeration of *Mycobacterium avium* subsp. *paratuberculosis* (MAP) *in vitro* is often a prerequisite in biological studies of paratuberculosis. A range of methods has been used for this purpose in the literature, in parallel with the evolution of laboratory techniques. We reviewed the different methods, their principle, inherent biases and the equivalence between methods. We identified two broad enumeration categories: quantification of cultivable MAP numbers versus total number of MAP cells. These are not directly comparable. The purpose of conducting the enumeration process should therefore guide the choice of the method to use.

5.2 Introduction

Historically the quantification of MAP in experimental studies has focused on inoculum doses. It was mainly reported as wet or dry weight of pure bacterial culture (Kluge et al., 1968; Karpinski and Zorawski, 1975). To the best of our knowledge, the first attempt to enumerate the number of viable bacilli in a sample was performed by Brotherston et al. (1961a). Nowadays a variety of enumeration methods is available, each with specific inherent technical characteristics and sources of biases (Behr and Collins, 2010).

The ability to detect and enumerate MAP is crucial to interpret the results of epidemiological studies of paratuberculosis (Reddacliff and Whittington, 2003). Taking into account biases associated with enumeration of MAP *in vitro* also contributes to standardize research using experimental models of PTB (Begg and Whittington, 2008). The exposure dose of MAP plays a predominant role in the physiopathology of MAP infection (Chapter 4). This dose effect is an important contribution to precise quantitative conclusions of this thesis. A meta-analysis of experimental challenge studies with MAP can quantify this effect, but adequate interpretation

of MAP doses in pathogenesis studies is hampered by the heterogeneity of the different enumeration techniques.

A review of the different *in vitro* enumeration methods of MAP is necessary to (1) clarify the similarities and the differences between these methods, and (2) elaborate guidelines to standardise the effect of dose in the meta-analysis (Chapter 6). These guidelines will ultimately enable comparisons between papers using different enumeration methods, as well as the evaluation of potential biases.

5.3 Different methods of MAP enumeration

Any attempt to enumerate MAP (in particular in clinical samples) relies on the accuracy of the method to detect MAP organisms in the first place. A lack of sensitivity is the first source of bias. This aspect is therefore reviewed in parallel with the aspect of MAP enumeration *per se*.

5.3.1 Culture based methods

Culture-based methods are the most common enumeration methods for MAP. They aim at determining the number of viable MAP in a clinical sample, or in a suspension obtained after subculture of MAP. This method is based on MAP ability to grow *in vitro*, therefore only MAP cells actually forming a colony are enumerated. Non-viable MAP and under some circumstances viable non-growing MAP will not be enumerated. Irrespective of the technique, MAP organisms are difficult to grow *in vitro* (Smith, 1953), and their detection on culture media can require incubation periods up to 3 months long (Merkal et al., 1964).

5.3.1.1 General sources of variation of viable cell counts

Any condition affecting the viability of MAP cells in a sample directly affects the accuracy of culture-based enumeration methods, more specifically:

- Storage: Raizman and Espejo (2011) studied MAP survival in stored faecal samples of naturally infected cows, by culture. The odds of observing a decrease in the MAP load from high to low or low to negative was 1.13 per month. The loss of viability was more likely for samples stored at -18°C compared to -70°C, but the observed difference was not significant. The number of thawing/refreezing cycles had no effect on survival time. Similarly, ovine strains of MAP showed a minimal loss of viability when stored at -80°C for over a year. In contrast, a MAP load decrease of one to two \log_{10} units of MAP was observed in the first three months of storage at -20°C (Reddacliff, 2002).

- Decontamination procedures: this preliminary treatment is critical for MAP culture from clinical samples, even more in liquid cultures due to a greater risk of bacterial contamination. This can have a significant impact on the viability of mycobacteria (Damato et al., 1983). Reddacliff et al. (2003b) found a reduction of three log₁₀ units in the MAP load contained in sheep faeces or tissues after routine decontamination protocols. As a result, an inherent lack of sensitivity of culture methods for clinical samples with a low infection rate was observed. The lower detection limit was at 250 MAP/g in faeces in liquid culture medium, and at best 80 MAP/g in tissues when using a method involving centrifugation.
- Other sample processing steps and laboratory manipulations before the enumeration cause a loss of bacteria from the initial suspension. Elguezabal et al. (2011) estimated this loss at 55% and 75%, by plate count and qPCR respectively.
- Dormancy: a dormant state exists during which MAP organisms are viable but non-cultivable (Whittington et al., 2004). This can affect culture-based enumeration methods when nutrient depletion occurs in culture medium, *i.e.* in late stages of growth (Elguezabal et al., 2011). This can increase growth time, thus artefactually underestimate the number of viable MAP.

Moreover, most enumeration methods are biased by the strong tendency of MAP cells to clump, both *in vitro* and *in vivo*, and to form aggregates with cells debris or broth medium. Hence one colony forming unit in culture may in fact correspond to a clump of several MAP cells, sometimes in “large numbers” (Merkal et al., 1964), rather than a clone from one unique MAP cell. The extent of clumping is variable. Brotherston et al. (1961a) mention “the presence of single bacilli or small clumps with rarely more than 10 bacilli per clump” in a suspension of cattle strain of MAP. By contrast, Klijn et al. (2001) evaluate the underestimation factor due to clumping at two to three log₁₀ units.

A thorough dispersion of MAP cells in suspension through appropriate laboratory procedures is therefore a prerequisite to avoid gross underestimation of MAP cell numbers. Possible treatments include the use of Tween-20 or Tween-80 acting as a dispersant (Hughes et al., 2001; Reddacliff, 2002; Bogli-Stuber et al., 2005), repeated passages through a fine gauge needle (Reddacliff et al., 2003a; Begg et al., 2010; Fernandez et al., 2015), filtering through a micro-pore (Lambrecht et al., 1988), vortexing (Bogli-Stuber et al., 2005; Elguezabal et al., 2011), bead-beating with silica beads (Kralik et al., 2012), continuous stirring of the broth (Hughes et al., 2001; O'Mahony and Hill, 2002), constant shaking at 300 rpm during incubation (Peñuelas-Urquides et al., 2013) and sonication (Stabel et al., 1997). If clumping cannot be

totally avoided, appropriate lab procedures can contribute to mitigate the problem. Some authors report to essentially achieve single bacilli suspensions of MAP (Lambrecht et al., 1988; Hughes et al., 2001). In contrast, other experiments highlight difficulties to overcome clumping despite preventive laboratory procedures, at least for bovine strains of MAP (Kralik et al., 2012). There is evidence that ovine MAP strain (type I) is readily emulsified in suspension, with only “occasional clumps of two or three organisms”, while bovine MAP strain (type II) tended to form “many large clumps of bacilli” despite the use of procedures to limit clumping (Reddacliff, 2002).

5.3.1.2 Cultivability of cattle strain versus sheep strain

MAP is a slow growing pathogen, although MAP type II organisms are readily cultivated from solid media. The isolation rate from bovine clinical samples is satisfactory (Whittington et al., 2001; Stevenson et al., 2002). On the other hand, strains isolated primarily from sheep (known today as type I or III strains) are particularly difficult to grow. Early attempts to isolate MAP from sheep (Taylor, 1951; Smith, 1953) and more recent ones (Whittington et al., 1999), both on solid and liquid media, highlight these difficulties. Nonetheless, liquid broths outperform solid media for the growth of MAP in general, especially for ovine strains (Smith, 1953; Whittington et al., 1999). The inherent lack of sensitivity of solid media for MAP type I strains means that the culture and enumeration of MAP from sheep samples (or from cattle cross-infected with strain type I) might be explained by a systematic bias towards the detection of the fastest growing MAP types (Whittington et al., 2001). Differential growth of cattle strains versus sheep strains was reported in Fernandez et al. (2014): plate counts and McFarland estimates (turbidity method) were very close ($< 0.5 \log_{10}$ unit difference) for two cattle strains. In contrast, plate counts were one to two \log_{10} units lower than McFarland estimates for a sheep strain. The authors report the “enormous difficulty” to grow this sheep strain on solid media.

Even within type II isolates from dairy cattle in the USA, a microbiological bias can be observed as liquid culture media shows greater sensitivity (Motiwala et al., 2005) and uncovers a greater diversity of genetic subtypes (Cernicchiaro et al., 2008) compared with solid media.

As a conclusion, sheep strains are more difficult to grow than cattle strains, which could introduce a differential bias in enumeration attempts. In particular, plate colony counts could grossly underestimate the inoculum dose prepared with sheep strains. Another differential bias can occur due to an increased tendency of the cattle strain to clump in suspension, considering that clumping affects MAP enumeration (see 5.3.1.1).

5.3.1.3 Viable count on solid media

This method is widely used to enumerate the inoculum dose in pathogenesis studies on PTB (Brotherston et al., 1961a; Stewart et al., 2004; Begg et al., 2005) or for epidemiological studies of ovine PTB. It gives an estimation of the number of colony forming units (CFU) growing on slopes or plates, from serial dilutions of an inoculum of MAP.

Culture of MAP on solid media is time consuming. Detectable growth commonly occurs within 12 weeks after inoculation (Merkal et al., 1964), but up to 52 weeks for sheep strains (Stevenson, 2015). Colonies of MAP can be visually difficult to detect and to count, hence the interpretation of plate counts can be subjective (Elguezabal et al., 2011). Results tend to be poorly reproducible and highly variable (Reddacliff, 2002; Elguezabal et al., 2011; Kralik et al., 2012), especially for enumeration of MAP from a clinical specimen rather than pure culture (Reddacliff, 2002). Finally, an inherent lack of sensitivity of solid media, particularly for the isolation of “slow growing” strains, limits the analytical sensitivity of the method (see 5.3.1.2). For this reason it is recommended not to use solid media “as a routine enumeration technique for MAP of ovine origin” (Reddacliff, 2002). However, it is still widely used for this purpose in ovine PTB pathogenesis studies, both for enumerating MAP from pure culture or from tissue homogenate (Delgado et al., 2013; Fernandez et al., 2015).

5.3.1.4 Methods involving liquid culture media:

Liquid media are sensitive substrates, detecting slow growing strains more readily than solid media. Their use improves the detection rate in clinical samples (Whittington et al., 1999; Motiwala et al., 2005), increases the accuracy of viable MAP numbers estimates and decreases the turn-over time (Damato et al., 1983; Damato and Collins, 1990).

5.3.1.4.1 Estimates based on light absorbance

This method uses the relationship between the turbidity of a liquid suspension of MAP (measured by a nephelometer) and the cell concentration. It thus represents a quick and easy technique to estimate bacterial numbers. Alternatively, the absorbance of the suspension can be related to MAP concentration, although this requires using a spectrophotometer. Either method can only be used for MAP in liquid culture, by measuring the absorbance or the turbidity directly from the broth (Lambrecht et al., 1988; Bogli-Stuber et al., 2005; Peñuelas-Urquides et al., 2013) or after re-suspending bacterial pellets obtained by centrifugation in PBS (Antognoli et al., 2007; Elguezabal et al., 2011; Fernandez et al., 2014; Fernandez et al., 2015). The applications are therefore limited.

Measures of turbidity are often expressed in McFarland units (Verna et al., 2007; Kralik et al., 2012; Fernandez et al., 2014), or alternatively in Brown's scale in older studies (Brotherston et al., 1961a). In microbiology, the McFarland scale is a reference for the estimation of bacterial suspensions concentration based on turbidity, but the standards were based upon numbers of *E. coli* organisms, with one McFarland unit corresponding to 3×10^8 cells of *E. coli* (Perilla et al., 2003). However, the physical properties of *E. coli* differ from that of mycobacteria, hence some authors recommend that McFarland units should not be used to enumerate MAP numbers directly according to the McFarland scale (Peñuelas-Urquides et al., 2013). Instead, McFarland units (as well as direct OD readings) need to be calibrated specifically for MAP enumeration, by comparing with number of viable MAP obtained by serial plate counting (Kralik et al., 2012) or direct visual counts (Hughes et al., 2001). Yet, one study shows an excellent fit between number of MAP estimated by qPCR and the McFarland standards based on *E. coli* (Kralik et al., 2012). This suggests that using the McFarland standards of *E. coli* could still provide better estimates than trying to produce a MAP-specific calibration based on culture, given the shortcomings of MAP cultivation. Turbidimetry, however, does not distinguish between live or dead cells. Hence McFarland units do not necessarily reflect the growing potential of MAP present in the sample/inoculum (Peñuelas-Urquides et al., 2013).

Turbidimetry performs better in concentrated MAP suspensions, with a detection limit of 10^7 cells (Reddacliff, 2002; Elguezabal et al., 2011). The precision of the relationship between number of mycobacterial cells and turbidity (or OD readings) is likely affected by the presence of clumps (Peñuelas-Urquides et al., 2013). This could contribute to the observed poor repeatability between trials (Reddacliff, 2002).

Nevertheless, turbidity measures allow a quick and easy - possibly inaccurate - estimate of MAP concentration. This is useful in the laboratory to obtain standard MAP suspensions of approximately equivalent of MAP concentrations. Where precise estimates of viable MAP numbers are needed, turbidity methods are often followed by culture-based method, giving a retrospective estimate of the dose of viable MAP (Brotherston et al., 1961a; Fernandez et al., 2014; Fernandez et al., 2015).

5.3.1.4.2 End point titration method

This method, also coined 'most probable number' (MPN), implies inoculating serial dilutions of MAP suspensions in liquid medium to grow the bacteria at decreasing concentrations, until no growth is observed. More accurate than direct colony count on solid media, this technique is expensive and time consuming to ensure the absence of growth at high dilutions (Reddacliff et

al., 2003a). The accuracy is also affected by the presence of clumps, especially towards the end point (Reddacliff, 2002).

This method was used in at least one sheep infection model to enumerate the number of colony forming units of MAP in inoculum doses (Reddacliff and Whittington, 2003), and in another study to calculate the excretion of viable MAP in infected sheep faeces (Whittington et al., 2000).

5.3.1.4.3 Time to growth in radiometric liquid media

An automated radiometric detection system for bacterial growth in liquid medium was developed using the Bactec instrument to analyse the amount of radioactive CO₂ released by bacterial metabolism (DeBlanc et al., 1971). This method, coined Bactec 460, was based on modified 12B medium (Shin et al., 2007). Early an automated detection of MAP (within 10 days) was achieved using the radiometric liquid culture medium BACTEC (Damato and Collins, 1990). This system also displayed enhanced sensitivity for sheep strains (Whittington et al., 1999), partially addressing the issue of differential growth of strains I versus II.

Using radiometric culture, MAP dose is estimated by linear regression of the cumulative growth response (*i.e.* readings of the quantity of radioactive CO₂ released) on time to detection and inoculum size. A statistical model thus enables to predict the number of viable MAP in suspension from observed growth measurements, “under controlled conditions” (Lambrecht et al., 1988). A simpler version consists in establishing equations relating the time to reach a threshold growth index (rather than an entire growth curve) and the inoculum size (Reddacliff et al., 2003a). This method was used for field isolates of S strains from faeces or tissues (Reddacliff et al., 2003a). In theory, it is possible to use these same equations for routine MAP enumeration in subsequent samples, with a precision of one to two log₁₀ units. The precision (compared with MPN estimates) was better for higher MAP concentrations: one log₁₀ unit in sheep clinical samples containing at least 10⁴ organisms and half a log₁₀ unit for inoculum sizes greater than 10³ organisms obtained from laboratory sub-cultures (Reddacliff et al., 2003a). Another advantage of this method is the fast turnover time and low-cost, especially compared with end-point titration, to achieve a similar precision. It is also less affected by the presence of MAP clumps in the broth (Lambrecht et al., 1988; Reddacliff et al., 2003a).

The discontinuation of the radiometric BACTEC 12B culture medium in 2012 illustrate the ongoing process of maintaining appropriated culture media for MAP organisms (Whittington et al., 2013), necessary for epidemiological studies. For cattle isolates, a non-radiometric liquid medium called MGIT ParaTB has been successfully used as an alternative to radiometric

Bactec. It automatically or manually detects bacterial growth by fluorescence (Shin et al., 2007; Kawaji et al., 2011). This system achieves early detection and high sensitivity. For enumeration purposes, standard growth curves of number of CFU in the inoculum versus time to detection (in days and hours) were validated for bovine strains of MAP (Shin et al., 2007). These equations produced precise estimates (prediction error below one \log_{10} unit) closely matching those obtained with radiometric Bactec. However, this media appeared less efficient for detecting strain of type I from clinical samples (Gumber and Whittington, 2007). An alternative modified Middlebrook 7H9 broth was developed and validated for this purpose. However, this alternative method is not automated and relies on end point titration (see 5.3.1.4.2) for MAP enumeration (Whittington et al., 2013).

5.3.2 Pelleted weight

This method consists in measuring the weight of a pellet of MAP after centrifugation from a MAP suspension. The pellet is usually obtained from a liquid culture medium or after re-suspension of MAP colonies harvested from a plate. The pellet weight can be measured as (1) 'wet weight' after simple draining (Hines et al., 2007), (2) 'dry weight' after MAP desiccation (Kluge et al., 1968), or (3) 'semi-dried' weight of organisms (Karpinski and Zorawski, 1975).

The direct measure of the weight of a pure culture (either dry or wet) can be related to a number of viable bacilli through other enumeration techniques, or by a theoretical calculation based on physical properties of MAP (see 5.4.3). This method can be biased by different sizes of MAP bacilli or differences in the water content for different strains (Elguezabal et al., 2011). It is only suited for concentration of MAP over 10^6 MAP/mL, to minimise the error due to extra water content. This error was approximately two \log_{10} units for suspensions around 10^5 MAP/mL (Elguezabal et al., 2011). An advantage is that the weight of pelleted bacteria is not affected by clumping or loss of growing ability; it is an easy way to quickly eyeball MAP quantities. Similar to turbidity estimates, the conversion between pelleted MAP weight and actual MAP numbers requires using published equivalence figures. Alternatively, a viable count by culture can be done in parallel, for retrospective validation.

Guidelines recommend a standard procedure to obtain the bacterial pellet: centrifuging for 10 minutes at 3000 g and draining the content for 5 minutes before weighting (Hines et al., 2007). This procedure, associated with retrospective CFU counts by serial plate dilution, is recommended as the reference method for reproducible MAP enumeration in experimental infection models of PTB (Hines et al., 2007).

5.3.3 Direct microscopic counts of MAP cells

Microscopic counts of MAP, either on a bacterial suspension or smears, are also frequently reported. This is faster than culture-based methods, but it leads to estimates of the total number of MAP in the sample, including non-viable organisms. Other acid-fast bacilli present in the clinical samples could also induce false positive results. Depending on the purpose, the enumeration of non-viable MAP can be irrelevant. To evaluate the concentration of inoculum doses for experimental infection models, methods counting total MAP numbers could overestimate the infective dose.

5.3.3.1 Direct count using counting chambers

This involves spreading a known volume of unstained MAP cells suspension on a slide equipped with a counting chamber (or haemocytometer). The counting chamber is a well containing a given volume of suspension. A counting grid enables counting the cells in representative microscopic fields. This can be extrapolated to estimate MAP concentration in the suspension.

The technique requires that the cells do not overlap and that their number is large enough to allow quantification; determining the appropriate dilution factor can thus be time consuming (Elguezabal et al., 2011). The presence of large clumps, media remnants, cell debris or other material can preclude the acquisition of reliable or even meaningful results with the counting chamber (Dennis et al., 2010; Elguezabal et al., 2011). This technique is thus only to be used in pure MAP culture. In clinical samples, a direct count of acid-fast bacilli on stained smears is preferable (see 5.3.3.2). Using a counting chamber also enables to evaluate the extent of clumping in suspension. Like all techniques based on MAP physical properties, it does not distinguish between viable and non-viable MAP. Hence, the number of infectious cells is likely overestimated.

Direct count in a counting chamber is less frequent than other enumeration techniques. It is usually performed in parallel with other techniques (Hughes et al., 2001; Reddacliff and Whittington, 2003; Begg et al., 2010).

5.3.3.2 Direct counts of AFB on stained smears

The most common colouration used to stain the wall of acid-fast bacilli in veterinary medicine is the Ziehl-Neelsen (ZN) colouration (Stewart et al., 2004; Verna et al., 2007; Delgado et al., 2009; Begg et al., 2010; Preziuso et al., 2012). Other colourations are sometimes used for

mycobacteria. They include haematoxylin-eosin (Whittington et al., 1999; Rocca et al., 2010; Delgado et al., 2013), ZN and haematoxylin-eosin (Pérez et al., 1996; Begg et al., 2010; Delgado et al., 2013), the Kinyuon method (Gwozdz et al., 2000a) or auramine staining (Damato and Collins, 1990).

5.3.3.2.1 Detection of MAP

Stained smears are primarily used to detect the presence of AFB from clinical samples, alongside tissue histopathology or to detect shedding in faeces (Whittington et al., 2000; Stewart et al., 2004; Bogli-Stuber et al., 2005).

However, MAP organisms are difficult to distinguish from other AFB (Merkal, 1973), causing a lack of specificity of this method. This is especially true in faecal smears with the presence of many other AFB. A study found that 76% of cattle with no other evidence of infection with MAP were AFB positive in faecal smears, including animals from PTB free herds (Merkal et al., 1968). The authors thus preclude the use of this method as a valuable diagnosis of faecal shedding. Furthermore, there is a lack of correlation between ZN faecal smears and faecal culture results, with reports of negative faecal smears from animals in the multibacillary stage of the disease. This confirms the unreliable nature of this test to detect shedding in sub-clinically infected sheep (Whittington et al., 2000).

In histopathology, ZN colouration targets the cell wall of any AFB; however, the presence of wall-deficient, coccoid MAP cells (or spheroplastic forms) was demonstrated in human samples of patients with Crohn's disease (Chiodini et al., 1986). Spheroplasts cannot be detected by standard staining techniques. In ruminants, most PTB lesion types are either abacillary or paucibacillary (Pérez et al., 1996), AFB being sparse or absent in these lesions. The presence of undetectable spheroplastic forms of MAP in clinical samples from ruminants with paucibacillary disease could partially explain this paucibacillary presentation. MAP organisms are significantly smaller and "less rod shaped" than other mycobacteria (Jeyanathan et al., 2006). An accurate detection of the bacilli thus requires using oil-immersion microscopy with an x1000 magnification, in particular for paucibacillary lesions. The x400 magnification appears insufficient for this purpose (Jeyanathan et al., 2007; Delgado et al., 2009). The clumping effect also affects more smears than MAP suspensions. This is especially true for the bovine strain, sometimes rendering the enumeration with this technique impossible (Reddacliff, 2002). Nonetheless, the presence of characteristic granulomatous lesions of graded severity is widely admitted as a specific diagnosis of MAP infection, irrespective of the presence of AFB, since abacillary lesions of PTB are common (Clarke and Little, 1996; Pérez et al., 1996).

5.3.3.2.2 Enumeration of MAP

Stained smears are usually used in experimental studies of PTB to estimate MAP doses in inoculum prepared directly from tissue homogenates (Gwozdz et al., 2000a; Stewart et al., 2004; Verna et al., 2007; Begg et al., 2010). Sometimes a retrospective confirmation by culture-based method is performed in parallel (Begg et al., 2005; Begg et al., 2010). Alternative techniques are usually preferred for pure culture inoculum, such as direct counts in counting chambers or turbidity estimates.

5.3.4 Direct PCR

The amplification of MAP DNA in a sample is a sensitive and specific detection method for infection and/or shedding. Quantitative PCR allows the enumeration of genomic equivalent of MAP organisms.

5.3.4.1 Detection of MAP

A multi-copy insertion element, IS900, which is specific to MAP, was identified in 1989 (Green et al., 1989). It has since been widely used as a probe for MAP DNA detection. Genome sequencing has shed light on the variation of this element in geographically and genetically distant MAP isolates. Despite contradictory evidence about the polymorphism of IS900, see Semret et al. (2006), current and robust evidence suggests a highly conserved and stable IS900. However, limited single nucleotide polymorphism exists, affecting only two loci, which are perfectly correlated with strain type (I/II/III) (Semret et al., 2006; Castellanos et al., 2009). IS900 was originally thought to be perfectly specific to MAP but “IS900-like” sequences with high homology to IS900 were later demonstrated in environmental mycobacteria other than MAP (Cousins et al., 1999; Englund et al., 2002). Such mycobacteria can induce false positive IS900 PCR signals (Tasara et al., 2005). This problem is circumvented by the use of PCR primers targeting areas of IS900 non-homologous to IS900-like sequences (Kawaji et al., 2007; Plain et al., 2014). Altogether, the specificity of IS900-based PCR is virtually perfect for diagnostic of infection/shedding in animals exposed to MAP (Möbius et al., 2008; Chiodini and Chamberlin, 2011; Plain et al., 2014), whether as a routine screening test in livestock or in research for experimental animal models.

Alternatively, a sequence unique to MAP was identified (Poupart et al., 1993; Tasara et al., 2005) and used as a specific PCR probe (Tasara et al., 2005; Möbius et al., 2008). However, this sequence is present as a single-copy in the MAP genome. This is a limiting factor of the

analytical sensitivity of an assay using this probe, compared to multiple copies of the IS900 probe (Ellingson et al., 1998; Kawaji et al., 2007; Abendano et al., 2014).

For detecting faecal shedding of MAP in cattle and sheep, direct faecal PCR using the IS900 probe presents sensitivity at least equivalent to liquid culture (Bogli-Stuber et al., 2005; Kawaji et al., 2007; Alinovi et al., 2009; Plain et al., 2014). Similar PCR techniques and probes were also successfully used to detect MAP in tissues of infected sheep (Delgado et al., 2012; Fernandez et al., 2015).

5.3.4.2 Enumeration of MAP

The use of real-time quantitative PCR allows monitoring by fluorescence the amount of template DNA amplified in real-time. The cycle threshold (Ct) value is the number of amplification cycles required to reach a threshold level of fluorescence. It is inversely proportional to the quantity of targeted DNA templates in the PCR reaction. It provides a good estimate of the number of MAP organisms or of genome equivalents. MAP quantitation requires calibrating each run of the PCR by including dilutions of external control standards of the target DNA (at known concentration). The relative quantity of target DNA present in the sample is thus estimated by interpolating the Ct value with that of the standard curve (Fang et al., 2002). This process is termed absolute quantification. The results are expressed either in number of target copies or in picograms of DNA in the template. Either quantity can be related to the total number of MAP cells in the sample using the published length of the whole MAP genome (Ahlstrom et al., 2015). Plasmids inserted with a copy of the target sequence or MAP genomic DNA can be used as standards (Fang et al., 2002; Sevilla et al., 2014). However, MAP genomic DNA should be preferred for robust enumeration (Yun et al., 2006).

IS900 is often used for quantitative PCR, as this multiple copy sequence is a reliable target for both detection and enumeration (O'Mahony and Hill, 2002; Plain et al., 2014). However, for the purpose of enumeration, some authors prefer single-copy sequences for the PCR probe, typically f57 (Elguezabal et al., 2011; Sevilla et al., 2014). The number of copies of IS900 in MAP genome varies with the strain, reportedly from 15 to 20 copies (Green et al., 1989) or 14 to 18 copies (Bull et al., 2000). As a result, if the number of copies in the template differs from that in the standard, enumeration could be affected. The extent of the error is low, necessarily less than $(20-14)/14 = 43\%$. This is negligible compared to other sources of variation, such as the presence of non-viable MAP, which can affect counts by several orders of magnitude (see 5.4.1.1).

While this method is not affected by clumping or by the presence of non-cultivable MAP in the sample, it cannot distinguish between viable and non-viable MAP. Moreover, at lower concentrations (typical in clinical samples), underestimation of MAP numbers could occur due to larger proportional DNA loss during the extraction process (Elguezabal et al., 2011). This pitfall can be avoided using magnetic bead extraction methods, known to have a better DNA extraction yield than conventional methods. With this technique, the analytical sensitivity of quantitative PCR is 10 MAP/gram of faecal sample (Plain et al., 2014; Sevilla et al., 2014), and the obtained estimates are more precise and more reproducible than when using plate counts (Elguezabal et al., 2011).

5.3.5 Other methods

Immunohistochemistry and *in situ* hybridisation are less common detection methods involving direct detection and visualisation (using a fluorescent label for example) of MAP specific antigens (immunohistochemistry) or specific DNA probes (*in situ* hybridisation) in the tissues of infected animals. However, neither method can be used to enumerate MAP cells. *In situ* hybridisation was developed as an alternative for the detection of the spheroplastic form of MAP (Hulten et al., 2000). It is mainly used in human medicine for the study of Crohn's disease and its link with MAP in human samples.

5.4 Equivalence between estimates from the different methods:

Different enumeration methods measure different parameters (*e.g.* viable/cultivable MAP or total MAP), each with inherent biases. We present here estimates of the relationships between the measures from different methods.

5.4.1 Viable MAP versus microscopic direct count

5.4.1.1 *Direct counts using a counting chamber versus end point titration:*

In a study designed to compare different methods of enumeration, the counts using a Thoma counting chamber were consistently and significantly higher than counts obtained by end point titration in most of the trials (Reddacliff, 2002). In some trials, estimated numbers of viable MAP were similar to total number estimates. In other trials, viable MAP counts were up to two

\log_{10} units lower than total counts. When suspensions were treated to reduce clumping, the differences between direct counts and MPN estimates decreased to less than half a \log_{10} unit, not statistically significant. This suggests that an apparent difference between a viable count and a total number of MAP is partially due to an underestimation of the number of viable MAP by culture methods because of organism clumping. However, in samples containing both viable and non-viable MAP, the use of direct counts can also overestimate the number of viable organisms by up to one order of magnitude (Reddacliff and Whittington, 2003). A difference of one \log_{10} unit means that up to 90% of the bacteria present in suspension might be non-viable.

5.4.1.2 Direct microscopic counts using a counting chamber versus plate count:

In one study, the number of organisms (ovine strain) in either cultures or tissue samples were determined by microscopic counting, and numbers were “confirmed retrospectively” by colony counts on solid medium (Begg et al., 2005). This suggests that results obtained by either method were not extremely different. In another study (Delgado et al., 2012), MAP concentration in two inocula (low and high dose) was estimated by direct microscopic counts to 3×10^8 MAP/mL and 1.2×10^3 MAP/mL respectively. Using culture on Lowenstein-Jensen and 7H11 media, retrospective estimates of doses resulted in 4×10^6 and 10^2 CFU respectively (Delgado et al., 2012). Plate counts thus underestimated MAP numbers by a factor 10 to 100, for these ovine strains. Very similar results were obtained for Cattle strains, with estimates by plate counting one to two \log_{10} units lower compared to direct microscopic count with a counting chamber (10^8 cells/mL of bacterial suspension, (Sevilla et al., 2014)).

5.4.1.3 Direct microscopic counts on ZN stained smears versus end point titration

In Begg et al. (2010), MPN and direct visual counts on ZN-stained smears were carried in parallel on a filtrated suspension from homogenate tissue samples of sheep. The number of viable MAP estimated by end point titration was 2.3×10^8 /mL while total numbers of MAP by direct microscopic count was 3.7×10^8 AFB/mL (Begg et al., 2010). The bacterial suspension was treated before enumeration to maximise MAP recovery (with a centrifugation step) and to minimise clumping (passage through a fine gauge needle twice). The observed difference was thus limited, suggesting that at least 60% of the MAP organisms were viable in this experiment.

5.4.2 Plate count versus end point titration

Experiments comparing different enumeration methods show that colony counts on plates consistently underestimate the number of viable MAP compared to end point titration (Reddacliff, 2002). For suspensions obtained from pure culture of various sheep strains and one bovine strain, the colony counts were smaller but the difference with MPN was limited (half to one \log_{10} unit) and not significant in most trials. For the bovine strain (suspension treated to limit clumping), the difference was less than half a \log_{10} unit and not significant. With some sheep strain cultures however, a high variation of plate colony counts between replicates was observed, and the magnitude of the difference with MPN was greater, up to two \log_{10} units. For sheep strains obtained directly from tissue homogenates, growth on plates gave inconsistent results. Absence of colonies was noted even for samples containing approximately 10^8 to 10^9 viable MAP as per end point titration. This highlights the shortcomings of enumerating viable MAP on solid media in clinical specimen from sheep. Begg and Whittington (2008) reported that “colony counts typically underestimate the viable count by several orders of magnitude compared to counts by limiting dilution in liquid media”.

5.4.3 Weight of pelleted bacteria versus “theoretical” total number or other methods

The experiment of (Brotherston et al., 1961a) originally attempted to enumerate viable MAP colony counts on solid media. The authors proceeded to limit the clumping effect, and they reported to have obtained “rarely more than 10 bacilli per clump”. They indicated that two milligrams (mg) wet weight of pure MAP culture was equivalent to approximately 10^8 to 10^9 CFU by plate serial dilution.

A retrospective verification of these estimates was attempted in Reddacliff (2002), based on MAP physical properties. Considering an average size of MAP at one micrometre long and specific gravity of similar to *Mycobacterium tuberculosis* (*M. tb.*), a “theoretical” number of 5×10^9 MAP/mg dry weight was calculated. Assuming 85% water content for MAP organisms, similar to *M. tb.*, this corresponds to a theoretical number of 7.5×10^8 MAP/mg wet weight. The authors compared this with estimates in Brotherston et al. (1961a). They accounted for the reported clumping with a 5-fold underestimation correction and for an 85% MAP water content. The resulting estimates of MAP doses corresponding to reports in Brotherston et al. (1961a) ranged from 1.6×10^9 to 1.6×10^{10} MAP/mg dry weight. These figures show a good agreement with theoretical numbers based on physical characteristics of MAP cells (Reddacliff,

2002). This indicates that CFU counts in Brotherston et al. (1961a) were relatively accurate and that bias due to clumping was probably no more than a 5-fold underestimate. However, it should be noted that the length of MAP organism may vary between one and two micrometres (Elguezabal et al., 2011).

Another study (Kluge et al., 1968) provided similar estimates with 1 mg dry weight of MAP suspension containing approximately 10^8 organisms as per plate counts. Other estimates were lower: Elguezabal et al. (2011) found 1 mg wet weight of MAP equivalent to 3.75×10^6 CFU (on average for eight different strains at different time points of the growth curve). This study also concluded that viable counts obtained by plating “grossly underestimates” the number of MAP, although the same experiment showed that 1 mg wet weight was also equivalent to only 3.39×10^7 MAP genome equivalent estimated by qPCR (less subject to underestimation than colony counting). It was not possible to establish distinct patterns in each strain, hence results were reported overall for both type I and II MAP strains (Elguezabal et al., 2011). Juste et al. (1994a) reported that 150 mg wet weight represented 1.36×10^6 CFU of bovine isolate. This represents less than 10^4 MAP/mg wet weight. This figure seems to be strongly underestimated, possibly due to excessive clumping.

In guidelines for experimental infection models of PTB (Hines et al., 2007), expert advice states that 1 mg pelleted wet weight averages approximately to 1×10^7 CFU, although no experimental evidence is provided.

5.4.4 McFarland units versus qPCR or direct microscopic count

Over eight different isolates including sheep and cattle strains, Elguezabal et al. (2011) found that one McFarland unit was equivalent to 1.2×10^8 genome equivalent by quantitative PCR. This is very close to the theoretical number of expected cells according to the McFarland standard (based on *E. coli*). It is also in line with other results from Kralik et al. (2012), and reveals an excellent fit between MAP cells numbers determined by qPCR and theoretical *E. coli* numbers according to the McFarland standard. The result is valid for cultures of MAP at different concentrations. Quantitative PCR and turbidity methods closely agree despite being very different techniques; both methods are thus likely accurate in enumerating the total number of MAP (see 5.4.5 and 5.4.6).

Similarly, Hughes et al. (2001) found a linear relationship between McFarland units and direct MAP counts in a counting chamber, with 1 McFarland units being equivalent to 10^8 cells/mL (total cell count).

5.4.5 McFarland units versus plate counts

The standard of one McFarland unit corresponds to 3×10^8 cells of *E. coli*/mL (Perilla et al., 2003). In theory, this cannot be extrapolated to MAP given different physical properties between the two species.

Overall for eight different MAP isolates including sheep and cattle strains, Elguezabal et al. (2011) found that one McFarland unit was equivalent to 1.3×10^7 CFU/mL by plate counting. In Fernandez et al. (2015), one McFarland unit of an ovine strain was equivalent to 5×10^7 CFU/mL by plate counting. Similar results were obtained for two cattle strains in Fernandez et al. (2014), with estimates by plate count less than half a \log_{10} units lower than the expected cell counts in McFarland unit (assuming one McFarland unit corresponds 1×10^8 cells/mL). For two sheep strains however, this difference was greater, with plate counts 1 to 2 \log_{10} units lower than expected. The authors assumed that this discrepancy was due to the difficulty of growing sheep strains rather than actual low MAP viability.

5.4.6 qPCR versus plate counts

For MAP organisms isolated in dairy herds, the Spearman correlation between the Ct value of qPCR and the CFU on Herrold Egg Yolk medium was estimated between -0.66 -for faecal pools containing five to several hundred individuals- to -0.76 for fresh environmental samples. This clearly indicates a good correlation between the two methods (Aly et al., 2010).

Using three different cattle strains of MAP in serial dilutions, Kralik et al. (2012) showed that culture on solid media consistently and significantly underestimated MAP numbers by about two \log_{10} units compared to qPCR. The authors mention that clumping could not be avoided. It is a potential explanation of the observed difference between the two methods, since clumping affects culture but not qPCR.

The established relationship between genome equivalent (qPCR) and CFU (plate count) likely depends on the phase of growth in liquid broth. Elguezabal et al. (2011) showed that qPCR underestimated MAP CFU numbers at low MAP concentrations due to a lack of analytical sensitivity. In later stages however, viable counts (CFU) underestimated the numbers of genome equivalents (up to a factor 1:187 after 142 days of culture). This is probably due to clumping, loss of viability or dormancy occurring in the late stages of *in vitro* culture. This discrepancy reflects biases in both enumeration methods. It likely results in an underestimate

of viable MAP numbers by culture-based methods and an overestimate by qPCR. To the best of our knowledge, the exact extent of each bias cannot be quantified precisely.

5.5 Summary

Each enumeration method has inherent bias. Moreover, the extents of the bias vary for each MAP isolate or strain (Shin et al., 2007; Elguezabal et al., 2011). No gold standard exists to detect or enumerate MAP organisms. All enumeration methods are evaluated relative to each other; hence, their absolute accuracy remains unknown.

Some methods can only detect “viable” MAP while others can account for both viable and non-viable MAP in the samples. One or the other has different clinical relevance. We used the word “viable” throughout this review, although “cultivable” may be a better term. Nevertheless, CFU on solid media is the reference for reporting doses in experimental challenge studies, despite important underestimation bias due to clumping and slow growth with this method (Reddacliff, 2002; Hines et al., 2007; Elguezabal et al., 2011; Kralik et al., 2012). The use of CFU as the gold standard for enumeration is thus questionable (Elguezabal et al., 2011). However, methods not based on culture cannot distinguish between viable and non-viable MAP. As such, they were reported to “overestimate the number of infectious units in the sample” (Hines et al., 2007), although the presence of non-viable MAP could be limited by strict observance of good laboratory practices (Elguezabal et al., 2011).

The purpose of MAP enumeration provides guidance as to the choice of the method and the interpretation of biases. For example, to enumerate MAP numbers in clinical samples, culture-based methods should be avoided. Indeed, laboratory processing of the samples prior to enumeration (storage, decontamination, and filtration) causes a loss of MAP viability that would affect the results.

Enumeration of MAP often aims at calculating inoculum doses for pathogenesis studies. In this case, enumeration of viable MAP would be more relevant. Any loss of viability occurring during procedures ahead of acquisition of the inoculum suspension would thus be accounted for. Colony counts on solid media are not reliable for ovine strains, in which case methods using liquid media are better suited. Culture-based methods are only suitable for dilutions of pure culture, not for tissue sample homogenate.

Methods enumerating total numbers of MAP should not be compared with those enumerating viable MAP. Moreover, they should not be used as a reference for each other. In particular, for

determining the analytical sensitivity of a MAP detection method such as qPCR, culture-based methods should not be used as a reference to avoid gross underestimations (Kralik et al., 2012). Instead, a direct count on ZN coloured smears, with oil-immersion microscopy (magnification x1000) is feasible. It provides more accurate results, and is well suited as a reference for qPCR.

Finally, although quantitative results differed across enumeration techniques, the variation was mostly within two orders of magnitude (two log₁₀ units) in a defined framework. This should be contrasted with variations in true MAP quantities contained in clinical samples or culture suspensions in which MAP enumeration is attempted.

5.6 Conclusion: application for interpreting inoculum doses of experimental challenge models

The effect of MAP dose on the outcome of infection with MAP is essential to evaluate for modelling ovine PTB. A meta-analysis of experimental challenge studies with MAP can quantify this dose effect across studies. Results of the present review identified different enumeration techniques with their inherent biases and specific purposes. This can serve as a guideline to conduct the meta-analysis, regarding the extraction and interpretation of MAP dose effects from experimental challenge experiments.

From this review, a general binary classification of enumeration methods follows: (1) methods quantifying the total number of MAP organisms irrespective of viability, and (2) methods enumerating the number of viable (or even cultivable) MAP. These two categories cannot be compared directly. Pooling studies using both methods together in a meta-analysis might therefore blur the effect of dose and/or introduce biases. For example, if culture-based methods perform differently with ovine versus bovine MAP strains, the estimation of the effect of strain in the meta-analysis might also be biased. The enumeration method used to calculate inoculum doses in each experiment needs to be included in the meta-analysis to adjust for potential confounding. More specifically, possible biases can be evaluated by exploring interactions between the dose, the enumeration method and the strain.

Some studies report wet or dry weight of bacterium pellets as a measure of inoculum. These weights can be converted in equivalent number of CFU according to guidelines in (Hines et al., 2007): 1 x 10⁷ MAP CFU/mg wet. This is the same order of magnitude as the number of

genome equivalent assessed by Elguezabal et al. (2011). This number corresponds approximately to 1.5×10^6 MAP CFU/mg dry weight, assuming a MAP water content of 85%. We acknowledge that other authors came up with figures several orders of magnitude higher (Brotherston et al., 1961a; Reddacliff, 2002). Nevertheless, the most important consideration is to be consistent across studies in the interpretation of experimental MAP doses while conducting the meta-analysis.

Following the guidelines aforementioned should help standardise the interpretation of inoculum doses from various sources, and enable adjusting for potential biases introduced by the enumeration method. It should therefore ease and improve the conduct of the meta-analysis.

Chapter 6. Meta-analysis of experimental infection of sheep with *Mycobacterium avium* subsp. *paratuberculosis* to inform mathematical modelling of ovine paratuberculosis

Nelly Marquetoux^a, Matthieu Vignes^b, Peter Wilson^c, Anne Ridler^c, Cord Heuer^a

^a EpiCentre, Institute of Veterinary, Animal and Biomedical Sciences, Massey University, New Zealand

^b Institute of Fundamental Science, Massey University, New Zealand

^c Institute of Veterinary, Animal and Biomedical Sciences, Massey University, New Zealand

6.1 Abstract

A meta-analysis of experimental infection of sheep with *Mycobacterium avium* subsp. paratuberculosis (MAP) was conducted to inform a mathematical model of ovine paratuberculosis. A total of 767 sheep inoculated with a known dose of MAP and from which relevant clinical outcomes were measured were identified for the meta-analysis. Generalised additive mixed models (GAMM) were used to analyse the impact of time from challenge on (1) the probability of occurrence of histological lesions in the intestine, (2) the probability of presenting markers of progression to severe disease, and (3) the probability of mild intestinal lesions versus diffuse severe lesions. Additionally, (4) a survival analysis was performed on a small sub-sample of animals to evaluate the rate of cure from transient shedding in sheep on a pathway to recovery. The effect of experimental covariates of biological importance at the host-level (age at inoculation, breed), at the pathogen-level (strain of MAP, inoculum dose) and related to the experimental conditions (type of inoculum, MAP enumeration method) were estimated. Our results show that MAP is highly infectious in sheep, with only 76 live organisms necessary to infect actively 50% of inoculated sheep. However, the virulence of MAP is low: 8.9×10^6 MAP organisms are necessary to cause progression to clinical disease in 50% of sheep infected as lambs or hoggets, and 7.7×10^9 MAP for sheep infected after one year of age. The obtained results were used secondarily to estimate parameters for a mathematical model of ovine paratuberculosis. All estimates and measured effects were driven by all available experimental data on ovine paratuberculosis and we conclude that the

model parameterisation based on this meta-analysis was a robust alternative to a more simple review process or using previously published model parameters from other species.

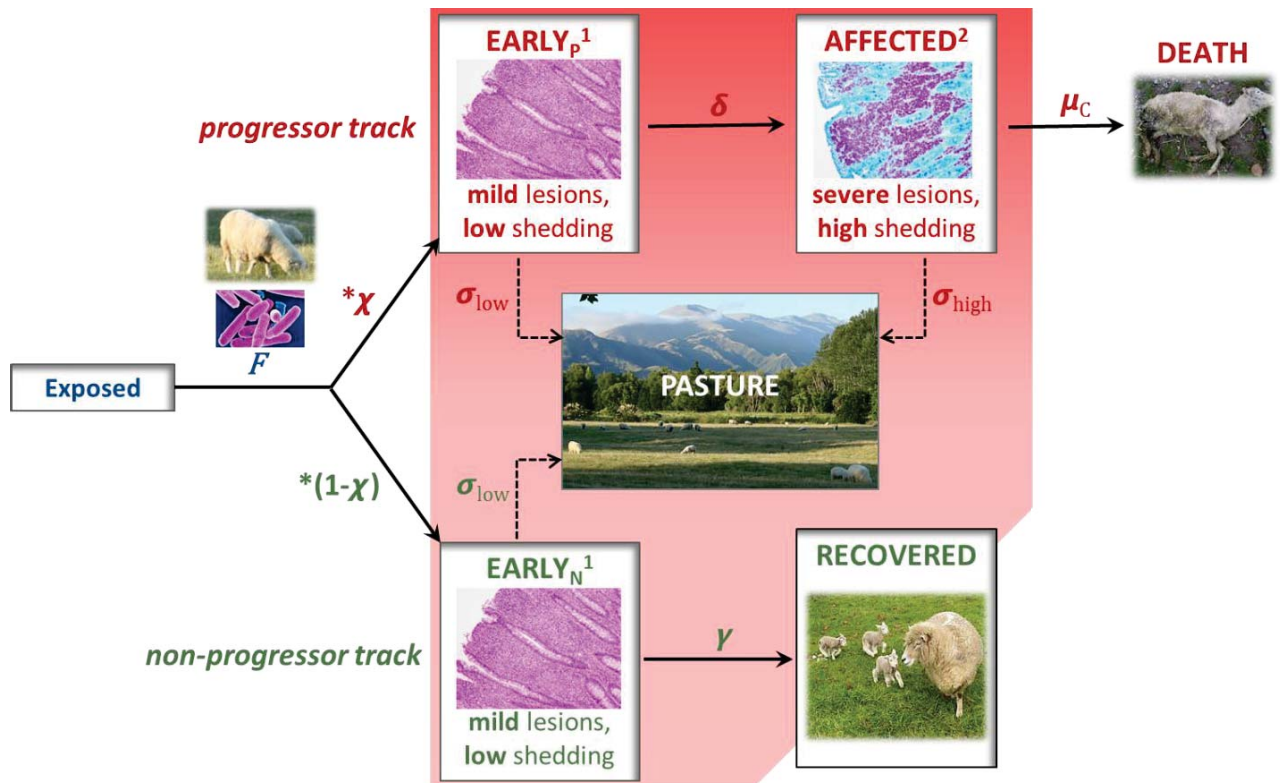
6.2 Introduction

Mathematical modelling of infectious diseases relies on a close understanding of the disease patho-physiology. A desirable property for a model is parsimony, while accurately capturing important phases of the disease. Developing the structure of such model and parameterizing it often appeals to experimental studies of physio-pathology in a controlled environment.

Paratuberculosis is a chronic infection with *Mycobacterium avium paratuberculosis* (MAP), affecting sheep and other ruminants. Late stages of infection are associated with the development of severe lesions in the intestine, which translates to subclinical production losses followed by the onset of clinical disease and ultimately death, detrimental to the economy of the farm. Evaluation of the economic impact of paratuberculosis can be addressed by mathematical modelling, providing the model adequately captures transitions from one stage to the next with respect to aspects of both transmission dynamics and possible production effects.

A preliminary literature review of the patho-physiology of paratuberculosis in sheep enabled us to develop a hypothesised structure for a mathematical model of ovine paratuberculosis (Chapter 4). The candidate model structure (Figure 6-1) illustrates the potential host-pathogen interaction of sheep infected with MAP. However, it was not possible to derive quantitative estimates for all these interactions directly from this review, due to methodological limitations, such as small numbers of animals in each study, confounding at the study level and lack of comparability between studies. This prompted the need for a more formal framework to derive quantitative data and to assess the robustness of assumptions generated in the review.

This individual-animal-based meta-analysis study firstly aimed to summarize all published accounts of experimental models of paratuberculosis in sheep and evaluate outcomes of exposure to MAP, such as infection, shedding, and progression to clinical stage. The second aim was to derive quantitative parameters for the mathematical model presented in Figure 6-1. We also evaluated the effect of MAP inoculum dose, MAP strain type, breed of the sheep and age at challenge on outcomes of infection. Finally, we explored the effects of possible artefactual confounders, such as diagnostic tests and methods of enumeration of the inoculum dose.



¹ sub-clinically infected with MAP, no visible production effects;

² affected by MAP, sub-clinically then clinically, experiencing production effects.

Figure 6-1: hypothesised model structure for transmission dynamics of ovine paratuberculosis. F is the rate of entry into active infection following exposure through contaminated environment. χ is the proportion of infected animals entering the progressor track, δ the rate of progression from mild to severe disease, γ the rate of exit from early, transient shedding into a recovered state, μ_c the rate of mortality due to clinical paratuberculosis, sigma the rate of shedding into the environment (high or low shedding).⁷

6.3 Materials and methods

We followed the Cochrane guidelines for the systematic selection of published reports for this meta-analysis and the checklist from the Preferred Reporting Items for Systematic reviews and Meta-Analyses (Moher et al., 2015). An outline of the meta-analysis method can also be found in Berman and Parker (2002).

6.3.1 Literature search

We used the Web of Science database as a source of publications encompassing the Web of Science Core Collection, Biological Abstracts, CABI: CAB Abstracts, Current Contents Connect,

⁷ References for the pictures: MAP bacterium from Oregon State University website (<http://smallfarms.oregonstate.edu/sfn/fl11Johnedisease>); histological lesions in the small intestine: (Smeed et al., 2007) Figures 2 and 3; Ewe and triplet lambs: https://en.wikipedia.org/wiki/Sheep_farming_in_New_Zealand; dead ewe: picture credit Stefan Smith; NZ sheep pasture: picture credit primary author.

FSTA (the food science resource), Journal Citation Reports, MEDLINE, and SciELO Citation Index. A search was carried out using all databases and the following terms: ((sheep OR ovine) AND (paratuberculosis OR johne*) AND (experimental OR vaccin* OR faec* OR shed*)). This identified 834 publications up until July 2015, narrowed down to 538 original science publications, reviews, clinical trials and thesis dissertations by excluding non-peer-reviewed reports.

To ensure that sheep included in this meta-analysis were comparable, we selected studies based on a set of pre-established criteria so that they were comparable in design and purpose. Papers were selected by title and abstract. Eligible papers were those in which experimental studies involved sheep inoculated with viable MAP organisms, irrespective of the purpose of the study or what clinical outcome was reported. Both physio-pathology studies and vaccine trials were eligible, but only unvaccinated control sheep challenged with MAP were recruited for the meta-analysis. Studies where MAP antigens or killed MAP were used as a challenge were dismissed. Review papers were not eligible for the meta-analysis; however, the references they contained were checked for eligibility. Abstracts of papers with eligible titles were read and where abstracts were not available, full text was retrieved. Sixty eight papers met the selection criteria (66 from the primary literature search, 2 from secondary references checks) and the full-text for these articles was retrieved through Massey University library.

Based on the full text copy, the selection was further restricted to experimental studies of sheep with at least one of the following monitored outcomes: infection by MAP in tissues, presence of histological lesions at *post-mortem*, faecal shedding. Essential elements of study design were also required: an estimation of the size of the MAP inoculum, age of sheep at inoculation and time elapsed from challenge to *post-mortem*.

Of the 68 full-text papers that were evaluated, 27 were excluded for the following reasons:

- two review papers (after checking that all eligible references had been considered in the search),
- three papers in foreign languages (one in Italian, one in Portuguese, one in Russian),
- eight papers due to unsuitable outcomes (immunologic/enzymatic aspects, intestinal absorption function in sheep),
- six papers where oral experimental challenge of unvaccinated sheep had not been performed (all sheep vaccinated, no challenge of the unvaccinated control group, natural infection rather than experimental challenge, *in-situ* intestinal infection rather than oral route),

- seven papers that did not provide study design details required for the meta-analysis,
- one paper for lack of consistency in the report of study design.

Seven of the papers excluded at this stage (for example reporting only immunologic results) had been reported in another paper that was included in the meta-analysis, thus excluding them did not cause a loss of information. Additionally, PhD theses related to selected published papers were searched manually, yielding three theses (Gwozdz, 1999; Reddacliff, 2002; Begg, 2004). These were used to provide more details about the study design and to double-check the accuracy of information primarily extracted from the corresponding published papers, as well as including animals that were not reported in the journal articles or more detailed outcomes.

The final meta-analysis included 44 peer-reviewed documents consisting of 41 published journal articles and 3 PhD theses.

6.3.2 Data extraction and standardisation

Individual sheep data were retrieved from all the studies (reconstructed from summary data if necessary), with the aim of matching the experimental protocol and the observed individual outcome. Outcomes that could not be inferred at the individual sheep level were dismissed. To avoid duplication, care was taken to identify and exclude cases where the same experiment was reported several times in different papers by the same authors. Any extra information in those cases was retained when, for example, the experimental outcome was different and also used to double-check the data. Each individual sheep was only included once (avoiding duplicates). When the information from the paper was confusing (example: numbers of sheep not adding up, uncertainty about the strain type of MAP) or some of it missing (example: age/breed of the sheep) authors were contacted by email to clarify. We tried to contact eleven authors and reached nine, of which eight gave useful information and sometimes additional data. The literature search and data extraction was performed by the primary author and the entire process was repeated twice several months apart.

To evaluate the effect of MAP inoculum dose on various pathological outcomes, the total dose administered singly or over successive challenges over a period of time was determined for all sheep from all the papers included. The time of inoculum is defined as when the first dose of MAP was administered. The concentration of MAP in the inoculum (dose) was expressed variously as follows (see Chapter 5):

- McFarland turbidity scale for a suspension of MAP,
- Direct microscopic count,
- Most probable number (MPN) in liquid culture ,
- Plate count,
- Pelleted bacterium weight (dry or wet weight): these were retro-converted into CFU equivalents using the equivalence published in recent guidelines (Hines et al., 2007),
- Mucosa weight of intestine tissue: in one study (Stewart et al., 2004) a subset of the inoculated sheep (10 animals) were dosed with a given weight of intestinal mucosa from a clinical case of paratuberculosis, with no estimation of MAP numbers. These observations were kept for the descriptive analysis but removed in all regression models where the effect of dose was evaluated.

These enumeration methods were divided into two categories: culture-based methods enumerating viable MAP (MPN, plate count, CFU equivalent of bacterium pelleted weight) or total viable and non-viable MAP organisms (turbidity, direct microscopic count).

6.3.2.1 Outcome definitions

The following outcomes were subjected to meta-analysis:

- Presence of MAP in the tissues (yes/no), either from small intestines or regional mesenteric lymph nodes, detected by bacteriology (tissue culture), immuno-histo-chemistry or tissue PCR. This outcome is a marker for the colonisation of the intestinal tract with MAP with or without tissue lesions.
- Presence of MAP-specific lesions of any grade in the wall of the small intestine by histological examination: this is a marker of active infection where the cellular immunity responds to the presence of MAP in tissues. The severity of lesions was determined when possible from the described individual histology.
 - Mild-moderate lesions (type 1 and 2) were considered markers for early disease stages from which it was possible to recover or progress to more severe disease.
 - Severe lesions presented a diffuse cellular infiltrate of macrophages and/or lymphocytes involving structures beyond the lamina propria in areas of the sub-mucosa and mucosa, such that the ultra-structure of the intestinal villusities was altered (atrophy). They were grade 3 lesions according to the Perez score (Pérez et al., 1996), also called lepromatous lesions in some early publications. The presence of these lesions was considered an early marker for onset of a clinical stage (sub-clinically affected, then clinically affected).

- Progressor: Binary covariate representing a marker of progression for every sheep. Progression was defined as presenting severe histological gut lesions or clinical signs. The presence of clinical signs was usually monitored by a loss of weight or low body condition score. If both conditions (histology with recording of lesion severity and assessment of clinical status of the animals) were fulfilled, and the individual correspondence could be established, the progressor covariate was set to 1 when the sheep was positive to either test (versus 0 if negative to both). If only one test was performed, this partial information informed the progressor status. Some sources did not provide detailed results with sheep ID but pooled results instead, so that both tests were performed but no formal correspondence at the individual level could be established between the different outcomes. In this case, the test that identified the largest number of sheep as progressors was used, and the information of the other test was dismissed to minimize sources of bias.
- Faecal shedding: for a small subset of animals, faecal shedding was monitored serially (more than once). We recorded the results of faecal shedding assessed by faecal culture and faecal PCR. Results obtained by faecal smears were dismissed due to the lack of sensitivity of this technique.

6.3.2.2 Covariate definitions

The covariates thought to have an impact on the outcome (from Chapter 4) and retrieved for each sheep were as follows:

- Time to *post-mortem* (t_{tpm}): most outcomes were evaluated at *post-mortem*, hence the time from first challenge to *post-mortem* was a variable of interest.
- Dose: the log of the total estimated inoculum dose received by each sheep during the challenge process.
- Enumeration method: a two-level covariate representing the enumeration method used in the paper to establish the inoculum dose, either MAP CFU using culture-based methods (a proxy for viable MAP or cultivable MAP) or enumerating the total number of MAP organisms in the inoculum irrespective of viability (qPCR, direct microscopic counts, turbidity estimates). A potential differential bias may exist between these because the enumeration of total MAP cells likely overestimated viable MAP counts (see Chapter 4). Models were fitted using the reported dose or a dose calculated according to guidelines of Hines et al. (2007). The potential bias was evaluated in all final models by including an interaction term between the dose and a binary variable representing the enumeration method, viable or total MAP.

- Inoculum type: a two-level covariate representing whether the inoculum was made of laboratory passaged MAP (pure culture of MAP) or directly from tissue homogenate of a clinical case of paratuberculosis.
- Strain: a two-level covariate representing the strain type (type I or “ovine strain” versus type II or “bovine strain”). The strain type was evaluated in a proportion of studies using PCR of the IS1311 fragment, which is considered perfectly specific. For studies not using molecular diagnostic tests, we determined the most likely strain by an educated guess using a combination of information about the cultural and biological characteristics of the strains, epidemiological information and in some cases by contacting the authors of the studies, guided by expert advice (Karen Stevenson⁸ and Marian Price-Carter⁹).
- Age of the sheep at dosing: four mutually exclusive methods of coding the effect of age in each model were used to find the best way to account for age in each distinct model (corresponding to a distinct dataset):
 - age as a continuous variable,
 - age category: lamb = 0 to 3 months old, hoggets = 4 to 12 months old, two-tooth = 13 to 24 months old, adult = more than 24 months old.
 - lamb: 1 if the sheep was less than 3 months old (0 otherwise).
 - young: 1 if the sheep was in its first year of age (0 otherwise).
- Breed: there was a great diversity of breeds (17 breeds and crosses plus unknown), hence they were categorised as “Romney and crosses”, “Merino and crosses”, “Other British breeds”, “Mediterranean and Middle East breeds”, or “others and unknown”.

A general assumption of all experimental challenge models included in this meta-analysis was that all enrolled sheep had not been infected by MAP prior to the time of inoculation (t_0). To take that into account, each animal in the dataset had two observations: one at t_0 with all outcome variables set to 0, and one at the actual time of *post-mortem* with the outcome variables observed at *post-mortem*, and with the same exposure variables at both time points.

⁸Moredun Research Institute, Pentlands Science Park, Bush Loan, Penicuik, EH26 0PZ, Scotland, UK

⁹Hopkirk Research Institute, AgResearch Grasslands, Tennent Drive, Private Bag 11008 Palmerston North 4442, New Zealand

6.3.3 Data analysis and parameter estimation

6.3.3.1 Probability of entering the actively infected compartment

We used the presence of histological lesions in the small intestine of sheep as a marker of active infection (as opposed to mere colonisation of the intestine with MAP) and a good proxy for shedding (see Chapter 4).

6.3.3.1.1 Modelling the probability of active infection over time

Histological examination was performed at *post-mortem*, representing a cross-sectional observation at one unique point in time. Due to the absence of follow-up of histological lesions and the potentially long periods of time that elapsed from challenge to *post-mortem*, the use of survival analysis (modelling incidence) was precluded.

Standard logistic regression with the outcome histology positive at *post-mortem* (0/1) was performed with the aim to evaluate the probability of active infection as a function of time since inoculation. We used Generalised Additive Mixed Models (GAMM), a semi-parametric method using cross-validation and a penalised likelihood approach where time (t_{tpm}) was processed by a non-parametric smoother function using regression splines (thin plate smoother) (Wood, 2003). Other covariates: dose, enumeration method, inoculum, strain and age were added in the parametric part of the model as a linear combination of covariates at logit scale. This was realised using the gam function from the mgcv package in R (Wood, 2006). Since there were two observations per sheep and individual sheep were clustered into experiments, experiment ID and individual sheep ID were included as random effects to account for clustering (Hu et al., 1998).

The model structure was as follows:

$$\text{logit}(\text{histological status})_{ij} \sim \text{intercept} + \sum_{k=1}^n \beta_k x_{ki} + f_{t_{tpm}}(t_{tpm})_i + U_{ij} + U_i + \varepsilon_i,$$

(model 1)

Where subscript i denotes each individual sheep and j the experiment ID, k is indexing covariates other than time in the parametric part of the model, f is a smoothing function of t_{tpm} for which no formal equation can be shown, U are the random effects for experiment and sheep ID and ε the residual error term.

An interaction term between dose and enumeration method was evaluated to test the existence of a potential experimental bias due to the use of different enumeration techniques for MAP inoculum doses. Variables were retained in the model based on biological significance, Wald test and lowest Akaike Information Criterion (AIC).

6.3.3.1.2 Deriving parameters for the expression of the force of infection (F)

The first model was built to predict the probability of being histology positive over time and has been called *model 1*. This probability is equivalent to an “epidemic curve”, *i.e.* the prevalence of active infection over time. This predicted probability of *model 1* was also a function of the inoculum dose, as dose was a significant covariate. We used this relationship between prevalence of active infection, time and MAP dose to derive parameters entering in the calculation of the force of infection for a mathematical model of indirect transmission of MAP to sheep (Figure 6-1): the rate of transition from exposed to actively infected, and the probability of success upon ingesting an infective dose.

All subsequent steps were carried out for values of the inoculum dose varying between 10^1 and 10^{12} MAP. Based on the shape of the predicted probability curve of *model 1*, in particular the existence of a plateau of infection after some time, it could be assumed that recovery events were negligible early on in the course of infection. The epidemic curve in this early phase was therefore equivalent to the cumulative incidence of active infection and the incidence rate can be derived. An appropriate distribution for the time from exposure to active infection is the Weibull distribution with two parameters (α , k), that allow the rate to vary with time. A special case is the exponential distribution with a constant rate. We fitted a Weibull (or exponential) distribution to the data which included both time at *post-mortem* and challenge dose.

The following Weibull cumulative probability function was used to model the cumulative probability of active infection. It depends on time (t) and dose:

$$P(\text{already infected at time } t)_{dose} = P(T < t)_{dose} = 1 - \exp^{-(\alpha_{dose} * t)^{k_{dose}}} \quad \text{Equation 1}$$

where P represents the predicted probabilities of *model 1*, T is the time to onset of infection (unobserved), t is the observed time to *post-mortem*, α and k are respectively the scale and shape parameters of the Weibull distribution ($k=1$ for the exponential distribution) and the subscript $_{dose}$ represents inoculum dose.

A Weibull distribution includes the limits 0 and 1. Hence if the observed probabilities obtained from *model 1* reached a plateau below 1 or didn't start exactly at 0, it would be difficult to fit a Weibull distribution. We therefore rescaled the predicted probability of active infection (*model 1*) to include the limits 0 and 1 as follows:

$$P_1(T < t)_{dose} = \frac{P(T < t)_{dose} - \min(P(T < t))_{dose}}{\max(P(T < t))_{dose} - \min(P(T < t))_{dose}} \quad \text{Equation 2}$$

where $\min(P(T < t)_{dose})$ corresponded to the minimum predicted probability of active infection of the early phase of onset (ie. the starting point, which happened to not be exactly 0 since corresponded to predicted probabilities) and $\max(P(T < t))_{dose}$ corresponded to the first local maximum (ie. the value of the plateau), both being dose specific. We henceforth refer to $\max(P(T < t))_{dose}$ as the 'plateau'. A simple transformation of Equation 1, in which $P(T < t)_{dose}$ was replaced by $P_1(T < t)_{dose}$ from Equation 2, leads to:

$$\log(-\log(1 - P_1(T < t)_{dose})) = k_{dose} * \log(\alpha_{dose}) + k_{dose} * \log(t) \quad \text{Equation 3}$$

We thus plotted $y = \log(-\log(1 - P_1(T < t)_{dose}))$ as a function of $\log(t)$ and fitted a straight line through the early phase of this curve i.e. between $t=0$ and $t=t_{max}$. t_{max} is the time chosen as the upper bound for the early phase which could be fitted by a Weibull distribution. It is the local maximum (first peak or plateau of infection) in the probability of active infection, occurring at day 214 post inoculation. According to Equation 3, the slope of this regression equals k_{dose} and the intercept equals $k_{dose} * \log(\alpha_{dose})$. From the coefficients of the linear regression corresponding to Equation 3 we could derive α_{dose} and k_{dose} the Weibull parameters corresponding for doses varying between 10 and 10^{12} .

These relationships are shown in Figure 6-2 (a-c).

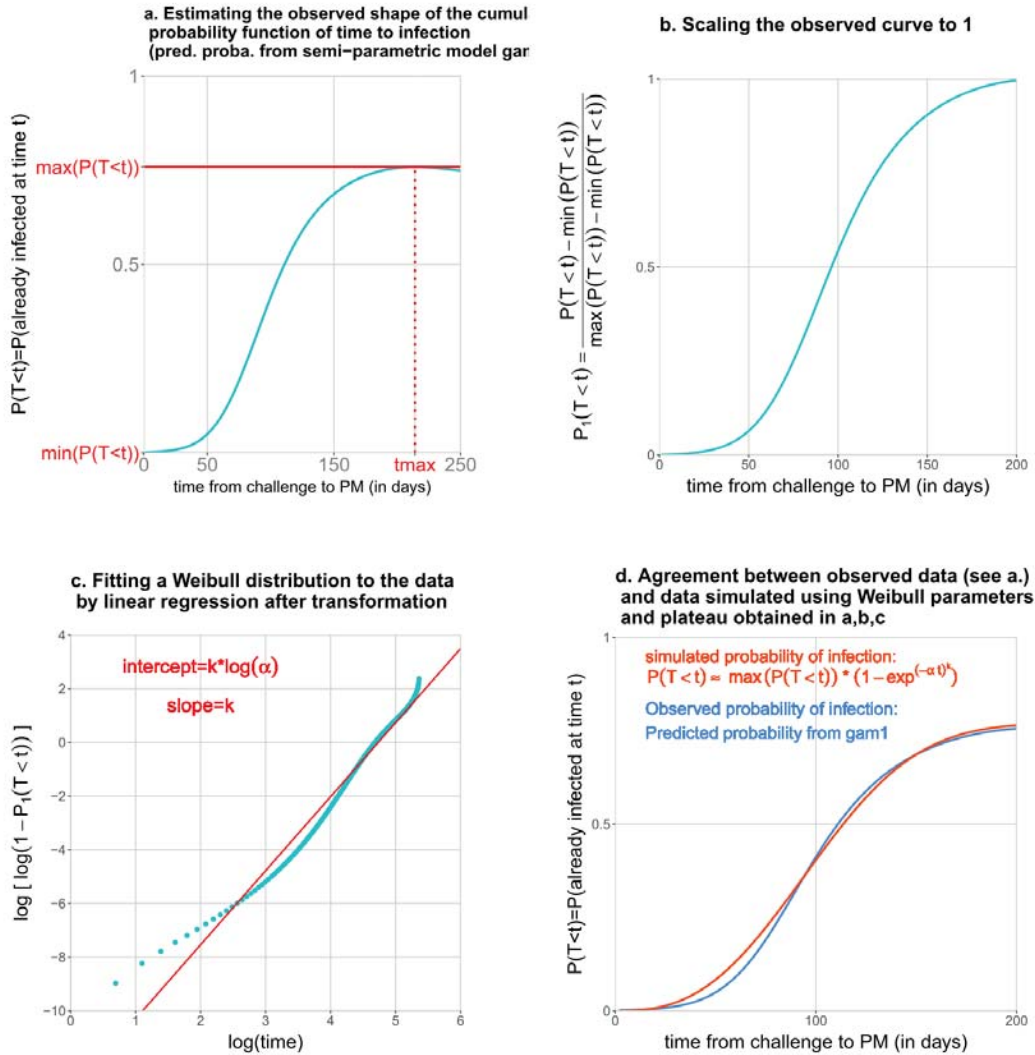


Figure 6-2: Steps of parameter estimation for the distribution of time from ingestion of MAP to onset of active infection from observed histological data of the meta-analysis for dose 10^4 MAP.

For this set of three parameters (α , k and plateau) we plotted the relationships $\alpha_{\text{dose}} \sim \log(\text{dose})$, $k_{\text{dose}} \sim \log(\text{dose})$ and $\text{plateau} \sim \log(\text{dose})$ and used mathematical transformations to predict these relationships, minimizing the mean square error as a goodness-of-fit criterion. The corresponding set of parameters obtained by this method was therefore fixed and independent of the dose. They could be used to simulate the distribution of time to infection as follows:

$$P(T < t)_{\text{dose}} = f(\text{plateau}, \text{dose}) * (1 - \exp^{-f(\alpha, \text{dose}) * t^{f(k, \text{dose})}}) \quad \text{Equation 4}$$

In Equation 4, we omitted the dose-dependent value $\min(P(T < t))$ as in Equation 3 to back transform the simulated probability of active infection scaled to one to the dose dependent plateau since the values of $\min(P(T < t))$ were close to 0, so that Equation 4 provided a good approximation. Figure 6-2, plot d. gives an example of the very good agreement between the probability curve predicted by *model 1* (blue curve) and the probability curve simulated with the three estimated parameters α , k and plateau $\max(P(T < t))$ (red curve).

6.3.3.2 Proportion of infected sheep entering the progressor pathway (χ)

Only a minority of sheep actively infected by MAP progress to show clinical signs associated with production effects. We therefore aim to 1- identify factors which trigger progression to clinical paratuberculosis and 2- estimate the proportion χ of infected sheep entering the progressor track.

The progressor state was defined by the presence of severe intestinal lesions or clinical signs at the time of *post-mortem*. As in the previous section, we used a GAMM (logit link) to model this point observation, with a non-parametric smoothing term to account for the time from inoculation to *post-mortem* (time of sacrifice, at which clinical observations were made).

$$\text{logit}(\text{progressor status})_{ij} \sim \text{intercept} + \sum_{k=1}^n \beta_k x_{ki} + f_{\text{ttpm}}(\text{ttpm})_i + U_{ij} + U_i + \varepsilon_i \quad (\text{model 2})$$

with letters and subscripts as described in *model 1*.

The probability χ is the dose dependent probability of an infected sheep progressing to an affected state. It can be written as:

$$\chi_{\text{dose}} = P(\text{progressor}|\text{infected})_{\text{dose}} = \frac{P(\text{progressor} \cap \text{infected})_{\text{dose}}}{P(\text{infected})_{\text{dose}}} = \frac{P(\text{progressor})_{\text{dose}}}{P(\text{infected})_{\text{dose}}}$$

Equation 5

where $P(\text{progressor})$ represents the cumulative probability of being a progressor among inoculated sheep over the course of infection (as opposed to the probability at any given time). Similarly, $P(\text{infected})$ represents the cumulative probability of active infection as assessed in the previous section, i.e. the probability that an inoculated sheep was “ever” actively infected.

With point observations at the time of sacrifice, we only observe point prevalence of progression over time, not the cumulative incidence. Unlike in the former section for actively infected sheep, progressor sheep do not tend to accumulate in the population since they are removed when clinical signs occur. We hence considered that the maximum of the curve of the predicted probability of progression versus ttpm (results of the fitted *model 2*) represented the best possible proxy, although underestimated, for the cumulative proportion. It corresponds to the observed proportion of progressors among all inoculated sheep, at the best possible time to observe this proportion (hence the closest from the cumulative proportion). For the cumulative probability of active infection, the first local maximum of the predicted probability versus time obtained in *model 1* was used as an adequate proxy, all the more that the shape of the curve obtained with *model 1* indicates a stable plateau of infection before recovery starts happening. The value of χ_{dose} can thus be calculated according to Equation 5, for the appropriate levels of the covariate pattern (depending on covariates present in the final models *model 1* and *model 2*). An illustration of this method and the calculation of χ can be seen in Figure 6-3.

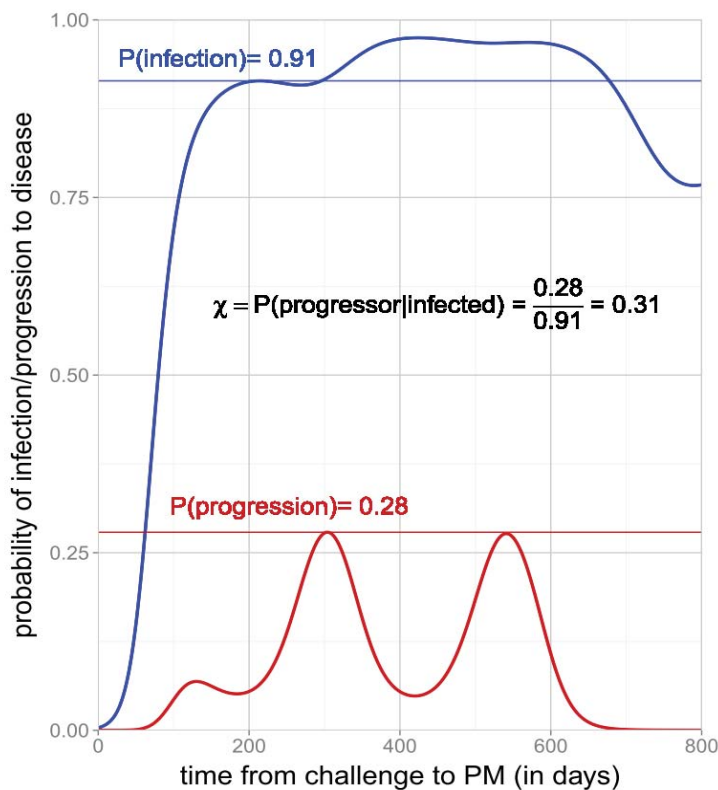


Figure 6-3: Method to estimate the value of χ from the predicted probabilities of *model 1* (in blue) and *model 2* (in red), for a specific set of covariates.

This process can be repeated for doses varying from 10 to 10^{12} MAP organisms. The relationship $\chi_{\text{dose}} = f(\log(\text{dose}))$ can thus be plotted and a simple mathematical transformation suggested by the shape of the curve can be used to predict these relationships, minimizing the mean square error as a goodness-of-fit criterion. The best fitting regression parameters for the equation $\chi_{\text{dose}} = f(\log(\text{dose}))$ are the parameters of interest, constant with respect to inoculum dose.

6.3.3.3 *Modelling the rate of progression from early disease to severe disease in the progressor track (δ)*

One clinical outcome that represents the progression from early infection to severe infection is the severity of intestinal lesions. In the absence of serial biopsies, the prevalence of these types of lesions was modelled as a function of time to describe the progression pattern. According to assumptions generated in Chapter 4, we assumed that sheep with severe lesions with diffuse infiltration start to be affected by the disease, while sheep with mild to moderate lesions with focal to multi-focal granuloma are not. For more descriptions of these histological types, see (Clarke and Little, 1996; Pérez et al., 1996). We therefore developed two models to describe the prevalence of both lesion types as was described earlier for previous GAMM, as follows:

$$\text{logit}(\text{mild} - \text{moderate lesions})_{ij} \sim \text{intercept} + \sum_{k=1}^n \beta_k x_{ki} + f_{\text{ttpm}}(\text{ttpm})_i + U_{ij} + U_i + \varepsilon_i \quad (\text{model 3})$$

$$\text{logit}(\text{severe lesions})_{ij} \sim \text{intercept} + \sum_{k=1}^n \beta_k x_{ki} + f_{\text{ttpm}}(\text{ttpm})_i + U_{ij} + U_i + \varepsilon_i \quad (\text{model 4})$$

with letters and subscripts as before.

Both models included time from inoculation to *post-mortem* as a smoothing term, to evaluate the effect of time on the probability of the outcome and when peaks would occur. We used the default smoothing (thin plate default with penalised likelihood) to build the final models adjusting for significant covariates. We then manually increased the smoothing (by reducing the maximum number of degrees of freedom allowed for the smooth term) in order to capture the main trend more appropriately, keeping the same set of covariates as in the final model with default smoothing.

Assuming a constant rate of change from an early mild infection stage (called X) to the following severe infection stage means there is an exponential decay. In this case, the

relationship between the progression rate δ and the median time t_{50} of remaining mildly infected (in X) is:

$$X(t_{50}) = X(t_0) * \exp^{-\delta * t_{50}} \quad \text{Equation 6}$$

Since by definition $X(t_{50})=0.5$ and $-\ln(0.5) = \ln(2)$:

$$\delta = \frac{\ln(2)}{t_{50}} \quad \text{Equation 7}$$

With knowledge of the shape of the probability of early lesions (as a proxy for the early infection stage) and the probability of severe lesions (as a proxy for the late infection stage) we can thus estimate the parameter δ . If those two curves each harbour a main peak at a given time (representing the time at which most of the sheep are currently in this particular infection stage), we can approximate the median time t_{50} spent in the early stage before entering the late stage as the lag in time between the two main peaks.

6.3.3.4 Modelling the rate of recovery from shedding in the non-progressor track (γ)

Recovery from paratuberculosis can encompass a range of outcomes: recovery from infection, from disease, or from shedding. It is therefore hard to demonstrate. Animals in the early active infection stage do not experience significant production effects; hence, the main difference between early infection and recovery in terms of within-flock infection dynamics would be transient shedding from the early infected animals (Chapter 4). We thus analysed longitudinal shedding data where available.

The duration of transient shedding for non progressors was defined as the time from the estimated onset of shedding to the estimated end of shedding for sheep with longitudinal shedding data. The onset of shedding was estimated as the middle of the time interval between the first positive sample and the previous (negative) sample, while the end of shedding (cure) was half way through the interval between the last positive sample and the first negative when all subsequent samples were negative. Parametric survival analysis (accelerated failure time model) was used to evaluate the rate of exit from transient shedding (*model 5*). An exponential and a Weibull distribution of time to event were evaluated (survreg

function of the survival package in R) (Therneau and Lumley, 2016). A frailty term was added to account for the lack of independence of sheep in the same study.

6.4 Results

6.4.1.1 Descriptive results

After accounting for experiments that were reported multiple times in different papers and papers that included more than one experiment, 767 sheep clustered in 38 experiments were subjected to the meta-analysis (Table 6-1).

Table 6-1: reference list for the 38 experiments included in the meta-analysis (n=767 sheep) with details of the experimental protocol

Reference(s) for each experiment	n	Dose ¹ (log10)	Breed	Strain ²	Age ³	Inf ⁴	Path ⁵	Clin ⁶	Shed ⁷
Begg et al. (2010)	3	10.2	merino	Ov	L	1	0	1	0
Begg et al. (2010)	9	5.1 - 8.1	merino	Ov	H	1	0	1	0
Begg et al. (2010) + Bower et al. (2011)	23	8.5	cross merino	Ov	H	1	1	1	0
Begg et al. (2010) + de Silva et al. (2010) + Bower et al. (2011)	18	8.4	merino	Ov	L	1	1	1	0
Begg et al. (2010) de Silva et al. (2010) + Bower et al. (2011)	12	8.2	merino	Ov	L	1	1	1	0
Begg 2010 + de Silva et al. (2010) + Bower et al. (2011) + de Silva et al. (2011) + Kawaji et al. (2011)	38	8.5 - 8.6	merino	Ov	H	1	1	1	1
Reddacliff and Whittington (2003) + Reddacliff (2002)	30	1.4 - 7.8	merino	Ov	H	1	1	0	0
de Silva et al. (2015)	36	9.4	merino	Ov	H	1	1	1	0
Thorel et al. (1992)	6	9.7	grivette	Bv	L	1	1	1	1
Williams et al. (1983)	9	8.7	unknown	Bv	H	1	0	1	0
Karpinski and Zorawski (1975)	13	9.8	merino cross	Bv	L	0	0	1	1
Begg et al. (2005) + Begg and Griffin (2005) + Begg (2004)	54	8 - 9.3	merino	Ov	L	1	1	1	0
Begg et al. (2005) + Begg (2004)	30	9.6	merino	Ov	L	1	1	1	0
Griffin et al. (2009)	30	7.6	merino	Ov	H	0	1	1	0
Begara-McGorum et al. (1998)	8	9.5	dorset	Bv	L	1	1	1	0
Beard et al. (2000)	5	9.5	suffolk*texel	Bv	L	1	0	0	0
Gilmour et al. (1969)	14	9.0	scottish*cheviot	Bv	L/H	1	0	0	0
Brotherston et al. (1961a) + Brotherston et al. (1961b) + Nisbet et al. (1962)	25	8.0 - 8.9	cheviot	Bv	L	1	1	1	0
Brotherston et al. (1961a) + Brotherston et al. (1961b) + Nisbet et al. (1962)	48	3.0 - 9.0	cheviot	Bv	L	1	1	1	0
Gilmour and Brotherston (1962)	7	9.0	cheviot	Bv	H	1	0	0	0

Reference(s) for each experiment	n	Dose ¹ (log10)	Breed	Strain ²	Age ³	Inf ⁴	Path ⁵	Clin ⁶	Shed ⁷
Gilmour et al. (1965a)	28	8.3	cheviot	Bv	H	1	1	1	0
Gilmour et al. (1965a)	18	8.0	cheviot*scottish	Bv	L/H/2T	1	1	0	0
Gilmour et al. (1965a)	9	8.0	cheviot	Bv	L	1	0	0	0
Gilmour and Brotherston (1966)	9	8.0	cheviot	Bv	L	1	0	0	0
Gilmour and Brotherston (1966)	9	8.0	cheviot	Bv	H	1	0	0	0
Gilmour and Angus (1973)	11	8.7	cheviot*blackface	Bv	H	1	1	1	0
Gilmour and Angus (1974)	10	9.0	cheviot	Bv	H	0	1	0	0
Gilmour et al. (1978)	49	9.0	cheviot*suffolk	Bv	H	0	1	1	0
Kluge et al. (1968)	18	10.1	corriedale	Bv	L	0	0	1	0
Degado et al. (2012) + Delgado et al. (2013)	38	3.6 - 8.2	churra	Ov	L/E	1	1	1	1
Juste et al. (1994b)	5	6.1	rasa	Bv	H	0	1	0	1
Verna et al. (2007)	24	9.0	churra	Ov/Bv	L	0	1	0	0
(Fernandez et al., 2014)	23	7.5 - 8.9	assaf	Ov/Bv	L	1	1	0	0
Fernandez et al. (2015)	14	8.2 - 9.3	churra	Ov	L	1	1	1	0
Kurade and Tripathi (2008) + Kurade et al. (2004)	20	10.9	crossbred	Ov	L	1	1	1	0
Gwozdz (1999) + Gwozdz et al. (2001) + Gwozdz and Thompson (2002)	30	9.5	romney cross	Ov	L	0	1	1	0
Gwozdz (1999) + Gwozdz et al. (2000a) + Gwozdz et al. (2000b) + Gwozdz et al. (2000c) + Gwozdz et al. (2000b)	14	8.6	romney cross	Ov	L	1	1	1	0
(Stewart et al., 2004) + Stewart et al. (2007)	20	8.7 - 10.8	merino	Ov/Bv	H	1	0	1	1

¹ Total inoculum dose per sheep in MAP numbers at the log10 scale (and range for experiments with different dose regimen)

² Strain type of MAP used: Ov=ovine (type II) or Bv=bovine (type I) or unknown

³ Age of the sheep at first inoculation: L=lamb (0-3 months), H=hoggets (4-12 months), 2T=two-tooth (13-24 months), E=ewes (>24 months)

⁴ Inf (0/1): data available about tissue infection with MAP (culture or PCR or immune-histo-chemistry)

⁵ Path (0/1): data available about histopathological examination of the intestine

⁶ Clin (0/1): data available about clinical symptoms of OJD

⁷ Shed (0/1): data available about longitudinal faecal shedding

Whereas age, MAP dose and time to euthanasia had little variability within experiment, there was substantial variation between experiments (Figure 6-4). The age of sheep at inoculation ranged from 1 day to ten years, with a median of 3 months. Only 30/767 (4%) animals were older than one year. The time between inoculation and *post-mortem* varied from one day to 4.5 years, with a median of 10 months post-inoculation and was evenly dispersed. The total inoculum dose ranged from 26 MAP to 7.2×10^{10} with a median dose of 5×10^8 . The large variation in these experimental conditions benefitted the analysis of their impact on the MAP infection response.

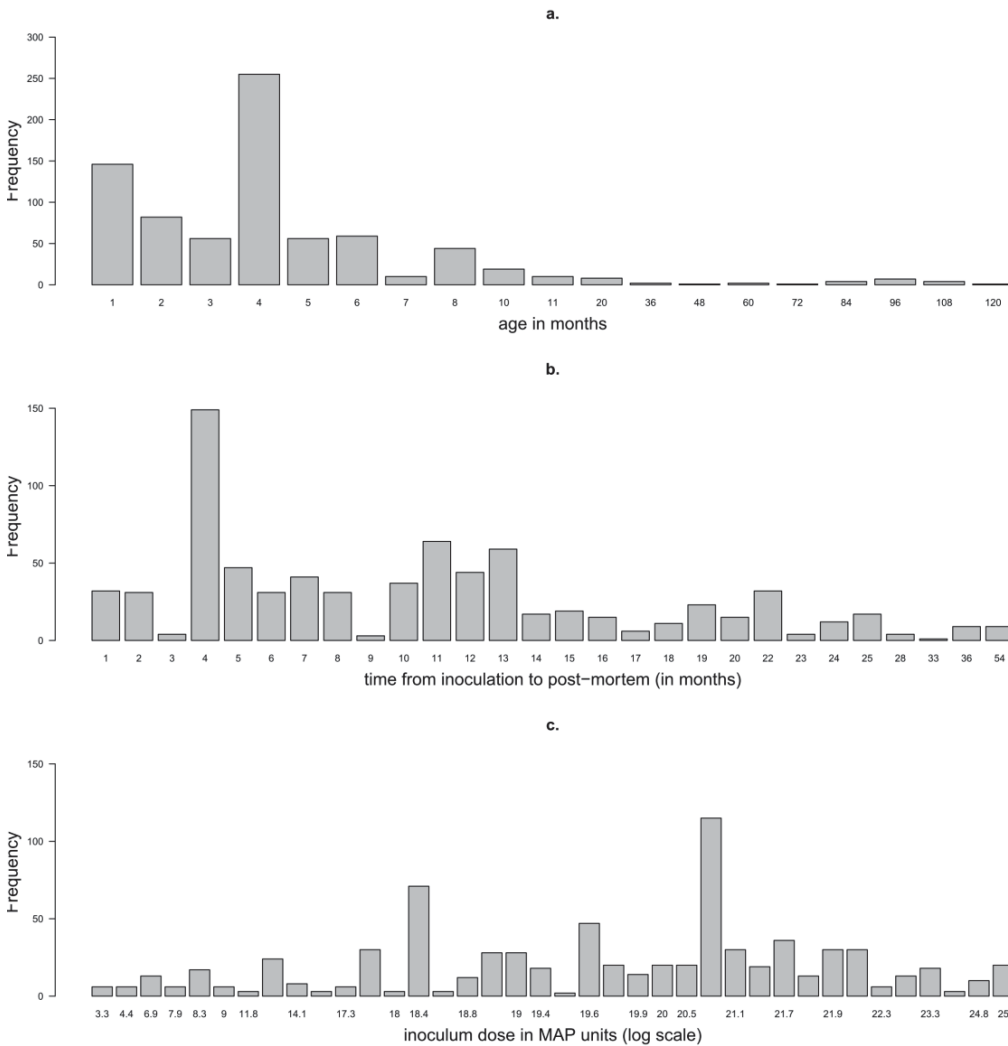


Figure 6-4: Distributions of the age at inoculation (a.) the time from inoculation to *post-mortem* (b.), and inoculum dose (c.) for individual sheep (across all experiments).

The pathological responses measured in the meta-analysis are listed in Table 6-2 with their frequency. Most sheep were infected with MAP at the time of *post-mortem* (specific lesions or

detectable infection of tissues) but the vast majority (72%) did not show signs of clinical disease. In the subset of 161 sheep monitored for faecal shedding, histological lesions and faecal shedding were detected with the same frequency (44% and 45% respectively, results not shown).

Table 6-2: frequency of different pathological outcomes for 767 sheep experimentally infected with MAP (all datasets combined)

	Tissue infection ^a	Histo. lesions ^b	Faecal shedding ^c	Clinical disease
Negative	267	247	87	483
Positive	443	378	72	104
ND ^d	57	142	608	180
% positive	62.4%	60.5%	45.3%	17.7%

^a culture or PCR or immunohistochemistry of intestinal tissue and/or mesenteric lymph nodes

^b in the small intestine

^c faecal culture or faecal PCR (at least one positive occurrence)

^d not done

Table 6-3 describes the correlation of different pathological responses in sheep for which the individual correspondence between outcomes measured in the study could be made. Markers of infection (presence of histological lesions in the guts, even mild or cultivable infection, Table 6-3a.) tended to agree (kappa coefficient=0.46, moderate agreement, $p < 0.0001$). Similarly, markers of progression to disease (presence of severe lesions in the guts or onset of clinical signs, Table 6-3b.) displayed “fair agreement” (kappa coefficient=0.28, $p < 0.0001$). On the other hand, infection and disease only showed “slight agreement” (kappa coefficient =0.17, $p < 0.0001$, Table 6-3c.) with the majority of animals (256/490=52%) infected with MAP but not affected by MAP.

Table 6-3: correspondence between different pathological outcomes measured at the time of *post-mortem*, for the subset of sheep for which it was possible to establish the individual correspondence between different outcomes from the data.

a.	Tissue infection ^b	
	Negative	Positive
Histo negative ^a	107	58
	53	225

b.	Clinical disease	
	Negative	Positive
Absence of severe lesions ^a	75	12
Presence of severe lesions ^a	30	20

Table 6-3 (continued): correspondence between different pathological outcomes measured at the time of *post-mortem*, for the subset of sheep for which it was possible to establish the individual correspondence between different outcomes from the data.

c.	Infected with MAP ^d	
	Negative	Positive
Affected by the disease ^c	129	256
	1	104

^a Histological lesions in the small intestine.

^b Detection of MAP by culture or PCR or immunohistochemistry of intestinal tissue and/or mesenteric lymph nodes.

^c Presence of either severe histological lesions in the guts or clinical signs of paratuberculosis, or both.

^d Presence of either histological lesions in the guts or detectable MAP in the guts or mesenteric lymph nodes, or both.

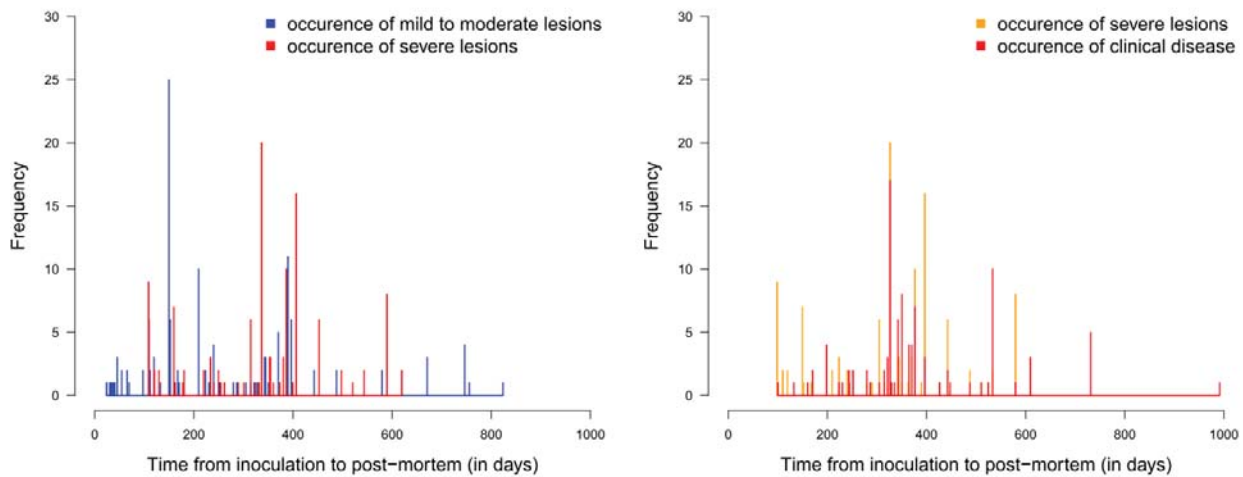


Figure 6-5: Raw daily frequency histogram of sheep with histological lesions of known type over time (left) and sheep detected with severe lesions or clinical signs over time (right), all datasets combined

The first histological lesions were detected at 23 days post challenge (mild-moderate) and the last were observed at 824 days (mild-moderate as well). The peak of mild to moderate lesions occurred earlier than the peak of severe lesions, which indicate they were appropriate markers for progression from early to severe pathology (Figure 6-5). The sheep harbouring mild lesions between 671 and 824 days post-challenge came from 3 distinct experiments and likely represented non-progressor sheep, since only six cases of clinical PTB were observed in the dataset after day 610, five of which were observed at day 732. We used the data shown in Figure 6-5 in subsequent parts of this manuscript to calculate a progression parameter δ from mild to severe lesions, for which only the relative position of the peaks matter, not the rest of

the distribution. Figure 6-5 (right panel) also shows that severe lesions occurred concomitantly with clinical signs. They were therefore combined as markers of progression for calculating the probability of progression upon infection with MAP (χ).

Regarding the subset of sheep with faecal shedding data, Figure 6-6 shows that the onset and decay of histological lesions and shedding follow a similar trend over time.

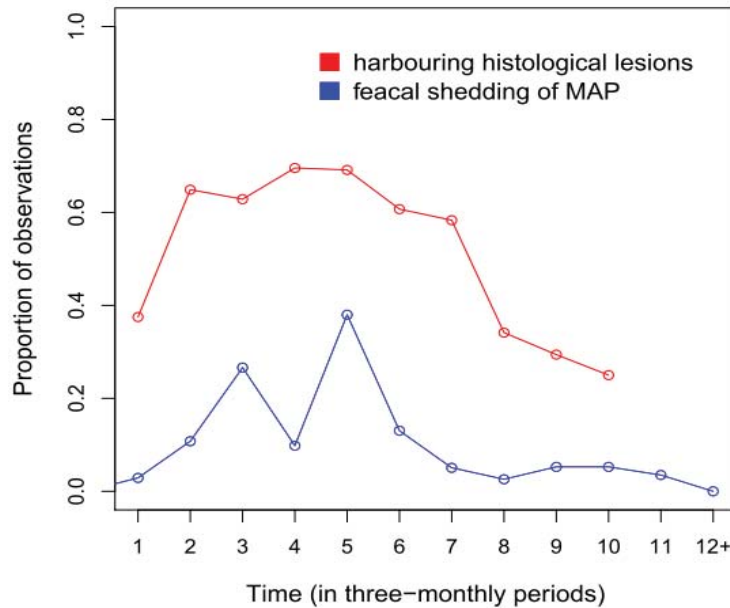


Figure 6-6: Monthly proportion of shedders (n=161, repeated measurements) and histological lesions of PTB at post-mortem (n=627).

We thereafter modelled some or a combination of the outcomes presented page 118 (using 5 different models), in order to derive four parameters for the compartmental model in Figure 6-1.

6.4.1.2 Modelling the probability of active infection

A first model was built to predict the probability of being histology positive over time, called *model 1*. A total of 1230 observations of 615 sheep were included in the analysis. Coefficients for covariates of the parametric part of the best fitting *model 1* for the presence or absence of histological lesions at *post-mortem* are presented in Table 6-4.

Table 6-4: results of the parametric part of *model 1* (presence/absence of histological lesions at *post-mortem*).

	Coefficient	Standard Error	P-value
log(dose)	0.27	0.04	< 0.0001
Strain Ovine (vs. Bovine)	-1.56	0.37	< 0.0001
Tissue homogenate inoculum (vs. pure culture)	1.59	0.32	< 0.0001

Increased doses, a bovine (vs. ovine) strain and fresh tissue homogenate (vs. culture-passaged MAP) were positively associated with the occurrence of histological lesions. However, age, either as a continuous or categorical variable, was not significant, hence was not included in the final model.

In the non-parametric part of the model, the smoothed term for time from inoculation to *post-mortem* was highly significant with seven estimated degrees of freedom, indicating a significant and non-linear effect of time at *post-mortem*. Random effects for sheep ID and experiment ID were both moderately significant.

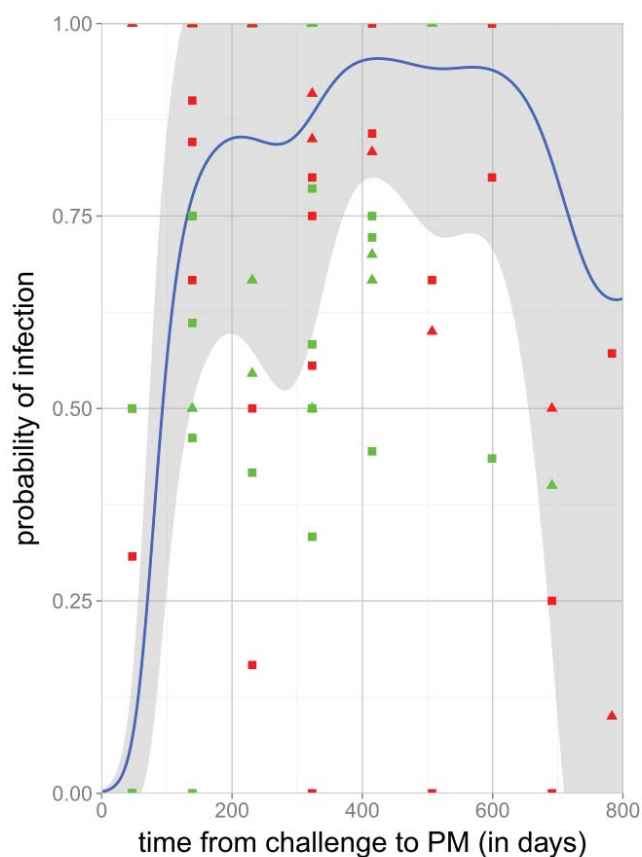


Figure 6-7: Predicted probability of active infection, i.e. presence of histological lesions in the guts versus time from *model 1* (blue curve) and 95% confidence interval (grey area) (covariate levels: MAP dose = 105, tissue homogenate inoculum, ovine strain). Points represent the raw data from individual experiments. Each point corresponds to the observed proportion of sheep histology positive in 3-monthly time slots, grouped by dose (red: observations with inoculum dose above the median dose; green: observations with inoculum dose below the median dose) and inoculum type (square: pure culture; triangle: tissue homogenate).

The predicted probability of active infection over time post-inoculation (*model 1*) is presented in Figure 6-7, alongside with display of raw data from individual experiments. This figure highlights the difficulty to interpret results from single experiments and the variability of outcomes between experiments. The predicted probabilities of infection at different doses are presented in Figure 6-8.

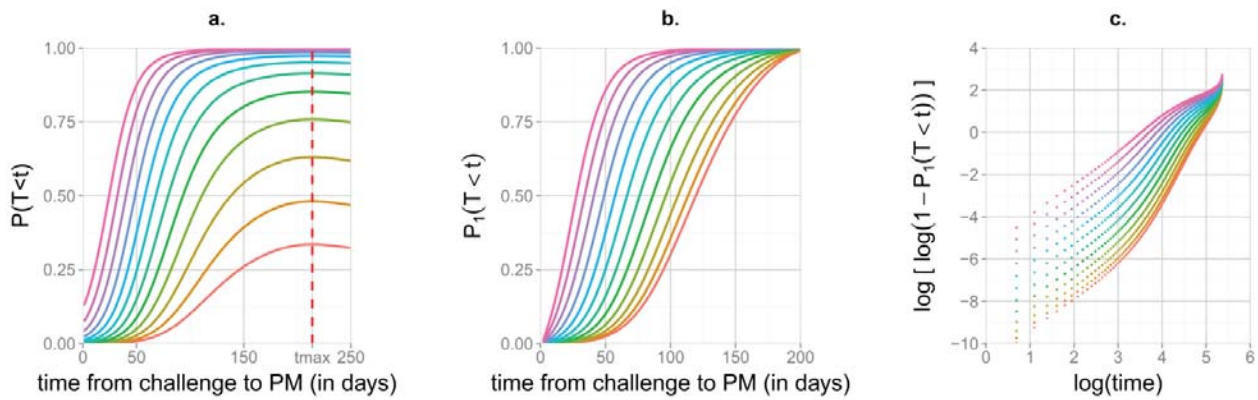


Figure 6-8: Predicted probabilities of active infection over time from *model 1* and successive transformations for the purpose of fitting a Weibull distribution (a = predicted probabilities; b= predicted probabilities scaled to one for each stratum, c = transformation to a linear form), stratified by increasing MAP challenge dose 10 to 10¹² MAP (ovine MAP strain, tissue homogenate inoculum).

The value of the plateau was the local maximum of the predicted probability of active infection in the early phase (Figure 6-2), occurring at day 214 after inoculation (Figure 6-8 a.), which we used to rescale the probability to one according to Equation 2 (Figure 6-8 b.). Parameters α_{dose} and k_{dose} (parameters of the Weibull distribution) and the value of the plateau were determined for each dose between 10¹ and 10¹² MAP. The best fitting equations were found for each relationship using regression, achieving an excellent fit ($r^2 \geq 0.99$) (Figure 6-9).

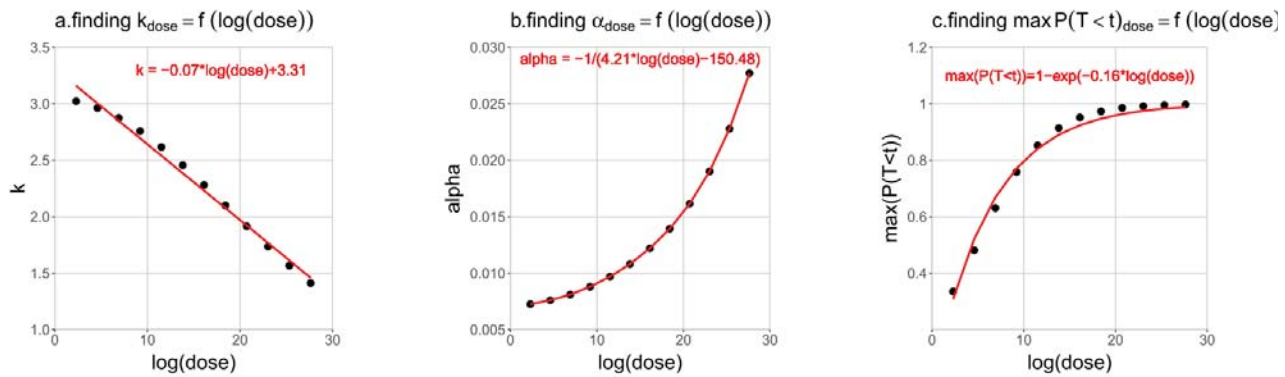


Figure 6-9: Relationships between the dose-dependent Weibull parameters α_{dose} and k_{dose} and the dose-dependent plateau $\max(P(T < t))_{\text{dose}}$ and the inoculum dose to model the probability of active infection as a function of time from inoculation to *post-mortem*.

Results of the regressions of the dose-dependent parameters as a function of the dose resulted in the following predictions:

Weibull parameters as a function of inoculum dose:

$$K = -0.07 * \log(dose) + 3.31 \quad (adjusted\ r^2 = 0.986)$$

$$\lambda = -1 / (4.21 * \log(dose) - 150.48) \quad (adjusted\ r^2 = 0.998)$$

Scaling parameter as a function of dose:

$$plateau = 1 - \exp(-0.16 * \log(dose)) \quad (adjusted\ r^2 = 0.992)$$

Hence the equation for the simulated probability of active infection was:

$$P(T < t)_{dose} = [1 - \exp(-0.16 * \log(dose))] * [1 - \exp^{-(-1 / (4.21 * \log(dose) - 150.48) * t)^{-0.07 * \log(dose) + 3.31}}]$$

The dose-dependent plateau $\max(P(T < t))$, limit of the cumulative infection probability, represents a variable overall “probability of success” of infection following MAP ingestion. It is complementary to the rate of infection α . Note that when dose = 76 MAP, plateau=50% hence 76 MAP is enough to actively infect 50% of sheep upon oral inoculation, indicative of the infectiousness of MAP in sheep.

The equations determined for parameters (α , K and plateau) can be used in the formulae of the force of infection of the mathematical model of ovine paratuberculosis presented in Figure 6-1.

6.4.1.3 Modelling the probability of progression

A second GAMM (*model 2*) was fitted to evaluate the probability of progression upon inoculation, approximated by the presence of severe lesions and/or clinical signs at the time of examination (*post-mortem*). There were 1358 observations (679 sheep) included in the analysis. The coefficients of the parametric part of this model are presented in Table 6-5.

Table 6-5: results of the parametric part of *model 2* (presence/absence of markers of progression at *post-mortem*)

	Coeff. estimate	Standard error	P-value
log(dose)	0.38	0.13	< 0.01
Tissue homogenate inoculum (vs. pure culture)	1.51	0.44	< 0.001
Age less than one year old (vs. more)	2.47	0.90	< 0.01

Increasing the dose of MAP, inoculation with fresh MAP from tissue homogenate rather than lab-passaged MAP, or being less than one year of age were all positively associated with markers of progressive paratuberculosis indicating current or imminent clinical disease ($p < 0.01$).

Concerning the non-parametric part of this model, the smooth term for time from inoculation to *post-mortem* was highly significant with seven estimated degrees of freedom, which means that there was a significant and non-linear effect of the time at which clinical observations were carried out. The random effect for experiment ID was highly significant while the one for sheep ID was non-significant ($p=0.83$), indicating that sheep in the same experiment were similar in their propensity to progress; most of the residual variability in the outcome was due to experiment.

The presence of the random effect for sheep ID did not affect the model fit, the size of the model coefficients or the shape of the relationship between inoculum dose and time. Nevertheless, the random effect was left in the model to ensure the same structure for *model 1* and *model 2*. The combined results of *model 1* and *model 2* are presented in Figure 6-10.

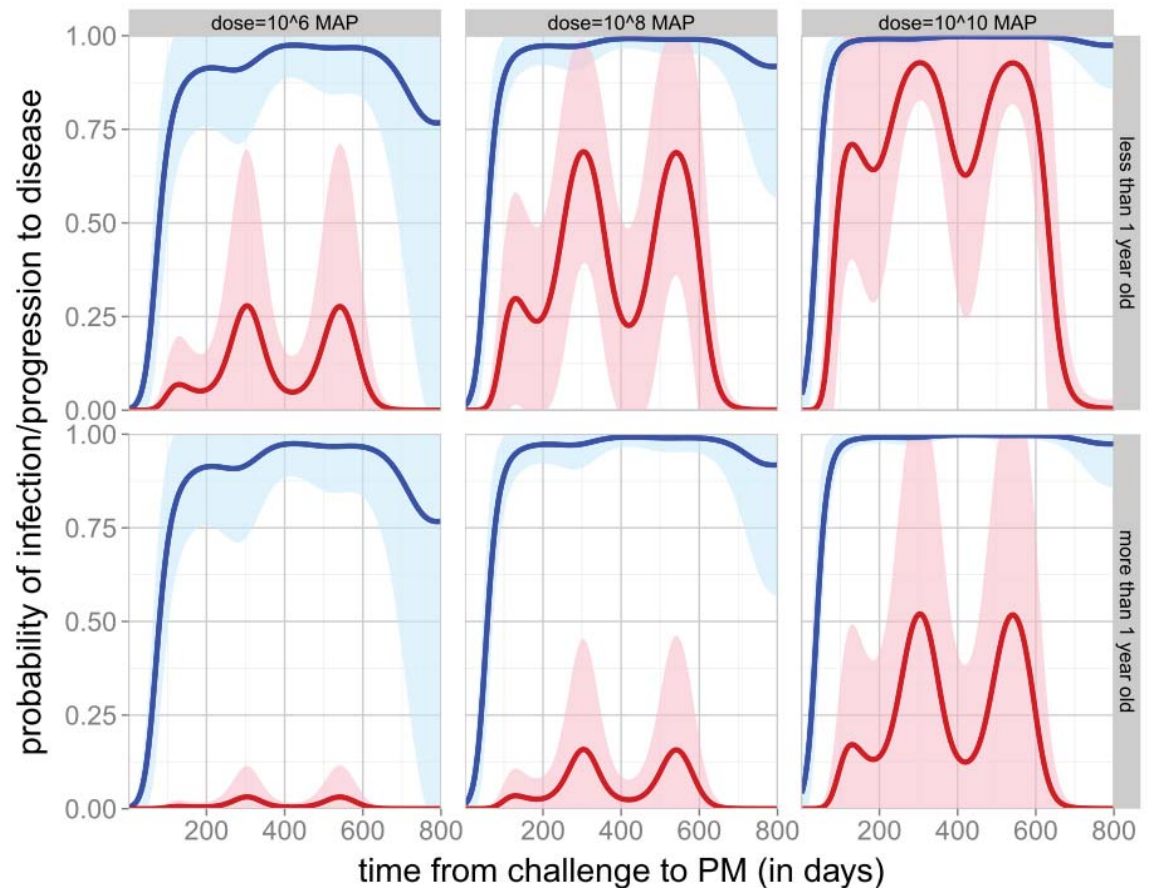


Figure 6-10: Predicted probability of active infection (blue) and progression (red) over time from inoculation to *post-mortem*, for combinations of age and inoculum dose, with confidence intervals (blue and red shading). All predicted probabilities were based on the ovine MAP strain (*model 1*) and tissue homogenate inoculum.

Unlike the probability of active infection, in blue in Figure 6-10 (predicted from *model 1*, see Table 6-4), the probability of progression depended significantly on the age, with a higher probability of progression when exposed before one year old. For the probability of active infection, based on the shape of the curves we selected the first local maximum occurring at day 214 as the best proxy for the cumulative incidence of infection as it appeared likely to match in time with the first observed peak of progression occurring on day 304, hence the results across the two curves appeared to be consistent. For the probability of progression, there were two local maxima of exactly the same height. Considering one or the other was therefore strictly the same.

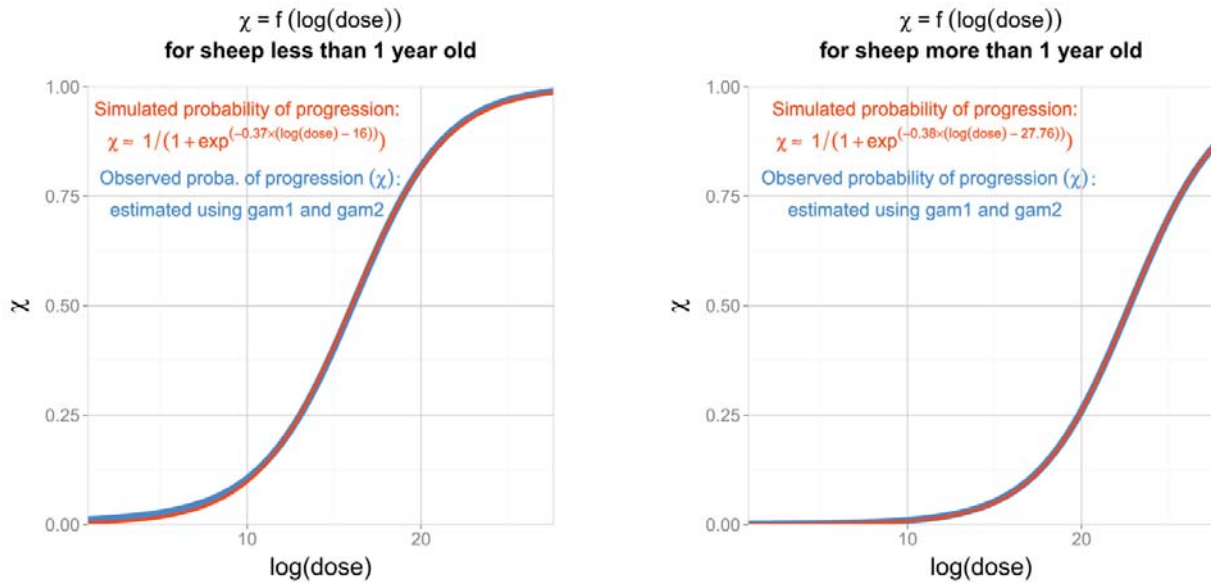


Figure 6-11: Estimated probability of progression upon infection (χ) as a function of inoculum dose for sheep less than one year old (left) and older sheep (right) showing data-driven predictions (obtained from *model 1* and *model 2*, in blue) and simulated (red) data.

For doses from 10 to 10^{12} MAP organisms, we calculated χ_{dose} according to Equation 5, using the predicted probabilities of *model 1* and *model 2* (see Figure 6-3). $\chi_{\text{dose}} = f(\log(\text{dose}))$ was then plotted and regression was performed and the best fit determined by minimising the least sum of squares. A sigmoid-like shape provided an excellent fit (in red in Figure 6-10) of the observed values (predicted from *model 1* and *model 2*) of χ . The best-fitting equations for $\chi_{\text{dose}} = f(\log(\text{dose}))$ were as follows:

$$\chi_{\text{young}} = \frac{1}{1 + \exp(-0.37 \times (\log(\text{dose}) - 16))} \quad \text{For sheep less than one year old,}$$

$$\chi_{\text{adult}} = \frac{1}{1 + \exp(-0.38 \times (\log(\text{dose}) - 27.76))} \quad \text{For sheep older than one year old.}$$

The above equation for χ can be used in the mathematical model of ovine paratuberculosis presented in Figure 6-1. Note that when dose = 8.89×10^6 MAP, $\chi_{\text{young}} = 50\%$, and when dose = 7.67×10^9 MAP, $\chi_{\text{adult}} = 50\%$. These doses, which trigger 50% of infected sheep to progress to a severe irreversible stage of PTB, represent the virulence of MAP in respectively young and adult sheep.

6.4.1.4 Modelling the rate of progression from early disease to severe disease in the progressor track (δ)

Two models were fitted to predict the probability of presenting mild-moderate lesions in the guts (*model 3*) or severe lesions (*model 4*). There were 1006 observations (503 sheep) for which precise histological description indicated the presence of mild to moderate lesions versus severe lesions.

Results of the final *model 3* for the presence of mild-moderate lesions (marker of early disease in Figure 6-1) are presented in Table 6-6. The random effect for experiment was significant as well as the smooth term for time from inoculation to *post-mortem*, with 8.7 estimated degrees of freedom indicating a non-linear pattern (Figure 6-12).

Table 6-6: results of the parametric part of the *model 3* for the presence of mild-moderate lesions at *post-mortem* (reference=no early lesions, ie. no specific lesions or severe lesions)

	Coeff. estimate	Standard error	P-value
log(dose)	0.39	0.09	<0.0001

Strain type and inoculum type were not significantly associated with the occurrence of mild lesions, although the trend was similar to that of the model for active infection (ovine strain protective against early lesions and tissue homogenate a risk factor). Age was only marginally significant hence not kept in the final model for parsimony, since what mattered was the shape of the curve (position of the peak) and not its height. The trend, however, was towards ewes being more likely to harbour mild lesions than lambs. The random effect for sheep ID was not significant and not kept in the final model. Since we were interested in the shape of the curve of the probability of mild lesions versus time, we modelled interactions between time and age or dose to explore possible variations of the shape. Even when the interaction improved the model fit, the peak locations in the curve were the same across covariate levels despite allowing for variation. Hence interactions were not retained.

Results of the final *model 4* for the presence of severe lesions (markers of severe, advanced stage of disease in Figure 6-1) are presented in Table 6-7. The random effect for experiment was significant. Although not significant, the smooth term for time from inoculation to *post-mortem* greatly reduced the AIC, indicating a better model. Degrees of freedom were estimated to 8.2, indicating a non-linear pattern (Figure 6-12).

Table 6-7: Results of the parametric part of *model 4* for the presence of severe lesions at *post-mortem* (reference=no severe lesions, i.e. no specific lesions or mild-moderate lesions)

	Coeff. estimate	Standard error	P-value
log(dose)	0.22	0.1045	0.03635
Age1 (less than 1 year old)	2.35	0.8839	0.00795
Tissue homogenate inoculum (vs. pure culture)	0.89	0.4425	0.04380

Increased MAP inoculum doses increased the odds of severe lesions in the guts. Strain type was not significant in this model while the use of tissue homogenate for inoculation increased the likelihood of developing severe lesions. Severe lesions were also much more likely to occur when sheep were challenged at less than one year of age compared to older animals. The random effect for sheep ID was not significant.

Given the presence of multiple peaks in the shape of the relationship between time and severe lesion occurrence (Figure 6-12), we explored whether differences in age, dose or inoculum type could be responsible for different “regimen” of progression, using interactions with time. The study of the curves with interactions did not reveal any clear pattern whereupon a particular covariate level would be associated with specific peak locations and none of these interactions improved the fit.

The shape of both curves (*model 3* and *model 4*) indicated when a “peak” of early versus severe lesions occurred. Since the GAMM relies on smoothing (non-parametric) and the data being not perfectly explained by the covariates that we could incorporate in the model, we obtained several peaks for both curves, corresponding to several regimen of progression for different sheep. It is possible to tune the amount of smoothing in order to average progression times of the different patterns to obtain a more global peak (see “intermediate smoothing”, Figure 6-12), without suppressing the actual shape of the curve with too much smoothing (see “more smoothing”, Figure 6-12).

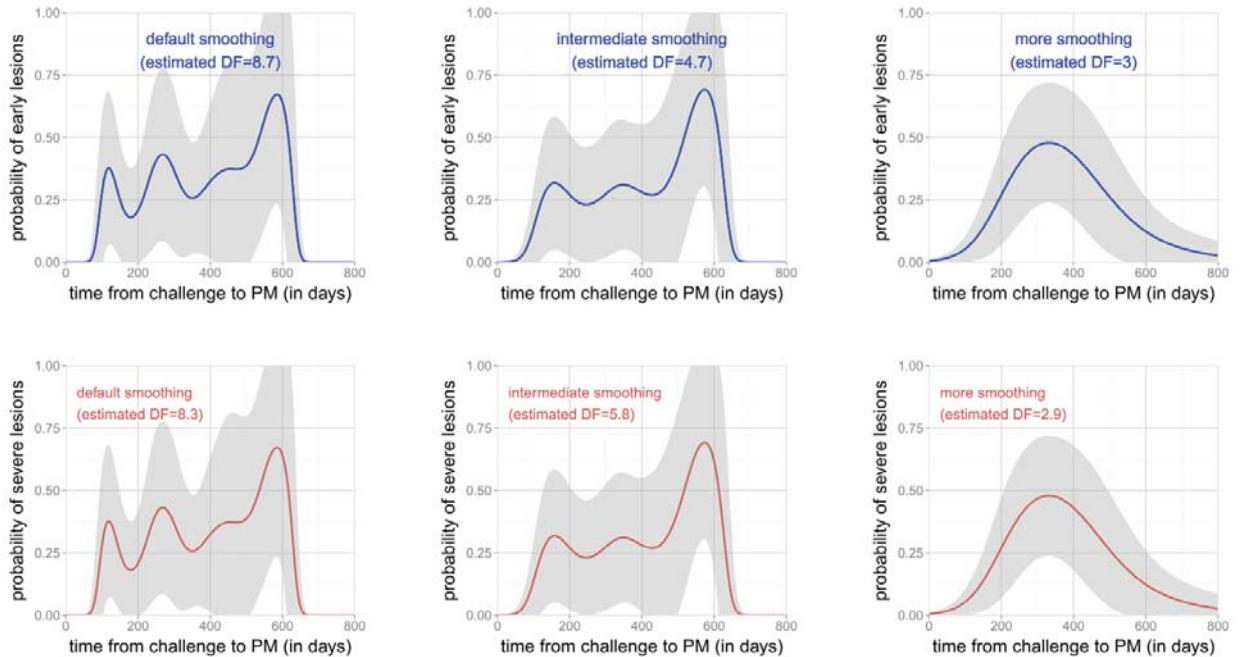


Figure 6-12: Illustration of the effect of smoothing on the curves and the appearance and position of the “main peak”

Results thereafter are based on the model with intermediate smoothing. The lag of time between the main peak of early lesions (occurring at 169 days post inoculation) and the main peak of severe lesions (occurring at 574 days post inoculation) was 405 days. Assuming this time represents a reasonable proxy for the median time spent in the compartment of mild disease before progressing to severe disease, the corresponding δ parameter was 0.0017.

This parameter δ can be used in the mathematical model of ovine paratuberculosis presented in Figure 6-1.

6.4.1.5 Modelling the rate of recovery from shedding in the non-progressor track (γ)

A small subset of sheep in this dataset ($n=159$) had longitudinal shedding information. Among those, 72 animals (45%) shed MAP at some point in time and contributed data to the analysis of shedding duration, using the parametric survival *model 5*. Among the 72 sheep entering the analysis, 26 stopped shedding according to our definition (see M&M page 128) and the remaining were censored at the end the observation period.

Between the Weibull and the exponential distribution, we elicited the exponential distribution based on a graphical comparison of the exponential and Weibull distributions, and a Kaplan-

Meier curve. The exponential distribution provided the best fit and was therefore selected and results presented in Table 6-8.

Table 6-8: Results of *model 5* (parametric survival using the exponential distribution) for factors associated with the duration of transient shedding in sheep classified as non-progressors (Figure 6-1).

	Coefficient	Standard error	P-value
Lamb (ref.: hogget)	2.44	0.636	1.26e-04
PCR (ref.: liquid culture)	2.81	0.693	5.05e-05
Solid culture (ref.: liquid culture)	-3.10	0.765	5.16e-05
Tissue homogenate inoculum (ref.: pure culture)	1.64	0.587	5.16e-03

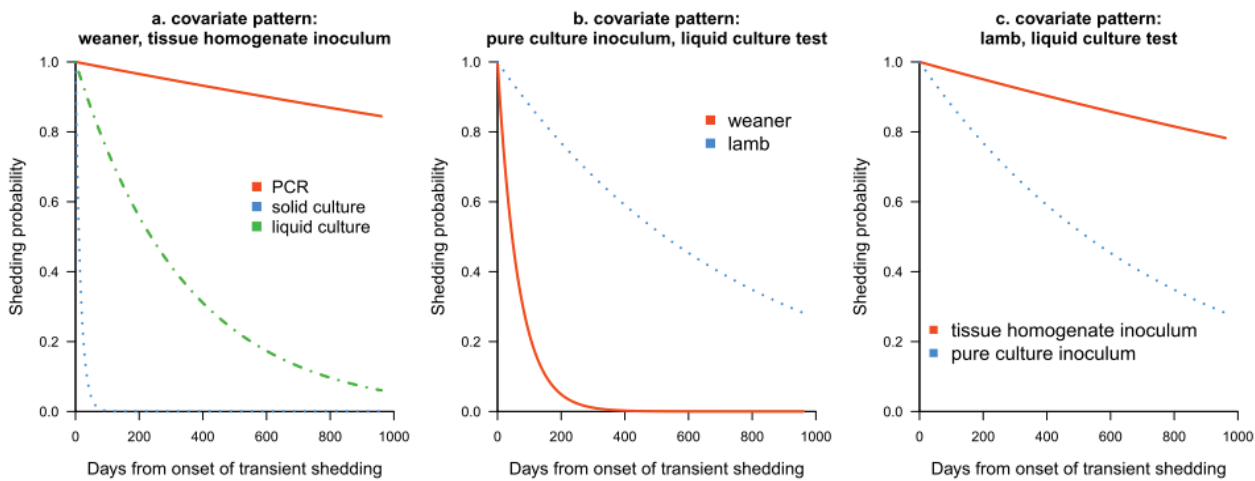


Figure 6-13: Parametric survival results (exponential distribution) for exit of transient shedding in sheep inoculated with MAP for various covariate patterns

The frailty term for experiment was completely non-significant and did not contribute to inflate the variance hence was not kept in the model.

From this survival model we could estimate rate of cure from transient shedding corresponding to parameters for a compartmental model (predictions using the following covariates: tissue homogenate inoculum, shedding detected by liquid culture):

- For lambs: $\gamma_{\text{lamb}} = 1/3917 = 0.000255 \text{ days}^{-1}$, indicating that at weaning a very small proportion of lambs shedding transiently would have already progressed to a non-shedding stage.
- For hoggets (> 3 months old): $\gamma_{\text{hoggets}} = 1/342.4 = 0.00292 \text{ days}^{-1}$.

The maximum age at inoculation in this dataset was 305 days old, hence the effect of age could not be evaluated in age groups older than this.

These parameters γ can be used for the mathematical model of ovine paratuberculosis presented in Figure 6-1.

6.5 Discussion

This meta-analysis aimed at estimating parameters for paratuberculosis modelling by pooling all published data existing about sheep experimentally dosed by MAP at the individual level as a robust and powerful means to assess the various sub-/clinical outcomes that follow MAP ingestion and infection. We describe the probability of sheep developing histological lesions over time, the probability of developing markers of severity of paratuberculosis over time and derive parameters for mathematical modelling of paratuberculosis in sheep. The analysis measured and adjusted for the effects of host (age, breed) and pathogen (dose, inoculum type, strain type) for the various outcomes of infection.

A recent meta-analysis of the dose-response effect of MAP inoculation in sheep used Poisson regression to parameterize a dose-response model of MAP infection (Breuninger and Weir, 2015). The study considered four studies where the dose effect was evaluated on different sets of animals. It included three studies that were also included in our meta-analysis. Due to the small study size, it was impossible to account for confounders such as age or time from challenge to *post-mortem* when the outcome of infection was determined. The authors described an apparent higher infectiousness in sheep of the bovine strain compared to ovine strain, but noted that this effect may have been due to age since sheep in the two compared experiments were of different ages. Our meta-analysis was larger and based on individual-sheep data rather than aggregate data which allowed a precise evaluation of the effect of dose by including studies with different inoculum doses as well as adjusting for confounding (Riley et al., 2010). Our results suggest that infection of sheep with a bovine MAP strain might produce more lesions, but that the lesions were not more severe than after infection with ovine MAP. Breuninger and Weir (2015) demonstrated a dose response effect with a pattern similar to our findings. Moreover, our findings agree with Breuninger and Weir (2015) in that the pattern of the dose-response effect was independent of the strain (ovine vs bovine).

Two meta-analyses of shedding patterns in cattle for informing mathematical modelling of bovine paratuberculosis resulted in similar findings as ours: one measured the effect of age and dose at exposure (Mitchell et al., 2011) and the other analysed shedding patterns of

experimental and natural infection (Mitchell et al., 2015). As with our work, both papers used an ‘individual-patient’ approach to apply standard statistical analysis rather than aggregate-level meta-analysis.

6.5.1 Probability of active infection

The force of infection in a compartmental model is the incidence rate at which susceptible individuals in the population become infected. It depends on the amount of infectious units to which the susceptible individuals are exposed. In the case of ovine paratuberculosis in a pastoral environment, the infectious compartment is represented by the amount of MAP organisms to which the animals are orally exposed.

We fitted the probability of active infection over time using time-dependant data of histological lesions at *post-mortem* to find parameters to use in the calculation of the force of infection. We derived three parameters for the force of infection: rate parameters from a Weibull distribution (α, k) and a dose-dependent plateau of active infection $\max(P(T < t))$.

The first appearance of histological lesions or the onset of faecal shedding can both be used as a proxy for entering the active infection stage. A preliminary review (Chapter 4) suggested that the presence of histological lesions in the intestinal wall and MAP faecal excretion are concomitant, especially at an early phase of transient shedding. Descriptive results in this meta-analysis confirm the concomitance of shedding and histological lesions in the guts (Figure 6-6).

We analysed both the onset of shedding (using survival analysis) and the presence of histological lesions at *post-mortem* (using GAMM). We concluded that data of histological lesions at *post-mortem* were more robust and only the analysis of these data are reported in the results of this manuscript and were used to estimate parameters for the mathematical model. The quality of the histological lesions dataset was considered better than longitudinal shedding data due to the following reasons:

- More power to detect and adjust for confounders: the meta-analysis had 627 sheep with histological lesions versus 159 with longitudinal shedding data. The former presented a greater range of covariate pattern allowing for more meaningful model building.
- The presence of histological lesions is considered a gold standard whereas detection of faecal shedding is hampered by the poor sensitivity of diagnostic tests. Results of Section

6.4.1.5 show that when using shedding data, the outcome depended heavily on the diagnostic test used.

- 50% of sheep with longitudinal shedding data only had 3 successive observations, and intervals between observations were sometimes very long, hence the difficulty to determine the onset of shedding using survival analysis.

Although the analysis using longitudinal faecal shedding were dismissed in this manuscript, they confirmed that the risk factors for onset of shedding were similar to those for onset of histological lesions, reinforcing the inferences obtained in 6.4.1.2. In particular, sheep infected with the bovine strain shed significantly earlier than sheep infected with the ovine strain, in line with results about the occurrence of histological lesions. Moreover, the time from challenge to shedding was significantly shorter in lambs than in animals older than three months old. This finding of transient shedding in lambs agrees with Mitchell et al. (2015) that transient shedding occurs in calves, and that this may affect the dynamics of PTB infection.

We used GAMM (logistic regression) to model the presence of histological data over time since inoculation, and secondarily derived the incidence of histological lesions based on the shape predicted by the model. The advantage of using logistic regression was that we did not need to assume that the time of observation was the time of onset, since we modelled the prevalence. The classical approach to estimate rates is survival analysis (modelling incidence), but this would require assuming that the time of observation was the time of onset of histological lesions. This, however, would be totally biased for observations occurring several months or years after inoculation. Our data consisted of point observations, which are not well suited for survival analysis. GAMM uses optimal smoothing procedures with penalised likelihood to evaluate the shape of the probability over time (Wood, 2006). Since the smooth term is non-parametric, it does not require an assumption about the shape, which is therefore purely data driven while accounting for the effect of other covariates in the parametric part of the model. Once this shape was known, we made an approximation based on the look of the data (early steep increase followed by a plateau of infection) to determine the part of the curve corresponding to cumulative incidence and used this part only to calculate parameters for the rate of infection and the plateau of infection. An advantage of using GAMM was that despite using one part of the obtained curve for parameters estimation, all other (later time points) observations were part of the model, and contributed to the estimation of the effect of other covariates. The part of the curve to use was data-driven rather than relying on an assumption.

The sigmoid shape of the predictive probability of histology lesions versus time (part before the plateau, Figure 6-8) was evocative of a Weibull distribution and not-compatible with an exponential distribution of time to active infection. There may be various other distributions that would provide a good fit, but the Weibull fit was excellent. With a parameter (k) greater than one, the Weibull fit indicated that the rate of onset of lesions increased over time. The pattern was independent of the age of infection. Because ODE cannot handle a rate varying with time since exposure, one would have to use partial differential equations or individual based stochastic modelling to model this process. To approximate the Weibull distribution, we therefore fitted a constant exponential rate instead. Detailed results from this alternative approach are described in Appendix B.

The meta-analysis revealed that, independently of the rate of infection, there existed a dose-dependent overall probability of “success” of infection with MAP, represented by the dose-dependent plateau $\max(P(T < t))$. Thus, the cumulative probability of active infection remains below one for low to medium doses and higher inoculum doses are required to infect all sheep. Our results (Figure 6-8 c) suggest a progressive effect of the dose. This is biologically plausible; it should be incorporated in compartmental, SIR-type model. The results indicate that there is considerable animal variation in the probability of becoming infected at a specific dose.

6.5.2 Probability of progression (χ)

Descriptive results (Figure 6-6) show that severe histological lesions occur with the onset of clinical disease. Hence the data provided good justification to combine the presence of either severe histological lesions (type 3 lesions) and/or clinical disease as a marker of progressive paratuberculosis. In the presence of such markers of progression, sheep are shedding high loads of MAP in their faeces, suffer subclinical to clinical disease resulting in production effects and are unlikely to recover from the disease (they will succumb to Johne’s disease or be culled).

We modelled the probability of progression following oral exposure to MAP (probability of presenting either severe lesions or clinical signs). We combined this with the probability of active infection, to estimate the probability of progression in actively infected animals (χ).

There was a very strong difference in the probability of progression for young animals (less than one year old) versus animals inoculated later on (coefficient for age less than one year =

2.5), but low numbers in the category of older sheep made predictions for this category less precise.

When modelling progression over time, there were two similar peaks of progression (Figure 6-10), likely representing two underlying populations of sheep following a different regimen, not explained by the model. The purpose was to estimate the maximum probability of progression. The value of the maximum (proportion) was not affected by the co-existence of different progression regimen. Still, we sought an explanation for these two peaks using interaction terms. A significant interaction between age and time indicated that lambs inoculated up to one month of age progressed quickly, with a unique peak around 300 days post-inoculation, while sheep older than four months of age presented a peak of progression centred on 400 days. However, for the intermediate age category (around weaning time) there were still several peaks of progression.

One goal of our meta-analysis was to derive parameters for a mathematical model in which age categories reflected the sheep production system of interest (four age groups representing lambs, hoggets, two-tooths and ewes). Consequently, the effect of age on progression was accounted for in the parametric part of the model, with categories reflecting the production system (less than one year old = lambs and hoggets versus more than a year old = two-tooth and ewes). Using these categories, interactions with time did not explain the presence of the double peak of progression.

To calculate the proportion of progressors among the infected (χ), we used the ratio of the first local maximum in the curve of infection over the first peak in progression. This assumes that the first peak in each curve represents the same population of sheep, possibly differing by their age at inoculation or other factors not accounted for. We used the maximum observed probability of progression as a proxy for the cumulative probability. For this time-dependant covariate, the cumulative probability is impossible to estimate *per se* from the meta-analysis data (point observations). We therefore used the maximum observed probability (peak of progression) as a proxy. This may underestimate the true cumulative probability because progressor sheep do not remain in this state for very long before succumbing to disease. To calculate χ , we also used the first local maximum of the curve of predicted probability of active infection versus time (*model 1*) as a proxy for the cumulative probability of active infection. The latter is likely close to the actual cumulative probability since the shape of the curve (presence of a plateau) suggests that recovery of infection is a relatively slow process. If the probability of progression (the numerator of χ) was actually underestimated, and the

probability of active infection (the denominator of χ) was unbiased, the parameter χ would be underestimated. It is nevertheless the closest realistic proxy we could obtain from the data, accounting for dose, age and type of inoculum.

6.5.3 Rate of progression from early to severe disease in the progressor track (δ)

We estimated the median time from entering active infection (early disease stage, not affected, associated with mild-moderate histological lesions) to progressing to an advanced stage (advanced, affected stage of disease associated with severe lesions and onset of clinical disease) as 405 days (13 months). This corresponds to a δ of 0.0017/day. We approximated the median time t_{50} as the peak time of mild to moderate lesions to the peak time of severe lesions, observed after modelling the prevalence of mild/moderate and severe lesions over time in two GAMM (*model 3* and *model 4*). However, it is not strictly correct to assume, as we did, that the difference between the peaks of prevalence of the two successive stages corresponds to the median time spent in the first stage. To evaluate the extent of the approximation we made, we used simulation and a theoretical compartmental model mimicking our method. We established that time quantiles obtained as the difference between the prevalence peaks of two successive infection stages (obtained with a combination of ranges of known parameters) was symmetrically distributed around the true median time (t_{50}) and in 50 % of the simulations the quantile fell between 33% and 64%. This means that the approximation we made (difference of peaks = t_{50}) was the most likely but the error was still large. To further support our estimate of δ , we also performed survival analysis on data from 30 naturally infected sheep of which serial intestinal biopsies were obtained by surgery of naturally infected sheep (Dennis et al., 2010). Although the latter constitutes anecdotal evidence (limited number of animals, for which the time of infection was unknown), this resulted in a median time spent in the early infection stage before progressing to a clinical stage (presence of multibacillary lesions or clinical paratuberculosis) of 10 months, which is coherent with our estimate of 13 months from the initial approach.

Another possible bias of this analysis was that all animals harbouring early lesions were assumed to progress to severe lesions. However, only a minority of animals actually progressed to severe lesions; most sheep entering the early stage recovered and did not develop clinical disease. The assumption would be justified if mild lesions occurred at about the same time in progressors and non-progressors, which is plausible. Hence, even though the

fate of animals sacrificed with mild lesions could not be determined, it is unlikely that taking them all into account in this analysis would drastically bias the results for the calculation of δ .

6.5.4 Rate of recovery from shedding in the non-progressor track (γ)

Early, low shedding of MAP is assumed to start at the same time as entry into active infection (histological lesions and shedding being supposedly concomitant), irrespective of the age at which exposure to MAP occurs. For animals entering the progressor track, early/low shedding is followed by the onset of high shedding as sheep progress from early stage to advanced paratuberculosis. For animals in the non-progressor track, we assume that this early shedding is transient (temporary) and the sheep later recover from their infection. This can be associated with recovery from shedding for the rest of their productive life when the sheep are not further exposed to MAP (Stewart et al., 2004). We estimated in this section the duration of this transient shedding stage, ending in recovery.

Recovery includes various aspects: recovery from mild disease and/or recovery from infection. Some sheep can totally clear up infection from their intestine (Dennis et al., 2010). Other infected sheep may pass through the stage of transient shedding and remain latent in the non-progressor track later on. This phenomenon is illustrated by “chronic” or “healing” histological lesions reported in several studies (Kluge et al., 1968; Gilmour et al., 1977). We elicited the presence of histological lesions as the marker of the actively infected stages. However, for recovery, the possible presence of chronic lesions in the absence of MAP organisms and MAP shedding could be misleading. For the dynamics of infection, it is irrelevant whether recovered animals still harbour healing lesions or are still latently infected by the bacteria as long as it is assumed that the recovered state is not shedding. Therefore the exit from the transient early infection compartment can be measured using duration of shedding as the outcome of interest. We thus defined “recovery” as “recovery from transient shedding”, a marker of evolution from early infection to recovery in the non-progressor track (Figure 6-1). Shedding data were quite sparse. Among 72 sheep with one or more PCR/culture positive faecal sample, 26 “stopped” shedding, hence were transient shedders according to our definition. The definition of “duration of shedding” was the time from the estimated onset of shedding to the middle of the interval between the last positive sample and the first negative when all subsequent samples were negative. There is evidence that for non-progressor sheep that were followed long enough, the recovery from shedding can be permanent (Stewart et al., 2004).

However, in our analysis there could be some underestimation of the shedding duration when only one negative sample was observed after the last positive sample (6 animals) because these animals were considered cured while they could actually be shedding intermittently. In all other cases, multiple negative samples followed the last positive case; hence cure from shedding was likely accurately determined. Because the last positive sample and the first observed negative sample were between five days and five months apart, the mean shedding duration could have been under or overestimated by up to 2.5 months, and the variance underestimated (Mitchell et al., 2015).

In the survival analysis, shedders still positive at the last sampling were censored and hence contributed to the analysis prior to being censored. However, a proportion of these animals might have been progressors that would not have later recovered from shedding but instead progressed to high shedding. These should ideally not be part of the population from which we estimate recovery from shedding, hence representing another possible bias. However, the proportion of progressors among the infected is likely low given the length of the follow-up. According to descriptive results in 6.4.1.1, most sheep still alive past 500 days were non-progressors.

The range of ages among the 72 sheep included in this analysis was from 30 to 300 days. Hence, the effect of age in animals older than a year could not be evaluated. There was a significant and important difference in shedding duration between lambs (less than 3 months old) versus sheep inoculated between three months old and 300 days, for which the transient shedding period was shorter. We can only assume that this effect would have been similar in sheep exposed as adults (more than one year of age). Dose of inoculum or strain type were not significantly associated with shedding duration.

Detecting faecal shedding can be biased by the sensitivity of diagnostic tests, which we accounted for in the analysis, adding the diagnostic test as a covariate. Relative sensitivity of the tests can be seen in Figure 6-13, whereupon qPCR detected shedding over a longer period of time than liquid culture, while plate culture detected very little shedding. This illustrates the poor sensitivity of solid medium and its inadequacy to grow MAP in particular the ovine strains. A qPCR, on the other hand can detect as few as one to 10 MAP/g of faeces which may not have a meaningful impact on the infection dynamics (Kawaji et al., 2011). The parameterization of shedding rates for the compartmental model in Figure 6-1 is explained in Chapter 4 and Appendix C. For the compartments of early disease, it was based on MAP excretion quantities from (Whittington et al., 2000) and comparative shedding levels between

paucibacillary and multibacillary sheep in the first year post-inoculation, from Kawaji et al. (2011). We thus evaluated the daily MAP quantity excreted by sheep in this compartment to 1740 organisms. Sheep on a track to recovery might shed lighter levels of MAP later on in the course of infection, but this was not taken into account by our parameterization. Since 1740 MAP is closer to the limit of detection of liquid culture and much higher than the limit of detection of qPCR and considering that qPCR can detect non-viable MAP, for consistency we predicted the recovery rate using liquid culture as the covariate for shedding test.

We used parametric survival analysis, better suited than Cox models to predict survival times and fit distributions to the data, hence estimating transition parameters for a compartmental transition model. Graphical comparison of a Weibull and an exponential distribution with a Kaplan-Meier curve indicated a better fit of the data with the exponential distribution. Given the complexity of using a time varying rate (Weibull) in a compartmental model and that in this case the Weibull distribution did not represent an obvious improvement in capturing the dynamics, we presented the results of parametric fit with the exponential distribution (constant rate) only. An exponential decay was well suited for our purpose of model parameterization. A similar approach using parametric survival was used in Mitchell et al. (2011) to study the effect of age on MAP shedding patterns in cattle. The lowest AIC however, was achieved in the model with Weibull distribution, although inferences about shedding duration were not impacted. We conclude that due to the small dataset (72 sheep) and some multi-collinearity in the covariates, inferences about the effect of covariates might have been not very robust, as indicated by variability of coefficients in models with different specifications (results not shown). However, inferences about overall shedding duration were robust.

6.5.5 Effects of covariates

Most animals used in the study were lambs or hoggets (only 30 animals were greater than one year of age), hence the effect of age at inoculation was difficult to evaluate. Only one study used adult sheep with a wide age range up to until 11 years (Delgado et al., 2012; Delgado et al., 2013).

We tested the effect of age at inoculation as a continuous variable (linear or not), or using categories corresponding to production groups relevant to the mathematical model of ovine paratuberculosis (lambs/hoggets/two-tooth and ewes) or as a dichotomous variable (less/more than one year old) in all models. The only model where a significant age effect

could be detected was the model of probability of progression. The odds of presenting markers of progression at any point in time were 12 times higher in animals inoculated before one year old (versus older than one year old). This resulted into estimating a different χ parameter in these two categories of age, which would have important repercussions for the simulated infection dynamics.

For all other parameters estimated, there was no difference between age groups, due to no significant age effect detected in the GAMMs. This, however, means that all estimates were driven by dynamics observed in young animals which were the majority in the dataset.

6.5.5.1 Effect of strain type

The strain type used in experimental studies (“ovine” or type I versus “bovine” or type II) is not always explicitly given, especially in older studies. In recent studies, the strains used for inoculation in experimental challenge were usually typed by PCR, which can be considered virtually perfect to distinguish the two main types of MAP. In numerous older studies, however, this was not the case. In such cases we used robust bacteriological and epidemiological criteria (educated guess) with the help of expert advice (Karen Stevenson¹⁰ and Marian Price-Carter¹¹) to determine the likely strain type. We also checked the robustness of the results obtained by running all models with different classification systems, *i.e.* if all the strains that were not typed had been ovine or alternatively bovine. The inferences remained the same in these models compared with models based on the educated guess.

The only model in which the strain type had a significant effect was modelling the prevalence of active infection (*model 1*): the bovine strain appeared as a risk factor for the occurrence of histology lesions (any grade) compared to ovine strain. The effect in the model of the presence of mild-moderate lesions in the guts (*model 3*) was similar but not significant. This is in line with the literature where an increased number of lesions, and more extensive lesions, were described in sheep inoculated with bovine MAP compared to ovine MAP, despite a tendency to later recover from the lesions caused by the bovine strain (Chapter 4). The main conclusion is that if the bovine strain seems more infectious than the ovine strain in sheep (more likely to cause active infection), the fate of sheep in terms of progression to clinical paratuberculosis is not significantly different between both strains.

¹⁰Moredun Research Institute, Pentlands Science Park, Bush Loan, Penicuik, EH26 0PZ, Scotland, UK

¹¹Hopkirk Research Institute, AgResearch Grasslands, Tennent Drive, Private Bag 11008 Palmerston North 4442, New Zealand

6.5.5.2 *Effect of breed*

Breed was partially collinear with strain type of MAP as all Romney and crosses and the vast majority of Merino and crosses were inoculated with an ovine strain while most other British breeds were inoculated with a bovine strain. This made it difficult to evaluate the effect of one versus the other. Moreover, breed was a proxy for the geographical region where the study was performed. In final models, the covariate strain type (only two levels) was preferred since breed did not improve the models over the effect of the strain type when the latter was significant.

In experiments undertaken in Australasia, both Romney and Merino crosses were infected with similar MAP strains, thus location and strain type did not confound the effect of breed. Results for these (not shown) suggest no obvious difference between those breeds in their susceptibility to MAP.

6.5.5.3 *Effect of experimental conditions*

One of the primary goals was to measure the effect of inoculum dose, thus the ‘infectiousness’ of MAP. We discarded one paper (Dukes et al., 1992) and another 10 sheep from an experiment that was included in the meta-analysis (Stewart et al., 2004) because these animals were dosed with tissue homogenate and the dose was reported as the weight of tissue, with no further attempt to enumerate the number of MAP. In our model, the “dose” corresponded to the total oral dose supposedly received by each animal (at the logarithmic scale). Most of the time, MAP was given in several inocula (up to 10) at various time intervals, with typically a few days between each dose. The total dose was the sum of all doses administered. The time from inoculation to *post-mortem* was calculated from the date of the first inoculum. To evaluate a potential effect of repeated doses, we tested the total number of doses administered as a continuous covariate in the two main models *model 1* (active infection) and *model 2* (progression). This was also a proxy for duration of the dosing regimen, although time intervals varied across studies. This effect was not significant and not kept in the models.

Experimental data are needed to measure the effect of MAP on the pathology of paratuberculosis. However, the effect of chronic exposure to MAP in a natural environment, although impossible to estimate, might trigger a different host response.

We also evaluated the possible bias due to MAP enumeration methods used to quantify the inoculum in experimental studies, on the estimated effect of dose. Each enumeration method comes with inherent biases and we classified them into two categories (Chapter 5). Culture-

based methods, counting viable/cultivable MAP) might underestimate MAP numbers. Physical methods counting total number of MAP might overestimate numbers by counting dead MAP cells. We used an interaction term between these two categories and the inoculum dose in the two main models (*model 1* and *model 2*). The effect of dose was very similar within each stratum and the interaction was not significant. Hence, the bias induced by enumeration methods was small compared to the amplitude of the effect of varying the inoculum doses itself. In this respect, this meta-analysis failed to generate robust conclusions about which enumeration method would seem more appropriate.

6.5.6 Methods

Meta-analysis can be defined as 'the statistical analysis of a large collection of analysis results from individual studies for the purpose of integrating the findings' (Glass, 1976). Systematic review and meta-analysis constitute the reference standard to generate synthetic evidence from diverse sources (Moher et al., 2015). Individual-patient meta-analysis in particular shows statistical advantages over 'aggregate data' meta-analysis, is more powerful and allows adjusting for confounding (Riley et al., 2010). They are more time- and resource-consuming than other methods for summarizing data but achieve a higher evidence level and therefore constitute the "gold-standard of systematic review" (<http://methods.cochrane.org/ipdma/about-ipd-meta-analyses>, Simmonds et al. (2005)).

Individual patient meta-analysis represents a challenge for data collection and extraction at individual-level. Published reports are sometimes ambiguous to interpret, hence the need for meaningful inclusion criteria and unbiased homogenisation of data from different studies to minimize biases. To alleviate ambiguity about the protocol we contacted eight authors for questions about the precise age or breed of sheep, the number of sheep, the strain of MAP used. We also called out for two experts of molecular biology of mycobacteria to help identify strain types in papers where typing was not done. A particular problem was encountered when the same research group reported the same experiment in several papers which required specific evaluation of the existence of duplicate sets of animals. This problem was noted in Berman and Parker (2002).

An important assumption of meta-analysis is that subjects enrolled in different studies come from the same underlying population; hence variation in the measured outcome is due mostly to the treatment effect (within-study variation) and random variation (Haidich, 2010). This (*i.e.* that the true effect is constant across studies) is the underlying assumption in meta-analysis adding study as a fixed effect (Dohoo, 2009). However, in practice variability between studies

always occurs, hence the necessity to explore heterogeneity. We incorporated between-study variation using random effect, thus assuming that the true effect varies across studies according to a normal distribution, which is standard in individual-patient meta-analysis (Berman and Parker, 2002; Riley et al., 2010). We had 38 distinct experiments in total in the meta-analysis, hence the use of random effects was appropriate, with the assumption that experiments represented a random sample of the 'population of experiments' and that their random effects are normally distributed around 0. The results therefore have a 'subject-specific' interpretation (here: study-specific) and can be thought of as a way to adjust for unmeasured study-level covariates (Hu et al., 1998). We did not further evaluate the left-over variability between experiments as the primary objective was to unify the findings while accounting for this variability.

Although the sheep in experimental infection studies were followed over time, most outcomes of interest in this meta-analysis were measured at the time of sacrifice, hence the studies were effectively cross-sectional and not longitudinal. With data corresponding to point observations, one can estimate the point prevalence of various paratuberculosis outcomes over time, but not the incidence. Parameters for a compartmental model are mostly rates (except the parameter χ in this study which is a proportion). The natural way to estimate rates is through survival analysis, which describes the distribution of time to event (onset or cure of a particular infection stage). Since the incidence depends only on the entry parameter (the incidence rate) and not upon the rate of exit, the point incidence (observed in survival data) and the cumulative incidence are directly related. In the present dataset, the distribution of time to onset was not available: we were working with prevalence data, which depends upon both onset and recovery. Because of that, we took an innovative approach to estimate the required mathematical parameters, based on the available data. We used a non-parametric smoothing function (GAMM) to describe the effect of time on the different outcomes of interest in the absence of longitudinal histological data in the study. We were thus able to derive parameters (rates or otherwise) from the observed data. These were necessarily biased but strongly relied on real-world observation as we made the best possible use of the existing experimental data available.

Finally, an assumption of this meta-analysis was that secondary infection by shedding from peers did not occur. We assumed that sheep enrolled in controlled trials were kept in conditions not favourable for secondary transmission (clean pens and paddocks). The presence of control animals was not a prerequisite for inclusion in this meta-analysis but was often reported. Control sheep, when reported, were always negative to all tests, thus corroborating

the assumption that secondary infection was not important. This phenomenon could have happened but the extent would have likely been negligible compared to the experimental inoculation process.

6.6 Conclusion

This study combined data from published experimental research of ovine paratuberculosis with the aim to provide robust parameter estimates for mathematical modelling. A total of 767 sheep contributed to this meta-analysis. Parameterizing mathematical models of infectious diseases often relies on reviewing the literature. However, we were confronted with difficulties in synthesizing evidence from disparate reports of experimental infection of sheep with MAP, with study-level confounders and small numbers increasing variability in the outcome. Meta-analysis represents the gold standard of evidence and allowed the estimation of data-driven parameters with more power, and adjusted for confounding. We were able to determine (1) the rate of infection and probability of success of infection upon oral ingestion of MAP, as a function of the dose ingested, (2) the probability of entering a pathway of progression to clinical disease upon infection with MAP as a function of the dose ingested, (3) a median time of 405 days to progress from early to severe disease (affected by MAP, onset of clinical disease, with production effects) in the progressor pathway, (4) a median time of 342 days for recovery from shedding for sheep entered the recovery track. Our results show that MAP is highly infectious in sheep, with only 76 live organisms necessary to actively infect 50% of inoculated sheep. However, the virulence of MAP is low: 8.9×10^6 MAP organisms are necessary to cause progression to clinical disease in 50% of sheep infected as lambs or hoggets, and 7.7×10^9 MAP for sheep infected after one year of age. These findings can be used to parameterize a mathematical model of ovine paratuberculosis in a pastoral environment. The main limitation is that all data available for the meta-analysis were from experimental infections. Extrapolations to natural challenge in commercial farming environments may not be valid for all parameters.

6.7 Acknowledgments

We thankfully acknowledge Marian Price Carter and Karen Stevenson for their expertise about MAP genetic diversity and their advice for assessing strains of MAP used in the literature. We are particularly grateful to Valentine Perez for providing additional raw data for one experiment, to Douglas Begg for sharing an expert view about the physio-pathology of OJD and

outcomes of experimental infection with MAP and Chris Jewell for very useful comments about the interpretation, the analysis and the display of these data.

Chapter 7. Modelling paratuberculosis in a typical sheep flock in New Zealand

Nelly Marquetoux^a, Matthieu Vignes^b, Carolyn Gates^a, Peter Wilson^c, Anne Ridler^c, Cord Heuer^a

^a *EpiCentre, Institute of Veterinary, Animal and Biomedical Sciences, Massey University, New Zealand*

^b *Institute of Fundamental Sciences, Massey University, New Zealand*

^c *Institute of Veterinary, Animal and Biomedical Sciences, Massey University, New Zealand*

7.1 Abstract

Pastoral sheep farming in New Zealand (NZ) is characterized by all-year grazing and strong seasonality of production cycles. Infection with *Mycobacterium avium* subspecies *paratuberculosis* (MAP) is endemic in 76% NZ sheep flocks. The organism causes ovine Johne's disease (OJD), a fatal chronic wasting disease associated with production loss and mortality in affected flocks.

We developed a deterministic state-transition model for MAP transmission dynamics in a typical NZ sheep flock and evaluated the cost of OJD on-farm and the cost-benefit of vaccination. The model structure was informed by a comprehensive literature review of experimental and natural infection of sheep with MAP and the model was parameterized using results from an earlier meta-analysis of experimental infection. The model considered the seasonal management typical of North Island hill country sheep flocks, with removals and replacements at specific times of the year. Novel aspects of within-flock dynamics of paratuberculosis were considered, as well as the influence of between-flock transmission, which have not been evaluated previously.

Transmission of MAP between sheep was driven primarily by pasture contamination. Seasonal events of lambing, culling and replacement, their impact on annual offtake rates and associated financial outputs were incorporated in the demographics part of the model. Age-related grazing management also influenced the level of pasture contamination. Different levels of MAP infection prevalence were simulated. These prevalence levels were associated with different clinical incidence of OJD. This allowed us to quantify the corresponding main production losses associated with mortalities due to OJD. For average NZ farms (with low incidence levels of OJD), the cost of PTB was estimated to be 0.3% of the potential farm-gate

revenue, hence negligible. At a level of 2% OJD mortalities in the ewes flock (representing very high incidence in NZ), the economic loss due to OJD represented 4% of farm-gate revenues.

Our simulations support a therapeutic effect of vaccination against OJD (changing the course of pathogenesis) rather than purely preventing the disease.

Results suggest that the vast majority of NZ pastoral sheep farms have a low impact of OJD and therefore would not economically benefit from vaccination. However, for the population of farms with high (1%) to very high (2%) annual clinical incidence of OJD in ewes, vaccination with Gudair™ drastically reduced OJD mortality in the flock and was thus cost-effective. A minimum of 0.97% OJD mortality in mixed age ewes was required for positive return on investment after 30 years of vaccination. Above 1% clinical incidence the time to return on investment was dropped rapidly. Farms with very high clinical incidence (2% cases/annum) could expect a positive return on investment after 5 years. At the 30 years horizon, such farms could expect 2.4 dollars of positive return (present value) for each dollar invested in vaccination, with a total net cumulated profit of vaccination of NZD 2435 per 100 ewes (present value). Meat price fluctuations had a strong impact on the economic evaluation. Purchasing 1% MAP-infected replacement ewes increased the overall farm contamination with MAP and resulted in higher OJD mortality. It substantially compromised the cost-effectiveness of vaccination for farms with 1% clinical incidence in the ewe flock. We also evaluated the influence of changing the replacement rate or reducing the exposure to MAP via rotational grazing on OJD levels. Given the negative impact of importing sheep potentially infected, we suggest that closed flocks are better candidates for vaccination strategies against OJD. This model could be adapted to study OJD in different sheep pastoral production systems in NZ or elsewhere, as well as other diseases with a strong environmental transmission component, such as leptospirosis.

7.2 Introduction

Johne's disease is the clinical manifestation of infection by *Mycobacterium avium* subspecies *paratuberculosis* (MAP). It causes losses to farms through deaths (Bush et al., 2006b), culling/disposing of clinically-affected animals and reduced carcass weights at slaughter (Morris et al., 2006). In New Zealand it is estimated that 76% of sheep flocks might be infected with MAP (Verdugo et al., 2014a). A nationwide farm survey conducted in 2010 indicated that only 5.4 % of randomly-selected flocks had confirmed clinical cases of OJD, while according to farmers' records the annual clinical incidence in farms infected with MAP (test positive) was

estimated to average three cases per 1000 ewes (95% confidence interval: 1 to 5). A study conducted in a research flock with high clinical incidence of OJD followed over 8 years estimated the overall annual clinical incidence in this “problem” flock was 1% in mixed-age ewes (Morris et al., 2006). These results from observational studies indicate that clinical OJD may be a limited burden in NZ sheep farms at the national scale. Nevertheless, for farmers experiencing high clinical incidence, controlling the disease may still be desirable.

Paratuberculosis control is challenging due to the poor performance of diagnostic tests for early detection of sub-clinically affected sheep and the persistence of MAP in the environment. An effective and safe killed vaccine (Gudair™) is commercially available for sheep in NZ (Reddacliff et al., 2006). Vaccination is widely used worldwide (Juste and Perez, 2011), with a focus on controlling the infection by reducing the amount of environmental contamination on the farm and reducing the economic burden through the prevention of clinical OJD (Reddacliff et al., 2006). In Australia vaccination programmes using Gudair™ proved to be successful at controlling infection and virtually eliminating clinical disease, even in flocks which previously experienced high OJD mortality (Windsor, 2006b). However, the use of this vaccine is associated with some limitations. Notably, it seems unlikely to eliminate shedding within a flock, even after prolonged vaccination. This has important consequences for control as the sustained presence of MAP continues to cause new infections (Reddacliff et al., 2006; Windsor, 2006b; Dhand et al., 2013; Dhand et al., 2016). Moreover, other management strategies may undermine the vaccination strategy, such as keeping unvaccinated cohorts of sheep on vaccinated farms (Eppleston et al., 2011), introducing infected sheep from other farms, or having stray sheep (Windsor, 2013). There is currently no evidence of this risk of relapse on farms that achieved very low prevalence of paratuberculosis and then stopped vaccinating. To the best of our knowledge, the cost-effectiveness of paratuberculosis vaccination on sheep farming in New Zealand has not yet been evaluated.

The cost-effectiveness of OJD control heavily depends on the economic burden of OJD on a farm. Strategies for reducing the OJD incidence, such as keeping flocks closed, can affect the cost-effectiveness of vaccination. Field trials for the evaluation of control measures are expensive and time consuming. Mathematical modelling offers an alternative to evaluate such outcomes.

Mathematical simulation models were widely used to study economic effects of control strategies for paratuberculosis in cattle (Marcé et al., 2010). However, the literature on modelling ovine paratuberculosis control is limited. We found two peer-reviewed spreadsheet

models of OJD and its control, both showing a benefit over cost of vaccination (Juste and Casal, 1993; Bush et al., 2008).

In the past two decades, the pathogenesis of ovine paratuberculosis has been extensively studied. This has provided data to allow a more accurate modelling of paratuberculosis dynamics and a more accurate estimate of the cost of OJD on sheep farms.

The aims of this study were to (1) use simulation modelling to evaluate the financial benefits of vaccination against ovine Johne's disease (OJD) in an all-year-pasture seasonal lambing sheep flock in New Zealand and (2) evaluate best management practices to increase the economic return from vaccination.

In this manuscript, paratuberculosis is a generic term to refer to any stage of infection with MAP, whether clinical or subclinical, while OJD is used interchangeably for clinical paratuberculosis.

7.3 Materials and methods

7.3.1 Model description

We developed a deterministic, compartmental mathematical model to simulate PTB for sheep in a pastoral environment. The model structure and main pathogenesis assumptions were based on a review of literature about MAP infection dynamics and pathogenesis (Chapter 4). Model parameter values were based on earlier work (Chapter 6). They reflect the quantitative effect of dose and age at infection. The model included plausible sheep flock demographics and a seasonal production system.

Transitions between infection stages can be described using a system of ordinary differential equations (ODE). These ODE were numerically solved in discrete time using first order (Euler), resulting in daily updates of quantities in each compartment. Model equations and parameter values are shown in Appendix C.

7.3.1.1 Demographic structure

Seasonal lambing and age-related sheep management influence both production outcomes and MAP transmission dynamics.

The model demographic structure was based on a typical self-replacing ('closed') New Zealand North Island hill country Romney sheep flock producing prime lamb for slaughter (

Figure 7-1: Modelled age compartment sizes of management groups (/100 lambing ewes), transitions between production groups, reproductive periods and timing of management events in a typical North Island hill country sheep flock.

). Keeping explicit track of calendar day reproduced the typical seasonal management of New Zealand sheep farms. The flock was divided into 4 management groups based on age: lambs (0 to 3 months), hoggets (>3 to 12 months), two-tooths (>12 to 24 months), and mixed-age ewes (>24 months of age). It was assumed that mixed-aged ewes and lambs grazed the same pasture. After weaning, hoggets grazed a separate pasture block. Two-tooth also grazed separately until joining the ewe flock at their first lambing. All animals were subjected to mortality at a rate specific for each age group.

The start of lambing was set to September 1st and the lambing period lasted 42 days (mid-point of the industry standard ranging from 34 to 51 days, Cranston L (2017)). The lambing percentage was 1.4 lambs/ewe. Lambs were weaned at a median age of three months, 16 weeks after the start of lambing, on December 22nd. At weaning, 20% of prime lambs were immediately drafted for slaughter and the remaining lambs were transferred to the replacement hogget management group. Fifteen percent of the remaining hoggets were drafted for slaughter every 21 days thereafter until either reaching the threshold number required for replacement ewes or reaching one year old and aging to the two-tooth group on September 1st of the following year. On that day any excess hoggets were sold as prime lamb. Past this age, the meat sent to slaughter was marketed as mutton instead of prime lamb.

Selective culling of ewes occurred once a year on January 15th, hence destocking the farm before wintering when pasture was limited. For simplicity, the joining of in-lamb replacement two-tooth into the mixed age ewe flock occurred on the first day of the lambing season as they reached two years of age.

The flock had an annual replacement rate of 25%, and it was self-replacing (baseline scenario). An additional safety margin of 3% was added to calculate numbers of hoggets and two-tooths to keep for replacement, accounting for losses on top of natural mortality. At the culling date, on January 15th, mixed-age ewes were removed from the flock. The number of ewes drafted for seasonal culling was determined to achieve a replacement rate of 25% for the baseline scenario of a paratuberculosis-free flock. General mortality and seasonal culling of ewes summed to 25% of the target flock size. This was achieved through a fixed culling proportion applied to the ewes present at culling time, calculated for the baseline scenario (paratuberculosis free). This proportion was kept constant in all subsequent scenarios and

applied to all ewes except those already affected by clinical OJD, which were assumed to die on pasture. Culled ewes were replaced by pregnant two-tooths to maintain the target flock size. Excess two-tooths were sold as mutton at two years of age. The safety margin was potentially exceeded in scenarios with additional mortality due to OJD. Purchase of extra-stock (in-lamb two-tooth ewes assumed to come from OJD-free flocks) was allowed to maintain flock size in flocks with higher clinical incidence of OJD when the 3% margin was not sufficient.

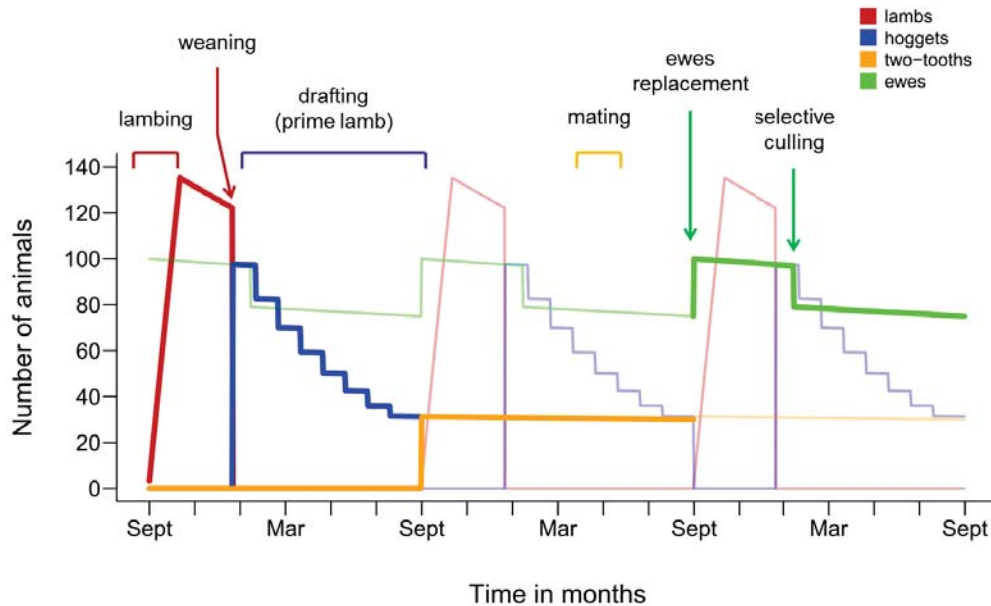


Figure 7-1: Modelled age compartment sizes of management groups (/100 lambing ewes), transitions between production groups, reproductive periods and timing of management events in a typical North Island hill country sheep flock.

7.3.1.2 Infection dynamics

The infection dynamics part of the model is shown in Figure 7-2. Sheep were exposed to MAP throughout their lifetime, specifically upon ingesting MAP from grazing a contaminated pasture. We modelled the transition rate F (force of infection) at which sheep entered a stage of active infection following exposure to MAP. F was updated at each time step for each age group as a function of the number of sheep exposed to MAP and the daily dose of MAP ingested per sheep (see Appendix C).

It was assumed that excreted MAP organisms were evenly distributed over the pasture. The total quantity of MAP on pasture (Env) thus depended on (1) the number of sheep shedding MAP and the shedding rates and (2) the decay rate of MAP on pasture. We identified two studies specifically measuring decay rates of MAP on pasture in an Australian farming

environment (Whittington et al., 2004; Eppleston et al., 2014). Results are summarised in Table 7-1.

Based on these studies, we selected a default value for the exponential decay rate of MAP on pasture (ψ) of 0.09. This represented shaded locations in the very dry Australian climate, hence more typical of milder New Zealand climate compared to unshaded locations for which extreme temperatures unrealistic for NZ were reached.

The number of MAP ingested by one animal per day (DA) was modelled by the following equation:

$$DA_{age}(i) = C \times Env_{pasture}(i-1) \times \frac{dmi_{age}}{\sum_{age}(dmi_{age} \times N_{age}(i-1))} \quad \text{Equation 1}$$

With age representing the age group (lamb, hogget, two-tooth or ewe), $Env_{pasture}$ representing MAP organisms present in the age-specific pasture block (ewes+lamb, hoggets, two-tooths), C a contact parameter representing the proportion of MAP available for ingestion of the total MAP on pasture, dmi_{age} the relative daily dry matter intake for this specific age group (ewe = 1, lamb = 0.3, hogget = 0.8, two-tooth = 1.3) to adjust the quantity of MAP ingested proportionally to age-specific dry matter intake from grass.

Here, the total number of MAP available through grazing was divided by N_{age} , the total number of sheep of each age group currently present on a pasture block. It assumes constant stocking density and that paddock size and grass growth match the feeding requirements of the animals in each age group.

Table 7-1: Summary of experiments of survival of MAP organisms on pasture

Paper	Sun exposure of the experimental locations	Season	Location	Method	Decay log ₁₀ /week	Exponential decay/week	Median survival time (days)	Exponential decay/day
1	shaded and unshaded	summer	pasture plot	linear regression ^a	0.55	1.27	NA	0.18
1	partially shaded	late spring	pasture boxes	linear regression ^a	0.25	0.58	NA	0.08
1	100% shaded	summer	pasture boxes	linear regression ^a	0.43	0.99	NA	0.14
1	100% shaded	summer	pasture boxes	linear regression ^a	0.10	0.23	NA	0.03
2	partially shaded	early spring	pasture boxes	survival analysis	NA	NA	82	0.01
1	unshaded	late spring	pasture plot	estimated ^b	1.50	3.45	NA	0.49
1	unshaded	late spring	pasture plot	estimated ^b	0.75	1.73	NA	0.25
1	unshaded	late spring	pasture plot	estimated ^b	1.25	2.88	NA	0.41
1	unshaded	late spring	pasture boxes	estimated ^b	1.25	2.88	NA	0.41
1	unshaded	late spring	pasture boxes	estimated ^b	0.35	0.81	NA	0.12
1	unshaded	summer	pasture boxes	estimated ^b	0.28	0.63	NA	0.09
1	unshaded	summer	pasture plot	estimated ^b	0.43	0.98	NA	0.14
1	unshaded	summer	pasture boxes	estimated ^b	0.35	0.81	NA	0.12
2	unshaded	early spring	pasture boxes	survival analysis	NA	NA	20	0.03
average across groups								
average shaded/partially shaded								
average fully unshaded								
range								
[0.01-0.49]								

1: (Whittington et al., 2004)

2: (Eppleston et al., 2014)

^alinear regression of log₁₀ (MAP dose) on time series of viable number counts of culture positive samples

^binferred from starting MAP concentrations and observed (assumed) maximum duration of survival

Parameter C, a proportion of viable MAP present on pasture being orally ingested by sheep through grazing, represented a contact ratio between sheep and MAP. To the best of our knowledge, it has never been determined. The rate of infection upon ingesting a given dose of MAP was known from the meta-analysis (Chapter 6). However, the dose of MAP ingested while grazing is unknown. We therefore adjusted parameter C to obtain scenario-based levels of infection and disease in the flock reflecting field observations.

Upon becoming actively infected with MAP, a proportion χ of animals entered the progressor track, while the remaining proportion $(1 - \chi)$ entered the non-progressor track (Figure 7-2). χ depended on the dose of MAP ingested and on the age group (see Appendix C).

Sheep in the progressor track progressed from early to severe disease at a constant rate (δ). Sheep in the severe disease compartment experienced production effects and clinical disease in the form of an additional PTB-related mortality rate μ_c . Sheep in the non-progressor track recovered from early disease at a rate γ . Recovered animals were neither shedding nor experiencing production effects, and were considered no longer susceptible to infection. They remained in this compartment until routine drafting, culling or death.

Animals in the early disease compartments (progressor P and non progressor N) shed MAP organisms into the environment (Env) at rate σ_{low} while animals in the severe disease compartment (affected A, sub-clinically then clinically) shed organisms at rate σ_{high} .

Drafting for meat removed animals at random and proportionally to the number of animals in each infection stage, except for animals in the affected stage (A) which were not subject to culling. These had no monetary value, and it was assumed they would die on farm and not be selected by the farmers for the slaughter plants.

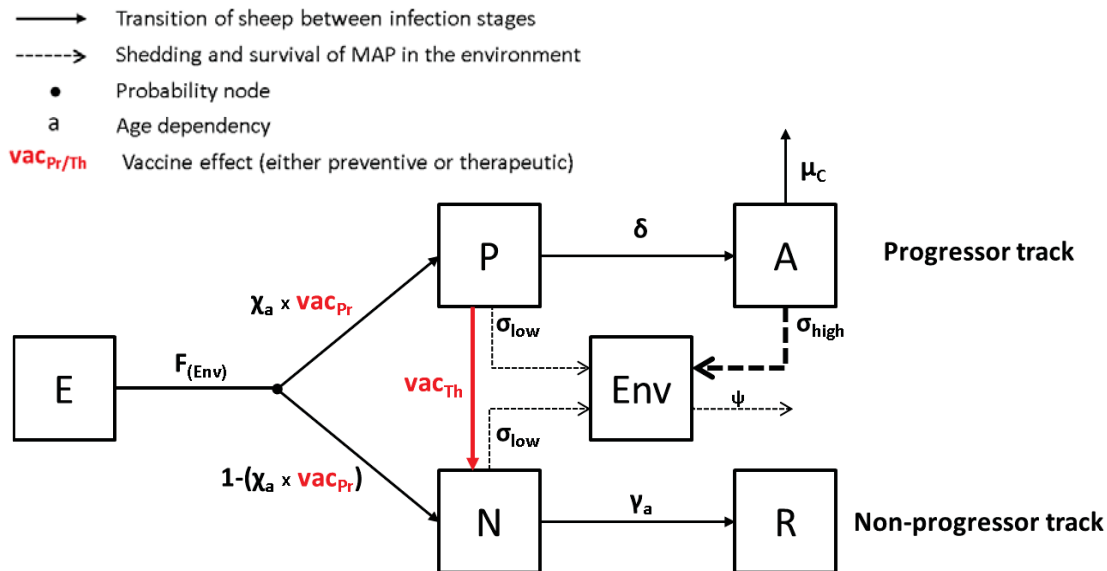


Figure 7-2 : Transitions between mutually exclusive disease states for ovine paratuberculosis (transmission from the environment Env, *i.e.* the pasture). E represents Exposed sheep. P (progressor track) and N (non-progressor track) represent sub-clinical infection associated with early/mild disease, low shedding and no visible production effects. A represents the (sub-clinically then clinically) Affected stage, experiencing production effects and high shedding. R represents a stage of Recovery from disease/shedding. Flock demographic parameters are not shown. Details of parameters and equations for transition between stages are given in Appendix C.

The infection state of lambs at birth depended on the infection state of their dam to consider the possibility of vertical transmission. According to Lambeth et al. (2004), 100% of clinically affected ewes and 1/54 sub-clinically affected ewes might have MAP infected foetuses. Based on that, we assumed that all lambs born to E and R ewes are assigned state E. Lambs born to ewes in the early/mild disease compartment (P or N) had a $(1 - \rho_{P/N})$ probability of being E at birth. The remaining proportion $\rho_{P/N}$ ($=1/54$) were born already infected, with a proportion χ entering the progressor track and $(1 - \chi)$ entering the non progressor track upon birth. All lambs born to ewes in the severe disease compartment were already infected (proportion of progressor/non-progressors according to χ).

7.3.1.3 Effect of vaccination

Gudair™ is a killed vaccine providing lifelong immunity with one dose and is the only vaccine registered against ovine paratuberculosis in Australia and NZ. A five year randomised controlled vaccine efficacy field trial was conducted in Australia from 1999 to 2004 in three heavily infected flocks with high mortalities, leading to Gudair™ registration (Reddacliff et al., 2006). This trial showed that vaccination of lambs at weaning (100% of the cohort) was followed by a 90% reduction of OJD mortality (across all age groups) compared to controls. These figures were confirmed in subsequent years by extensive research about Gudair™

vaccine efficacy in Australia. We used the observed 90% decrease in mortality to estimate a parameter for vaccine efficacy, which then could be used in subsequent simulations.

We modelled a preventive effect or a therapeutic effect of vaccination (Figure 7-2) and attempted to validate either of these against the observed 90% reduction of OJD mortality. A therapeutic effect of vaccination consisted of switching a proportion of infected sheep from the progressor track to the non progressor track, by adding a transition rate from P (early disease progressor) to N (early disease non-progressor). A preventive vaccine effect consisted of reducing the χ parameter (proportion of sheep entering the progressor track upon infection) to a fraction of its baseline value. Both effects were simulated using the parameter *vac* (a rate for therapeutic effect, a proportion for preventive effect). We reproduced the Merino flock in the Gudair™ trial (Reddacliff et al., 2006) by (1) keeping most weaners in the flock until 2-years of age (by increasing the safety margin to keep weaners for replacement to 70% instead of 3%), (2) vaccinating all weaners as was done in the Reddacliff trial, not just 30% and (3) setting the clinical incidence in ewes to 5% (pre-vaccination). The parameter *vac* was then adjusted so that vaccination at weaning reduced the overall OJD mortality from 15% in the absence of vaccination by 90%, *i.e.* to 0.5%, mimicking the effect of vaccine in the Gudair™ trial.

7.3.2 Farm gate profit of sheep farming

7.3.2.1 Benefit of sheep farming

We used figures from the sheep industry (Table 7-2) to calculate the annual benefit in NZD generated by the simulated system of production. The main income for this production system comes from prime lamb carcasses for which we used two input prices:

- National industry prices for year 2010-2011 represented an outlier year with the highest prime lamb/mutton price for the decade 2005-2015,
- National industry prices for year 2012-2013 corresponded exactly to the average meat price for the decade 2005-2015, for both mutton and prime lamb.

The total annual benefit of sheep farming was the sum of carcasses revenue and fleece revenue, minus the cost of purchasing replacement ewes (where applicable). In farms with no vaccination, the annual farm gate profit was equal to the annual benefit (Figure 7-3).

Table 7-2: Parameters to evaluate the annual economic benefit of sheep farming (Romney type production, North Island farming system).

		2010-11 ^e	2012-13 ^f
Carcass value (NZD/head):	Lamb ^a	118	85
	Mutton ^a	92	61
Greasy fleece value (NZD/kg):	Fine ^b	9.55	10.48
	Medium ^b	4.43	6.46
	Strong ^b	4.12	3.17
Wool production kg/head (Shorn wool greasy ^c)		4.66	4.86
Shearing cost NZD/head (full contract Romney North island) ¹²		3.6	3.6
Purchase in-lamb replacement two-tooths (NZD/head) ^d		105	105

^aannual average farm-gate price for export, returns include skin and wool-pull payment net of processing charges (all grades weighted schedule, year ending September)

^bSeason average Auction wool prices, cents/kg greasy, year finishing in June

^cWool production, excludes wool on sheepskin

^dAssumed price

^eHigh price scenario

^fBaseline scenario = decade average

Reference: Beef and Lamb economic services¹³: Beef and Lamb mid-season update 2015-16, Beef and Lamb mid-season update 2011-12, Beef and Lamb Compendium of NZ farm facts 2016.

7.3.2.2 Production effects of paratuberculosis

On top of the cost of mortality due to clinical paratuberculosis, animals in the severe disease compartment suffered production effects. Little information exists about production effects of paratuberculosis in sheep in NZ. Based on Morris et al. (2006), we accounted for sub-fertility in ewes in the severe stage by setting the lamb rate for the latter to 0.87 of that of other ewes. Significantly lower live weights in clinically affected ewes were also noted (Morris et al., 2006), but need not be incorporated in our model since animals in the 'Affected' compartment were assumed to die on-farm, and not be subject to culling/drafting. Therefore they had no economic value.

7.3.2.3 Cost of vaccination

Vaccination was done at a convenient time for the farmer *i.e.* when yarding and handling of the animals would occur in the general management cycle. The recommendation is to vaccinate only replacement stock to be more cost-effective. Hence for all practical purposes, we simulated vaccination at weaning of 30% of the lamb crop weaned (corresponding to lambs

¹² Expert opinion: Anne Ridler (IVABS, Massey University, Palmerston North, New Zealand) and Peter Anderson (The Vet Centre Marlborough, Blenheim, New Zealand)

¹³ <http://www.beeflambnz.com/information/economic-reports/>

needed for replacement plus a small margin). The cost of vaccine including labour (Gudair™ vaccination is labour intensive) was NZD 3.5 per vaccinated sheep.

The annual farm gate profit on vaccinated farms was the total farm benefit minus the total cost of vaccination (Figure 7-3).

7.3.3 Simulation scenarios

7.3.3.1 Baseline

The baseline for simulations was a self-replacement flock with management as described above and free of OJD. All simulation outcomes are reported relative to 100 lambing ewes and can be extrapolated to any flock size. Typical flock size for North Island Hill country sheep flock in NZ would be about 2000 mixed-age ewes.

7.3.3.2 Cost of OJD

For simulations with MAP infection/OJD present in the flock, we seeded the infection through pasture contamination of the ewe/lamb paddock ($Env_{(0)} = 2 \times 10^{12}$ MAP). The outcomes of OJD scenarios are reported after 30 years of simulation, which we call equilibrium. Different levels of clinical paratuberculosis at equilibrium were generated by adjusting parameter C. We simulated three scenarios:

1. *Average scenario*: 0.2% OJD annual mortality in the mixed age ewes, typical for New Zealand farms reporting clinical paratuberculosis.
2. *High clinical incidence scenario*: 1% OJD annual mortality in the mixed age ewes, representing high clinical incidence for NZ.
3. *Very high clinical incidence scenario*: 2% OJD annual mortality in the mixed age ewes.

For each scenario, the annual cost of OJD was the difference of farm gate profit between the baseline OJD-free scenario and the OJD scenario (without vaccination) at equilibrium (Figure 7-3).

7.3.3.3 Cost-effectiveness of vaccination

Vaccination started on scenarios of disease at equilibrium after 30 years simulations, leading to a new equilibrium after another 30 years. The annual clinical incidence of OJD after vaccination was monitored and the cost-effectiveness of vaccination over time was evaluated.

We used the following definitions:

- Benefit of vaccination: difference in revenue between (1) the scenario with disease after onset of vaccination and (2) the scenario with disease/no vaccination at equilibrium. The benefit of vaccination represents the averted loss due to vaccination.
- Net profit of vaccination: difference between the cost of vaccination and the benefit of vaccination.

Benefit, cost and net profit were either expressed as annual or accumulated from the onset of vaccination. A discount rate of 6%¹⁴ was applied to determine the present dollar value, to make costs and benefit comparable over time.

- Return on investment was the time until the net cumulative discounted profit of vaccination became positive.
- Break-even was the time until the annual net discounted benefit of vaccination became positive.
- Benefit-cost ratio over time: cumulative discounted benefit of vaccination divided by the cumulative discounted cost of vaccination. It represented the return (in NZD) that could be expected for each NZD invested from that point onwards. The Benefit-cost ratio exceeded one when return on investment was reached.

The principle of the economic analysis and calculation of net profit of vaccination is explained in Figure 7-3.

¹⁴ <http://www.treasury.govt.nz/publications/guidance/planning/costbenefitanalysis/currentdiscounrates>

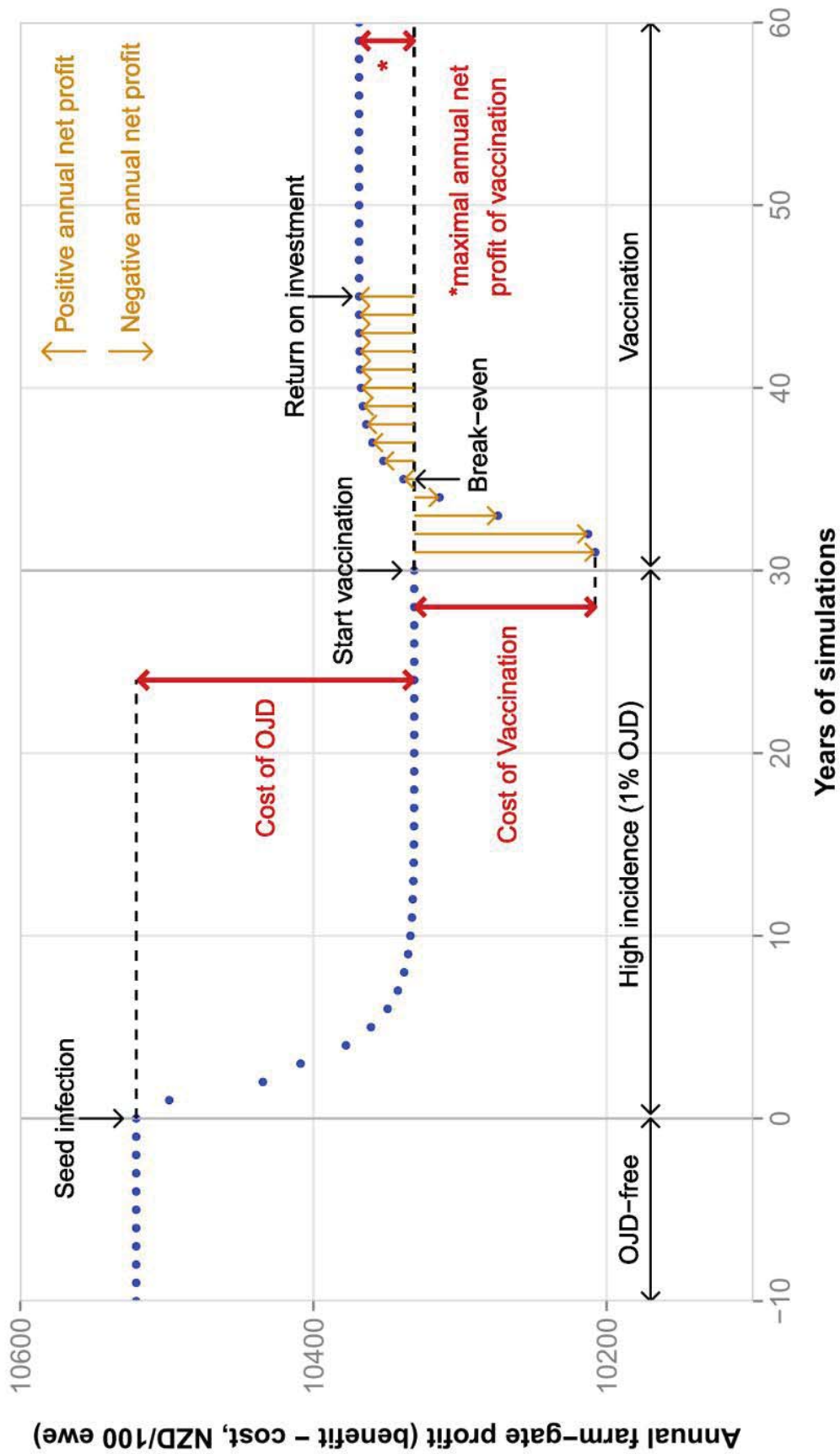


Figure 7-3 Evaluation of the cost of OJD and of the cost effectiveness of vaccination over time, showing the evolution of annual farm gate profit after seeding MAP infection and after the onset of vaccination. This figure is for explanatory purposes only and benefits/costs are not discounted.

7.3.3.4 Effect of sheep trade

In the baseline scenario, the sheep flock was closed (self-replacing). Purchase of replacements would only be required in situations with very high clinical OJD incidence, when the safety margin for replacement was not sufficient. Only susceptible animals from an OJD-free farm would then be purchased. To study the effect of trade, we shifted to a baseline scenario of purchasing one pregnant two-tooth per 100 ewes every year, in addition to extra replacements potentially needed due to OJD. Purchased two-tooth ewes joined the ewe flock at lambing. The baseline was to purchase one uninfected (susceptible) ewe. The alternative was to purchase an infected ewe instead (in early progressive stage P or early non-progressing stage N, unvaccinated) and see whether this would compromise the vaccination strategy. For a given level of clinical incidence with baseline purchase scenario (one un-infected animal/year), vaccination started. Ten years later, the alternative purchase scenario was adopted (one infected ewe/year) and subsequent changes were monitored.

7.3.3.5 Effect of market price fluctuations and alternative flock management strategies

We investigated the effect of higher farm-gate price by using market prices of the year 2011 (record high for decade 2005-2015) versus decade-average prices of 2013 (Table 7-2) in simulations of the cost-effectiveness of vaccination.

We additionally evaluated the impact of two alternative flock management strategies, separately or in addition to vaccination. First, we varied the replacement rate in the ewe flock of $\pm 5\%$ (setting it to 20% or 30% instead of the baseline 25%). Secondly, we decreased the contact between sheep and MAP from the pasture (C) by a factor 10 to mimic pasture spelling as an alternative to set stocking. For these scenarios, the baseline was the same as described page 166, in particular it was a closed flock. We assessed the effect of these scenarios on the infection and disease dynamics. For variations in the ewe replacement rate we also evaluated the impact on the farm gate profit by calculating the cumulative net profit of the alternative strategy compared to the baseline (without vaccination).

7.3.4 Sensitivity analysis

We evaluated variation of the parameters with the greatest uncertainty: the contact rate C (proportion of MAP present in the pasture ingested by sheep through grazing), was the incidence calibrating parameter of unknown value and was varied from 10^{-7} to 1 to see the

effect on infection dynamics. We also evaluated plausible variations of MAP individual shedding rates and ψ (MAP survival on pasture).

7.4 Results

Similar to ‘the real world’ seasonal farm management of culling, replacement and lamb sales, the number of sheep in the four age groups fluctuated throughout the year. Results are shown at ‘equilibrium’ after 30 years of simulation. The flock size did not have any impact on the prevalence of infection or clinical incidence of disease in this deterministic model approach. Hence all results are expressed as a percentage of the number of lambing ewes (*i.e.* /100 ewes at lambing) and can be extrapolated to typical flock sizes of North Island hill country farms.

7.4.1 Infection dynamics

Environmental exposure to MAP (via the dose available/sheep) was driving levels of infection prevalence and incidence of clinical disease in the flock. According to findings in Chapter 6, the built-in dose-dependent plateau of infection influenced equilibrium prevalence by giving an upper limit.

For the ‘average’ scenario (0.2% annual clinical incidence), the daily exposure to MAP from grazing and the value of the corresponding plateau of infection are shown in Table 7-3. The daily dose of MAP ingested per animal depended on which paddock they were and on the relative amount of grass ingested for animals in different age groups (for lambs versus ewes that were kept in the same paddock). It ranged from a few hundred to a few thousand MAP organisms. The corresponding parameter value for the plateau of infection (Table 7-3) gives an idea of the theoretical upper limit for the prevalence of infection. It represents the prevalence that would be reached over time in this age group, if there were no demographic events. This theoretical cumulative prevalence of infection could not be above 72% in the ‘average OJD’ scenario.

Table 7-3: Annual range of daily exposure to MAP from grazing for each age group, and the corresponding values taken by the plateau of infection, for an annual clinical incidence of OJD of 0.2% (NZ national average)

	Lambs	Hoggets	Two-tooth	Ewes
Annual range of daily MAP dose ingested (#/sheep)	250-295	0.02-2641	2572-2902	835-1352
Annual range of values taken by the plateau of infection ¹ (%)	59-67%	41-72%	72%	66-68%

¹ The plateau of infection is a dose-dependent model parameter, representing the maximum proportion of sheep that could become actively infected upon ingesting a given dose of MAP, over time if all other conditions remained constant.

By limiting the prevalence of infection, the plateau of infection also limited the clinical incidence of OJD in the flock. The effect of the plateau on the infection dynamics can be seen by removing it (setting it to one), all other parameters held constant. The incidence of clinical disease in ewes was consequently doubled (0.39% instead of 0.2%).

7.4.2 Cost of OJD

The annual farm-gate net income corresponding to the baseline scenario in a farm free of paratuberculosis is presented in Table 7-4.

Table 7-4: Total annual farm-gate profit (in NZD/100 ewes) for a self-replacing North Island Hill country Romney flock at baseline (no paratuberculosis).

Farm gate profit /100 ewes:	Average prices (2013)	High prices (2011)
Sale prime lamb (NZD)	7757.7	10769.6
Sale mutton meat (NZD)	1275.6	1923.9
Sale fleece (NZD)	1487.6	1965.5
Purchase replacement (NZD)	0	0
Total (NZD)	10521	14659

Compared to this baseline, the loss of profit due to paratuberculosis in an average NZ flock (0.2% clinical incidence) would be about NZD 36 in an average year (up to NZD 53 in a year with particularly high meat price). This represents only 0.35% of farm-gate profit, hence negligible economic impact. The cost of OJD reached NZD 438 in an average year (up to NZD 590 for particularly high meat price) in a flock with annual clinical incidence of 2% in mixed-age ewes (Figure 7-4). This represents about 4% of potential annual farm gate revenue. The main economic impact of paratuberculosis was a decrease in sale of mutton carcasses attributable to higher OJD mortality (Figure 7-4).

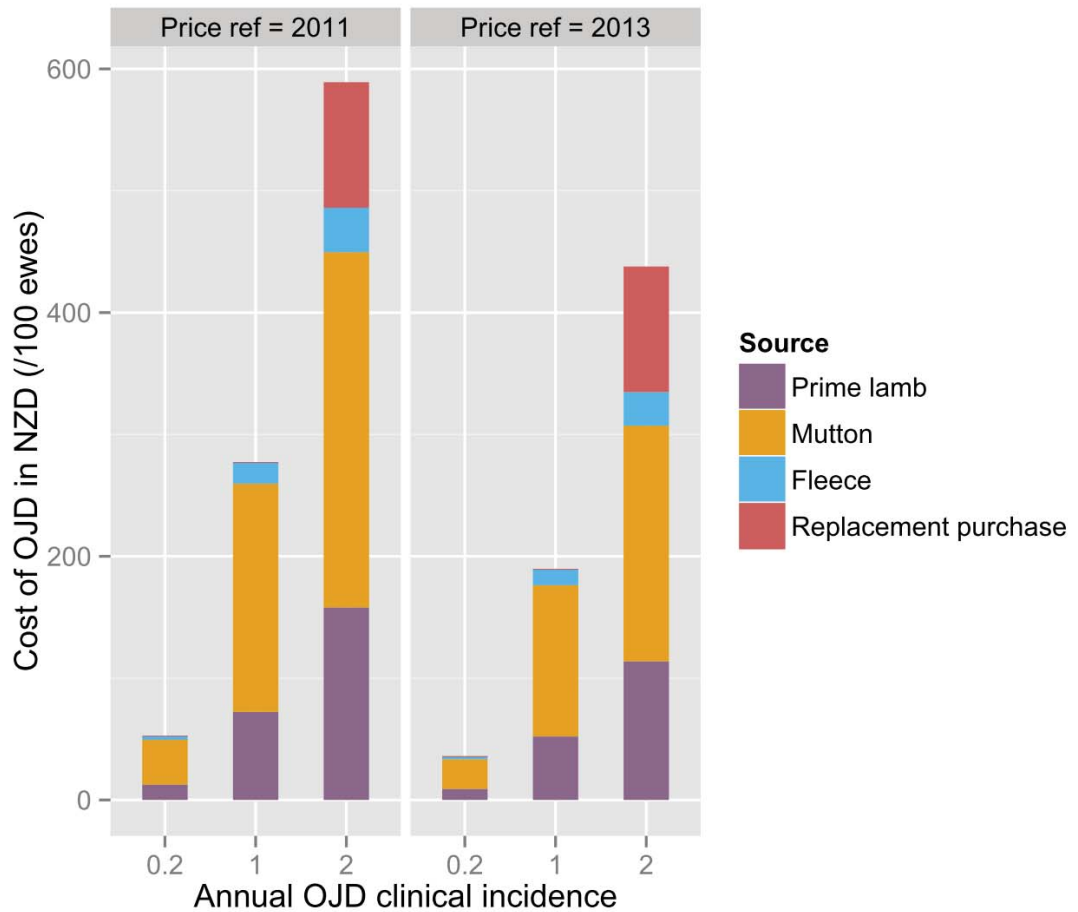


Figure 7-4: Loss in revenue due to paratuberculosis in the flock, in NZD/year/100 ewes, for different levels of clinical incidence and different reference years for farm-gate prices.

7.4.3 Vaccine effect

Starting with a clinical incidence of OJD corresponding to observations (pre-vaccination) in the vaccine efficacy trial flocks reported in (Reddacliff et al., 2006), we attempted to simulate the observed decrease in OJD mortality, using either a preventive or a therapeutic vaccine effect (Figure 7-2).

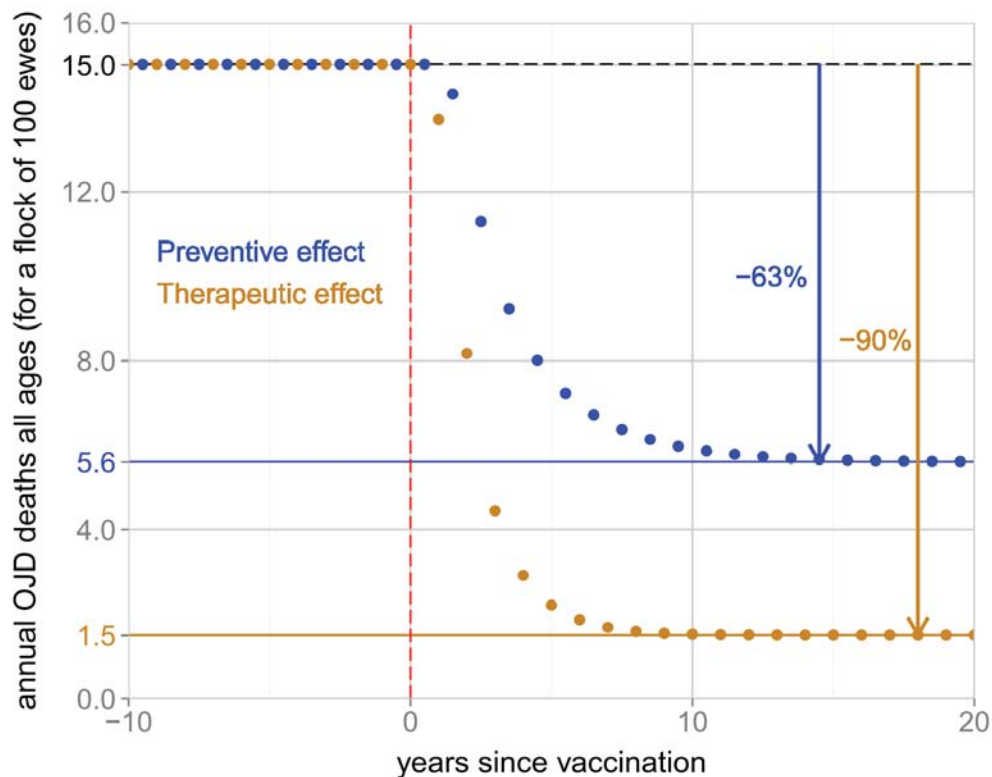


Figure 7-5: Simulation of Gudair™ trial conditions (Reddacliff et al., 2006) showing the effect of vaccine on the total number of OJD deaths in the flock (for 100 lambing ewes in the flock). Two possible vaccine effects were simulated (separately): a preventive vaccine effect (in blue) or a therapeutic effect (orange); the red dashed line represents onset of vaccination (whole flock).

A preventive vaccine effect only (preventing the entry into the progressor pathway upon infection) was compared to a therapeutic vaccine effect only (modifying the pathogenic pathway in sheep already infected) in Figure 7-2. Simulation showed that a preventive vaccine effect on mortality was smaller than a therapeutic effect. The maximum possible preventive effect (obtained by reducing χ to 0 in vaccinated sheep) allowed a decrease from 15 to 5.7 annual OJD deaths (62% decrease) (Figure 7-5). Despite the resulting overall reduction of MAP infection pressure in the flock, the preventive vaccination effect was limited since vaccination occurred at weaning when 50% of lambs were already infected. For animals already infected at weaning, the vaccine with preventive effect was not effective as it was assumed that vaccination had no effect on further progression. Conversely, using a therapeutic vaccine effect allowed the mortality level to drop: vac_{th} set to 0.0136 corresponded to a 90% decrease in mortality, as reported by the Gudair™ trial conditions (Figure 7-5).

With this parameter vac_{th} for the vaccine effect in our baseline model, OJD was not eradicated. Rather, a new equilibrium at a much lower level of clinical incidence was reached, even for low initial levels of clinical incidence in the flock. For example, for our scenario of very high clinical incidence of OJD (pre-vaccination), the total mortality due to OJD in the flock went from 5.2% to 0.77% at equilibrium after onset of vaccination, hence a decrease of 85%. On the other hand, the prevalence of infection (proportion of sheep ever infected, including recovered) decreased only very slightly (from 87.3 to 85.6%) since vaccination did not prevent infection *per se*. There was a decrease by a factor 10 order of magnitude in the total amount of MAP in the lambing/ewes paddock. Since MAP is highly infectious even at low doses, this decrease in overall contamination had a high impact on clinical incidence but not on prevalence of infection.

7.4.4 Cost-effectiveness of vaccination

Looking at a horizon of 30 years and using market meat prices corresponding to the average for the decade 2005-2015, a threshold around 1% of clinical incidence in the mixed-age ewes for vaccination cost-effectiveness is apparent (Figure 7-6). At 0.97% clinical OJD, at a 30 years horizon and for average meat prices, the cumulative benefit of vaccination becomes higher than the cumulative cost of vaccination (Figure 7-6 a.), hence the benefit-cost ratio became higher than one (Figure 7-6 b.) and a positive return on investment is achieved (Figure 7-6 c.). At this level of clinical incidence, break-even (when the annual net profit of vaccination becomes positive) was reached in 5 years (Figure 7-6 d.).

Around 1% clinical OJD in the ewe flock, the time frame for positive return on investment declined very rapidly: 30 years at 0.97% clinical OJD in the flock, 15 years at 1.1% OJD and 10 years at 1.27% (Figure 7-6). Higher meat prices than usual triggered better and faster economic return from vaccination.

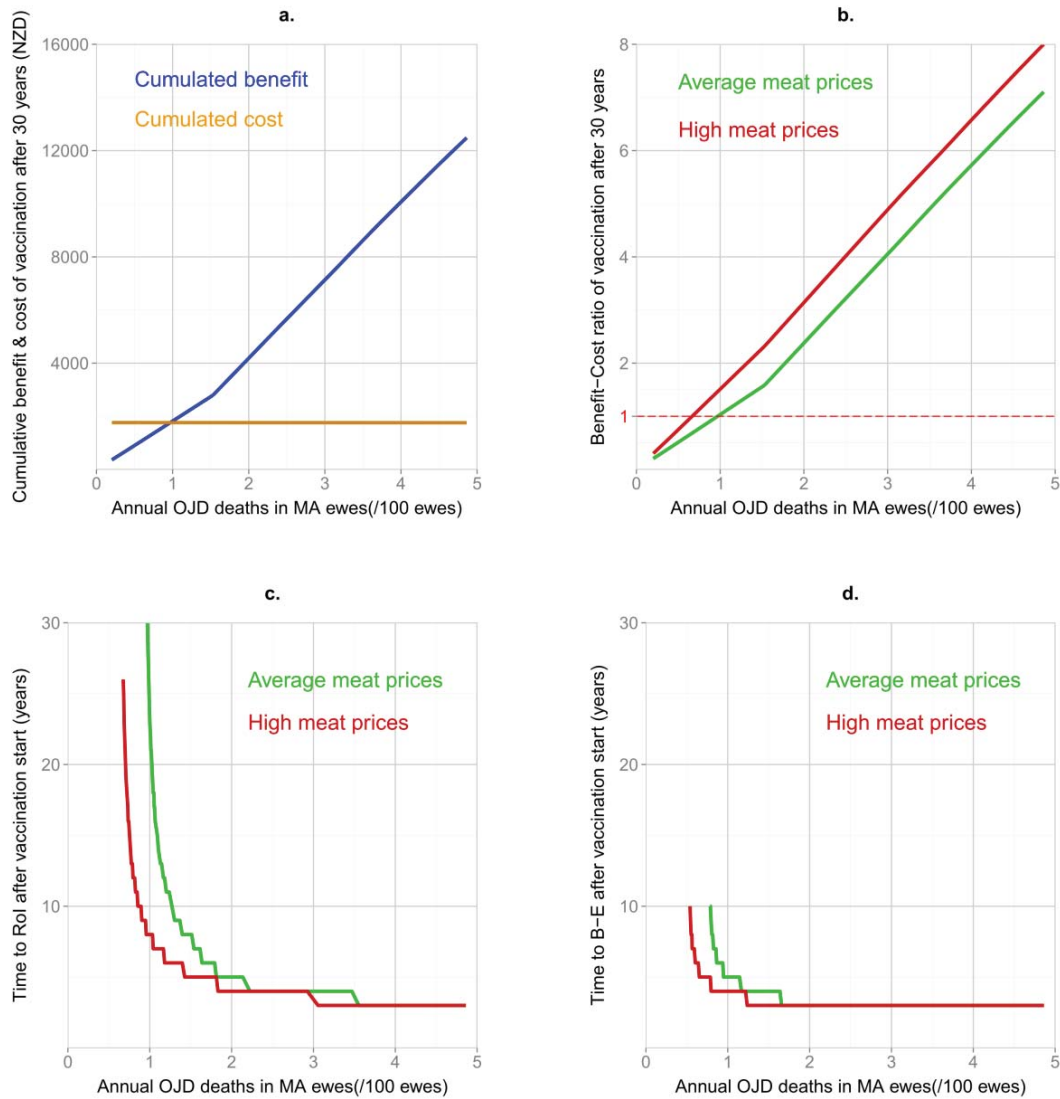


Figure 7-6: Cost-effectiveness of vaccination with varying levels of pre-vaccination OJD clinical incidence in the flock using present value (discounting rate 6%): a. cumulative benefit and cost of vaccination at equilibrium (30 years after vaccination start, for 100 ewes in the flock, with average meat prices), b. benefit-cost ratio of vaccination at equilibrium, c. time to return on investment (RoI) after onset of vaccination, d. time to break-even (B-E) after onset of vaccination.

Table 7-5 shows different measures of vaccination cost-effectiveness for different scenarios of clinical OJD incidence and farm gate prices. In a very high clinical incidence scenario (2% OJD in mixed age ewes) and using average meat prices, the cumulative net profit was NZD 2435 (present value, per 100 ewes) after 30 years of vaccination. For each dollar invested, 2.4 dollars were earned in return. After 30 years, the annual net profit of vaccination would be NZD 43.6 (/100 ewes) in an average year and NZD 65.4 in a year with high market prices.

Table 7-5: Cumulative net profit, Benefit cost ratio, time to return on investment (RoI) and time to break-even (B-E) for different scenario of levels of clinical incidence and meat price scenario

OJD Scenario	Price scenario	Annual net profit of vaccination (NZD/100 ewes)	Cumul. net profit of vaccination (NZD/100 ewes) ¹	Benefit-cost ratio ¹	Time to RoI (yrs)	Time to B-E (yrs)
Average CI (0.2% OJD):	Average price	-17.5	-1402	0.20	>30	>30
	High price	-13.9	-1234	0.30	>30	>30
High CI (1% OJD):	Average price	6.5	57.1	1.03	23	5
	High price	19.9	890	1.51	8	4
Very high CI(2% OJD):	Average price	43.6	2435	2.38	5	3
	High price	65.4	3779	3.15	4	3

¹ After 30 years of vaccination

7.4.5 Effect of purchasing infected stock

Here we modified the baseline scenario from a self-replacing flock to purchasing one uninfected pregnant two-tooth (/100 ewes) each year in the progressing stage (P) of OJD. The purchased two-tooth joined the mixed-age ewe flock at lambing. The alternative scenario of interest was then, by contrast, to purchase an infected ewe in the early progressor stage.

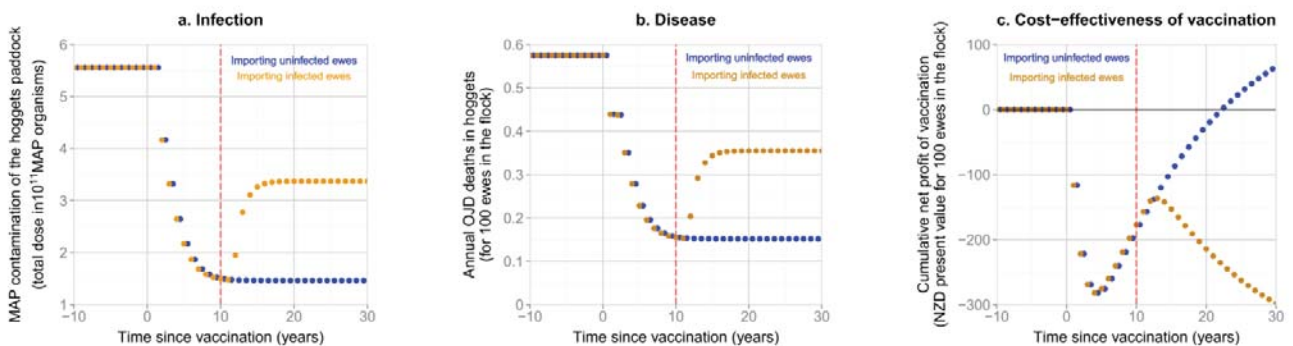


Figure 7-7: Effect of vaccination and purchase of ewes in a flock with high clinical incidence of OJD (1% in ewes pre-vaccination), in two different scenarios, describing (a.) MAP infection, (b.) OJD incidence level and (c.) cost-effectiveness of vaccination (using average market prices). The baseline scenario (in blue) was to purchase one uninfected ewe/100 ewes/year. The alternative scenario (in orange) was to purchase one infected ewe/100 ewes/year (in the P compartment) after the red dashed line.

Figure 7-7 shows the negative impact of importing one infected animal per year. The purchase affected the infection and disease dynamics in all age ewe groups, not only the ewe's flock receiving the purchased ewe. Direct and indirect effects resulted in higher overall farm contamination in all paddocks, and higher infection and disease equilibrium. The introduction of infected stock on the farm thus compromised the effectiveness and cost-effectiveness of vaccination, as can be seen in Figure 7-7 (c.) for a flock with high clinical incidence (1% annual OJD in ewes pre-vaccination). In this example, the cumulative net profit of vaccination after 30 years dropped from +NZD 69.2 to -NZD 298.5 upon importing one infected ewe/year, for each 100 ewes in the flock.

On the other hand, importing an infected ewe but in the non-progressor track (N instead of P) had very little impact (results not shown). The effect of importing a sheep in the early progressor track comes from increasing the overall contamination of the farm environment with MAP, due to high shedding occurring in the late stage of the progressor track.

7.4.6 Effect of changing the replacement rate and pasture spelling

Decreasing the replacement rate from 25 to 20% decreased the number of hoggets and two-tooths needed for replacement, hence the number of susceptible sheep becoming infected shedding and progressing to disease. The result was to decrease the overall MAP contamination and the impact of OJD on-farm (Figure 7-8 a. and b.). In scenarios with replacement rate of 20% (resp. 30%), annual OJD mortality in the ewe flock respectively decreased by 16% (resp. increased by 15%). Nevertheless, vaccination had a much stronger impact on infection and disease than changing the replacement rate to 20% or 30%. In combination with vaccination, both these scenarios had exactly the same effect as vaccination only on MAP contamination and OJD levels (can be seen in the blue curve in Figure 7-8 a. and b.).

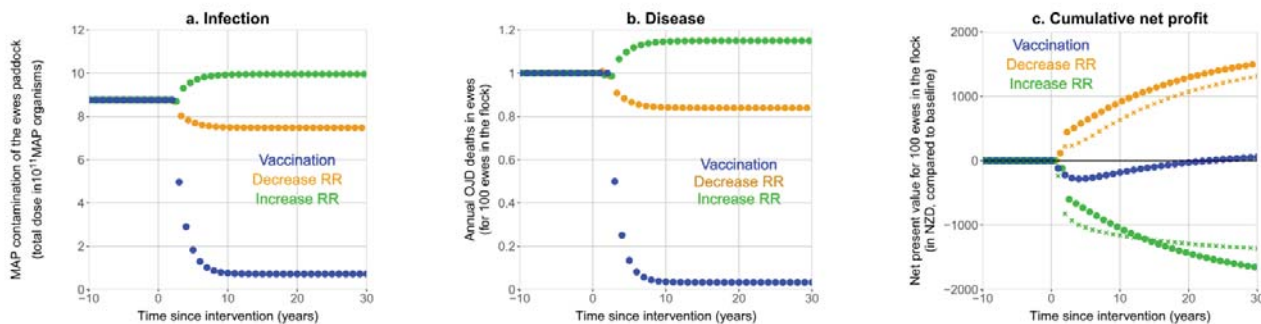


Figure 7-8: Effect of changing the replacement rate (RR) from 25 to 20% (in orange) or to 30% (in green) and vaccination (in blue) and in a flock with high clinical incidence of OJD (1% in ewes pre-intervention), describing (a.) MAP infection, (b.) OJD mortality and (c.) cumulative net profit of alternative strategy compared to the baseline (using average market prices). Crosses in plot c. represent combination of RR changes and vaccination. These are not shown in plot a. and b. as they are blended with the blue curve.

Decreasing the flock replacement rate was associated with much higher farm gate profit, due to an increase in the prime-lamb carcasses sold, irrespective of the improvement in the OJD farm status. Increasing the replacement rate has the opposite economic effect. This is reflected in Figure 7-8 c. In scenarios without vaccination, decreasing the replacement rate of 5% resulted in a cumulative net profit after 30 years of +NZD 1510 (net present value per 100 ewes in the flock), while increasing the replacement rate by 5% is associated with a cumulative

net profit of -NZD 1668 after 30 years. Hence, changing the flock replacement rate also influence the cost-effectiveness of vaccination (Figure 7-8 c.). The economic benefit (or cost) directly due to decreasing (or increasing) OJD in the flock cannot be derived using this simulation since the baseline economics in the flock changes when shifting scenarios for replacement rate, but was likely limited.

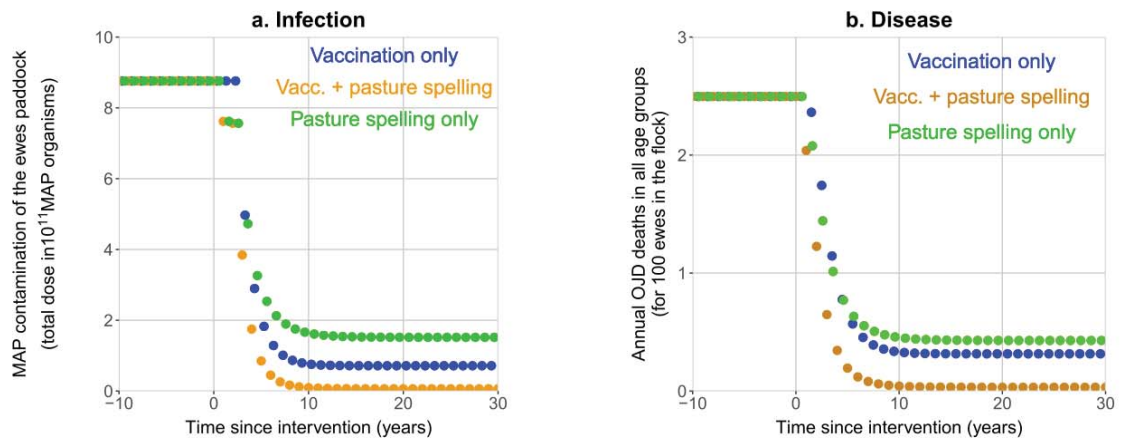


Figure 7-9: Effect of pasture spelling (in green) and vaccination (in blue) or both (in orange) in a flock with high clinical incidence of OJD (1% in ewes pre-intervention), describing (a.) MAP infection and (b.) OJD mortality.

Pasture spelling, even in the absence of vaccination, decreases the exposure of grazing sheep with MAP, hence driving the infection dynamics of MAP down (Figure 7-9 a.) and decreasing the impact of OJD on farm (Figure 7-9 b.). Combined with vaccination, it improves the outcomes of vaccination.

7.4.7 Sensitivity analysis

With the current parameterization, there was a difference of about 10^4 MAP organisms between shedding levels of low versus high shedding stages in the model. Thus, the dynamics of infection is driven almost entirely by super-shedders, despite the fact that low shedders shed during extended periods of time, and are many more in the flock. As a result, reducing the daily low-shedding rate from 2.4×10^6 MAP/day to 0 or multiplying it by 10 had very little effect on the infection prevalence and OJD incidence at equilibrium (results not shown). Similarly, a 10-fold increase of the high shedding rate had only a minor impact on the model outcomes, considering the magnitude of this parameter (8.3×10^{10} MAP/day). On the other hand, reducing the high shedding rate to the low shedding level (2.4×10^6 MAP/day) caused OJD to become almost extinct in the flock. For combinations of initial seeding dose of MAP on

pasture and contact rate C for which infection was sustainable, MAP load in the pasture reached very low equilibrium (oscillating around 10^7 - 10^8 total number of MAP in each pasture), but there were almost no clinical cases. Below a given threshold (combination of seeding level and C), MAP was not sustainable.

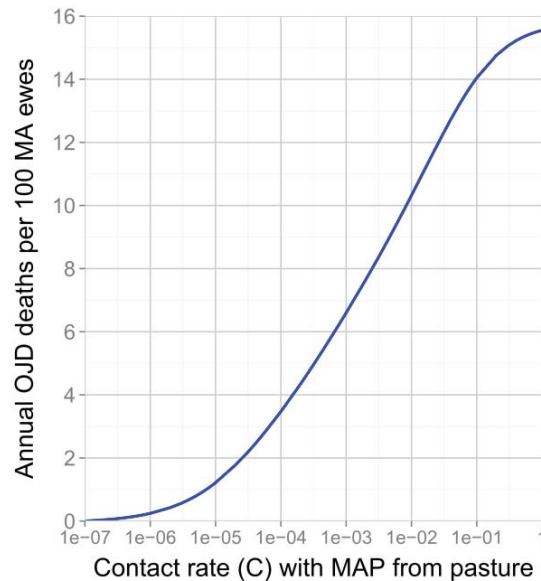


Figure 7-10: effect of contact rate C (proportion of MAP in pasture that is ingested by sheep through grazing) on the disease dynamics.

The effect of varying parameter C (proportion of MAP present on pasture ingested through grazing) is shown in Figure 7-10. Under the current parameterization, the model could simulate up to 16 OJD mortalities per 100 ewes per annum in the flock. Such a high level of clinical incidence is not plausible for New Zealand. On the other hand, for clinical incidences considered high in NZ (1 to 2%), the value of C suggests that the actual ratio of MAP available for ingestion was about 10 in 1 million of MAP organisms on pasture. The remaining MAP organisms on the ground would thus likely be unavailable for ingestion.

Varying parameter ψ (MAP decay rate in the environment) had the same effect as varying C (results not shown).

7.4.8 Model validation

Comparison of the main production outcomes obtained by the model and that from the industry obtained from national statistics are shown in Table 7-6. Figures from the industry were very close to the demographics of the model.

Table 7-6: lamb crop, comparison between industry figures and outcomes from the model (in an OJD-free flock)

	Industry figures	Model predictions
Ewe tailing percentage North Island ¹	129.5	133.7
Early drafting North Island, % of total ²	23.5	26.7

¹ Number of lambs tailed / number of ewes put to ram (2T and older),

² First quarter lamb processed between October and December, as a percentage of the total lamb processed for that year,

Ref: Beef and Lamb NZ, Lamb crop 2014-15 (ewe numbers from Statistics New Zealand, Beef + Lamb New Zealand Economic Service Lamb Crop Survey).

Field data were compiled in an earlier study (Chapter 4). They informed on the distribution of disease stages in flocks affected with OJD. Comparison of distributions obtained from the model and a summary of observational field data are shown in Table 7-7.

Table 7-7: Infection dynamics observed in the simulations (for various annual OJD levels and two age groups) compared to that of observational studies

		Prevalence of histo+ ² (%)	Prev. severe disease ³ (%)
1% OJD	MA ewes	8.2	0.9
	Two-tooths	46	2.1
2% OJD	MA ewes	10.5	1.8
	Two-tooths	52.5	4.4
5% OJD	MA ewes	19.3	4.4
	Two-tooths	67	12.9
Field experiments ¹ (average)		14	6
Field experiments ¹ (range)		3-87	1-54

¹ Ref: Chapter 4,

² Presence of histological lesions consistent with paratuberculosis, equivalent to model compartments N+P+A,

³ Presence of severe histological lesions of paratuberculosis, equivalent to model compartment A.

The distribution of various disease stages was within the range observed in Australian flocks with high clinical incidence (Chapter 4). The model was, however, unable to simulate values of the upper range of what was found in these field studies, in particular for the prevalence of severe lesions. The maximum in the scenarios simulated in Table 7-7 was 13% of sheep with severe lesions (in the two-tooth group in a flock with 5% OJD in mixed-age ewes), while the maximum observed in the Australian field studies was 54%.

Data on the age-distribution of clinical cases of paratuberculosis in a flock can be found in (Bush et al., 2006b; Reddacliff et al., 2006). These studies carried longitudinal follow-up and monitored the age of animals succumbing to OJD. They found approximately 75% of OJD mortality occurring in mixed-age ewes versus 25% occurring in sheep younger than two years

old. The former proportion was much lower in our model, with only around 40% of mortalities occurring after two years of age (variable depending on OJD incidence level).

7.5 Discussion

Our model incorporated well documented within-flock dynamics of MAP infection in sheep, as well as realistic seasonal demographics typical of self-replacing hill country sheep breeding farms in New Zealand.

According to our simulations, the vast majority of farms in NZ do not have an economic incentive to vaccinate against OJD. However, for farms with a high annual clinical incidence of OJD (1% and above) positive returns would start occurring within 5 years of vaccination and return on investment achieved in 23 years. However, MAP infection would not be eradicated from the farm in the simulated scenarios. The benefit of vaccination in high OJD incidence farms could be jeopardized by importing infected stock from other farms.

7.5.1 Dynamics of infection

Model parameters were based on a systematic review and a meta-analysis of experimental infection and disease expression in sheep (Chapter 6), rather than adapting models developed for cattle.

7.5.1.1 Modelling indirect transmission from the environment

Most models of paratuberculosis are based on dairy cows in intensive farming systems, thus primarily modelling direct transmission between animals. MAP bacteria can survive for up to 55 weeks in the farm environment (Whittington et al., 2004). In a pasture-based production system, most infections are therefore acquired from the environment.

We therefore modelled indirect transmission of MAP through pasture grazing which addresses infection dynamics in a pastoral environment, as in Humphry et al. (2006) for beef herds and Heuer et al. (2012) for deer. Hence, the equilibrium between MAP shedding, MAP survival on pasture and MAP consumption through grazing determined the level of MAP infection in the flock and subsequent disease outcomes. Our results highlight that MAP infection is sustainable in sheep flocks under pastoral conditions typical of NZ.

Based on experimental inoculation trials, we had evidenced estimates of the infectiousness and pathogenicity for a given dose of MAP after oral inoculation (Chapter 6). These

parameters, however, needed to be extrapolated for natural infection under NZ pastoral conditions.

However, it remains uncertain at a given a dose of live MAP in the environment, what proportion of this dose would actually be ingested through grazing (parameter C). By adjusting this parameter to reproduce the infection prevalence and OJD incidence observed in field studies, the model informed about the likely fraction of infectious MAP from the environment (*i.e.* 1:100,000 to 1:1,000,000). This parameter C can also represent a proxy for physical features of the pasture which can alter the dose of MAP available for the sheep. Such effects were described in epidemiology studies of farm-level PTB in sheep. Differences in soil type were an important explanatory factor for both herd-level PTB seropositivity in Spain (Reviriego et al., 2000) and levels of OJD mortalities in Australia (Lugton, 2004). Pasture quality was also associated with clinical expression of the disease with a high proportion of improved pasture being a risk factor (Lugton, 2004). The authors speculated that sheep might graze closer to the ground on improved pastures, actually increasing their probability of contact with MAP. Adjusting C to simulate various levels of OJD in the flock, as we did, might thus mimic such physical effects. It can also be used to simulate variations of the grazing management not currently represented in the model, such as pasture spelling or co-grazing of other susceptible species. The physical effect of such practice is a dilution of the MAP dose on pasture and therefore the contact rate between MAP on pasture and grazing sheep.

We modelled a fixed decay rate of MAP in the environment with a parameter estimate based on studies of MAP survival on pasture. MAP decay rates in the environment are essentially highly variable between locations and experiments (Whittington et al., 2004; Eppleston et al., 2014). The main explanation is an increased decay with increased maximum temperature of the soil surface (Whittington et al., 2004). In addition, the absence of shade causes a 14-fold increase of the hazard of a sheep strain of MAP to be inactivated (Eppleston et al., 2014). Other features likely to impact on MAP decay and survival are interactions with protozoa and insects, dormancy and the formation of biofilm and aerosol (Rowe and Grant, 2006). MAP decay can demonstrate substantial variation from one farm to the next. This in turn could account for a large part of the variation in the distribution of clinical OJD between farms. In view of the substantial variations and little justification in MAP environmental decay rates used in other paratuberculosis models with indirect transmission from the environment, we relied on decay rates measured from specific experiments (Table 7-1). However, NZ milder and more humid climatic conditions are likely more suitable for MAP survival compared to South Australia where these experiments were carried out. We further investigated this by varying ψ

in the sensitivity analysis. For a baseline at 1% clinical incidence in the flock, decreasing ψ 10-fold while keeping C constant shifted the annual OJD mortalities in ewes from 1% to 2.7%. Simultaneously, the load of MAP in the ewe paddock was about two \log_{10} units higher. In order to reach the same equilibrium as before (1% clinical incidence in ewes), C needed to be reduced about 10-fold (1 in 1,063,830 MAP ingested versus 1 in 138,889); infection dynamics in both scenarios were then exactly the same. In conclusion, the impact on infection dynamics was similar when varying C or the decay rate of MAP on pasture (ψ).

The calculation of feed intake from pasture was based on the proportion of grass (hence MAP) ingested by each sheep, simply dividing the total amount of available MAP in the pasture by the total number of sheep present. We compared our method with an alternative calculation adapted from former PTB modelling work explicitly modelling the dry matter intake and grass growth (Heuer et al., 2012). Both methods were equivalent as they both assumed that available pasture was equivalent to feed requirements, and yielded very similar simulation outcomes (results not shown). Epidemiological studies of ovine PTB at the flock-level confirmed this approach. They found that flock level sero-positivity to PTB (Reviriego et al., 2000) as well as clinical incidence/PTB mortalities (Lugton, 2004) were independent of stocking density.

We seeded infection in the flock using an initial load of MAP in the ewe paddock (2×10^{12} MAP in total). For a fixed contact rate C, a threshold existed for initial MAP paddock contamination, below which infection in the flock waned off. This indicates that naïve flocks need a minimum environmental MAP contamination to establish endemic infection. Additionally, infection is likely to disappear in very low prevalence flocks under field conditions. However, we simulated seeding infection with a single high shedder in a flock of one million ewes which triggered an endemic equilibrium. This clearly emphasizes the predominant role of trade not just to sustain infection in a flock, but also to seed a new infection in a healthy flock. However, it should be noted that for small flock sizes, stochasticity might not allow infection to settle in a flock in most instances.

The model also included a 'plateau of infection' limiting the force of infection for a given exposure dose to MAP. The effect was an important limiting feedback on MAP levels and OJD incidence, biologically plausible and thus reflecting more realistically the within-flock dynamics.

7.5.1.2 Technical limitations

We used a deterministic compartmental model based on ODE, with inherent limitations. Firstly, it does not model entire individual sheep, but rather daily averaged transitions from one compartment to another with sheep considered as a continuous quantity. Moreover, it does not take into account the variability inherent to realisation of biological phenomenon (stochasticity). Hence our deterministic model was biased towards continued sustenance of MAP when fadeout could occur by chance in the real world, *e.g.* for small flocks. Secondly, standard compartmental models assume constant transmission rates, which may not be realistic for chronic infections. We showed in Chapter 6 that the onset rate of active infection after inoculation (which in effect corresponds to the rate of exit from latent infection) was better fitted with a simple Weibull distribution allowing the rate to increase over time. The Weibull rate is a naturally plausible model for the exhaustion over time leading to generalised failure of immune control, classically described as a switch effect (Koets and Gröhn, 2015). We, however, approximated this by using a constant rate (exponential distribution).

Finally, the infection rate in the model we presented depended on the dose of MAP that sheep were exposed to. Each update only depended on the previous iterations: this ‘*memoryless*’ feature prevented modelling a cumulative dose effect for each sheep over time. The total exposure time to MAP was not taken into account. Not accounting for past MAP exposure beyond one time step may or may not be a reasonable proxy. In the real-world, chronic exposure to MAP might either overcome host defences, or conversely could contribute to development of immunity. These scenarios could not be investigated in the meta-analysis (Chapter 6). Hence it would be difficult to incorporate such effects without data to validate resulting outcomes.

Adopting an individual-based, stochastic model instead of this compartmental deterministic model would address the aforementioned technical limitations, by (1) explicitly modelling individual sheep and keeping track of time and (2) modelling stochastic noise. This could be the object for future work.

7.5.2 Flock demographics

The demographic structure of the model reflected realistic seasonal management of the sheep flock, resulting in fluctuation of the population size. A model with constant population size would be too constrained. In addition, the proposed population structure was well suited for detailed evaluation of production outcomes and economics.

The selective culling of ewes was modelled to achieve a 25% replacement rate in a paratuberculosis-free flock with natural mortality of 8% per year. In this scenario, 17 ewes (for 100 ewes present at lambing) are thus 'available' for selective culling due to failure to conceive, failure to rear a lamb, old age, bad teeth or poor condition. We tried two modelling options for the culling of these 17 ewes: (1) a fixed proportion (*i.e.* removing a proportion x of the remaining ewes in the flock (N) on the culling day, equal to $n=17$ ewes in a paratuberculosis-free flock), or (2) a fixed number (*i.e.* removing $n=17$ ewes on the culling day). In a flock with extra-mortalities due to OJD, the actual ewe turnover increases and the replacement rate then exceeds 25%. In such a flock with OJD N is smaller at any point in time compared to a paratuberculosis-free flock. Hence using option 1, n (number of ewes culled= $x*N$) becomes less than 17 in case of extra-OJD mortality, representing a 'self-adjustment' of selective culling to increased OJD mortality in the flock. Alternatively, with option 2 the number of culled ewes is always 17 irrespective of OJD mortality levels. The economic impact of OJD (via increased ewe turn-over) is therefore stronger using option 2 compared to option 1. This illustrates the fact that selling slightly fewer carcasses is a recommended strategy to avoid purchasing replacing ewes. It also diminishes the risk of purchasing potentially infected animals. Management decisions and the way they are modelled affect economic outputs of the model to an extent similar to simulated control strategies, highlighting that results in the form of absolute figures cannot be generalised to all sheep farms. All our simulation results were based on option 1.

7.5.3 Model validation

Our model simulated different levels of severity of OJD similar to the range observed in New Zealand (Verdugo, 2013). The production outcomes from the model were close to industry statistics about lamb harvest and reproductive performance (Table 7-6). Infection dynamics were within the range of field observations (Table 7-7). However, the model could not simulate the high extremum reported in the literature, such as 87% of sheep in the flock presenting histological lesions and 54% of sheep presenting severe lesions. These figures are extremely high and it is possible that the sheep in these field studies were in fact not selected at random and represented a population affected by the disease. In any case, such high figures are not plausible for NZ sheep flocks.

Unlike field observations, the clinical incidence of OJD in the model had a peak in young animals (hoggets/two-tooth), with only about 40% of total OJD mortality occurring in adult ewes. Field experiments in which OJD mortalities were monitored in all age groups across

several years indicate that mortalities of mixed-age ewes made up around 75% of all OJD mortalities in the flock (Bush et al., 2006a; Reddacliff et al., 2006). These experimental data were obtained from only two studies and pertained to commercial Merino flocks in Australia, hence different conditions. Nevertheless it suggests that the distribution of mortality observed in our simulations may be somewhat skewed.

According to our simulations, a high proportion of animals were exposed to MAP on pasture from birth, hence became infected before weaning. For sheep in the progressor track, the time to clinical disease thus depended on parameter δ (median time to progression of 405 days). Clinical cases died relatively quickly (median time of 7.4 months according to rate μ_c). Hence, a possible reason for an early peak of clinical disease was an overestimate of the progression parameter δ on the basis of experimental infections if progression was faster after artificial than natural challenge. However, our δ estimate compares favourably to that obtained by analysing serial biopsy data from naturally infected sheep (Dennis et al., 2010). Therefore the δ parameter estimated from experimental infection appeared to be a reasonable proxy for natural infection.

Another possible explanation is that our current model assumed that recovered sheep were not susceptible to new infection. An alternative would be to allow them to become infected again in the face of ongoing challenge. The effect of this would be to shift the age distribution of clinical cases towards older animals. The basis for the current model assumptions and parametrization came from experimental studies where sheep were only dosed once at the beginning of the study. Thus, there was no evidence from which to derive parameters for re-infection after recovery, hence this could not be considered in the model. The assumption that recovered sheep were not susceptible to new infection might not be realistic in a farming environment where ongoing challenge occurs throughout life. The meta-analysis results (Chapter 6) show unambiguously that adult sheep are as susceptible to MAP infection as are lambs. Preventing recovered animals to become infected again assumes that MAP infection results in a life-long immunisation. We are not aware of any evidence justifying that assumption. In the face of ongoing challenge with MAP, recovered sheep might become susceptible again after some period of time as cell-mediated immunity wanes off and/or due to an overwhelming infection pressure. Considering a time-varying infection rate starting low and increasing over time (discussed above) might also contribute to a more realistic age distribution of mortality.

Future modelling of ovine paratuberculosis could incorporate such modifications to make the age-dependent mortality distribution resemble field observations better. This might have an impact on the estimated cost-benefit of vaccination. If the proportion of OJD mortality occurring in ewes is more than the assumed 40% in our model, the total cost of OJD for a fixed level of clinical incidence in ewes would have been overestimated, hence overestimating the cost-benefit of vaccination.

7.5.4 Interventions to control OJD

7.5.4.1 Vaccination

Simulation modelling of the cost-effectiveness of OJD vaccination in sheep flocks, although rare, is not novel; Vaccination was deemed cost-effective by Juste and Casal (1993) and Bush et al. (2008) using spreadsheet models. In addition to reducing the incidence of clinical OJD, vaccination triggers a reduction in the number of shedders and consequently the overall MAP contamination. However, it does not totally eliminate either shedding nor high-shedding (Reddacliff 2004). Vaccination is therefore ineffective to eradicate MAP infection (Fridriksdottir et al., 2000; Dhand et al., 2016). Eradication is not a realistic goal for control because MAP persists in the environment. Instead, the focus of control should be on reducing the cost due to clinical disease, mortality and the associated production limiting effects (Juste and Perez, 2011).

7.5.4.1.1 Vaccine efficacy

To model the efficacy of Gudair™, we used observations from a field randomised controlled vaccine efficacy trial conducted in three heavily infected flocks with high mortalities (Reddacliff et al., 2006). Vaccinated and control sheep were run together on the same pasture, hence potentially causing an underestimation of vaccine efficacy. However, heavy MAP challenge was ensured throughout the study by retaining ewes affected by paratuberculosis and co-grazing them with the trial flock. Main results were a 90% decrease in mortality and shedding. However, severe disease and high shedding remained possible in vaccinated sheep. Subsequent observational studies tested additional assumptions about vaccine efficacy and confirmed the initial findings. Analysis from a convenient sample of 37 sheep flocks in New South Wales (NSW) Australia estimated the median individual-level shedding prevalence to have decreased from 2.72 to 0.72 in five years after the onset of vaccination (Dhand et al., 2013). This 73% decrease in the prevalence of shedders was observed in sheep flocks representative of the population of farms in NSW, with a low average pre-vaccination

prevalence. It suggests that vaccination has a strong protective impact on moderately as well as heavily infected flocks. However, 30 out of 37 flocks were still shedding after five years of vaccination with four flocks having above 2% post-vaccination prevalence and one above 5%. This suggests that vaccine efficacy varies between flocks and further confirms that it does not suppress shedding. To evaluate specifically the effect of initial prevalence levels, a longitudinal study was conducted in 12 flocks with low, medium or high initial paratuberculosis mortality pre-vaccination, which were then followed for over a decade after onset of vaccination (Dhand et al., 2016). The study, closing one decade of research on Gudair™, mostly confirmed findings from the vaccine efficacy study reported in Reddacliff et al. (2006). The effect of vaccination did not appear to depend on the initial within-flock prevalence. On average, the within-flock prevalence of shedders dropped by 98%. However, there was variation between flocks and shedding, although markedly decreased, was not eradicated. Persistence of detectable shedding existed in 3 out of the 8 flocks still enrolled at the end of the study despite 10 years of sustained vaccination. We simulated vaccine efficacy in our model based on the results observed in the initial vaccine efficacy trial (Reddacliff et al., 2006), in line with findings of subsequent studies. Using this, our simulations concur with the field observations of Dhand et al. (2016) that MAP shedding persists over ten years after the onset of vaccination and that MAP eradication is not achieved by vaccination (Fridriksdottir et al., 2000).

7.5.4.1.2 Preventive versus therapeutic vaccine effect

The recommendation for Gudair™ vaccination is to vaccinate lambs at docking or at weaning (replacements only). The rationale for early vaccination is to prevent infection. However, it is likely that lambs in a contaminated environment or born from shedding ewes are exposed to MAP in a matter of days if not hours post-partum, hence preventing infection may not be realistic.

As highlighted by Juste and Perez (2011), “the real goal of vaccination is to prevent clinical cases, which is achieved by modifying the course of pathogenesis of the disease rather than preventing infection and colonization in the animal”. In that respect, our simulations showed that a preventive effect of vaccination (preventing the entrance in the progressor track in vaccinated sheep) was not compatible with field observations about vaccine efficacy when animals were vaccinated at weaning. Instead, a therapeutic effect of the vaccine (switching sheep already infected from the progressor to the non-progressor track) was more compatible with the observed high vaccine efficacy in reducing OJD mortalities. This is in line with current research assumptions that vaccination in sheep “modifies the immunopathologic processes”

leading to clinical disease, so that vaccinated sheep “are able to arrest the progression of the infection and the ensuing lesions” (Juste and Perez, 2011).

Additional anecdotal observations from a heavily infected flock of over 8000 sheep in Australia suggests that vaccinating 3 month-old weaners or 8 month-old hoggets appeared to have a similar effect. In another trial however, vaccination of two year-old sheep had a limited impact on reducing mortalities while still limiting the prevalence of shedders (Windsor, 2006a). The authors noted that adequate vaccine efficacy in weaners was achieved despite intensive exposure since birth. Collectively these observations, like our simulations, corroborate a therapeutic effect of the vaccine.

7.5.4.1.3 Cost-effectiveness of vaccination

Annual clinical OJD incidence observed in sheep flocks in NZ is typically low (2-3 per 1000; Verdugo (2013)). Our simulations highlighted that at this level of incidence, the cost of OJD was negligible (around 0.3% of potential farm-gate revenue). Hence a majority of farms in this country may not benefit economically from vaccination. However, in farms with 2% annual OJD levels, economic losses due to OJD could reach over NZD 500/100 ewes. Hence, for this minority of flocks with high to very high clinical incidence, vaccination is an effective and cost-effective means of OJD control.

For farms with OJD mortality of 1% and above (in mixed age ewes), vaccination was cost-effective at an horizon of 30 years and the time to return on investment rapidly decreased, being of 10 years post vaccination at a clinical incidence level of 1.27%. The annual net profit from vaccination fluctuated with meat price and could reach up to NZD 65 (present value) for every 100 ewes in a flock with very high OJD (2%). In the latter, a positive return of 2.4 dollars for every dollar invested in vaccination was achieved in 30 years (using average meat prices).

Vaccination was simulated at weaning, a convenient management practice as the lambs are then being drafted manually. It also allows vaccinating selected replacement hoggets only, compared to costly blanket vaccination at docking. An additional benefit of vaccinating replacements only is the absence of injection site lesions in prime-lamb carcasses. For these reasons it is the method recommended by the vaccine supplier and the baseline for all our simulations.

A breach to the vaccination scenario, such as failure to vaccinate in one given year or vaccinating only some of the replacement lambs delayed the time to return on investment (results not shown). This is in line with evidence from the field in Australia that keeping cohorts

of unvaccinated Merino wethers into their second year of age increases MAP shedding in the flock and therefore pasture contamination (Eppleston et al., 2011). Our simulations show that OJD vaccination often requires several decades before the farmer could see an economic return on investment. Moreover, vaccination does not eradicate infection. This advocates for long-term commitment to an OJD vaccination programme - some even suggest permanent (Juste and Perez, 2011).

A previous spreadsheet model suggested that vaccination was highly cost-effective at controlling paratuberculosis whereas test-and-cull was not (Juste and Casal, 1993).

More recently, another spreadsheet model was used to simulate more detailed financial impact of OJD in Australian sheep farms (Bush et al., 2008). This model used a farm-level gross margin approach, but incorporated essential demographics and production outcomes as well as data on age-dependent OJD. The financial evaluation was detailed, included the cost of animal husbandry practices, and discounted cost and benefits. The model investigated break-even times after vaccination onset for a range of different sheep production systems. Although the financial modelling was specific to Australian Merino and Merino-crosses production systems, results obtained were compatible with our results. In particular, break-even in flocks with over 3% clinical incidence (corresponding to 'very high incidence' scenario in our model) was reached in 3 years in cross-Merino operations and 10 years in pure Merino operations, versus 3-4 years with our model. They also predicted earlier break-even in farms with higher OJD mortality. The model was based solely on the financial impact of OJD mortality. The dynamics of paratuberculosis in the flock was not modelled, curtailing the possibility to model the biological effect of various control strategies as we did in this work. In addition to OJD mortality, our model considered sub-clinical effects and indirect OJD effects, in particular around the management of replacement ewes in response to OJD. In a high incidence scenario, the margin of extra replacement hoggets to compensate animals lost to OJD was consumed, so the farmer had to purchase extra replacement stock to keep the flock size constant. If purchase of extra replacements were not allowed, a high OJD incidence in the flock would result in destocking below a few percent of the target flock size, resulting in a lower lamb crop. In that case the financial impact of OJD would be far greater than presented in this work (results not shown). These findings demonstrate that management practices have crucial consequences on the impact of OJD beyond losses attributable to OJD mortality alone. These effects were explicitly taken into account in the demographics part of our model.

Finally, our analysis of the value of vaccination was based on purely economic grounds. Other factors, such as animal welfare and emotional consequences of seeing sheep with OJD might play a role in farmer's decisions about whether or not to vaccinate.

7.5.4.2 Biosecurity

Previous work has shown that commercial livestock trade networks in NZ are structurally prone to disease spread between farms (Marquetoux et al., 2016b). Moreover, livestock movements between farms in the past four years were a specific risk factor for harbouring common strains of MAP on farm: livestock trade is a risk for introducing and maintaining MAP infection on farm (Marquetoux et al., 2016a). Our approach integrates within- and between-farm spread of MAP to quantify the effect of sheep trade.

In open flocks, results showed that replacing 1% of the mixed-age ewe flock with purchased ewes shedding MAP (in the progressor track) was detrimental to OJD control, and jeopardized the cost-effectiveness of vaccination. This was the case in farms close to the vaccine "cost-effectiveness threshold" of 1% clinical incidence in ewes, for which the net present benefit of vaccination turned negative upon purchasing infected ewes (Figure 7-7). For farms with very high clinical incidence (2%), the averted loss due to vaccination was overwhelming and vaccination was always cost-effective.

This is in line with observations from the field in Australia, where purchasing unvaccinated sheep was a risk factor for increased OJD levels on vaccinating farms (Windsor, 2013). These results are to be considered by farmers when implementing control of OJD. Indeed, our simulations showed that ongoing introduction of infected sheep could jeopardize the effectiveness and cost-effectiveness of vaccination on some flocks, or at least considerably decrease the return from vaccination. Farmers tend to worry about vaccine efficacy, as indicated by low vaccination uptake in NZ even on high OJD farms. We conclude that biosecurity can have substantial impact on the dynamics of disease, an effect of which farmers may often be unaware.

Currently, due to MAP persistence in the environment, poor biosecurity and in the absence of a certification scheme, controlling the spread at local, regional or national level appears difficult.

7.5.4.3 Alternative management strategies

All management decisions have an impact on the infection/disease dynamics. Unlike previous models, our model allowed exploring the impact of different management practices on OJD.

Measures resulting in lower numbers of young sheep on the farm (for example lower replacement rate) were associated with lower OJD mortality. This effect was due to a smaller number of susceptible weaned lambs retained in the flock, thus reducing the number of infected/disease progressors. Such changes in management also have a strong impact on farm gate profit irrespective of OJD. Compared to the baseline replacement rate of 25%, a 5% reduction in the replacement rate resulted in a cumulative net profit of NZD 1510 (per 100 ewes) after 30 years, due mostly to more prime lamb carcasses sold/year in addition to lower levels of OJD in the flock (Figure 7-8). On the contrary, increasing the replacement rate of 5% had the opposite effect. This shows the overall benefit of improving the flock longevity, both on farm gate profit and on OJD outcomes in the flock. However, these economic results do not take into account the costs associated with changing the replacement rate. For example, reducing the ewe turn-over requires an investment to improve the general flock health and productivity.

Our simulations also showed that decreasing the contact between sheep and MAP from the pasture (mimicking the spelling of pasture by rotational grazing as an alternative to set-stocking) reduced the impact of OJD on farm. This was displayed in Figure 7-9 for illustrative purposes only, since this simulation is the result of dividing the contact rate C by ten to mimic pasture spelling, which was arbitrary. For this reason we did not perform a net profit analysis.

These results illustrate how management decisions, seemingly independent of OJD, can have a strong impact on (1) the infection dynamics and OJD levels and (2) farm gate profits, hence also can influence the cost-effectiveness of vaccination. Hence such management decisions should not be taken independently of the PTB status of the farm, when OJD control is a farming objective.

No clear effect of breed on the susceptibility to OJD could be detected from experimental observations (Chapter 6), although field observations suggest that Merino are more susceptible to OJD than other breeds (Morris et al., 2006). Based on our simulations, we propose that the observed increased susceptibility to disease in Merino may be mostly due to differences in management. In particular, Merino breeders keep a much higher proportion of young sheep (post-weaning) on the farm to be shorn, compared to Romney flocks. Our simulations suggested that this could lead to higher OJD incidence levels. Such management differences could be as important in differences observed in the field as an inherent susceptibility of Merino to OJD.

Climatic stress, pasture availability, market prices and management of higher impact diseases probably have a stronger impact on economic returns of sheep farming than OJD. However, general management practices, such as biosecurity, grazing, and seasonal culling can have a strong impact on OJD, perhaps to the extent that vaccination may lose its cost efficiency.

7.6 Conclusion

We developed a model to study ovine paratuberculosis in NZ pastoral sheep farms, driven by indirect transmission through the environment. The infection dynamics part of the model was based on a systematic literature review and a meta-analysis of pathogenesis of ovine paratuberculosis. We therefore believe the parametrization was robust. The model also resembled typical demographics of New Zealand sheep flocks and adequately simulated the seasonal management system of Romney farms. To our knowledge, this was unprecedented.

The cost of OJD on an average NZ sheep farms with an annual clinical incidence of 0.2% in ewes was negligible. We evaluated the control of OJD in NZ sheep farms using Gudair™ vaccination and explored plausible biological effects of the vaccine. Our simulations suggested that preventing progression to OJD was not sufficient to reduce OJD while a cure from sub-clinical disease compared more favourably with field observations about vaccine efficacy. Farms with high clinical incidence (above 1% annual OJD mortality in mixed-age ewes) would benefit financially from vaccination. At this level of OJD incidence, the model predicted a foreseeable positive return, after 23 years. Above 1% incidence of OJD, the time to return on investment quickly dropped. For farms with very high clinical incidence of OJD (2% annual mortality in ewes), the benefit-cost ratio after 30 years was 2.4. Fluctuations of market prices, however, had a strong impact on the cost-effectiveness of vaccination, at least in the short term. Moreover, breaches in biosecurity appeared to play an important role in MAP dynamics, influenced the effectiveness of vaccination and impacted on the farm economic performance. Importing only one infected ewe per 100 ewes each year was sufficient to jeopardize the cost-effectiveness of vaccination for farms close to the threshold incidence for cost-effectiveness (1% OJD mortality in ewes). Self-replacing flocks are therefore better candidates to implement control of OJD by vaccination.

7.7 Acknowledgements

This study was funded by the New Zealand Johne's Disease Research Consortium and Landcorp Farming Ltd. Stipends were granted by Massey University and New Zealand International Doctoral Research Scholarship.

Chapter 8. General discussion

This general discussion brings together the context of this thesis, presents a critique of content and methods, a proposal for future research, and ends with concluding comments.

This work was about understanding the transmission of MAP in livestock populations, particularly sheep, in New Zealand. Transmission is driven by the specific epidemiological context of livestock industries in this country, in particular pasture-based seasonal farming, and a high frequency of livestock traffic between farms.

This thesis encompasses consideration of MAP infection dynamics from the individual-sheep level through to the level of the meta-population of farms, with dynamics within a flock at the intermediate level. Key aspects were:

- (1) Producing evidence of between-farm transmission of MAP via livestock movement;
- (2) Producing a synthesis of MAP infection dynamics and pathogenesis in individual sheep using existing data, mostly experimental;
- (3) Using findings from the above to simulate ovine paratuberculosis in a typical commercial New Zealand sheep farm and draw inferences about the epidemiology, the economics and the control of ovine paratuberculosis.

Overall, OJD has a low impact in New Zealand, with only half of infected farms reporting clinical disease. The clinical incidence 95% quantile ranges from 0.09% to 0.24% (average 0.16%, Verdugo (2013)). Nevertheless, some farms are more impacted than others. Currently there is limited robust evaluation of the economic cost of OJD and its control. One aim of this work was therefore to integrate the within-farm and between-farms transmission with OJD economics, to provide guidance for on-farm control in farms highly exposed to OJD in New Zealand. Our inferences about the epidemiology of paratuberculosis might nevertheless be relevant to contexts other than New Zealand.

8.1 Overview of results

The pattern of livestock movement in New Zealand presents specific features inherent to seasonal pastoral farming systems, which favour the spread of infectious diseases in general. This was analysed in Chapter 2, identifying in particular small-world features and strong

positive correlations between movements in and out of a farm that were particularly favourable to disease spread. We identified hub farms playing a central role in this network. Targeting those farms for risk-based movement control was efficient to decrease the potential for pathogen transmission, by cutting the network into smaller, more isolated clusters.

The next step was to assess if the livestock contact pattern between farms might actually play a role in the transmission of paratuberculosis. Chapter 3 merged aspects of molecular epidemiology and social network analysis to assess the specific risk of MAP transmission between farms in the New Zealand context. By using specific methodology adapted to dependent observations, *i.e.* a problem of matrices correlations, we were able to show robust associations between cross-sectional strain type distribution on-farm and past livestock movement. These results strongly support the role of livestock movement in spreading MAP between farms, suggesting that strains of MAP can establish in a flock following the introduction of infected animals. However, this conclusion is based upon observational, cross-sectional data and thus shows associations rather than evidence of causation, although the associations are biologically plausible.

For the purpose of building a mathematical model of ovine paratuberculosis, we established the current understanding of patho-physiology of ovine paratuberculosis in Chapter 4. We identified relevant infection stages and synthesized this information to build the compartmental model structure. Further, we carried a review of enumeration methods of MAP *in vitro*, aiming to guide the interpretation and comparison of inoculum dose in experimental infection models (Chapter 5). We were able to generate important assumptions about patho-physiology of paratuberculosis and possible biases associated with experimental infection. The review of literature was initially meant to estimate parameters for the mathematical model. However, we were confronted with the shortcomings of the review process, precluding robust quantitative parameter estimations directly from this review.

The shortcomings above mentioned prompted us to carry out a systematic review and meta-analysis (Chapter 6) in addition to the narrative reviews in Chapters 4 and 5. This allowed us to test hypotheses generated in Chapter 4 while taking into account findings in Chapter 5, thus precisising the effect of MAP exposure dose, age at exposure, strain type and sheep breed. The meta-analysis was also used to quantitatively estimate important parameters for the model of ovine paratuberculosis, while adjusting for study-level confounding.

We then merged the findings of all previous chapters in an exercise of modelling ovine paratuberculosis in a pastoral sheep farm typical of New Zealand (Chapter 7). This model

incorporated up-to-date science on infection dynamics, with robust parameters reflecting the patho-physiology of ovine paratuberculosis, indirect transmission from pasture, and realistic demographics with typical seasonal management. Conclusions could thus be drawn about infection dynamics, cost of ovine paratuberculosis, biological effectiveness and cost-effectiveness of vaccination and the impact of movements of animals between farms, tailored for New Zealand sheep farming.

8.2 Farm-to-farm transmission of paratuberculosis (Chapters 2 and 3)

This aspect has not been formally assessed prior to this work. Both our methods and inferences represent a novelty in the field. In these studies we used social network analysis of livestock movements merged with molecular epidemiology to explore the role of livestock movements as a risk factor for disease spread in general, MAP spread in particular.

8.2.1 Assessing the impact of livestock movements on MAP spread

Infection with MAP is highly endemic in New Zealand, with about 80% of sheep flocks in New Zealand infected with MAP (Verdugo et al., 2014a). It would seem difficult to infer farm-to-farm spread of MAP when nearly all farms are infected. However, we added another layer of epidemiological information with strain typing of farm isolates, which enabled us to seek associations between livestock movements and MAP strain type distribution. Hence, even in this context of high endemicity, it was notable that the data clearly suggested that farms clustered in the livestock movements were more likely to share the same strains of MAP.

This could also be explained by the fact that the studied network of farms was densely connected, with a total of 1.15 million head of livestock involved in farm-to-farm movements over four years, and all farms in this network being directly or indirectly connected. Figures in which this network can be visualized (in Chapter 2) give a fair impression of the intense movements and resulting potential for transfer of infection occurring between the farms. In this context, despite the endemicity of paratuberculosis infection, movement of livestock does apparently still play an important role in MAP distribution between New Zealand farms. Moreover, a very common grazing practice in New Zealand, called ‘agistment’, consists of grazing livestock off on another farm for a season and bringing it back to the farm of origin;

this is to make the best use of feed throughout the country. We identified in Chapter 2 this very specific practice as a high risk for pathogen spread in general, due to the back-and-forth pattern of these movements. We can speculate that this might also contribute to spreading MAP infection from farm to farm.

The data for the analysis in Chapter 3 consisted of snapshots of livestock movements between farms and snapshots of strain type distribution on farms. The focus of the analysis was thus to test for associations between these. However, these data were not adapted to quantify the absolute risk of importing livestock. Different measures of farm clustering in the livestock movement's network were computed as proxies for how closely connected via livestock movements every two farms were. These were used as risk factors for the analysis. We thus obtained ORs for these 'movement related' risk factors. These ORs measure the strength of association between the risk factors and the fact that two farms presented the same strains of MAP. Nevertheless, these can't be interpreted quantitatively, *i.e.* it was impossible to use this analysis to determine a probability of transmission of MAP per animal, or per farm.

8.2.2 Spatial spread and comparison with TB

The data presented in Chapter 2 and 3 combined information about movement and farm spatial location. We used a multivariate approach that enabled us to effectively tease out the effect of different covariates on the outcome of interest, namely farms sharing the same strain of MAP. Local spread could happen from run-off waters, wildlife, stray livestock or over-the-fence contact. Our analysis revealed that livestock movement rather than spatial proximity was a risk for between-farm transmissions. This does not mean that local transmission of MAP from neighbouring farms cannot happen, but it may not be the main source of cross-contamination. Biosecurity efforts should therefore focus on livestock movement.

Farm-to-farm transmission of MAP has not previously been formally assessed as far as we have been able to ascertain. However, mechanisms of transmission of bovine tuberculosis between farms are well studied (Skuce et al., 2012). Recent work about the molecular epidemiology of bovine tuberculosis (TB) using whole genome sequencing (WGS) of *Mycobacterium bovis* in dairy cows in New Zealand identified highly variable spatial propagation rates of *M. bovis*, suggesting various diffusion mechanisms other than local spread, among which livestock movement presumably can play an important role (Joseph Crisp (University of Glasgow) and Marian Price-Carter (AgResearch New Zealand), unpublished). This is consistent with our findings.

It should be noted, however, that the population studied for this thesis was not the most suited to evaluate local transmission of MAP, because farms were distributed around the country. The effect of local transmission of Mycobacteria from farm to farm might appear more clearly in studies of small settings of closely clustered farms, as employed by Biek et al. (2012). Their study indicated that the TB cases that occurred on five farms were explained by a mixture of both long term within-herd maintenance of the pathogen and new introductions from environmental reservoirs (“over the fence” cattle contacts with neighbour farms, infectious badgers, etc.). Actual cattle movements between farms explained little of the described epidemic (Biek et al., 2012). On a wider scale however, national cattle movements were more important predictors for the global spread of TB in the UK than environmental, topographic and anthropogenic factors (Gilbert et al., 2005). This thus appears a corollary of mycobacterial infection in livestock.

8.2.3 Genetic resolution and influence of species

A key aspect of this work was merging social network analysis with molecular epidemiology. The analysis of between-farm transmission relied upon VNTR-SSR strain typing of MAP. Genotyping proved useful in the past decade for epidemiological studies of paratuberculosis (Amonsin et al., 2004; Thibault et al., 2008) but the more recent advent of whole genome sequencing (WGS) has highlighted important shortcomings of this method (Ahlstrom et al., 2015). Most importantly, VNTR genotyping lacks resolution in identifying the genetic diversity of MAP isolates. We believe, however, that this would have only biased our results towards the null. Nevertheless, there is little doubt that WGS of MAP isolates from New Zealand, as is currently performed at Massey University, would enable much finer resolution in epidemiological studies, as it did for bovine tuberculosis. While recognizing the important limitations of VNTR typing, we believe genotyping data were robust enough for testing associations based on farms harbouring the same versus different strains. We emphasize that our study did not attempt to directly infer transmission events, which would have been inappropriate. However, it should be noted that when it comes to inferences about transmission, research on bovine tuberculosis has shown that WGS is not a panacea either (Worby et al., 2014). All these aspects are detailed in the discussion of Chapter 3.

Our analysis was also adjusted for potential confounding due to relative specificity of MAP strains for certain livestock species. One covariate in the model of Chapter 3 was thus informing whether each pair of farms was hosting a common species or not. Beef and dairy cattle were classified as different species since previous research showed that these tend to

mostly harbour different strains of MAP (Verdugo et al., 2014b). This choice was therefore being conservative in our inference. As a consequence, the effect of species in the results of the model increased at the expense of the livestock movement effects, possibly masking some of those effects. However, this did not remove the effect of livestock movements, which remained highly significant, with comparable strength in the model. We therefore conclude that our inferences about livestock movements as a risk factor for spreading MAP in the population are robust.

8.2.4 Methods

Social network analysis (SNA) is not novel but application to veterinary epidemiology is recent. Chapter 2 uses SNA techniques to describe the pattern of livestock movement in one nationwide farming enterprise, which we think is fairly typical of the New Zealand livestock movement pattern. We then derived inferences about pathogen transmission in general, in this specific network of farms. In Chapter 3, our aim was to look for associations between movement pattern and strain type distribution, to assess the plausibility of transmission of MAP between farms. Literature about social network analysis *per se* and its use in preventive veterinary medicine has become plethoric in recent years (Martínez-López et al., 2009). Similarly, a body of literature exists about spread of infection in networks (physics, computer science, infectious diseases) with a focus on simulation modelling (Danon et al., 2011). However, there are very few examples, in the field of infectious diseases, of making inferences in networks using real-world data (Firestone et al., 2011; Biek et al., 2012; VanderWaal et al., 2014), rather than simulation modelling.

We had knowledge about an existing network of contact via livestock movements between farms, as well as observed cross-sectional distribution of MAP strain types in the same population of farms. We were not interested in simulating MAP spread in the observed network to see what could happen in theory. Instead, we wanted to test for possible associations between the different kind of farm-to-farm relationships that might be present in the observed data, in particular between observed livestock movements and strain type sharing. Hypothesis testing in network data requires the use of specific methods appropriately dealing with lack of independence inherent to relational data. We investigated social network methodologies borrowed mostly from the field of social sciences, in particular Exponential Random Graph Modelling (ERGM) and permutation methods (Krackhardt, 1988; Welch, 2011).

Exponential Random Graph Modelling would have been appropriate for testing our hypothesis formulated in terms of whether epidemiological links (livestock movements, spatial proximity) and social determinants (farm type, species) gave rise to ties in the MAP ‘transmission’ network (*i.e.* farms sharing the same strains of MAP). ERGM is a statistical method used to test for determinants of network tie formation and for specific network structures, hence providing the additional benefit of shedding light on this aspect (Robins et al., 2007). However, with regard to our data, ERGM was not suited to simultaneously handle directed and undirected relationships, and valued and unvalued edges, which characterized our data. Moreover, we presented a description of important structural features of the network used in this work (based on simple social network analysis) in Chapter 2. Additional refinements or more formal testing for the network structure was unnecessary as it would not further contribute to answering the research question. The research question was quite simple, *i.e.* assessing potential associations between the observed data about the proximity in the livestock movement network and the odds of sharing the same strains of MAP. Hence we turned to permutation methods to test this hypothesis on this farm network. The field of permutation tests for relational data is in itself rather specialised and the relevant literature emphasizes shortcomings and potential biases associated with some of the methods (Legendre and Fortin, 2010). The technique we selected, quadratic assignment procedure using double semi-partialling, was very well suited to answer the research question while teasing apart confounding effects, for robust inferences. We crafted the methodology very specifically to address our research question and the available data. This resulted in a rather novel approach in veterinary epidemiology and, as far as we have been able to ascertain, is unprecedented in studies of the epidemiology of paratuberculosis.

8.3 Within-flock transmission (Chapters 4, 5, 6)

8.3.1 From physiopathology of ovine paratuberculosis to within-flock dynamics

Modelling within-flock MAP infection dynamics is an exercise of capturing the intra-host dynamics of MAP infection and taking it to the level of the flock. We needed to understand possible disease patterns and excretion levels from individual sheep to derive flock-level dynamics of MAP infection.

In Chapter 4 and 6, we used a literature review and a meta-analysis to study host-pathogen interactions at three levels:

(1) The cellular and tissue level with the immunological response of the host and subsequent associated histopathology.

(2) The individual sheep level with the different clinical outcomes resulting from MAP infection as well as individual excretion levels, thus informing the important stages of infection that a sheep can encounter.

(3) The population level with the probabilities associated with the different stages and rates of transitions from one stage to the next.

This was a productive process as it helped us to fully measure how physio-pathology at the animal level and within-herd infection/disease dynamics are in fact a continuum of host-pathogen interaction.

8.3.2 Evaluating the effect of MAP dose

Measuring the effect of MAP inoculum dose from experimental infection models was an essential aspect of this work as it represents the infectiousness of MAP and its virulence. The dose of exposure to MAP represents a key parameter for a model of indirect MAP transmission: the force of infection. Assessing the effect of dose thus requires accurately evaluating the actual dose of MAP used in experimental studies in the first place. Therefore, Chapter 5 reviewed enumeration methods of MAP *in vitro* to evaluate the magnitude and direction of possible bias in the estimation of MAP doses in experimental challenge models. This was instrumental for a correct interpretation of the protocol of these experimental studies. The review provided insights about possible biases in the estimation of the dose effect due to enumeration methods, that were further tested in the meta-analysis (Chapter 6). It also informed about the criteria for data extraction in the meta-analysis.

8.3.3 Methods to estimate model parameters

The literature review in Chapter 4 highlighted disparate studies and heterogeneous results, biased by study level confounding (determined by study design) and by limited power. It was impossible to determine covariate effects from individual studies due to a lack of different covariate patterns, or confounding. Even though experimental challenge models are controlled, it often appeared difficult in practice to overcome confounding. For example, one

study was aimed at the effect of strain type but the animals in each group were inoculated at a different age (Stewart et al., 2004). It was also frequent that groups dosed by either pure culture or gut homogenate were confounded by the inoculum dose, either because dose could only be assessed retrospectively (Begg et al., 2005) or because MAP enumeration in tissue homogenate, which was more difficult, was not attempted (Stewart et al., 2004), or even because by design, the two groups were inoculated one year apart (Fernandez et al., 2015). In this situation, it is very difficult to tease apart all the different effects.

On the other hand, experimental studies of MAP infection in sheep have been carried out with a similar purpose and design, and indeed mostly by few research groups producing most of the research. This made the studies easily comparable, although we needed to use a formal framework, *i.e.* a meta-analysis. The rationale was two-fold: to draw robust inferences, and make the best use of all available data.

We thus decided to carry out an ‘individual-patient’ meta-analysis, consisting of extracting available information at the level of each sheep enrolled in the studies. This was labour intensive but resulted in one large dataset of 767 sheep, for which we individually retrieved the dose of MAP inoculum, the age at inoculation, the breed, the strain of MAP used, the type of inoculum, the time of follow up as well as various clinical outcomes. This was a very precious mine of information as it was then possible to perform multivariate analysis, thus estimating the effect of the different experimental conditions while adjusting for them. We used this dataset to estimate a set of parameters for the model presented in Chapter 7.

Essential parameters of state-transition models are rates. However, most of the data from the meta-analysis were point observations, not longitudinal observations. Hence it was not possible to use classical survival models for the analysis. To circumvent this limitation we modelled the effect of time from inoculation to observation, using a semi-parametric smoother (generalized additive mixed models). This enabled us to approximate the dynamics of infection/disease despite the absence of longitudinal data. It was a key element to derive population parameters from individual sheep data, since each sheep contributed one observation time to the observed dynamics and we were interested in the overall resulting dynamics. This was an original way to estimate dynamic parameters from these data.

An advantage of this approach was that the parametric part of the model enabled us to adjust for covariate effect, and estimate the covariate effects, while the non-parametric part gave a description of the probability of the outcomes as a function of time. Despite that the smoother was non-parametric, the observed predicted probability of active infection appeared to fit a

Weibull distribution very closely. For other outcomes however, the observed dynamics did not lend themselves to straightforward parameter estimation, requiring specifically tailored and imaginative parameter estimation and relying on more restrictive assumptions. We are well aware that not all our working assumptions were very robust. However, we are also satisfied that the estimates were driven by data, emanating from more than seven hundred robust observations. Some of the hand-crafted methods to estimate parameters represented quite a methodologic stretch. Nevertheless they allowed us to make the most of this noisy, yet powerful dataset. We trust therefore that our results were a good representation of an 'average' dynamics of MAP infection.

A note about the use of random effects in the meta-analysis: when analysing outcomes at the individual-sheep level, sheep were clustered within-study which needed to be accounted for in the analysis. Using study as a random effect is considered a gold standard for individual-patient meta-analysis. We want to emphasise however, that there were several possible levels of clustering for the sheep: research group (a country/university conducting ovine paratuberculosis over sometimes decades), paper (reporting one or several experiments), experiment, or even the set of animals (sub-group of sheep infected with exactly the same experimental conditions). Adding a random effect, if the covariate pattern is fixed within each cluster (for example the set of animals), can hamper the detection of the true covariate effect. Indeed the random effect can partially 'absorb' some of the variability due to the covariates. We observed this in our analysis when adding a random effect at a level that was not meaningful, *i.e.* the set of sheep with exactly the same experimental conditions (resulting in one random effect by covariate pattern). This problem was also noted by (Mitchell et al., 2011) and was circumvented by using robust standard errors. In our analysis, the clustering was accounted for at the level of the experiment (modelled as a random effect): all the sheep in an individual trial, potentially including animals with different experimental conditions (different dose regimen, different types of inoculum etc.). There was sometimes more than one experiment described in one paper while on other occasions the same experiment was described across several papers. With all the exploratory work that went into the analysis, we can conclude that this was an appropriate way to account for clustering of sheep.

8.3.4 From experimental infection to natural challenge

For this work, we needed to extrapolate parameters estimated in experimental challenge data to model natural paratuberculosis. Controlled trials are the only means by which we can measure the effect of the conditions of infection as precisely as we did in the meta-analysis.

Therefore they provide a powerful basis for parametrization of mathematical models of infectious diseases. However, the extrapolation of pathological mechanisms observed in experimental conditions to naturally occurring paratuberculosis might represent a stretch of imagination.

The first striking condition that comes to mind as unnatural in experimental studies is the dose of MAP to which sheep are being exposed. When conducting research of ovine paratuberculosis, one wants to ensure that a suitable proportion of the inoculated sheep will encounter the outcome of interest. Hence the median inoculum dose used in challenge trials was around 10^8 MAP, which intuitively can seem higher than likely in a natural exposure situation. However, a study of fecal excretion of MAP by sheep with natural paratuberculosis showed that the contribution of multibacillary sheep to environmental contamination could be nearly 10^{11} MAP per day. Each gram of faeces from a multibacillary sheep could contain around 10^8 , which is close to the median inoculum dose encountered in experimental studies. Hence, high amounts of MAP exposure can still be encountered in a natural environment. Moreover, our systematic review provided experimental data with a wide range of inoculum doses. We were thus able to determine fairly precisely the quantitative effect of dose. In other words, it was possible to evaluate in the meta-analysis the dynamics associated with low dose exposure, which was thus incorporated into the model. The back-up loop between environment contamination and sheep infection in the model was controlling the average exposure dose per sheep, via the tuning parameter, and low exposure doses could be achieved.

Shedding patterns might also differ between natural and experimental challenge. A powerful analysis highlighted the differences between the shedding patterns of over 3000 naturally infected cows with that of experimentally infected cows (Mitchell et al., 2015). In natural infection, high shedding stages were rare and terminal, nearly always followed by being removed from the herd within a year. In experimental challenge however, transient shedding of high doses was common in early stages of infection. The shedding pattern of experimentally infected cows was more complex with many transitions between shedding stages, faster progression rates to high shedding and an unnaturally high proportion of animals becoming high shedders. In our model, this might be partially accounted for by the dose-dependent proportion of sheep entering the progressor versus non-progressor track.

More importantly, we feel that repeated, continuous challenge occurring in natural paratuberculosis might also drive potential differences between natural and experimental

paratuberculosis. However, we were not able to detect an effect of the length of inoculation period or the number of single inoculums in the meta-analysis. Ongoing challenge might presumably trigger an increased resistance to infection for sheep exposed in the long run, but not yet infected. Moreover, sheep, once recovered from infection might be re-infected by MAP in the face of ongoing challenge. These mechanisms are unknown and none are currently implemented in the model. As a result, our simulation results might be partially unrealistic. More about this can be seen in discussion of Chapter 7.

8.3.5 Modelling within-flock dynamics

Based on the meta-analysis of experimental infection with sheep (Chapter 6), the mathematical model presented in Chapter 7 incorporates age-dependency and dose-dependency for important parameters, notably the proportion of infected sheep entering the progressor track. It also includes realistic demographics mimicking seasonal management and separate pasture block for each age group. Because of the explicit demographic part of this model which needed a daily update, we did not use a standard ODE solver (usually Runge-Kutta order 4) to numerically integrate the ODE system of equations for the infection dynamics part. Instead, we implemented a simpler first order Euler numerical approximation with daily updates matching the demographic part. Simulation modelling is only a representation of the real world and our method was just a different approximation. However, it was a novel way to blend detailed daily farm demographics with dynamics of infection with MAP.

We used this model primarily to evaluate the effect of vaccination. However, this model could also allow evaluation of the effect of various grazing management with respect to age groups. For example, the model can be used to compare the effect of set-stocking versus rotational grazing on OJD at times of scarce pasture resource for selected age groups (*e.g.* hoggets, two-tooths, mixed age ewes) However, we are aware that though these questions are interesting from a theoretical standpoint, farmers' management decisions are influenced by animal's feed requirements, and hence in practice there may not be much flexibility as to their grazing options.

8.4 Control of ovine PTB

8.4.1 Vaccination

In all livestock production systems, and all countries, paratuberculosis has been spreading extensively since MAP was first identified in 1895, to reach a widespread global endemic status

(Kennedy and Benedictus, 2001). Eradicating infection using mainly test-and-cull strategies has proved largely unsuccessful. However, vaccination against paratuberculosis was repeatedly deemed both an efficient and a profitable means of control in all species in most studies where this evaluation was made (Bastida and Juste, 2011).

In a review and meta-analysis of paratuberculosis control, Bastida and Juste (2011) stated that vaccination might bring up to 20 times higher economic return than any test-and-cull strategy. These results were available as early as the nineteen nineties. The authors therefore point out the current paradoxical situation where paratuberculosis control is mostly unsuccessful, while the use of an effective control measure (vaccination) has been mostly dismissed in favour of expensive test-and-cull strategies, which have in turn largely been unsuccessful. In the past decade, the paradigm of paratuberculosis control has started to shift from eradicating infection to controlling the disease.

This mind shift might be favourable for wider uptake of vaccination for controlling paratuberculosis. This perspective is all the more desirable given a potential public health threat due to the link with Crohn's disease in humans (Feller et al., 2007; Waddell et al., 2015), although the existence of a causal link is still debated. While MAP is ubiquitous and shedding rates by clinical cases can be colossal, one of the main effects of vaccination is to reduce the amount of shedding and the prevalence of shedders, thus reducing overall MAP contamination in the general environment, and presumably in the food chain. The examples of Iceland and Australia, tackling ovine paratuberculosis, are particularly relevant. In both countries, extensive and expensive depopulation of sheep farms was carried out in an attempt to eradicate infection. This approach failed and widespread ovine paratuberculosis epidemics occurred with heavy losses. Subsequent vaccination contributed to resolving clinical paratuberculosis, thus bringing huge benefit to the sheep industries in both countries (Fridriksdottir et al., 2000).

Hence all the existing evidence, whether simulation modelling or observational studies, unambiguously demonstrates the value of vaccination for paratuberculosis control. Our work is one additional piece of evidence supporting that proposition. The added value of our results is an economic study of vaccine cost-benefit tailored for prime-lamb producers in New Zealand. We incorporated direct and indirect costs of OJD by coupling the economic model to the infection and demographics model. This shows that 'highly impacted' farms (over 1% clinical incidence in mixed age ewes in the New Zealand epidemiologic context) would likely economically benefit from vaccination. However, it is important to understand that purely

from an economic standpoint, the return on investment takes many years. Hence, this strategy requires consistency to pay off over time. We propose that this work will contribute to improve the uptake of vaccination by highly impacted prime-lamb producers in New Zealand, as is already the case for Merino farmers.

8.4.2 Biosecurity on Farms

Our results support the role of livestock movements in spreading MAP infection from farm to farm, and our simulations show the resulting impact on on-farm control. Introducing infected, shedding sheep onto a farm on a regular basis by opening the flock might jeopardize control by vaccination.

The role of livestock movement in disseminating MAP infection between farms is certainly highly relevant to countries like Australia where the epidemiologic situation is much contrasted, with OJD-free areas and OJD-impacted areas. In Australia, livestock movement control is key in the national control strategy for Johne's disease. Our work provides evidence to support this strategy in the Australian context. Moreover it also highlights, maybe more unexpectedly, the impact of livestock movement in the New Zealand context of widespread endemic MAP infection. In fact, our simulation results are likely transferrable to pastoral sheep farming situations in different countries, since important working assumptions are common to many.

Biosecurity would appear relevant to consider, at least in theory, in an integrated approach to paratuberculosis control. This aspect should be emphasized in the farming community as it is likely overlooked. However, given that in New Zealand 80% of sheep farms are infected with MAP, it seems illusory to rely on biosecurity as it would be very difficult for farmers to source MAP-free stock. Moreover, farmers in New Zealand mostly trade livestock through agents serving as intermediates between farmers. This is also not favourable for implementing a trade-based control of OJD. Moreover, given the low average impact of ovine OJD on productivity in New Zealand, there is really little incentive to add constraints on livestock trade which are an important feature of New Zealand pastoral farming systems, more dictated by climatic variation and regional pasture availability.

8.4.3 What is the real incentive for control?

A significant goal of this PhD thesis was to develop a robust framework (a compartmental model) to evaluate control strategies against OJD. We evaluated the effectiveness of

vaccination in terms of OJD incidence, and the cost-effectiveness of vaccination. However, we want to highlight that economic return is not necessarily the alpha and omega of farm management.

Firstly, farmers care about the health and well-being of their animals irrespective of economic endpoints. Windsor (2014) identified extrinsic motivations for farmer's actions beyond strict monetary outcomes, involving status and peer recognition. The intrinsic (intangible) motivations involved satisfaction, pride, sense of achievement and fulfilment. This is well illustrated by the Australian experience of OJD. Because of all the emotional involvement that goes into farmer's management and response to diseases, the epidemic of OJD with high mortalities that occurred in the early 2000's in New South Wales (Australia) had far reaching social and psychological consequences, enough to disrupt affected rural communities (Windsor, 2014). In that experience, the use of the Gudair™ vaccine, by virtually resolving OJD-related mortalities, proved an "enormous benefit to the sheep industry and rural communities" (Windsor, 2013; Windsor, 2014), likely well beyond the pure economic incentive that we highlighted in our work.

Secondly, we often consider animal "production" mainly (if not solely) from a productivity perspective, driven by profit maximization. This is almost a philosophical standpoint as it highlights our propensity to see other forms of life as a mere resource, and ourselves as the "Masters and possessors of Nature" as Descartes put it four centuries ago. Such classical views of Judeo-Christian heritage are now dated, although it heavily influences to this day our contribution, as veterinarians, to farming systems. This can be seen by the importance of animal production, reproduction and herd health management in veterinary science.

In this respect, and more specifically about control of paratuberculosis, I would like to quote *in extenso* a paragraph from Juste and Perez (2011), as an insightful comment and faithful representation of my own ideas on this matter: "The simplicity and robustness of Koch postulates, which allowed the early success of some countries in the eradication of tuberculosis by a testing and culling strategy, led the veterinary community to think that the only reasonable goal in the control of most infectious diseases was full eradication. This has proved an optimistic perspective, because many microorganisms can survive in hidden reservoirs and because the perspective on animal welfare, ecological balance, biodiversity, drug and antibiotic usage, and sustainable production is forcing a change of paradigm in the approach to animal disease control. Thus, considerations about the role of natural population regulation factors have shown that killing individuals is part of the ecological balance and that

it can be achieved not only by superior predators but also by microscopic agents that, in the end, are also part of the general biodiversity of any system. The loss of animals in programs based on testing and culling of non-zoonotic infections and the wasting-associated rapid turnover of animals based on productivity are not always socially acceptable; thus, more sustainable strategies are demanded.”.

On this part, I conclude that production and economics are only a narrow scope of veterinary science and animal ‘production’ systems. For the future, a paradigm shift is desirable both from the perspective of the veterinary profession and at the society level. This could lead us to reconsider our role and responsibility and the role of other life forms (including pathogenic agents), in the global and interdependent ecosystem that is the common “good” to all lives. In this perspective, the rationale to control paratuberculosis could be considered in a more holistic approach to farming (including animal welfare and One Health approach), rather than a simple question of cost and benefit.

8.5 Future work

One caveat of this work is robust field data measuring the true impact of OJD in New Zealand. A precise evaluation of the situation seems like essential background knowledge to address the situation efficiently. Evidence about production effects in sheep in New Zealand, presented in the General Introduction of this thesis, is rather anecdotal and based on clinical disease (Morris et al., 2006). This knowledge gap, however, is not trivial to address. The prevalence of subclinical infection and associated production effects, in the absence of good diagnostic tests for subclinical stages of JD in live animals, is and will remain largely unknown. Individual-level cross-sectional studies of production effects in the case of chronic infection can be hampered by the ‘healthy worker’ effect, *i.e.* when animals testing positive to diagnostic tests are actually the non-progressors (resistant ones) while the progressors died earlier. Farm-level studies on production effects are biased by farm-level confounding and great variation between farms. Similarly, the figures of clinical incidence of OJD in New Zealand presented in the General Introduction pertain to survey results. Farmers were asked to provide their best guess estimate about their losses to JD (Verdugo, 2013), with all the biases and uncertainty involved in this process. However, robust data of the true impact of JD are essential both to better justify the work presented in this thesis and to provide more robust input for economic modelling. Hence we feel our results would greatly benefit from deeper scrutiny about these questions.

At the inception of this PhD, a study involving prospective cohort studies on commercial farms in New Zealand, with longitudinal follow-up over three years, was considered. The proposed study design would have allowed investigation of: (1) the predictive ability of diagnostic tests, (2) subclinical production effects at the individual level, (3) incidence of clinical disease and associated production effects. This approach was adopted for dairy farms in the USA: herds were followed for four to seven years with regular testing, enabling to document precisely the effect of paratuberculosis on calving and culling rates (Smith et al., 2010). These results were essential inputs for mathematical modelling of the impact of paratuberculosis on dairy farming (Al-Mamun et al., 2016) . However, funding for this project in New Zealand was not forthcoming; hence the possibility to shed light on these aspects was not pursued. A precise picture of the impact of paratuberculosis in the population seems an essential prerequisite to control attempt. In our case however, it is well recognized that the impact of OJD on the majority of sheep farms in New Zealand is low. Results of the simulation modelling chapter (Chapter 7) are thus most relevant to a minority of farms experiencing economically significant losses, not the average farm.

Stochastic modelling incorporating uncertainty in parameters would give a better grasp of stochasticity of the results and could answer questions of the type “how many farms would benefit from vaccination in this scenario and how many would not?” or “what is the threshold of clinical incidence above which 90% of farms would clear clinical OJD, indicated by fade-out?”. In fact, it would be really interesting to move from compartmental modelling to individual-based modelling. The latter, by modelling each sheep individually, would allow (1) incorporating stochasticity; (2) keeping track of time of exposure for each sheep, (3) using time-varying rates and (4) modelling discrete sheep.

Recent research carried at Massey University (unpublished) suggests a significantly higher economic impact of OJD on pure Merino farms compared to Romney farms in New Zealand. Our model could easily be modified to mimic a typical Merino flock and study conditions of vaccination cost-effectiveness for Merino producers. The ability to model the impact of OJD on-farm for different incidence levels and different production systems is also an essential starting input to modelling the economic impact of OJD nationally.

Further studies investigating the hypothesis that MAP strains might have differential virulence are also currently being undertaken at Massey University. Our model could contribute by evaluating the virulence of competing strains in a pastoral environment. The structure of the

model could also be used to study other sheep diseases with an environmental compartment, such as leptospirosis which is a major disease of interest in New Zealand.

8.6 Concluding comments

The farming system in New Zealand involves a high frequency of livestock mixing between farms, inherent to the pasture-based system and the fact that breeding farms may be different to store lamb farming. Livestock movements are also dependant on weather and pasture availability, often requiring sale and purchase of animals. It is known that livestock movements are important contributors to the spread of infectious diseases in general. However, farmers in New Zealand overlook livestock movements as a specific risk regarding paratuberculosis, and therefore this risk is not mitigated. While paratuberculosis is not a major problem on most sheep farms in New Zealand, this work highlights that moving animals between farms or premises does contribute to the observed pattern of MAP infection on farm. This should reinforce the notion that biosecurity is important in paratuberculosis control. However, this risk remains difficult to mitigate with high endemic farm levels of MAP infection. A certification program, in which farms would determine their paratuberculosis status and implement on-farm control accordingly, could serve as basis for risk-based livestock trade.

We developed a simulation model specifically tailored for New Zealand pastoral Romney sheep farms. This model blended a MAP infection dynamics component, with indirect MAP transmission through the environment, and a production component incorporating seasonal flock demographics and timed farm management events. These features enabled an economic evaluation of OJD on farm.

Using this approach, we evaluated the effectiveness and cost-effectiveness of vaccination, and highlighted the value of vaccination in high incidence farms. Break-even could be reached in 5 years on farms with 1% clinical incidence of OJD in ewes, although return on investment would take 23 years, thus requiring a continued effort from the farmer. For farms with 2% clinical OJD in ewes, the benefit-cost ratio of vaccination after 30 years was 2.4 according to our work. However, the cost-effectiveness of vaccination varies with fluctuation of market prices and variation in management around drafting prime lambs, culling and replacement. Moreover, cost-effectiveness can be hampered in open flocks by importing infected sheep on the farm on an annual basis. For this reason we do not want to highlight a precise threshold of disease above which vaccination would be cost-effective, like a recipe for success for the farmers. Instead, this thesis conveys that vaccination is epidemiologically effective, drastically reducing

the burden of OJD and MAP contamination in the environment, on most farms. Our results unambiguously show that highly impacted flocks have a clear economic incentive for vaccination, providing they commit in the long run. Gudair™ vaccination is not popular in lamb producing sheep farmers in New Zealand, despite a proportion of sheep farms experiencing high mortalities due to paratuberculosis. These, however, would highly benefit from an OJD vaccination program. This work thus provides robust direction to assist farmer's decision-making and veterinary advice. It may therefore contribute to a better uptake of vaccination by sheep farmers who experience paratuberculosis as a problem.

Chapter 9. References

- Abbott, K., Whittington, R., McGregor, H., 2004. Exposure Factors Leading to Establishment of OJD Infection and Clinical Disease.
- Abendano, N., Tyukalova, L., Barandika, J.F., Balseiro, A., Sevilla, I.A., Garrido, J.M., Juste, R.A., Alonso-Hearn, M., 2014. Mycobacterium Avium subsp Paratuberculosis Isolates Induce In Vitro Granuloma Formation and Show Successful Survival Phenotype, Common Anti-Inflammatory and Antiapoptotic Responses within Ovine Macrophages Regardless of Genotype or Host of Origin. Plos One 9.
- Abendaño, N., Tyukalova, L., Barandika, J.F., Balseiro, A., Sevilla, I.A., Garrido, J.M., Juste, R.A., Alonso-Hearn, M., 2014. Mycobacterium Avium subsp. Paratuberculosis Isolates Induce In Vitro Granuloma Formation and Show Successful Survival Phenotype, Common Anti-Inflammatory and Antiapoptotic Responses within Ovine Macrophages Regardless of Genotype or Host of Origin. PLOS ONE 9, e104238.
- Ahlstrom, C., Barkema, H.W., Stevenson, K., Zadoks, R.N., Biek, R., Kao, R., Trewby, H., Haupstein, D., Kelton, D.F., Fecteau, G., Labrecque, O., Keefe, G.P., McKenna, S.L., De Buck, J., 2015. Limitations of variable number of tandem repeat typing identified through whole genome sequencing of Mycobacterium avium subsp. paratuberculosis on a national and herd level. BMC Genomics 16, 161.
- Al-Mamun, M.A., Smith, R.L., Schukken, Y.H., Gröhn, Y.T., 2016. Modeling of Mycobacterium avium subsp. paratuberculosis dynamics in a dairy herd: An individual based approach. Journal of Theoretical Biology 408, 105-117.
- Albert, R., Barabasi, A.-L., 2002. Statistical mechanics of complex networks. Review of Modern Physics 74.
- Alinovi, C.A., Ward, M.P., Lin, T.L., Moore, G.E., Wu, C.C., 2009. Real-time PCR, compared to liquid and solid culture media and ELISA, for the detection of Mycobacterium avium ssp. paratuberculosis. Vet Microbiol 136, 177-179.
- Aly, S.S., Anderson, R.J., Adaska, J.M., Jiang, J., Gardner, I.A., 2010. Association between Mycobacterium avium subspecies paratuberculosis infection and milk production in two California dairies. Journal of Dairy Science 93, 1030-1040.
- Amonsin, A., Li, L.L., Zhang, Q., Bannantine, J.P., Motiwala, A.S., Sreevatsan, S., Kapur, V., 2004. Multilocus Short Sequence Repeat Sequencing Approach for Differentiating among Mycobacterium avium subsp. paratuberculosis Strains. Journal of Clinical Microbiology 42, 1694-1702.
- Anderson, M.J., Legendre, P., 1999. An empirical comparison of permutation methods for tests of partial regression coefficients in a linear model. Journal of Statistical Computation and Simulation 62, 271-303.
- Anderson, R., May, R., 1991. Infectious Diseases of Humans, Dynamics and Control. Oxford University Press.
- Anderson, R.M., May, R.M., 1979. Population biology of infectious diseases: Part I. Nature 280, 361-367.
- Antognoli, M.C., Hirst, H.L., Garry, F.B., Salman, M.D., 2007. Immune Response to and Faecal Shedding of Mycobacterium avium ssp. paratuberculosis in Young Dairy Calves, and the Association Between Test Results in the Calves and the Infection Status of their Dams. Zoonoses and Public Health 54, 152-159.
- Aznar, M.N., Stevenson, M.A., Zarich, L., León, E.A., 2011. Analysis of cattle movements in Argentina, 2005. Preventive Veterinary Medicine 98, 119-127.
- Bansal, S., Grenfell, B.T., Meyers, L.A., 2007. When individual behaviour matters: homogeneous and network models in epidemiology. Journal of The Royal Society Interface 4, 879-891.

- Barabási, A.-L., Albert, R., 1999. Emergence of Scaling in Random Networks. *Science* 286, 509-512.
- Bastian, M., Heymann, S., Jacomy, M., 2009. Gephi: an open source software for exploring and manipulating networks. *International AAAI Conference on Weblogs and Social Media*.
- Bastida, F., Juste, R.A., 2011. Paratuberculosis control: a review with a focus on vaccination. *Journal of Immune Based Therapies and Vaccines* 9, 8-8.
- Batagelj, V., Mrvar, A., Pajek - Program for large Network Analysis. Home page: <http://vlado.fmf.uni-lj.si/pub/networks/pajek/>.
- Beard, P.M., Rhind, S.M., Sinclair, M.C., Wildblood, L.A., Stevenson, K., McKendrick, I.J., Sharp, J.M., Jones, D.G., 2000. Modulation of gamma delta T cells and CD1 in *Mycobacterium avium* subsp paratuberculosis infection. *Veterinary Immunology and Immunopathology* 77, 311-319.
- Begara-McGorum, I., Wildblood, L.A., Clarke, C.J., Connor, K.M., Stevenson, K., McInnes, C.J., Sharp, J.M., Jones, D.G., 1998. Early immunopathological events in experimental ovine paratuberculosis. *Veterinary Immunology and Immunopathology* 63, 265-287.
- Begg, D., 2004. Immune profiles in sheep following experimental infection with *Mycobacterium paratuberculosis* University of Otago, Dunedin, New Zealand
- Begg, D.J., de Silva, K., Carter, N., Plain, K.M., Purdie, A., Whittington, R.J., 2011. Does a Th1 over Th2 dominancy really exist in the early stages of *Mycobacterium avium* subspecies paratuberculosis infections? *Immunobiology* 216, 840-846.
- Begg, D.J., de Silva, K., Di Fiore, L., Taylor, D.L., Bower, K., Zhong, L., Kawaji, S., Emery, D., Whittington, R.J., 2010. Experimental infection model for Johne's disease using a lyophilised, pure culture, seedstock of *Mycobacterium avium* subspecies paratuberculosis. *Veterinary Microbiology* 141, 301-311.
- Begg, D.J., Griffin, J.F.T., 2005. Vaccination of sheep against M-paratuberculosis: immune parameters and protective efficacy. *Vaccine* 23, 4999-5008.
- Begg, D.J., O'Brien, R., Mackintosh, C.G., Griffin, J.F.T., 2005. Experimental infection model for Johne's disease in sheep. *Infection and Immunity* 73, 5603-5611.
- Begg, D.J., Whittington, R.J., 2008. Experimental animal infection models for Johne's disease, an infectious enteropathy caused by *Mycobacterium avium* subsp paratuberculosis. *Veterinary Journal* 176, 129-145.
- Behr, M.A., Collins, D.M. (Eds.), 2010. *Paratuberculosis Organism, Disease, Control*.
- Berman, N.G., Parker, R.A., 2002. Meta-analysis: Neither quick nor easy. *BMC Medical Research Methodology* 2, 10.
- Biek, R., O'Hare, A., Wright, D., Mallon, T., McCormick, C., Orton, R.J., McDowell, S., Trewby, H., Skuce, R.A., Kao, R.R., 2012. Whole Genome Sequencing Reveals Local Transmission Patterns of *Mycobacterium bovis* in Sympatric Cattle and Badger Populations. *PLoS Pathogens* 8, e1003008.
- Blondel, V., D., Guillaume, J.-L., Renaud, L., Etienne, L., 2008. Fast unfolding of communities in large networks. *Journal of Statistical Mechanics: Theory and Experiment* 2008, P10008.
- Bogli-Stuber, K., Kohler, C., Seitert, G., Glanemann, B., Antognoli, M., Salman, M., Wittenbrink, M., Wittwer, M., Wassenaar, T., Jemmi, T., Bissig-Choisat, B., 2005. Detection of *Mycobacterium avium* subspecies paratuberculosis in Swiss dairy cattle by real-time PCR and culture: a comparison of the two assays. *J Appl Microbiol* 99, 587 - 597.
- Borgatti, S.P., Everett, M.G., Johnson, J.C. (Eds.), 2013. *Analyzing Social Networks*. SAGE publications Ltd.
- Bower, K.L., Begg, D.J., Whittington, R.J., 2011. Culture of *Mycobacterium avium* subspecies paratuberculosis (MAP) from blood and extra-intestinal tissues in experimentally infected sheep. *Veterinary Microbiology* 147, 127-132.
- Brett, E., 1998. *Johne's Disease: An Economic Evaluation of Control Options for the New Zealand Livestock Industries*. Agriculture New Zealand. Wellington.
- Breuninger, K.J., Weir, M.H., 2015. Development of an Interspecies Nested Dose-Response Model for *Mycobacterium avium* subspecies paratuberculosis. *Risk Analysis* 35, 1479-1487.

- Brotherston, J.F., Gilmour, N.J.L., Samuel, J.M., 1961a. Quantitative studies of *Mycobacterium johnei* in tissues of sheep .1. Routes of infection and assay of viable *M. johnei*. *Journal of Comparative Pathology and Therapeutics* 71, 286.
- Brotherston, J.F., Samuel, J.M., Gilmour, N.J.L., 1961b. Quantitative studies of *Mycobacterium johnei* in tissues of sheep .2. Protection afforded by dead vaccines *Journal of Comparative Pathology and Therapeutics* 71, 300.
- Bull, T.J., Hermon-Taylor, J., Pavlik, I., El-Zaatari, F., Tizard, M., 2000. Characterization of IS900 loci in *Mycobacterium avium* subsp. *paratuberculosis* and development of multiplex PCR typing. *Microbiology* 146, 2185-2197.
- Bush, R.D., Toribio, J.A., Windsor, P.A., 2006a. The impact of malnutrition and other causes of losses of adult sheep in 12 flocks during drought. *Australian Veterinary Journal* 84, 254-260.
- Bush, R.D., Windsor, P.A., Toribio, J.A., 2006b. Losses of adult sheep due to ovine Johne's disease in 12 infected flocks over a 3-year period. *Australian Veterinary Journal* 84, 246-253.
- Bush, R.D., Windsor, P.A., Toribio, J.A., Webster, S.R., 2008. Financial modelling of the potential cost of ovine Johne's disease and the benefit of vaccinating sheep flocks in southern New South Wales. *Australian Veterinary Journal* 86, 398-403.
- Butts, C.T., 2008. Social Network Analysis with sna. *Journal of Statistical Software* 24, 1-51.
- Carrington, P.J., Scott, J., Wasserman, S. (Eds.), 2005. *Models and methods in social network analysis*. Cambridge University Press Cambridge.
- Castellanos, E., Aranaz, A., de Juan, L., Álvarez, J., Rodríguez, S., Romero, B., Bezos, J., Stevenson, K., Mateos, A., Domínguez, L., 2009. Single Nucleotide Polymorphisms in the IS900 Sequence of *Mycobacterium avium* subsp. *paratuberculosis* Are Strain Type Specific. *Journal of Clinical Microbiology* 47, 2260-2264.
- Cernicchiaro, N., Wells, S.J., Janagama, H., Sreevatsan, S., 2008. Influence of type of culture medium on characterization of *Mycobacterium avium* subsp. *paratuberculosis* subtypes. *Journal of Clinical Microbiology* 46, 145-149.
- Chiodini, R.J., Chamberlin, W.M., 2011. What Is *Mycobacterium avium* subsp. *paratuberculosis*? *Applied and Environmental Microbiology* 77, 1923-1924.
- Chiodini, R.J., Van Kruiningen, H.J., Merkal, R.S., 1984. Ruminant paratuberculosis (Johne's disease): the current status and future prospects. *The Cornell veterinarian* 74, 218-262.
- Chiodini, R.J., Van Kruiningen, H.J., Thayer, W.R., Coutu, J.A., 1986. Spheroplastic phase of mycobacteria isolated from patients with Crohn's disease. *Journal of Clinical Microbiology* 24, 357-363.
- Christley, R.M., Robinson, S.E., Lysons, R., French, N.P., 2005. Network analysis of cattle movement in Great Britain. In: Mellor, D.J., Russell, A.M., Wood, J.L.N. (Eds.), *Proceedings of the Society for Veterinary Epidemiology and Preventive Medicine Meeting*, Inverness, Scotland, 234-244.
- Clarke, C.J., 1997. The pathology and pathogenesis of paratuberculosis in ruminants and other species. *Journal of Comparative Pathology* 116, 217-261.
- Clarke, C.J., Little, D., 1996. The pathology of ovine paratuberculosis: Gross and histological changes in the intestine and other tissues. *Journal of Comparative Pathology* 114, 419-437.
- Clauset, A., Shalizi, C.R., Newman, M.E.J., 2009. Power-Law Distributions in Empirical Data. *SIAM Review* 51, 661-703.
- Cocito, C., Gilot, P., Coene, M., de Kesel, M., Poupart, P., Vannuffel, P., 1994. Paratuberculosis. *Clinical Microbiology Reviews* 7, 328-345.
- Collins, D.M., De Zoete, M., Cavaignac, S.M., 2002. *Mycobacterium avium* subsp. *paratuberculosis* strains from cattle and sheep can be distinguished by a PCR test based on a novel DNA sequence difference. *Journal of Clinical Microbiology* 40, 4760-4762.
- Collins, D.M., Gabric, D.M., Delisle, G.W., 1990. Identification of 2 groups of *Mycobacterium paratuberculosis* strains by restriction endonuclease analysis and DNA hybridization. *Journal of Clinical Microbiology* 28, 1591-1596.

- Corner, L.A.L., Pfeiffer, D.U., Morris, R.S., 2003. Social-network analysis of *Mycobacterium bovis* transmission among captive brushtail possums (*Trichosurus vulpecula*). *Preventive Veterinary Medicine* 59, 147-167.
- Cousins, D.V., Whittington, R., Marsh, I., Masters, A., Evans, R.J., Kluver, P., 1999. *Mycobacteria* distinct from *Mycobacterium avium* subsp. *paratuberculosis* isolated from the faeces of ruminants possess IS 900-like sequences detectable by IS 900 polymerase chain reaction: implications for diagnosis. *Molecular and Cellular Probes* 13, 431-442.
- Cranston L, R.A., Kenyon P, Greer A. , 2017. *Livestock Production in New Zealand*. Massey University Press, Auckland, New Zealand.
- Cross, P.C., Lloyd-Smith, J.O., Johnson, P.L.F., Getz, W.M., Sherratt, J., 2005. Duelling timescales of host movement and disease recovery determine invasion of disease in structured populations. *Ecology Letters* 8, 587-595.
- Csárdi, G., T. Nepusz, 2006. The igraph software package for complex network research. *InterJournal Complex Systems*, 1695.
- Damato, J.J., Collins, M.T., 1990. Growth of *Mycobacterium paratuberculosis* in radiometric, middlebrook and egg-based media. *Veterinary Microbiology* 22, 31-42.
- Damato, J.J., Collins, M.T., Rothlauf, M.V., McClatchy, J.K., 1983. Detection of mycobacteria by radiometric and standard plate procedures. *Journal of Clinical Microbiology* 17, 1066-1073.
- Danon, L., Ford, A.P., House, T., Jewell, C.P., Keeling, M.J., Roberts, G.O., Ross, J.V., Vernon, M.C., 2011. *Networks and the Epidemiology of Infectious Disease. Interdisciplinary Perspectives on Infectious Diseases 2011*.
- de Lisle, G.W., 2002. Johne's disease in New Zealand: the past, present and a glimpse into the future. *New Zealand Veterinary Journal* 50, 53-56.
- de Lisle, G.W., Yates, G.F., Montgomery, R.H., 2003. The emergence of *Mycobacterium paratuberculosis* in farmed deer in New Zealand — a review of 619 cases. *New Zealand Veterinary Journal* 51, 58-62.
- de Silva, K., Begg, D., Carter, N., Taylor, D., Di Fiore, L., Whittington, R., 2010. The early lymphocyte proliferation response in sheep exposed to *Mycobacterium avium* subsp *paratuberculosis* compared to infection status. *Immunobiology* 215, 12-25.
- de Silva, K., Begg, D., Whittington, R., 2011. The interleukin 10 response in ovine Johne's disease. *Veterinary Immunology and Immunopathology* 139, 10-16.
- de Silva, K., Begg, D.J., Plain, K.M., Purdie, A.C., Kawaji, S., Dhand, N.K., Whittington, R.J., 2013. Can early host responses to mycobacterial infection predict eventual disease outcomes? *Preventive Veterinary Medicine* 112, 203-212.
- de Silva, K., Plain, K.M., Begg, D.J., Purdie, A.C., Whittington, R.J., 2015. CD4(+) T-cells, gamma delta T-cells and B-cells are associated with lack of vaccine protection in *Mycobacterium avium* subspecies *paratuberculosis* infection. *Vaccine* 33, 149-155.
- DeBlanc, H.J., DeLand, F., Wagner, H.N., 1971. Automated Radiometric Detection of Bacteria in 2,967 Blood Cultures. *Applied Microbiology* 22, 846-849.
- Dekker, D., Krackhardt, D., Snijders, T.B., 2007. Sensitivity of MRQAP Tests to Collinearity and Autocorrelation Conditions. *Psychometrika* 72, 563-581.
- Delgado, F., Etchechoury, D., Gioffré, A., Paolicchi, F., Blanco Viera, F., Mundo, S., Romano, M.I., 2009. Comparison between two in situ methods for *Mycobacterium avium* subsp. *paratuberculosis* detection in tissue samples from infected cattle. *Veterinary Microbiology* 134, 383-387.
- Delgado, L., Garcia Marin, J.F., Munoz, M., Benavides, J., Juste, R.A., Garcia-Pariente, C., Fuertes, M., Gonzalez, J., Ferreras, M.C., Perez, V., 2013. Pathological Findings in Young and Adult Sheep Following Experimental Infection With 2 Different Doses of *Mycobacterium avium* Subspecies *paratuberculosis*. *Veterinary Pathology* 50, 857-866.
- Delgado, L., Juste, R.A., Munoz, M., Morales, S., Benavides, J., Carmen Ferreras, M., Garcia Marin, J.F., Perez, V., 2012. Differences in the peripheral immune response between lambs and

- adult ewes experimentally infected with *Mycobacterium avium* subspecies paratuberculosis. *Veterinary Immunology and Immunopathology* 145, 23-31.
- Delignette-Muller, M.L., Dutang, C., 2015. *Fitdistrplus: An R Package for Fitting Distributions*. 2015 64, 34.
- Dennis, M.M., Reddacliff, L.A., Whittington, R.J., 2010. Longitudinal Study of Clinicopathological Features of Johne's Disease in Sheep Naturally Exposed to *Mycobacterium avium* Subspecies Paratuberculosis. *Veterinary Pathology Online*.
- Dhand, N.K., Eppleston, J., Whittington, R.J., Windsor, P.A., 2016. Changes in prevalence of ovine paratuberculosis following vaccination with Gudair®: Results of a longitudinal study conducted over a decade. *Vaccine* 34, 5107-5113.
- Dhand, N.K., Johnson, W.O., Eppleston, J., Whittington, R.J., Windsor, P.A., 2013. Comparison of pre- and post-vaccination ovine Johne's disease prevalence using a Bayesian approach. *Preventive Veterinary Medicine* 111, 81-91.
- Dhand, N.K., Sergeant, E., Toribio, J.-A.L.M.L., Whittington, R.J., 2010. Estimation of sensitivity and flock-sensitivity of pooled faecal culture for *Mycobacterium avium* subsp. paratuberculosis in sheep. *Preventive Veterinary Medicine* 95, 248-257.
- Didelot, X., Gardy, J., Colijn, C., 2014. Bayesian Inference of Infectious Disease Transmission from Whole-Genome Sequence Data. *Molecular Biology and Evolution*.
- Diekmann, O., Heesterbeek, J.A.P., Metz, J.A.J., 1990. On the definition and the computation of the basic reproduction ratio R_0 in models for infectious diseases in heterogeneous populations. *Journal of Mathematical Biology* 28, 365-382.
- Dohoo, I.W., Martin; Stryhn, Henrik, 2009. *Veterinary Epidemiologic Research*.
- Dorjee, S., Revie, C.W., Poljak, Z., McNab, W.B., Sanchez, J., 2013. Network analysis of swine shipments in Ontario, Canada, to support disease spread modelling and risk-based disease management. *Preventive Veterinary Medicine* 112, 118-127.
- Drewe, J.A., Eames, K.T.D., Madden, J.R., Pearce, G.P., 2011. Integrating contact network structure into tuberculosis epidemiology in meerkats in South Africa: Implications for control. *Preventive Veterinary Medicine* 101, 113-120.
- Dubé, C., Ribble, C., Kelton, D., 2010. An analysis of the movement of dairy cattle through 2 large livestock markets in the province of Ontario, Canada. *Canadian Veterinary Journal* 51, 1254-1260.
- Dubé, C., Ribble, C., Kelton, D., McNab, B., 2009. A Review of Network Analysis Terminology and its Application to Foot-and-Mouth Disease Modelling and Policy Development. *Transboundary and Emerging Diseases* 56, 73-85.
- Dukes, T.W., Glover, G.J., Brooks, B.W., Duncan, J.R., Swendrowski, M., 1992. Paratuberculosis in Saiga antelope (*Saiga tatarica*) and experimental transmission to domestic sheep *Journal of Wildlife Diseases* 28, 161-170.
- Eguíluz, V.M., Klemm, K., 2002. Epidemic Threshold in Structured Scale-Free Networks. *Physical Review Letters* 89, 108701.
- Elguezabal, N., Bastida, F., Sevilla, I., Gonzalez, N., Molina, E., Garrido, J., Juste, R., 2011. Estimation of *Mycobacterium avium* subsp. paratuberculosis growth parameters: strain characterization and comparison of methods. *Appl Environ Microbiol* 77, 8615 - 8624.
- Ellingson, J.L.E., Bolin, C.A., Stabel, J.R., 1998. Identification of a gene unique to *Mycobacterium avium* subspecies paratuberculosis and application to diagnosis of paratuberculosis. *Molecular and Cellular Probes* 12, 133-142.
- Englund, S., Bölske, G., Johansson, K.-E., 2002. An IS900-like sequence found in a *Mycobacterium* sp. other than *Mycobacterium avium* subsp. paratuberculosis. *FEMS Microbiology Letters* 209, 267-271.
- Eppleston, J., Begg, D.J., Dhand, N.K., Watt, B., Whittington, R.J., 2014. Environmental Survival of *Mycobacterium avium* subsp. paratuberculosis in Different Climatic Zones of Eastern Australia. *Applied and Environmental Microbiology* 80, 2337-2342.

- Eppleston, J., Windsor, P., Whittington, R., 2011. Effect of unvaccinated Merino wether lambs on shedding of *Mycobacterium avium* subspecies paratuberculosis in flocks vaccinating for ovine Johne's disease. *Australian Veterinary Journal* 89, 38-40.
- Fang, Y., Wu, W.-H., Pepper, J.L., Larsen, J.L., Marras, S.A.E., Nelson, E.A., Epperson, W.B., Christopher-Hennings, J., 2002. Comparison of Real-Time, Quantitative PCR with Molecular Beacons to Nested PCR and Culture Methods for Detection of *Mycobacterium avium* subsp. paratuberculosis in Bovine Fecal Samples. *Journal of Clinical Microbiology* 40, 287-291.
- Fecteau, M.E., Whitlock, R.H., Buergelt, C.D., Sweeney, R.W., 2010. Exposure of young dairy cattle to *Mycobacterium avium* subsp. paratuberculosis (MAP) through intensive grazing of contaminated pastures in a herd positive for Johne's disease. *Can Vet J* 51, 198-200.
- Feller, M., Huwiler, K., Stephan, R., Altpeter, E., Shang, A., Furrer, H., Pfyffer, G.E., Jemmi, T., Baumgartner, A., Egger, M., 2007. *Mycobacterium avium* subspecies paratuberculosis and Crohn's disease: a systematic review and meta-analysis. *The Lancet Infectious Diseases* 7, 607-613.
- Fernandez, M., Benavides, J., Sevilla, I.A., Fuertes, M., Castano, P., Delgado, L., Francisco Garcia Marin, J., Garrido, J.M., Ferreras, M.C., Perez, V., 2014. Experimental infection of lambs with C and S-type strains of *Mycobacterium avium* subspecies paratuberculosis: immunological and pathological findings. *Veterinary Research* 45.
- Fernandez, M., Delgado, L., Sevilla, I.A., Fuertes, M., Castano, P., Royo, M., Ferreras, M.C., Benavides, J., Perez, V., 2015. Virulence attenuation of a *Mycobacterium avium* subspecies paratuberculosis S-type strain prepared from intestinal mucosa after bacterial culture. Evaluation in an experimental ovine model. *Research in Veterinary Science* 99, 180-187.
- Firestone, S.M., Ward, M.P., Christley, R.M., Dhand, N.K., 2011. The importance of location in contact networks: Describing early epidemic spread using spatial social network analysis. *Preventive Veterinary Medicine* 102, 185-195.
- Fortunato, S., Castellano, C., 2007. Community Structure in Graphs. ArXiv e-prints.
- Fridriksdottir, V., Gunnarsson, E., Sigurdarson, S., Gudmundsdottir, K.B., 2000. Paratuberculosis in Iceland: epidemiology and control measures, past and present. *Veterinary Microbiology* 77, 263-267.
- Garcia, A.B., Shalloo, L., 2015. Invited review: The economic impact and control of paratuberculosis in cattle. *Journal of Dairy Science* 98, 5019-5039.
- Gardy, J.L., Johnston, J.C., Sui, S.J.H., Cook, V.J., Shah, L., Brodtkin, E., Rempel, S., Moore, R., Zhao, Y., Holt, R., Varhol, R., Birol, I., Lem, M., Sharma, M.K., Elwood, K., Jones, S.J.M., Brinkman, F.S.L., Brunham, R.C., Tang, P., 2011. Whole-Genome Sequencing and Social-Network Analysis of a Tuberculosis Outbreak. *New England Journal of Medicine* 364, 730-739.
- Geraghty, T., Graham, D.A., Mullaney, P., More, S.J., 2014. A review of bovine Johne's disease control activities in 6 endemically infected countries. *Preventive Veterinary Medicine* 116, 1-11.
- Gilbert, M., Mitchell, A., Bourn, D., Mawdsley, J., Clifton-Hadley, R., Wint, W., 2005. Cattle movements and bovine tuberculosis in Great Britain. *Nature* 435, 491-496.
- Gilmour, N.J.L., Angus, K.W., 1973. Effect of revaccination on *Mycobacterium johnei* infection in sheep. *Journal of Comparative Pathology* 83, 437-445.
- Gilmour, N.J.L., Angus, K.W., 1974. Absence of immunogenicity of an oral vaccine against *Mycobacterium johnei* in sheep. *Research in Veterinary Science* 16, 269-270.
- Gilmour, N.J.L., Angus, K.W., Mitchell, B., 1977. Intestinal infection and host response to oral administration of *Mycobacterium johnei* in sheep. *Veterinary Microbiology* 2, 223-235.
- Gilmour, N.J.L., Angus, K.W., Mitchell, B., 1978. Intestinal infection and host response to oral administration of *Mycobacterium johnei* in sheep. *Veterinary Microbiology* 2, 223-235.
- Gilmour, N.J.L., Brotherston, J.G., 1962. Quantitative studies of *Mycobacterium johnei* in tissues of sheep .4. Distribution of *M. johnei* shortly after oral dosing. *Journal of Comparative Pathology and Therapeutics* 72, 165-&.

- Gilmour, N.J.L., Brotherston, J.G., 1966. Further Studies on Immunity to Mycobacterium Johnei in Sheep - Relationship between Hypersensitivity and Host Response to Infection. *Journal of Comparative Pathology* 76, 341-&.
- Gilmour, N.J.L., Halhead, W.A., Brothers.Jg, 1965a. Studies of immunity to Mycobacterium johnei in sheep *Journal of Comparative Pathology and Therapeutics* 75, 165-&.
- Gilmour, N.J.L., Halhead, W.A., Brotherston, J.G., 1965b. Studies of immunity to Mycobacterium johnei in sheep. *Journal of Comparative Pathology* 75, 165-173.
- Gilmour, N.J.L., Singleton, L., Ross, G.W., 1969. Studies on the hypersensitivity and immunity caused by Mycobacterium johnei PMKOJ adjuvant vaccine in sheep. *Journal of Comparative Pathology* 79, 341-346.
- Girvan, M., Newman, M.E.J., 2002. Community structure in social and biological networks. *Proceedings of the National Academy of Sciences of the United States of America* 99, 7821-7826.
- Glass, G.V., 1976. Primary, Secondary, and Meta-Analysis of Research. *Educational Researcher* 5, 3-8.
- Gonda, M.G., Chang, Y.M., Shook, G.E., Collins, M.T., Kirkpatrick, B.W., 2007. Effect of Mycobacterium paratuberculosis infection on production, reproduction, and health traits in US Holsteins. *Preventive Veterinary Medicine* 80, 103-119.
- Green, E.P., Tizard, M.L., Moss, M.T., Thompson, J., Winterbourne, D.J., McFadden, J.J., Hermon-Taylor, J., 1989. Sequence and characteristics of IS900, an insertion element identified in a human Crohn's disease isolate of Mycobacterium paratuberculosis. *Nucleic Acids Research* 17, 9063-9073.
- Griffin, J.F.T., Hughes, A.D., Liggett, S., Farquhar, P.A., Mackintosh, C.G., Bakker, D., 2009. Efficacy of novel lipid-formulated whole bacterial cell vaccines against Mycobacterium avium subsp paratuberculosis in sheep. *Vaccine* 27, 911-918.
- Gumber, S., Whittington, R.J., 2007. Comparison of BACTEC 460 and MGIT 960 systems for the culture of Mycobacterium avium subsp. paratuberculosis S strain and observations on the effect of inclusion of ampicillin in culture media to reduce contamination. *Veterinary Microbiology* 119, 42-52.
- Gumbrell, R.C., 1986. The history and current status of ovine Johne's disease in New Zealand. The society of Sheep and Beef Cattle Veterinarians of the New Zealand Veterinary Association.
- Gwozdz, J.M., 1999. Mycobacterium paratuberculosis infection in sheep: aspects of diagnosis and immunity. Massey University, Palmerston North, New Zealand.
- Gwozdz, J.M., Thompson, K.G., 2002. Antigen-induced production of interferon-gamma in samples of peripheral lymph nodes from sheep experimentally inoculated with Mycobacterium avium subsp paratuberculosis. *Veterinary Microbiology* 84, 243-252.
- Gwozdz, J.M., Thompson, K.G., Manktelow, B.W., 2001. Lymphocytic neuritis of the ileum in sheep with naturally acquired and experimental paratuberculosis. *Journal of Comparative Pathology* 124, 317-320.
- Gwozdz, J.M., Thompson, K.G., Manktelow, B.W., Murray, A., West, D.M., 2000a. Vaccination against paratuberculosis of lambs already infected experimentally with Mycobacterium avium subspecies paratuberculosis. *Australian Veterinary Journal* 78, 560-566.
- Gwozdz, J.M., Thompson, K.G., Murray, A., Reichel, M.P., Manktelow, B.W., West, D.M., 2000b. Comparison of three serological tests and an interferon-gamma assay for the diagnosis of paratuberculosis in experimentally infected sheep. *Australian Veterinary Journal* 78, 779-783.
- Gwozdz, J.M., Thompson, K.G., Murray, A., West, D.M., Manktelow, B.W., 2000c. Use of the polymerase chain reaction assay for the detection of Mycobacterium avium subspecies paratuberculosis in blood and liver biopsies from experimentally infected sheep. *Australian Veterinary Journal* 78, 622-624.
- Haidich, A.B., 2010. Meta-analysis in medical research. *Hippokratia* 14, 29-37.
- Harris, N.B., Barletta, R.G., 2001. Mycobacterium avium subsp. paratuberculosis in Veterinary Medicine. *Clinical Microbiology Reviews* 14, 489-512.

- Hasonova, L., Pavlik, I., 2006. Economic impact of paratuberculosis in dairy cattle herds: a review. *Vet. Med.* 51, 193-211.
- Hethcote, H.W., 1978. An immunization model for a heterogeneous population. *Theoretical Population Biology* 14, 338-349.
- Heuer, C., Mitchell, R.M., Schukken, Y.H., Lu, Z., Verdugo, C., Wilson, P.R., 2012. Modelling transmission dynamics of paratuberculosis of red deer under pastoral farming conditions. *Preventive Veterinary Medicine*.
- Hines, M.E., II, Stabel, J.R., Sweeney, R.W., Griffin, F., Talaat, A.M., Bakker, D., Benedictus, G., Davis, W.C., de Lisle, G.W., Gardner, I.A., Juste, R.A., Kapur, V., Koets, A., McNair, J., Pruitt, G., Whitlock, R.H., 2007. Experimental challenge models for Johne's disease: A review and proposed international guidelines. *Veterinary Microbiology* 122, 197-222.
- House, T., Keeling, M.J., 2011. Insights from unifying modern approximations to infections on networks. *Journal of The Royal Society Interface* 8, 67-73.
- Hu, F.B., Goldberg, J., Hedeker, D., Flay, B.R., Pentz, M.A., 1998. Comparison of Population-Averaged and Subject-Specific Approaches for Analyzing Repeated Binary Outcomes. *American Journal of Epidemiology* 147, 694-703.
- Hubert, L., Schultz, J., 1976. Quadratic assignment as a general data analysis strategy. *British Journal of Mathematical and Statistical Psychology* 29, 190-241.
- Hughes, V.M., Stevenson, K., Sharp, J.M., 2001. Improved preparation of high molecular weight DNA for pulsed-field gel electrophoresis from mycobacteria. *Journal of Microbiological Methods* 44, 209-215.
- Hulten, K., Karttunen, T.J., El-Zimaity, H.M.T., Naser, S.A., Collins, M.T., Graham, D.Y., El-Zaatari, F.A.K., 2000. Identification of cell wall deficient forms of *M. avium* subsp. paratuberculosis in paraffin embedded tissues from animals with Johne's disease by in situ hybridization. *Journal of Microbiological Methods* 42, 185-195.
- Humphry, R.W., Stott, A.W., Adams, C., Gunn, G.J., 2006. A model of the relationship between the epidemiology of Johne's disease and the environment in suckler-beef herds. *The Veterinary Journal* 172, 432-445.
- Hunnam, J.C., Heuer, C., Stevenson, M., Wilson, P., 2009. National slaughterhouse - based surveillance for Johne 's disease in New Zealand farmed deer. *The Deer Branch New Zealand Veterinary Association*.
- Jeyanathan, M., Alexander, D.C., Turenne, C.Y., Girard, C., Behr, M.A., 2006. Evaluation of In Situ Methods Used To Detect *Mycobacterium avium* subsp. paratuberculosis in Samples from Patients with Crohn's Disease. *Journal of Clinical Microbiology* 44, 2942-2950.
- Jeyanathan, M., Boutros-Tadros, O., Radhi, J., Semret, M., Bitton, A., Behr, M.A., 2007. Visualization of *Mycobacterium avium* in Crohn's tissue by oil-immersion microscopy. *Microbes and Infection* 9, 1567-1573.
- Jones, J.H., Handcock, M.S., 2003. An assessment of preferential attachment as a mechanism for human sexual network formation.
- Juste, R.A., Casal, J., 1993. An economic and epidemiologic simulation of different control strategies for ovine paratuberculosis. *Preventive Veterinary Medicine* 15, 101-115.
- Juste, R.A., García Marín, J.F., Peris, B., Sáez de Ocariz, C., Badiola, J.J., 1994a. Experimental infection of vaccinated and non-vaccinated lambs with *Mycobacterium paratuberculosis*. *Journal of Comparative Pathology* 110, 185-194.
- Juste, R.A., Marin, J.F.G., Peris, B., Deocariz, C.S., Badiola, J.J., 1994b. Experimental infection of vaccinated and non-vaccinated lambs with *Mycobacterium paratuberculosis* *Journal of Comparative Pathology* 110, 185-194.
- Juste, R.A., Perez, V., 2011. Control of Paratuberculosis in Sheep and Goats. *Veterinary Clinics of North America: Food Animal Practice* 27, 127-138.
- Kao, R.R., 2002. The role of mathematical modelling in the control of the 2001 FMD epidemic in the UK. *Trends in Microbiology* 10, 279-286.

- Kao, R.R., Danon, L., Green, D.M., Kiss, I.Z., 2006. Demographic structure and pathogen dynamics on the network of livestock movements in Great Britain. *Proceedings of the Royal Society B: Biological Sciences* 273, 1999-2007.
- Kao, R.R., Haydon, D.T., Lycett, S.J., Murcia, P.R., 2014. Supersize me: how whole-genome sequencing and big data are transforming epidemiology. *Trends in Microbiology* 22, 282-291.
- Karpinski, T., Zorawski, C., 1975. Experimental paratuberculosis of sheep. I. Clinical, allergical, bacteriological and post-mortem examinations. *Bulletin of the Veterinary Institute in Pulawy* 19, 59-63.
- Kawaji, S., Begg, D.J., Plain, K.M., Whittington, R.J., 2011. A longitudinal study to evaluate the diagnostic potential of a direct faecal quantitative PCR test for Johne's disease in sheep. *Veterinary Microbiology* 148, 35-44.
- Kawaji, S., Taylor, D.L., Mori, Y., Whittington, R.J., 2007. Detection of *Mycobacterium avium* subsp. paratuberculosis in ovine faeces by direct quantitative PCR has similar or greater sensitivity compared to radiometric culture. *Veterinary Microbiology* 125, 36-48.
- Keeling, M.J., 1999. The Effects of Local Spatial Structure on Epidemiological Invasions. *Proceedings: Biological Sciences* 266, 859-867.
- Keeling, M.J., Eames, K.T.D., 2005. Networks and epidemic models. *J. R. Soc. Interface* 2, 295-307.
- Kennedy, D.J., Benedictus, G., 2001. Control of *Mycobacterium avium* subsp paratuberculosis infection in agricultural species. *Revue Scientifique Et Technique De L Office International Des Epizooties* 20, 151-179.
- Keyfitz, B.L., Keyfitz, N., 1997. The McKendrick partial differential equation and its uses in epidemiology and population study. *Mathematical and Computer Modelling* 26, 1-9.
- Kiss, I.Z., Green, D.M., Kao, R.R., 2006. The network of sheep movements within Great Britain: Network properties and their implications for infectious disease spread. *Journal of The Royal Society Interface* 3, 669-677.
- Klijn, N., Herrewegh, A.A.P.M., De Jong, P., 2001. Heat inactivation data for *Mycobacterium avium* subsp. paratuberculosis: implications for interpretation. *Journal of Applied Microbiology* 91, 697-704.
- Kluge, J.P., Merkal, R.S., Monlux, W.S., Larsen, A.B., Kopecky, K.E., Ramsey, F.K., Lehmann, R.P., 1968. Experimental paratuberculosis in sheep after oral intratracheal or intravenous inoculation - Lesions and demonstration of etiologic agent *American Journal of Veterinary Research* 29, 953-&.
- Koets, A.P., Gröhn, Y.T., 2015. Within- and between-host mathematical modeling of *Mycobacterium avium* subspecies paratuberculosis (MAP) infections as a tool to study the dynamics of host-pathogen interactions in bovine paratuberculosis. *Veterinary Research* 46, 60.
- Kossinets, G., Watts, D.J., 2006. Empirical Analysis of an Evolving Social Network. *Science* 311, 88-90.
- Krackhardt, D., 1987. QAP partialling as a test of spuriousness. *Social Networks* 9, 171-186.
- Krackhardt, D., 1988. Predicting with networks: Nonparametric multiple regression analysis of dyadic data. *Social Networks* 10, 359-381.
- Kralik, P., Beran, V., Pavlik, I., 2012. Enumeration of *Mycobacterium avium* subsp. paratuberculosis by quantitative real-time PCR, culture on solid media and optical densitometry. *BMC Research Notes* 5, 114.
- Kurade, N.P., Tripathi, B.N., 2008. Lymphoproliferative response and its relationship with histological lesions in experimental ovine paratuberculosis and its diagnostic implications. *Veterinary Research Communications* 32, 107-119.
- Kurade, N.P., Tripathi, B.N., Rajukumar, K., Parihar, N.S., 2004. Sequential development of histologic lesions and their relationship with bacterial isolation, fecal shedding, and immune responses during progressive stages of experimental infection of lambs with *Mycobacterium avium* subsp paratuberculosis. *Veterinary Pathology* 41, 378-387.
- Lambeth, C., Reddacliff, L.A., Windsor, P., Abbott, K.A., McGregor, H., Whittington, R.J., 2004. Intrauterine and transmammary transmission of *Mycobacterium avium* subsp paratuberculosis in sheep. *Australian Veterinary Journal* 82, 504-508.

- Lambrecht, R.S., Carriere, J.F., Collins, M.T., 1988. A model for analyzing growth kinetics of a slowly growing *Mycobacterium* sp. *Applied and Environmental Microbiology* 54, 910-916.
- Legendre, P., Fortin, M.-J.E., 2010. Comparison of the Mantel test and alternative approaches for detecting complex multivariate relationships in the spatial analysis of genetic data. *Molecular Ecology Resources* 10, 831-844.
- Li, L., Alderson, D., Doyle, J.C., Willinger, W., 2005. Towards a Theory of Scale-Free Graphs: Definition, Properties, and Implications. *Internet Mathematics* 2, 431-523.
- Lockhart, C.Y., Stevenson, M.A., Rawdon, T.G., Gerber, N., French, N.P., 2010. Patterns of contact within the New Zealand poultry industry. *Preventive Veterinary Medicine* 95, 258-266.
- Lombard, J.E., 2011. Epidemiology and Economics of Paratuberculosis. *Veterinary Clinics of North America: Food Animal Practice* 27, 525-535.
- Lombard, J.E., Garry, F.B., McCluskey, B.J., Wagner, B.A., 2005. Risk of removal and effects on milk production associated with paratuberculosis status in dairy cows. *Journal of the American Veterinary Medical Association* 227, 1975-1981.
- Lugton, I.W., 2004. Cross-sectional study of risk factors for the clinical expression of ovine Johne's disease on New South Wales farms. *Australian Veterinary Journal* 82, 355-365.
- Mantel, N., 1967. The Detection of Disease Clustering and a Generalized Regression Approach. *Cancer Research* 27, 209-220.
- Marcé, C., Ezanno, P., Weber, M.F., Seegers, H., Pfeiffer, D.U., Fourichon, C., 2010. Invited review: Modeling within-herd transmission of *Mycobacterium avium* subspecies paratuberculosis in dairy cattle: A review. *Journal of Dairy Science* 93, 4455-4470.
- Marquetoux, N., Heuer, C., Wilson, P., Ridler, A., Stevenson, M., 2016a. Merging DNA typing and network analysis to assess the transmission of paratuberculosis between farms. *Preventive Veterinary Medicine* 134, 113-121.
- Marquetoux, N., Stevenson, M.A., Wilson, P., Ridler, A., Heuer, C., 2016b. Using social network analysis to inform disease control interventions. *Preventive Veterinary Medicine*.
- Martínez-López, B., Perez, A.M., Sánchez-Vizcaíno, J.M., 2009. Social Network Analysis. Review of General Concepts and Use in Preventive Veterinary Medicine. *Transboundary and Emerging Diseases* 56, 109-120.
- May, R.M., Lloyd, A.L., 2001. Infection dynamics on scale-free networks. *Physical Review E* 64, 066112.
- McGregor, H., 2009. Aspects of the biology, transmission and control of Ovine Johne's disease. University of Sydney.
- McGregor, H., Dhand, N.K., Dhungyel, O.P., Whittington, R.J., 2012. Transmission of *Mycobacterium avium* subsp paratuberculosis: Dose-response and age-based susceptibility in a sheep model. *Preventive Veterinary Medicine* 107, 76-84.
- Merkal, R.S., 1973. Laboratory Diagnosis of Bovine Paratuberculosis. *Journal of the American Veterinary Medical Association* 163, 1100-1103.
- Merkal, R.S., Kenneth, E.K., Larsen, A.B., Thurston, J.R., 1964. Improvements in the Techniques for Primary Cultivation of *Mycobacterium paratuberculosis*. *Am. J. Vet. Res.* 25, 1290-1293.
- Merkal, R.S., Larsen, A.B., Kopecky, K.E., Ness, R.D., 1968. Comparison of Examination and Test Methods for Early Detection of Paratuberculous Cattle. *Am. J. Vet. Res.* 29, 1533-1538.
- Miller, J.C., Davoudi, B., Meza, R., Slim, A.C., Pourbohloul, B., 2010. Epidemics with general generation interval distributions. *Journal of Theoretical Biology* 262, 107-115.
- Mitchell, R.M., Medley, G.F., Collins, M.T., Schukken, Y.H., 2011. A meta-analysis of the effect of dose and age at exposure on shedding of *Mycobacterium avium* subspecies paratuberculosis (MAP) in experimentally infected calves and cows. *Epidemiology and Infection* 140, 231-246.
- Mitchell, R.M., Schukken, Y., Koets, A., Weber, M., Bakker, D., Stabel, J., Whitlock, R.H., Louzoun, Y., 2015. Differences in intermittent and continuous fecal shedding patterns between natural and experimental *Mycobacterium avium* subspecies paratuberculosis infections in cattle. *Veterinary Research* 46, 66.

- Möbius, P., Hotzel, H., Raßbach, A., Köhler, H., 2008. Comparison of 13 single-round and nested PCR assays targeting IS900, ISMav2, f57 and locus 255 for detection of *Mycobacterium avium* subsp. paratuberculosis. *Veterinary Microbiology* 126, 324-333.
- Moher, D., Shamseer, L., Clarke, M., Ghersi, D., Liberati, A., Petticrew, M., Shekelle, P., Stewart, L., Group, P.-P., 2015. Preferred reporting items for systematic review and meta-analysis protocols (PRISMA-P) 2015 statement. *Systematic Reviews* 4, 1.
- Morris, C.A., Hickey, S.M., Henderson, H.V., 2006. The effect of Johne's disease on production traits in Romney, Merino and Merino x Romney-cross ewes. *New Zealand Veterinary Journal* 54, 204-209.
- Motiwala, A.S., Li, L., Kapur, V., Sreevatsan, S., 2006. Current understanding of the genetic diversity of *Mycobacterium avium* subsp. paratuberculosis. *Microbes and Infection* 8, 1406-1418.
- Motiwala, A.S., Strother, M., Theus, N.E., Stich, R.W., Byrum, B., Shulaw, W.P., Kapur, V., Sreevatsan, S., 2005. Rapid Detection and Typing of Strains of *Mycobacterium avium* subsp. paratuberculosis from Broth Cultures. *Journal of Clinical Microbiology* 43, 2111-2117.
- Mucha, P.J., Richardson, T., Macon, K., Porter, M.A., Onnela, J.-P., 2010. Community Structure in Time-Dependent, Multiscale, and Multiplex Networks. *Science* 328, 876-878.
- Nisbet, D.I., Brotherston, J.G., Gilmour, N.J.L., 1962. Quantitative studies of *Mycobacterium johnei* in tissues of sheep .3. Intestinal pathology. *Journal of Comparative Pathology and Therapeutics* 72, 80-&.
- O'Brien, R., Mackintosh, C.G., Bakker, D., Kopečna, M., Pavlik, I., Griffin, J.F.T., 2006. Immunological and molecular characterization of susceptibility in relationship to bacterial strain differences in *Mycobacterium avium* subsp paratuberculosis infection in the red deer (*Cervus elaphus*). *Infection and Immunity* 74, 3530-3537.
- O'Mahony, J., Hill, C., 2002. A real time PCR assay for the detection and quantitation of *Mycobacterium avium* subsp. paratuberculosis using SYBR Green and the Light Cycler. *Journal of Microbiological Methods* 51, 283-293.
- Oakey, J., Gavey, L., Singh, S.V., Platell, J., Waltisbuhl, D., 2014. Variable-number tandem repeats genotyping used to aid and inform management strategies for a bovine Johne's disease incursion in tropical and subtropical Australia. *Journal of Veterinary Diagnostic Investigation*.
- Ortiz-Pelaez, A., Pfeiffer, D.U., Soares-Magalhães, R.J., Guitian, F.J., 2006. Use of social network analysis to characterize the pattern of animal movements in the initial phases of the 2001 foot and mouth disease (FMD) epidemic in the UK. *Preventive Veterinary Medicine* 76, 40-55.
- Pastor-Satorras, R., Vespignani, A., 2001. Epidemic Spreading in Scale-Free Networks. *Physical Review Letters* 86, 3200-3203.
- Peñuelas-Urquides, K., Villarreal-Treviño, L., Silva-Ramírez, B., Rivadeneyra-Espinoza, L., Said-Fernández, S., de León, M.B., 2013. Measuring of *Mycobacterium tuberculosis* growth. A correlation of the optical measurements with colony forming units. *Brazilian Journal of Microbiology* 44, 287-289.
- Pérez, V., Marín, J.F.G., Badiola, J.J., 1996. Description and classification of different types of lesion associated with natural paratuberculosis infection in sheep. *Journal of Comparative Pathology* 114, 107-122.
- Perilla, M., Ajello, G., Bopp, C., Elliott, J., Facklam, R., 2003. Manual for the laboratory identification and antimicrobial susceptibility testing of bacterial pathogens of public health importance in the developing world. Atlanta, Georgia, United States Centers for Disease Control and Prevention [CDC], National Center for Infectious Diseases.
- Pinter-Wollman, N., Hobson, E.A., Smith, J.E., Edelman, A.J., Shizuka, D., de Silva, S., Waters, J.S., Prager, S.D., Sasaki, T., Wittemyer, G., Fewell, J., McDonald, D.B., 2013. The dynamics of animal social networks: analytical, conceptual, and theoretical advances. *Behavioral Ecology*.
- Plain, K.M., Marsh, I.B., Waldron, A.M., Galea, F., Whittington, A.-M., Saunders, V.F., Begg, D.J., de Silva, K., Purdie, A.C., Whittington, R.J., 2014. High-Throughput Direct Fecal PCR Assay for Detection of *Mycobacterium avium* subsp. paratuberculosis in Sheep and Cattle. *Journal of Clinical Microbiology* 52, 745-757.

- Ponnusamy, D., Periasamy, S., Tripathi, B.N., Pal, A., 2013. Mycobacterium avium subsp paratuberculosis invades through M cells and enterocytes across ileal and jejunal mucosa of lambs. *Research in Veterinary Science* 94, 306-312.
- Porphyre, T., Stevenson, M., Jackson, R., McKenzie, J., 2008. Influence of contact heterogeneity on TB reproduction ratio R0 in a free-living brushtail possum *Trichosurus vulpecula* population. *Vet. Res.* 39.
- Poupart, P., Coene, M., Van Heuverswyn, H., Cocito, C., 1993. Preparation of a specific RNA probe for detection of Mycobacterium paratuberculosis and diagnosis of Johne's disease. *Journal of Clinical Microbiology* 31, 1601-1605.
- Pradhan, A.K., Mitchell, R.M., Kramer, A.J., Zurakowski, M.J., Fyock, T.L., Whitlock, R.H., Smith, J.M., Hovingh, E., Van Kessel, J.A.S., Karns, J.S., Schukken, Y.H., 2011. Molecular Epidemiology of Mycobacterium avium subsp. paratuberculosis in a Longitudinal Study of Three Dairy Herds. *Journal of Clinical Microbiology* 49, 893-901.
- Preziuso, S., Magi, G.E., Renzoni, G., 2012. Detection of Mycobacterium avium subsp. paratuberculosis in intestinal and mammary tissues and in lymph nodes of sheep with different techniques and its relationship with enteric lesions. *Small Ruminant Research* 105, 295-299.
- R Development Core Team, 2014. R: A language and environment for statistical computing. R Foundation for Statistical Computing. Home page: <http://www.R-project.org/>, Vienna, Austria.
- Raizman, E.A., Espejo, L.A., 2011. Long-Term Survival of Mycobacterium avium subsp. paratuberculosis in Fecal Samples Obtained from Naturally Infected Cows and Stored at -18°C and -70°C . *Veterinary Medicine International* 2011.
- Reddacliff, L., Eppeleston, J., Windsor, P., Whittington, R., Jones, S., 2006. Efficacy of a killed vaccine for the control of paratuberculosis in Australian sheep flocks. *Veterinary Microbiology* 115, 77-90.
- Reddacliff, L.A., 2002. Aspects of the Pathogenesis of Ovine Johne's Disease. Faculty of Veterinary Science. University of Sydney, New South Wales, Australia.
- Reddacliff, L.A., McGregor, H., Abbott, K., Whittington, R.J., 2004. Field evaluation of tracer sheep for the detection of early natural infection with Mycobacterium avium subsp paratuberculosis. *Australian Veterinary Journal* 82, 426-433.
- Reddacliff, L.A., Nicholls, P.J., Vadali, A., Whittington, R.J., 2003a. Use of Growth Indices from Radiometric Culture for Quantification of Sheep Strains of Mycobacterium avium subsp. paratuberculosis. *Applied and Environmental Microbiology* 69, 3510-3516.
- Reddacliff, L.A., Vadali, A., Whittington, R.J., 2003b. The effect of decontamination protocols on the numbers of sheep strain Mycobacterium avium subsp. paratuberculosis isolated from tissues and faeces. *Veterinary Microbiology* 95, 271-282.
- Reddacliff, L.A., Whittington, R.J., 2003. Experimental infection of weaner sheep with S strain Mycobacterium avium subsp paratuberculosis. *Veterinary Microbiology* 96, 247-258.
- Reviriego, F.J., Moreno, M.A., Domínguez, L., 2000. Soil type as a putative risk factor of ovine and caprine paratuberculosis seropositivity in Spain. *Preventive Veterinary Medicine* 43, 43-51.
- Riley, R.D., Lambert, P.C., Abo-Zaid, G., 2010. Meta-analysis of individual participant data: rationale, conduct, and reporting. *BMJ* 340.
- Robins, G., 2013. A tutorial on methods for the modeling and analysis of social network data. *Journal of Mathematical Psychology* 57, 261-274.
- Robins, G., Pattison, P., Kalish, Y., Lusher, D., 2007. An introduction to exponential random graph (p*) models for social networks. *Social Networks* 29, 173-191.
- Robinson, S.E., Everett, M.G., Christley, R.M., 2007. Recent network evolution increases the potential for large epidemics in the British cattle population. *Journal of The Royal Society Interface* 4, 669-674.
- Rocca, S., Cubeddu, T., Nieddu, A.M., Pirino, S., Appino, S., Antuofermo, E., Tanda, F., Verin, R., Sechi, L.A., Taccini, E., Leoni, A., 2010. Detection of Mycobacterium avium spp. paratuberculosis

- (Map) in samples of sheep paratuberculosis (Johne's disease or JD) and human Crohn's disease (CD) using liquid phase RT-PCR, in situ RT-PCR and immunohistochemistry. *Small Ruminant Research* 88, 126-134.
- Rowe, M.T., Grant, I.R., 2006. *Mycobacterium avium* ssp. paratuberculosis and its potential survival tactics. *Letters in Applied Microbiology* 42, 305-311.
- Sanson, R.L., 2005. A survey to investigate movements off sheep and cattle farms in New Zealand, with reference to the potential transmission of foot-and-mouth disease. *New Zealand Veterinary Journal* 53, 223-233.
- Scott, J., 2013. *Social Network Analysis*, third edition. SAGE Publications Ltd
- Semret, M., Turenne, C.Y., Behr, M.A., 2006. Insertion Sequence IS900 Revisited. *Journal of Clinical Microbiology* 44, 1081-1083.
- Sergeant, E., 2002. Development of computer models to describe the epidemiology of Johne's disease in sheep.
- Sergeant, E.S.G., Marshall, D.J., Eamens, G.J., Kearns, C., Whittington, R.J., 2003. Evaluation of an absorbed ELISA and an agar-gel immuno-diffusion test for ovine paratuberculosis in sheep in Australia. *Preventive Veterinary Medicine* 61, 235-248.
- Sevilla, I.A., Garrido, J.M., Molina, E., Geijo, M.V., Elguezabal, N., Vázquez, P., Juste, R.A., 2014. Development and Evaluation of a Novel Multicopy-Element-Targeting Triplex PCR for Detection of *Mycobacterium avium* subsp. paratuberculosis in Feces. *Applied and Environmental Microbiology* 80, 3757-3768.
- Shin, S.J., Han, J.H., Manning, E.J.B., Collins, M.T., 2007. Rapid and Reliable Method for Quantification of *Mycobacterium paratuberculosis* by Use of the BACTEC MGIT 960 System. *Journal of Clinical Microbiology* 45, 1941-1948.
- Shirley, M.D.F., Rushton, S.P., 2005. Where Diseases and Networks Collide: Lessons to be Learnt from a Study of the 2001 Foot-and-Mouth Disease Epidemic. *Epidemiology and Infection* 133, 1023-1032.
- Simmonds, M.C., Higginsa, J.P.T., Stewartb, L.A., Tierneyb, J.F., Clarke, M.J., Thompson, S.G., 2005. Meta-analysis of individual patient data from randomized trials: a review of methods used in practice. *Clinical Trials* 2, 209-217.
- Skuce, R.A., Allen, A.R., McDowell, S.W.J., 2012. Herd-Level Risk Factors for Bovine Tuberculosis: A Literature Review. *Veterinary Medicine International* 2012, 10.
- Smeed, J.A., Watkins, C.A., Gossner, A.G., Hopkins, J., 2010. Expression profiling reveals differences in immuno-inflammatory gene expression between the two disease forms of sheep paratuberculosis. *Veterinary Immunology and Immunopathology* 135, 218-225.
- Smeed, J.A., Watkins, C.A., Rhind, S.M., Hopkins, J., 2007. Differential cytokine gene expression profiles in the three pathological forms of sheep paratuberculosis. *BMC Veterinary Research* 3, 1-11.
- Smith, H.W., 1953. Modifications of Dubos's media for the cultivation of *Mycobacterium johnei*. *The Journal of Pathology and Bacteriology* 66, 375-381.
- Smith, R.L., Strawderman, R.L., Schukken, Y.H., Wells, S.J., Pradhan, A.K., Espejo, L.A., Whitlock, R.H., Van Kessel, J.S., Smith, J.M., Wolfgang, D.R., Gröhn, Y.T., 2010. Effect of Johne's disease status on reproduction and culling in dairy cattle. *Journal of Dairy Science* 93, 3513-3524.
- Snijders, T.A.B., 2011. *Statistical Models for Social Networks*. In: Cook, K.S., Massey, D.S. (Eds.), *Annual Review of Sociology*, Vol 37. Annual Reviews, Palo Alto, 131-153.
- Snijders, T.A.B., Pattison, P.E., Robins, G.L., Handcock, M.S., 2006. New specifications for Exponential Random Graphs Models *Sociological Methodology* 36, 99-153.
- Stabel, J.R., Steadham, E.M., Bolin, C.A., 1997. Heat inactivation of *Mycobacterium paratuberculosis* in raw milk: are current pasteurization conditions effective? *Applied and Environmental Microbiology* 63, 4975-4977.
- Stevenson, K., 2015. Genetic diversity of *Mycobacterium avium* subspecies paratuberculosis and the influence of strain type on infection and pathogenesis: a review. *Veterinary Research* 46, 64.

- Stevenson, K., Hughes, V.M., de Juan, L., Inglis, N.F., Wright, F., Sharp, J.M., 2002. Molecular Characterization of Pigmented and Nonpigmented Isolates of *Mycobacterium avium* subsp. paratuberculosis. *Journal of Clinical Microbiology* 40, 1798-1804.
- Stewart, D.J., Vaughan, J.A., Stiles, P.L., Noske, P.J., Tizard, M.L.V., Prowse, S.J., Michalski, W.P., Butler, K.L., Jones, S.L., 2004. A long-term study in Merino sheep experimentally infected with *Mycobacterium avium* subsp paratuberculosis: clinical disease, faecal culture and immunological studies. *Veterinary Microbiology* 104, 165-178.
- Stewart, D.J., Vaughan, J.A., Stiles, P.L., Noske, P.J., Tizard, M.L.V., Prowse, S.J., Michalski, W.P., Butler, K.L., Jones, S.L., 2007. A long-term bacteriological and immunological study in Holstein-Friesian cattle experimentally infected with *Mycobacterium avium* subsp paratuberculosis and necropsy culture results for Holstein-Friesian cattle, Merino sheep and Angora goats. *Veterinary Microbiology* 122, 83-96.
- Sweeney, R.W., 1996. Transmission of paratuberculosis. *The Veterinary clinics of North America. Food animal practice* 12, 305-312.
- Tasara, T., Hoelzle, L.E., Stephan, R., 2005. Development and evaluation of a *Mycobacterium avium* subspecies paratuberculosis (MAP) specific multiplex PCR assay. *International Journal of Food Microbiology* 104, 279-287.
- Taylor, A.W., 1951. Varieties of *Mycobacterium johnei* isolated from sheep. *The Journal of Pathology and Bacteriology* 63, 333-336.
- Therneau, T.M., Lumley, T., 2016. Package 'survival'.
- Thibault, V.C., Grayon, M., Boschioli, M.L., Hubbans, C., Overduin, P., Stevenson, K., Gutierrez, M.C., Supply, P., Biet, F., 2007. New Variable-Number Tandem-Repeat Markers for Typing *Mycobacterium avium* subsp. paratuberculosis and *M. avium* Strains: Comparison with IS900 and IS1245 Restriction Fragment Length Polymorphism Typing. *Journal of Clinical Microbiology* 45, 2404-2410.
- Thibault, V.C., Grayon, M., Boschioli, M.L., Willery, E., Allix-Béguet, C., Stevenson, K., Biet, F., Supply, P., 2008. Combined Multilocus Short-Sequence-Repeat and Mycobacterial Interspersed Repetitive Unit-Variable-Number Tandem-Repeat Typing of *Mycobacterium avium* subsp. paratuberculosis Isolates. *Journal of Clinical Microbiology* 46, 4091-4094.
- Thompson, K.G., West, D.M., Anderson, P.V.A., Burnham, D.L., 2002. Subclinical Johne's Disease in Sheep. *New Zealand Society of Animal Production*.
- Thorel, M.F., Vialard, J., Manfroni, F., Bernardot, J., Ostyn, A., Vandeveld, J., 1992. Experimental paratuberculosis in sheep after oral or intravenous inoculation - Pathogenicity and biological diagnosis. *Annales De Recherches Veterinaires* 23, 105-115.
- VanderWaal, K.L., Atwill, E.R., Isbell, L.A., McCowan, B., 2014. Linking social and pathogen transmission networks using microbial genetics in giraffe (*Giraffa camelopardalis*). *Journal of Animal Ecology* 83, 406-414.
- Verdugo, C., 2013. Epidemiology of *Mycobacterium avium* subspecies paratuberculosis infection on sheep, beef cattle and deer farms in New Zealand. Institute of Veterinary, Animal and Biomedical Sciences. Massey University, Palmerston North, New Zealand.
- Verdugo, C., Jones, G., Johnson, W., Wilson, P., Stringer, L., Heuer, C., 2014a. Estimation of flock/herd-level true *Mycobacterium avium* subspecies paratuberculosis prevalence on sheep, beef cattle and deer farms in New Zealand using a novel Bayesian model. *Preventive Veterinary Medicine* 117, 447-455.
- Verdugo, C., Pleydell, E., Price-Carter, M., Prattley, D., Collins, D., de Lisle, G., Vogue, H., Wilson, P., Heuer, C., 2014b. Molecular epidemiology of *Mycobacterium avium* subsp. paratuberculosis isolated from sheep, cattle and deer on New Zealand pastoral farms. *Preventive Veterinary Medicine* 117, 436-446.
- Verdugo, C., Wilson, P.R., Heuer, C., 2008. Association between species combination on-farm and *Mycobacterium* - like lesions in deer at slaughter. *Proceedings of the Deer Branch of the New Zealand Veterinary Association* 25, 69-72.

- Verna, A.E., Garcia-Pariente, C., Munoz, M., Moreno, O., Garcia-Marin, J.F., Romano, M.I., Paolicchi, F., Perez, V., 2007. Variation in the immuno-pathological responses of lambs after experimental infection with different strains of *Mycobacterium avium* subsp. *paratuberculosis*. *Zoonoses and Public Health* 54, 243-252.
- Vernon, M.C., 2011. Demographics of cattle movements in the United Kingdom. *BMC Veterinary Research* 7, 31-31.
- Vernon, M.C., Keeling, M.J., 2009. Representing the UK's cattle herd as static and dynamic networks. *Proceedings of the Royal Society B: Biological Sciences* 276, 469-476.
- Vestergaard, C.L., Génois, M., 2015. Temporal Gillespie Algorithm: Fast Simulation of Contagion Processes on Time-Varying Networks. *PLoS Computational Biology* 11, e1004579.
- Volkova, V.V., Howey, R., Savill, N.J., Woolhouse, M.E.J., 2010. Sheep Movement Networks and the Transmission of Infectious Diseases. *PLoS ONE* 5, e11185.
- Waddell, L.A., Rajić, A., StÄrk, K.D.C., McEwen, S.A., 2015. The zoonotic potential of *Mycobacterium avium* ssp. *paratuberculosis*: a systematic review and meta-analyses of the evidence. *Epidemiology and Infection* 143, 3135-3157.
- Watts, D.J., Strogatz, S.H., 1998. Collective dynamics of 'small-world' networks. *Nature* 393, 440-442.
- Welch, D., 2011. Is Network Clustering Detectable in Transmission Trees? *Viruses* 3, 659-676.
- Whittington, R.J., Marsh, I., McAllister, S., Turner, M.J., Marshall, D.J., Fraser, C.A., 1999. Evaluation of Modified BACTEC 12B Radiometric Medium and Solid Media for Culture of *Mycobacterium avium* subsp. *paratuberculosis* from Sheep. *Journal of Clinical Microbiology* 37, 1077-1083.
- Whittington, R.J., Marshall, D.J., Nicholls, P.J., Marsh, I.B., Reddacliff, L.A., 2004. Survival and Dormancy of *Mycobacterium avium* subsp. *paratuberculosis* in the Environment. *Applied and Environmental Microbiology* 70, 2989-3004.
- Whittington, R.J., Reddacliff, L.A., Marsh, I., McAllister, S., Saunders, V., 2000. Temporal patterns and quantification of excretion of *Mycobacterium avium* subsp. *paratuberculosis* in sheep with Johne's disease. *Australian Veterinary Journal* 78, 34-37.
- Whittington, R.J., Sergeant, E., 2001. Progress towards understanding the spread, detection and control of *Mycobacterium avium* subsp. *paratuberculosis* in animal populations. *Australian Veterinary Journal* 79, 267-278.
- Whittington, R.J., Taragel, C.A., Ottaway, S., Marsh, I., Seaman, J., Fridriksdottir, V., 2001. Molecular epidemiological confirmation and circumstances of occurrence of sheep (S) strains of *Mycobacterium avium* subsp. *paratuberculosis* in cases of paratuberculosis in cattle in Australia and sheep and cattle in Iceland. *Veterinary Microbiology* 79, 311-322.
- Whittington, R.J., Whittington, A.-M., Waldron, A., Begg, D.J., de Silva, K., Purdie, A.C., Plain, K.M., 2013. Development and Validation of a Liquid Medium (M7H9C) for Routine Culture of *Mycobacterium avium* subsp. *paratuberculosis* To Replace Modified Bactec 12B Medium. *Journal of Clinical Microbiology* 51, 3993-4000.
- Williams, E.S., Snyder, S.P., Martin, K.L., 1983. Experimental infection of some North-American wild ruminants and domestic sheep with *Mycobacterium paratuberculosis* - Clinical and Bacteriological findings. *Journal of Wildlife Diseases* 19, 185-191.
- Windsor, P., 2006a. Research into vaccination against ovine Johne's disease in Australia. *Small Ruminant Research* 62, 139-142.
- Windsor, P.A., 2013. Understanding the efficacy of vaccination in controlling ovine paratuberculosis. *Small Ruminant Research*.
- Windsor, P.A., 2014. Managing control programs for ovine caseous lymphadenitis and paratuberculosis in Australia, and the need for persistent vaccination. *Veterinary Medicine: Research & Reports* 5, 11-22.
- Windsor, P.A., Whittington, R.J., 2010. Evidence for age susceptibility of cattle to Johne's disease. *The Veterinary Journal* 184, 37-44.
- Windsor, R., 2006b. Research into vaccination against ovine Johne's disease in Australia. *Small Ruminant Research* 62, 139-142.

- Wood, S.N., 2003. Thin Plate Regression Splines. *Journal of the Royal Statistical Society. Series B (Statistical Methodology)* 65, 95-114.
- Wood, S.N., 2006. *Generalized Additive Models: an introduction with R*.
- Woolhouse, M.E.J., Dye, C., Etard, J.F., Smith, T., Charlwood, J.D., Garnett, G.P., Hagan, P., Hi, J.L.K., Ndhlovu, P.D., Quinnell, R.J., Watts, C.H., Chandiwana, S.K., Anderson, R.M., 1997. Heterogeneities in the transmission of infectious agents: Implications for the design of control programs. *Proc. Natl. Acad. Sci. USA* Vol. 94 pp. 338-342.
- Woolhouse, M.E.J., Shaw, D.J., Matthews, L., Liu, W.-C., Mellor, D.J., Thomas, M.R., 2005. Epidemiological implications of the contact network structure for cattle farms and the 20–80 rule. *Biology Letters* 1, 350-352.
- Worby, C.J., Lipsitch, M., Hanage, W.P., 2014. Within-Host Bacterial Diversity Hinders Accurate Reconstruction of Transmission Networks from Genomic Distance Data. *PLoS Computational Biology* 10, e1003549.
- Yun, J.J., Heisler, L.E., Hwang, I.I.L., Wilkins, O., Lau, S.K., Hycza, M., Jayabalasingham, B., Jin, J., McLaurin, J., Tsao, M.-S., Der, S.D., 2006. Genomic DNA functions as a universal external standard in quantitative real-time PCR. *Nucleic Acids Research* 34, e85-e85.

Chapter 10. Appendices

10.1 Appendix A (Chapter 3)

10.1.1A.1. Inter-dependencies and hypothesis testing in social network analysis

Dyadic observations are inherently dependent (Dekker et al., 2007) and therefore structural auto-correlation is present in the data. Sources of dependency include (but are not limited to):

1. Reciprocity: “the presence of a tie from i to j may increase the chances of a tie from j to i , irrespective of nodal attributes” (Robins, 2013). For instance, if farm i sends animals to farm j , it may be more likely that animals are also moved from farm j to farm i . Specifically on pastoral farms in New Zealand and LD farms in particular, a common practice consists in transferring young stock for periods of time to farms with good pasture availability and later return them to their farm of origin for their productive life; this results in a high reciprocity in the contact pattern (Marquetoux et al., 2016b).
2. Transitivity: Snijders (2011) states: “if there is a tendency toward transitivity, the existence of the two ties $X_{ij} = X_{jh} = 1$ will lead to an increased probability of the tie $X_{ih} = 1$, the closure of the triangle”. For example if farm i and j share common strains of MAP and so do farm j and h , it necessarily follows that farm i and h also share common strains of MAP.
3. Row/column auto-correlation (also called “sender” and “receiver” effects): all observations within one row/column of a matrix pertain to the same social player, hence they would be correlated if this social player presents specific features that can result in popularity or expensiveness (Carrington et al., 2005; Scott, 2013). In the case of a sociomatrix of livestock movements, a finishing farm might have a high number of on-farm livestock movements and very few off-farm movements to other farms, whereas breeding farms would present the opposite pattern.
4. Block auto-correlation that can arise when a social tie represents the fact of sharing similar categorical attributes (for example, a matrix representing whether any two farms host the same livestock species will harbour block auto-correlation for groups of farms of the same versus different production type).

For this kind of dependent data, standard testing procedures can produce inflated type 1 errors to the point of “rendering significance tests unusable for all practical purposes” (Dekker et al., 2007). Ordinary least squares or logistic regression on network data produce accurate estimates for measures of association, but alternative methods are required to appropriately evaluate the uncertainty around these measures of associations.

All inferences in this study were therefore based upon a non-parametric permutation method derived from the Mantel test (Mantel, 1967) developed for testing spurious relationships between network variables organised in sociomatrices (Krackardt, 1987). This procedure specifically addresses the statistical issue of dependency arising in pairwise relationships and was generalised for multivariable regression as the Multiple Regression Quadratic Assignment Procedure (MR-QAP) (Krackardt, 1988). The principle is to test whether nodes tend to be assigned to certain positions within a network matrix, hence the coined term of “QAP” (Hubert and Schultz, 1976).

10.1.2A.2. Results of univariate analysis

The crude associations showed that all distance measures, whether network related (SPL) or spatial distance, were negatively associated sharing the same strains and were significant at an alpha level of 0.05 (Table A1). Two farms tended to harbour the same MAP strain when they were close, belonged to the same network community, hosted the same livestock species or were located on the same island. P-values of standard statistical tests were smaller than p-values from QAP, except for spatial distance. This suggests that dependencies between observations existed in the network matrices so that classical significance tests resulted in erroneously small p-values. The MR-QAP procedure inflated p-values and thus accounted for these dependencies although the inferences remained the same with both methods.

Table A1: Crude analysis of predictors for any two farms harbouring the same VNTR/SSR type of MAP (p-value for the odds ratio (OR) calculated using univariable QAP, with p-value obtained by standard logistic regression assuming independence between dyads provided as a comparison)

Predictor	OR	Standard p-value	QAP p-value*
Undirected SPL	0.4 ^a	1.81e-11	< 0.0001
Directed SPL	0.5	< 2e-16	< 0.0001
Same community	3.0	4.14e-07	0.0004
Same species	4.9 ^b	2.29e-12	< 0.0001
Same island	2.6	7.36e-07	0.002
Spatial distance (on a 100 km scale)	0.95	0.049	0.049

* MC p-values, note that it is not possible to directly obtain standard error estimates with this method.

^a interpretation: For each additional step along the shortest undirected path between farms (following livestock movement event records), the odds that two farms shared the same strains of MAP decreased by a factor 0.4.

^b interpretation: if a pair of farms hosted the same livestock species, the odds of harbouring the same MAP strains were 4.9 times as high as when they hosted different species.

10.1.3 A.3. Supplementary Figures

Source farm	Destination farm	Directed SPL	Un-directed SPL
A	B	2	1
B	A	1	1
A	C	1	1
C	A	2	1
B	C	1	1
C	B	1	1
A	D	NA	2
D	A	3	2
B	D	NA	2
D	B	2	2
C	D	NA	1
D	C	1	1

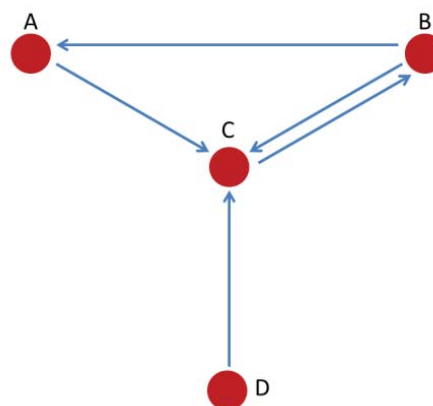


Figure A1: Examples of the calculation of the directed and un-directed shortest path length (SPL) in a theoretical network of four farms (red circles) linked by livestock movements (blue arrows).

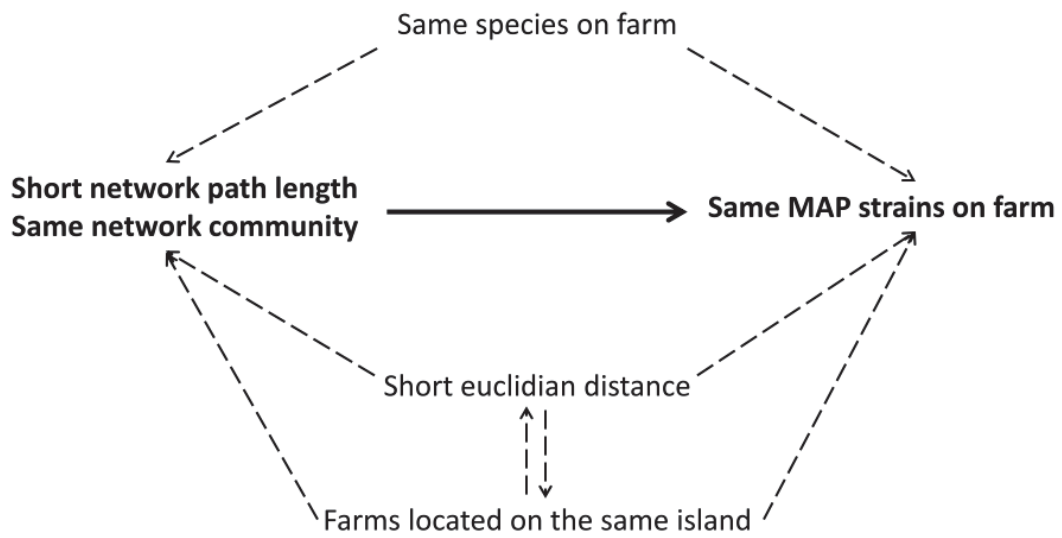


Figure A2: Hypothesized causal diagram (in bold the association of interest, in dashed possible confounding effects)

10.2 Appendix B (Chapter 6)

An important result of Chapter 6 was that the probability of being histology positive after inoculation was accurately fitted with a Weibull cumulative probability function. This modelled a rate of infection (corresponding to the transmission parameter in a SIR model) increasing with time since inoculation, after adjusting for the age of the sheep at exposure.

The “standard” way to model transitions in a compartmental model is to assume a constant rate (exponential distribution of time to transition). Implementing rates varying with time since exposure in compartmental models is not trivial and cannot be achieved through a standard Ordinary Differential Equations (ODE) system (Miller et al., 2010). Instead, it requires shifting to partial differential equations (Keyfitz and Keyfitz, 1997), or individual-based modelling in systems that can keep track of time (Vestergaard and Génois, 2015), instead of ODE or Markov chains.

In order to fit a simpler ODE model, we need to fit the probability of active infection with an exponential distribution (constant rate of becoming infected over time).

10.2.1 B.1. Method 1: overall fit

We used the same methods as described in 3.1.1 (Figure B1) but assuming that k in Equation 1 was equal to one, which corresponded to an exponential distribution (constant rate of infection over time). Hence the regression performed to determine the parameter α_{dose} (Figure B1 c.) was:

$$\log(1 - P_1(T < t)_{dose}) = -\alpha_{dose} * time$$

Equation B1

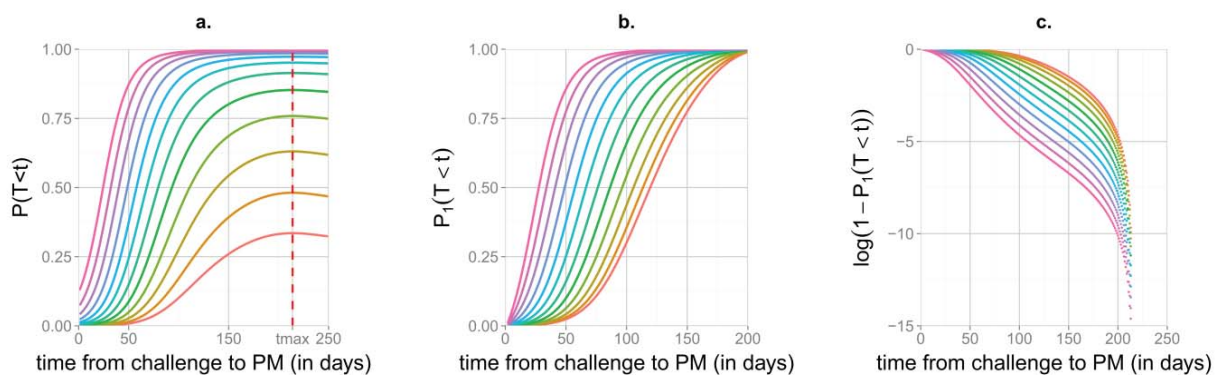


Figure B1: Predicted proportion of sheep with histological lesions of PTB over time from model1 (a) and Exponential model (b= scaling to one, c=transformation to a linear form) stratified by increasing MAP challenge dose 10 to 10^{12} MAP (ovine MAP strain, tissue homogenate inoculum).

This method is fitting an exponential distribution to the whole curve of observed probability of active infection. We obtained the results observed in Figure B2.

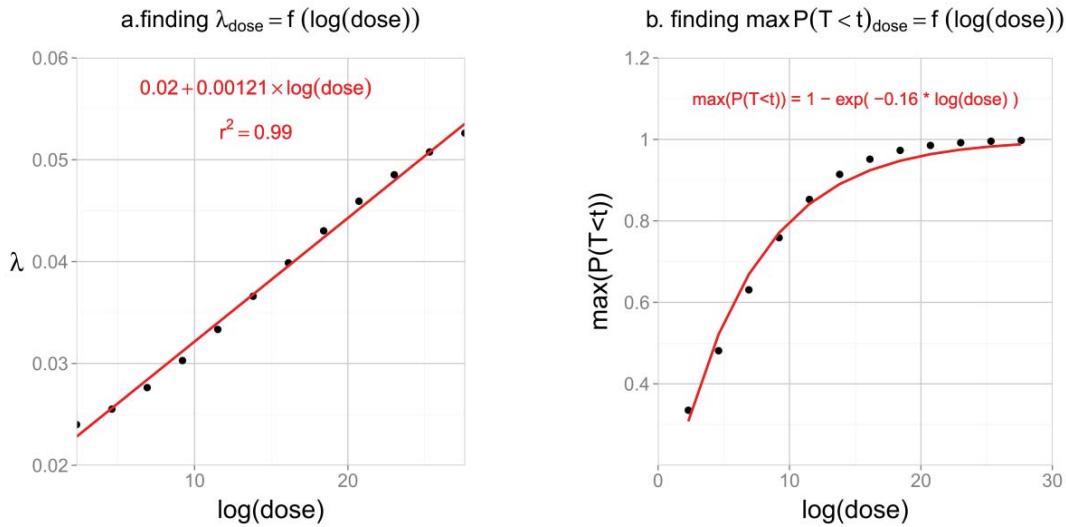


Figure B2: Relationships between the dose-dependent Exponential parameters α_{dose} and the dose-dependent plateau $\max(P(T < t))_{\text{dose}}$ and the inoculum dose to model the probability of active infection as a function of time from inoculation to *post-mortem* (method 1).

10.2.2B.2. Method 2: fitting using the median time

An alternative method was to use the median time to infection (t_{50}) to estimate the corresponding exponential parameter, according to:

$$\alpha = \frac{\log\left(\frac{100}{50}\right)}{t_{50}} \quad \text{Equation B2}$$

We estimated t_{50} from the predicted probabilities of *model 1* for each dose, then estimated the corresponding α and fitted a simple mathematical transformation to the observed relationship (Figure B3 a).

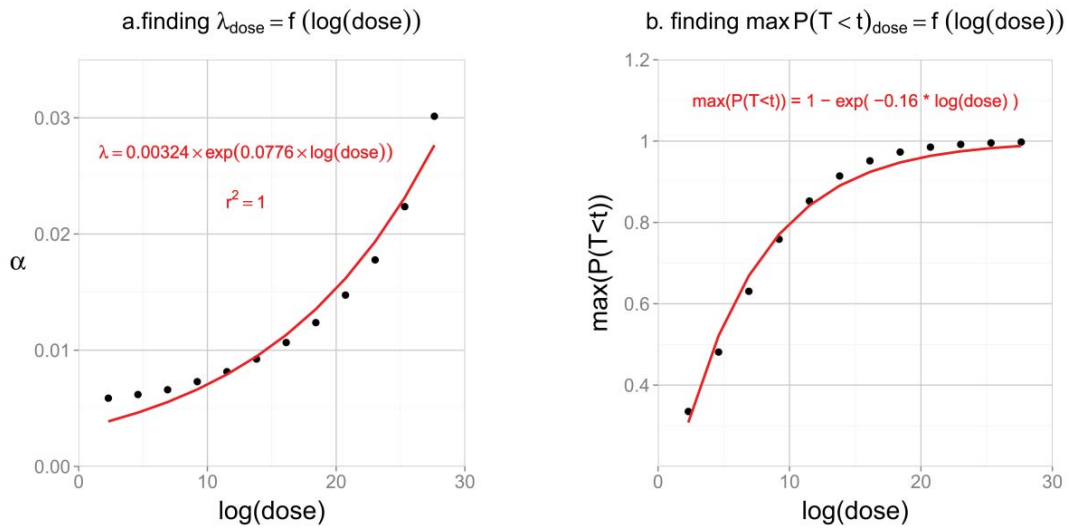


Figure B3: Relationships between the dose-dependent Exponential parameters α_{dose} and the dose-dependent plateau $\max(P(T < t))_{\text{dose}}$ and the inoculum dose to model the probability of active infection as a function of time from inoculation to *post-mortem* (method 2).

This method is fitting an exponential distribution to the observed data using the median time only, rather than fitting the overall shape (which is not well suited for an exponential fit).

10.2.3 B.3. Results

Irrespective of the method chosen to evaluate the rate of infection, the observed dose-dependent plateau of infection was always the same. The method to fit the plateau as a function of inoculum dose was described in section 6.3.3.1 of Chapter 3 and raised the equation:

$$\max(P(T < t)) = 1 - \exp(-0.16 * \log(\text{dose})) \quad (\text{adjusted } r^2 = 0.992)$$

The equation for the exponential parameter α as a function of dose depended on the method used:

Method 1: $\alpha = 0.02 + 0.00121 * \log(\text{dose}) \quad (\text{adjusted } r^2 = 0.992)$

Method 2: $\alpha = 0.00324 * \exp(0.0776 * \log(\text{dose})) \quad (\text{adjusted } r^2 = 1)$

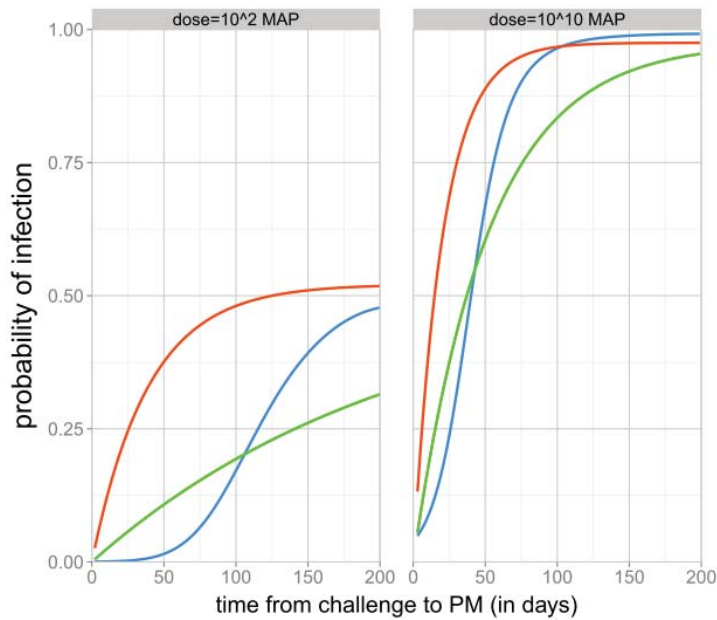


Figure B4: Estimated probability of active infection versus time since exposure for two different inoculum doses showing data-driven predictions (obtained from *model 1* in blue) or simulated (fitted using method 1 in red and method 2 in green).

Figure B4 shows that an exponential distribution is a poor fit for the observed distribution obtained on the predicted probabilities from *model 1*. Method 1 (in red) is an overall fit, thus closer to the observed behaviour (in blue) near the plateau, however, underestimates the time to infection greatly for nearly all individuals, especially at lower doses. Method 2 (in green) accurately captures the median time to infection, hence underestimating time to infection in the early stage and overestimating it after t_{50} . The plateau of infection is therefore reached later than that of the observed curve (in blue).

10.3 Appendix C (Chapter 7)

10.3.1 C.1. Model Ordinary Differential Equations

We explicitly present here the system of ODE depicted in Figure 2 of Chapter 7.

$$\frac{dE_{age}}{dt}(t) = -\lambda(DA_{age}) \cdot [E_{age}(t) - (1 - plateau(DA_{age})) \cdot E_{age,0}] - \mu_{age} \cdot E_{age}$$

$$\frac{dP_{age}}{dt}(t) = +\lambda(DA_{age}) \cdot \chi_{age}(DA_{age}) \cdot [E_{age}(t) - (1 - plateau(DA_{age})) \cdot E_{age,0}] - \delta \cdot P_{age}(t) - \mu_{age} \cdot P_{age}$$

$$\frac{dN_{age}}{dt}(t) = +\lambda(DA_{age}) \cdot [1 - \chi_{age}(DA_{age})] \cdot [E_{age}(t) - (1 - plateau(DA_{age})) \cdot E_{age,0}] - \gamma_{age} \cdot N_{age}(t)$$

$$\frac{dA_{age}}{dt}(t) = +\delta \cdot P_{age}(t) - (\mu_{age} + \mu_c) \cdot A_{age}$$

$$\frac{dR_{age}}{dt}(t) = +\gamma_{age} \cdot P_{age}(t) - \mu_{age} \cdot R_{age}$$

$$\begin{aligned} \frac{dEnv_{pasture}}{dt}(t) &= -(C + \psi) \cdot Env_{pasture} + \sigma_{low} \cdot \sum_{age \in pasture} (P_{age} + N_{age}) \\ &+ \sigma_{high} \cdot \sum_{age \in pasture} A_{age} \end{aligned}$$

where

- $age \in \{\text{lamb, hogget, two-tooth, ewe}\}$, the age group of sheep.
- $pasture \in \{\text{lamb+ewe (e-l), hogget (h), two-tooth (tt)}\}$, the age-specific pasture block.
- The model compartments E, N, P, A, R, Env are defined in Figure 2 of Chapter 7.
- DA_{age} is the daily dose of MAP per sheep available through grazing, calculated according to Equation 1 in section 1.2. of Chapter 7
- λ is the dose-dependent rate of infection. The force of infection $F_{(Env)}$ is then $\lambda(DA_{age}) \cdot [E_{age}(t) - (1 - plateau_{DA_{age}}) \cdot E_{age,0}]$, with $plateau$ the dose-dependent limit of cumulative infection and $E_{age,0}$ is the initial population at risk used to code the plateau effect.
- μ_{age} is the age-specific natural mortality, and μ_c is the mortality due to clinical PTB in the Affected compartment.

- χ_{age} is proportion of infected entering the progressor track.
- δ is the progression rate from P to A.
- γ_{age} is the rate of recovery from N to R.
- C is the proportion of viable MAP present on pasture being orally ingested by sheep through grazing and ψ is the decay rate of MAP in the environment. $\sigma_{low}/\sigma_{high}$ are the low/high shedding rates.

Parameter value and equations for the dose-dependent parameters are specified in Algorithm (I).

Initial conditions for the system of ODEs are updated at each demographics event according to Algorithm (II).

The system of ODEs above is solved using a first order Euler approximation. It leads to update equations for model compartments presented in Algorithm (I).

10.3.2 C.2. Euler method: first order approximation of ODE solutions

Given (1) the complexity of computing exact solutions for the system of ODEs presented above and (2) the many demographics events which involved new initial conditions, we used the Euler method to approximate the exact solutions. The principle is explained below with a simple example.

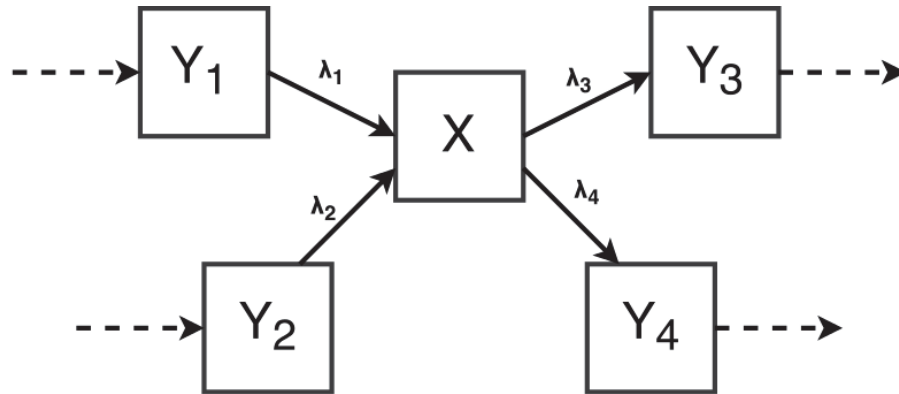


Figure C1: illustrative compartmental model

The differential equation driving the infinitesimal change in the compartment X above (Figure C1) is:

$$\frac{dX}{dt}(t) = \lambda_1 \cdot Y_1 + \lambda_2 \cdot Y_2 - \lambda_3 \cdot X - \lambda_4 \cdot X \text{ and } X(t_0) = X_0$$

with λ 's representing the transition rates. The Euler method is an approximation of the exact solution of this equation, straightforward to implement due to an explicit formulation. If X is differentiable, it is possible to write:

$$X(t + dt) = X(t) + \frac{1}{1!} dt \frac{dX}{dt}(t) + o(dt)$$

where $o(dt)$ can be assumed negligible compared to dt . The increment in X can thus be approximated using an incremental numerical solver for X(t) at time steps $t_0, t_0+dt, t_0+2 \cdot dt, \dots$ from the initial condition at t_0 .

If $dt = 1$ (daily update):

$$\begin{aligned} X(t + 1) &= X(t) + \frac{1}{1!} \frac{dX}{dt}(t) + o(1) \\ &\approx X(t) + \frac{1}{1!} \frac{dX}{dt}(t) \\ &= X(t) + \lambda_1 \cdot Y_1 + \lambda_2 \cdot Y_2 - \lambda_3 \cdot X - \lambda_4 \cdot X \end{aligned}$$

This approximation is used to daily update the model compartments with respect to infection and mortality as presented in Algorithm (I).

$\mathbf{E}(i) <- \mathbf{E}(i-1) - \lambda_i \cdot [\mathbf{E}(i-1)] - (1 - \text{plateau}_i) \cdot \mathbf{E}_{i,ol}$ $\mathbf{P}(i) <- \mathbf{P}(i-1) + \chi_i \cdot \lambda_i \cdot [\mathbf{E}(i-1)] - (1 - \text{plateau}_i) \cdot \mathbf{E}_{i,ol} - \delta \cdot \mathbf{P}(i-1)$ $\mathbf{A}(i) <- \mathbf{A}(i-1) + \delta \cdot \mathbf{P}(i-1)$ $\mathbf{N}(i) <- \mathbf{N}(i-1) + (1 - \chi_i) \cdot \lambda_i \cdot [\mathbf{E}(i-1)] - (1 - \text{plateau}_i) \cdot \mathbf{E}_{i,ol} - \psi_i \cdot \mathbf{N}(i-1)$ $\mathbf{R}(i) <- \mathbf{R}(i-1) + \psi_i \cdot \mathbf{N}(i-1)$	$\mathbf{E}_h(i) <- \mathbf{E}_h(i-1) - \lambda_h \cdot [\mathbf{E}_h(i-1)] - (1 - \text{plateau}_{u_h}) \cdot \mathbf{E}_{h,ol}$ $\mathbf{P}_h(i) <- \mathbf{P}_h(i-1) + \chi_h \cdot \lambda_h \cdot [\mathbf{E}_h(i-1)] - (1 - \text{plateau}_{u_h}) \cdot \mathbf{E}_{h,ol} - \delta \cdot \mathbf{P}_h(i-1)$ $\mathbf{A}_h(i) <- \mathbf{A}_h(i-1) + \delta \cdot \mathbf{P}_h(i-1)$ $\mathbf{N}_h(i) <- \mathbf{N}_h(i-1) + (1 - \chi_h) \cdot \lambda_h \cdot [\mathbf{E}_h(i-1)] - (1 - \text{plateau}_{u_h}) \cdot \mathbf{E}_{h,ol} - \psi_h \cdot \mathbf{N}_h(i-1)$ $\mathbf{R}_h(i) <- \mathbf{R}_h(i-1) + \psi_h \cdot \mathbf{N}_h(i-1)$	$\mathbf{E}_{tt}(i) <- \mathbf{E}_{tt}(i-1) - \lambda_{tt} \cdot [\mathbf{E}_{tt}(i-1)] - (1 - \text{plateau}_{u_{tt}}) \cdot \mathbf{E}_{tt,ol}$ $\mathbf{P}_{tt}(i) <- \mathbf{P}_{tt}(i-1) + \chi_{tt} \cdot \lambda_{tt} \cdot [\mathbf{E}_{tt}(i-1)] - (1 - \text{plateau}_{u_{tt}}) \cdot \mathbf{E}_{tt,ol} - \delta \cdot \mathbf{P}_{tt}(i-1)$ $\mathbf{A}_{tt}(i) <- \mathbf{A}_{tt}(i-1) + \delta \cdot \mathbf{P}_{tt}(i-1)$ $\mathbf{N}_{tt}(i) <- \mathbf{N}_{tt}(i-1) + (1 - \chi_{tt}) \cdot \lambda_{tt} \cdot [\mathbf{E}_{tt}(i-1)] - (1 - \text{plateau}_{u_{tt}}) \cdot \mathbf{E}_{tt,ol} - \psi_{tt} \cdot \mathbf{N}_{tt}(i-1)$ $\mathbf{R}_{tt}(i) <- \mathbf{R}_{tt}(i-1) + \psi_{tt} \cdot \mathbf{N}_{tt}(i-1)$	$\mathbf{E}_e(i) <- \mathbf{E}_e(i-1) - \lambda_e \cdot [\mathbf{E}_e(i-1)] - (1 - \text{plateau}_{u_e}) \cdot \mathbf{E}_{e,ol}$ $\mathbf{P}_e(i) <- \mathbf{P}_e(i-1) + \chi_e \cdot \lambda_e \cdot [\mathbf{E}_e(i-1)] - (1 - \text{plateau}_{u_e}) \cdot \mathbf{E}_{e,ol} - \delta \cdot \mathbf{P}_e(i-1)$ $\mathbf{A}_e(i) <- \mathbf{A}_e(i-1) + \delta \cdot \mathbf{P}_e(i-1)$ $\mathbf{N}_e(i) <- \mathbf{N}_e(i-1) + (1 - \chi_e) \cdot \lambda_e \cdot [\mathbf{E}_e(i-1)] - (1 - \text{plateau}_{u_e}) \cdot \mathbf{E}_{e,ol} - \psi_{tt} \cdot \mathbf{N}_e(i-1)$ $\mathbf{R}_e(i) <- \mathbf{R}_e(i-1) + \psi_{tt} \cdot \mathbf{N}_e(i-1)$	<p><i>Everyday:</i></p> <p>“Infection dynamics”</p>
$\mathbf{E}(i) <- \mathbf{E}(i) - \mu_e \cdot \mathbf{E}(i-1)$ <p>and \mathbf{R}_i</p> $\mathbf{A}(i) <- \mathbf{A}(i) - (\mu_i + \mu_C) \cdot \mathbf{A}(i-1)$	$\mathbf{E}_h(i) <- \mathbf{E}_h(i) - \mu_h \cdot \mathbf{E}_h(i-1)$ <p>\mathbf{N}_h and \mathbf{R}_h</p> $\mathbf{A}_h(i) <- \mathbf{A}_h(i) - (\mu_h \cdot \mathbf{A}_h(i) - (\mu_h \cdot \mathbf{A}_h(i) + \mu_C) \cdot \mathbf{A}_h(i-1))$	$\mathbf{E}_{tt}(i) <- \mathbf{E}_{tt}(i) - \mu_{tt} \cdot \mathbf{E}_{tt}(i-1)$ <p>\mathbf{N}_{tt} and \mathbf{R}_{tt}</p> $\mathbf{A}_{tt}(i) <- \mathbf{A}_{tt}(i) - (\mu_{tt} \cdot \mathbf{A}_{tt}(i) - (\mu_{tt} \cdot \mathbf{A}_{tt}(i) + \mu_C) \cdot \mathbf{A}_{tt}(i-1))$	$\mathbf{E}_e(i) <- \mathbf{E}_e(i) - \mu_e \cdot \mathbf{E}_e(i-1)$ <p>\mathbf{N}_e and \mathbf{R}_e</p> $\mathbf{A}_e(i) <- \mathbf{A}_e(i) - (\mu_e \cdot \mathbf{A}_e(i) - (\mu_e \cdot \mathbf{A}_e(i) + \mu_C) \cdot \mathbf{A}_e(i-1))$	<p><i>Everyday:</i></p> <p>“Mortality”</p>
$\mathbf{Env}_{i,e}(i) <- (1-C) \cdot \mathbf{Env}_{i,e}(i-1) + \sigma_{low} \cdot (\mathbf{P}_e + \mathbf{N}_e + \mathbf{N}_e) + \sigma_{high} \cdot (\mathbf{A}_e + \mathbf{A}_e) - \psi \cdot \mathbf{Env}_{i,e}(i-1)$	$\mathbf{Env}_h(i) <- (1-C) \cdot \mathbf{Env}_h(i-1) + \sigma_{low} \cdot (\mathbf{P}_h + \mathbf{N}_h) + \sigma_{high} \cdot \mathbf{A}_h - \psi \cdot \mathbf{Env}_h(i-1)$	$\mathbf{Env}_{tt}(i) <- (1-C) \cdot \mathbf{Env}_{tt}(i-1) + \sigma_{low} \cdot (\mathbf{P}_{tt} + \mathbf{N}_{tt}) + \sigma_{high} \cdot \mathbf{A}_{tt} - \psi \cdot \mathbf{Env}_{tt}(i-1)$	$\mathbf{Env}_e(i) <- (1-C) \cdot \mathbf{Env}_e(i-1) + \sigma_{low} \cdot (\mathbf{P}_e + \mathbf{N}_e) + \sigma_{high} \cdot \mathbf{A}_e - \psi \cdot \mathbf{Env}_e(i-1)$	<p><i>Everyday:</i></p> <p>“Update MAP in paddock”</p>
$\mathbf{E}_w(i) <- \mathbf{E}(i) \cdot p_{vac} \cdot \text{switch}_{vac}$ $\mathbf{E}(i) <- \mathbf{E}(i) - \mathbf{E}_w(i)$ <p>\mathbf{N}_w and \mathbf{R}_w / update \mathbf{P}_i, \mathbf{N}_i and \mathbf{R}_i</p> <p>For infection dynamics specific to vaccinated sheep (including the vaccine effect), see M&M</p>	NA	NA	NA	<p><i>Once a year at</i></p> <p>vac_{date}, <i>from</i></p> <p>vac_{year} <i>on</i>^v</p> <p>“Vaccination of lambs”</p>

^v: from vac_{date} onwards, each compartment is duplicated in one un-vaccinated and one vaccinated version existing in parallel. Both versions are updated similarly using the steps described in the algorithm.

(II) Population demographics algorithm

Lamb (l)	Hogget (h)	Two tooth (tt)	Ewe (e)	Events
NA	NA	NA	$E_e(i) <- E_e(i) - \text{prop}_{\text{cull}} \cdot E_e(i)$ $P_e(i) <- P_e(i) - \text{prop}_{\text{cull}} \cdot P_e(i)$ $N_e(i) <- N_e(i) - \text{prop}_{\text{cull}} \cdot N_e(i)$ $R_e(i) <- R_e(i) - \text{prop}_{\text{cull}} \cdot R_e(i)$	<p>Once a year at $t = \text{cull}_{\text{date}}$:</p> <p>“Ewe culling + replacement”</p>
NA	NA	<p>If $(\text{num}_{\text{two-tooth}}^* > \text{num}_{\text{keep,tt}}^{\uparrow})$</p> <p>Culling of $\text{num}_{\text{two-tooth}} - \text{num}_{\text{keep,tt}}$</p> <p>$\text{num}_{\text{two-tooth}} <- 0$ Else {</p> <p>$\text{num}_{\text{keep,tt}} <- \text{num}_{\text{two-tooth}}$</p> <p>$\text{num}_{\text{two-tooth}} <- 0$}</p>	$E_e(i) <- E_e(i) + \text{num}_{\text{keep,tt},E} + \text{num}_{\text{buy}}$ $P_e(i) <- P_e(i) + \text{num}_{\text{keep,tt},P}$ $N_e(i) <- N_e(i) + \text{num}_{\text{keep,h},N}$ $M_e(i) <- M_e(i) + \text{num}_{\text{keep,h},M}$ $R_e(i) <- R_e(i) + \text{num}_{\text{keep,h},R}$	<p>Once a year at $t = \text{rep}_{\text{date}}$:</p> <p>“Replacing culled ewes with two-tooth turning 2 YO”</p>
NA	<p>If $(n_{\text{hogget}}^* > \text{num}_{\text{keep,h}}^{\uparrow})$</p> <p>Culling of $n_{\text{hogget}} - \text{num}_{\text{keep,h}}$ (unvaccinated hoggets in priority)</p> <p>$n_{\text{hogget}} <- 0$ Else {</p> <p>$\text{num}_{\text{keep,h}} <- n_{\text{hogget}}$</p> <p>$n_{\text{hogget}} <- 0$}</p>	$E_{\text{tt}}(i) <- E_{\text{tt}}(i) + \text{num}_{\text{keep,h},E}$ $P_{\text{tt}}(i) <- P_{\text{tt}}(i) + \text{num}_{\text{keep,h},P}$ $N_{\text{tt}}(i) <- N_{\text{tt}}(i) + \text{num}_{\text{keep,h},N}$ $M_{\text{tt}}(i) <- M_{\text{tt}}(i) + \text{num}_{\text{keep,h},M}$ $R_{\text{tt}}(i) <- R_{\text{tt}}(i) + \text{num}_{\text{keep,h},R}$	<p>Once a year at $t = \text{aging}_{\text{hogget}}$:</p> <p>“Hoggets aging at 1 YO + culling extra”</p>	
$E_l(i) <- E_l(i) + \text{lamb}_{\text{rate}} \cdot [E_e(i) + R_e(i)] + (1 - \rho_M) \cdot \text{lamb}_{\text{ratePV}} \cdot [P_e(i) + N_e(i)] + (1 - \rho_M) \cdot \text{lamb}_{\text{rateM}} \cdot M_e(i)$	NA	NA	NA	<p>While $(\text{lamb}_{\text{start}} < \text{day} < \text{lamb}_{\text{end}})$:</p> <p>“Lambing season”</p>

10.3.4C.4. Updating the value of the underlying initial population at risk of infection (exposed to MAP) $E_{age,0}$ after demographic events

The model encompasses a plateau effect limiting the force of infection. This plateau (limit of the cumulative infection) applies to a theoretical “underlying” initial population at risk of infection, which needs to be updated with demographic events.

Notations:

- t_e : event time.
- “+” (plus) or “-” (minus) superscript refer to the value of a quantity before or after a demographic event occurred. For example, E^- is the number of exposed before the event, and E^+ the number of exposed after the event.
- Plateau^{new/old}: value of the dose-dependent plateau used in the force of infection (theoretical limit of cumulative infection when $t \rightarrow \infty$) after (new) or before (old) a demographic event. Needs updating since it depends on the MAP dose available/sheep from the environment. This can vary because of that because the dose available per sheep can be changed after a demographics event only, not as a direct effect of change in sheep number. Not like:
- $E_{age,0}^{new/old}$: the (imaginary) initial population size which corresponds to the current infection dynamics for a specific age group (l, h, tt, e), again after (new)/before (old) the event.

An event corresponds to remove (culling/aging/mortality) or add (aging/replacing) sheep from/to an age group. After each event the value $E_{age,0}^{old}$ (underlying theoretical population at risk of infection before the event) needs updating to $E_{age,0}^{new}$ (after the event), to take into account demographic changes in the infection dynamics.

The update in the absence of the event would be:

$$E_{age}^-(t_e+1) <- E_{age}^-(t_e) - \lambda_{age} \cdot [E_{age}^-(t_e) - (1 - \text{plateau}^{old}) \cdot E_{k,0}^{old}].$$

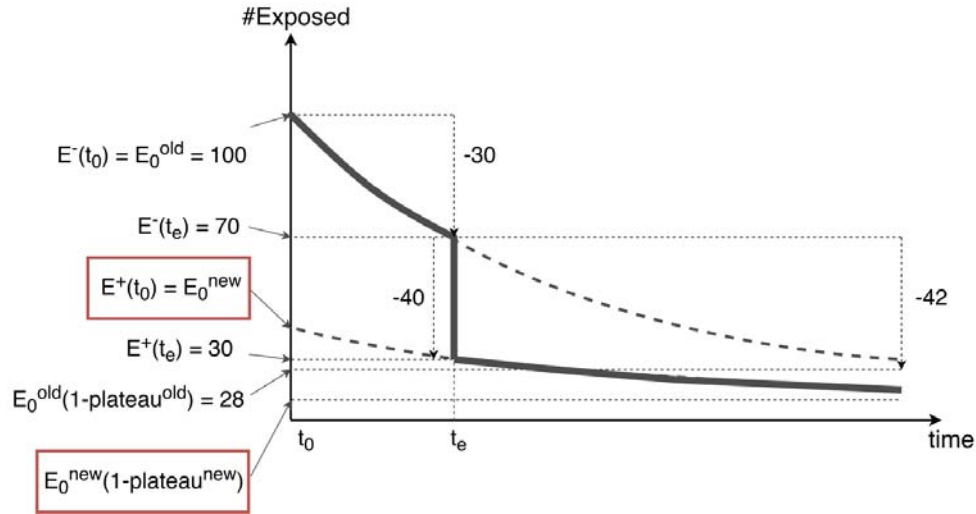


Figure C1: a schematic representation of the plateau update in the model after a removal (e.g. culling) event. The plain curve shows the number of Exposed sheep versus time.

In the example in Figure C1, the number of Exposed sheep removed is $E^-(t_e) - E^+(t_e) = 70 - 30 = 40$.

A new dynamics follows the removal of sheep at t_e , according to the following equation:

$$E_{age}^+(t_e+1) <- E_{age}^+(t_e) - \lambda_{age} \cdot [E_{age}^+(t_e) - (1\text{-plateau}^{new}) \cdot E_{age,0}^{new}].$$

Without the event, the increment in the new number of infected between t_e and t_e+1 would have been $E_{age}^-(t_e) - E_{age}^-(t_e+1) = \lambda_{age} \cdot [E_{age}^-(t_e) - (1\text{-plateau}^{old}) \cdot E_{age,0}^{old}]$. After the event occurred, the increment in the new number of infected between t_e and t_e+1 is: $E_{age}^+(t_e) - E_{age}^+(t_e+1) = \lambda_{age} \cdot [E_{age}^+(t_e) - (1\text{-plateau}^{new}) \cdot E_{age,0}^{new}]$.

The ratio of sheep remaining in the Exposed compartment after event is $E^+(t_e)/E^-(t_e)$. If sheep are assumed to be removed randomly from all compartments, we can write the following continuity equation which expresses that the fraction of removed sheep is the same among infected versus exposed sheep:

$$\lambda_{age} \cdot [E_{age}^-(t_e) - (1\text{-plateau}^{old}) \cdot E_{age,0}^{old}] \cdot E(t_e^+) = E(t_e^-) \cdot \lambda_{age} \cdot [E_{age}^+(t_e) - (1\text{-plateau}^{new}) \cdot E_{age,0}^{new}].$$

Solving this equation leads to:

$$E_{age,0}^{new} = E_{age,0}^{old} \frac{E(t_e^+)}{E(t_e^-)} \cdot \frac{1 - \text{plateau}^{old}}{1 - \text{plateau}^{new}}$$

The same equations apply if the event corresponds to adding sheep that follow the same infection dynamics, i.e. from the same infected flock, for example aging from one age group to the next.

The case of introducing naïve sheep (e.g. purchasing replacement ewes from an uninfected flock) is depicted in Figure C2.

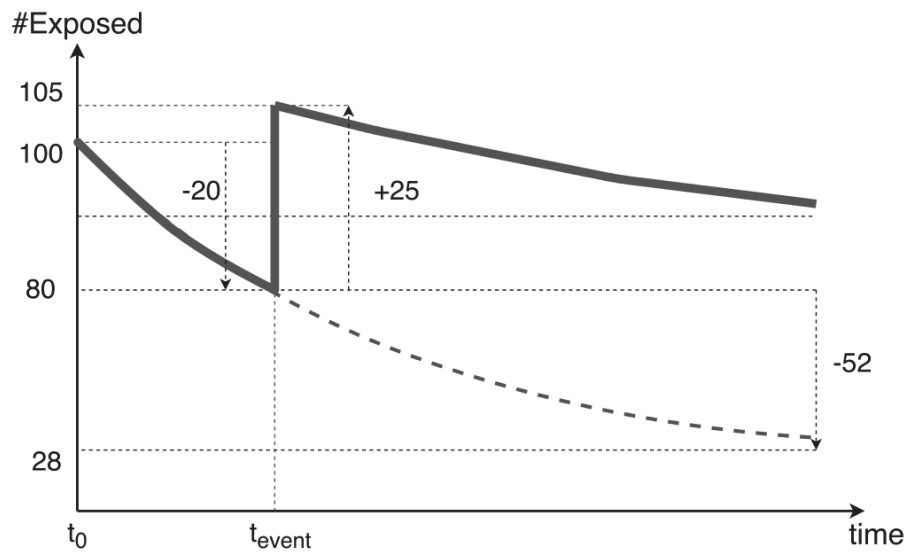


Figure C2: Schematic representation of the plateau update in the model after an introduction of naïve sheep (e.g. purchase replacement in E compartment) event. The plain curve shows the number of Exposed sheep versus time.

In this case, the updating equation for the value of the underlying initial population at risk (exposed to MAP) $E_{age,0}$ is:

$$E_{age,0}^{new} = n_{add} + E_{age,0}^{old} \frac{E^+(t_e) - n_{add}}{E^-(t_e)} \cdot \frac{1 - \text{plateau}^{old}}{1 - \text{plateau}^{new}}$$

With n_{add} the number of sheep added to the flock at this particular event.

Note: when purchasing infected ewes, the latter don't contribute to the update of the underlying population at risk of infection.

10.3.5C.5. Calculation of death rate due to paratuberculosis parameters (μ_c) and shedding parameters (σ_{low} and σ_{high})

Most key parameters for infection dynamics of PTB in sheep were estimated using a meta-analysis of ovine experimental infection. Two parameters needed to be estimated separately.

10.3.5.1 *Rate of death due to paratuberculosis (μ_c)*

In experimental infection models, the definition of clinical disease varies across studies. The trigger to euthanize an animal ranges from a subtle 10% weight loss to the animal being moribund, depending on the study. Hence the time spent in the affected compartment before succumbing to OJD could not be estimated in the meta-analysis of experimental infection because (1) observations of severe disease at *post-mortem* were by definition concomitant to euthanasia making it impossible to determine a progression from one to the other, and (2) the time of euthanasia was biased and not representative of the time a sheep would “naturally” succumb to the disease.

Instead, we used anecdotal evidence from a unique study of natural infection in sheep where serial biopsies of the intestine were performed (Dennis et al., 2010). It allowed us to estimate the timeline. It should be noted, however, that most clinically affected sheep in this study were euthanized as they reached a critical stage, potentially biasing the results towards underestimating the time sheep remained clinical (and shedding) in a flock.

In this study, sheep from a naturally infected flock were followed for three years. 12/77 died of clinical paratuberculosis after having developed intestinal lesions of various grades, as asserted by serial biopsies.

Based on observed histological results from intestinal samples at different time points, we elaborated the likely monthly course of progression in these sheep (table C1).

loads of MAP) for longer periods as highlighted by our estimation of μ_c , commensurately contributing to pasture-contamination.

10.3.5.2 *Shedding rates*

Based on a review of literature (Chapter 4), we determined that among severely infected animals subject to the onset of clinical signs, 17% presented paucibacillary lesions at *post-mortem*, and 83% presented with multibacillary lesions. Moreover, based on Whittington et al. (2000) we determined a plausible daily shedding level of 10^{11} MAP/day for multibacillary sheep and $2.4 \cdot 10^6$ MAP/day for paucibacillary sheep (see Chapter 4). From the above figures, we calculated corresponding adjusted shedding levels for the different shedding compartments of the model:

- σ_{low} (P/N early disease compartments) = $2.4 \cdot 10^6$ MAP/day
- σ_{high} (A affected compartment) = $(0.17 \cdot 2.4 \cdot 10^6) + (0.83 \cdot 10^{11}) = 8.3 \cdot 10^{10}$ MAP/day.